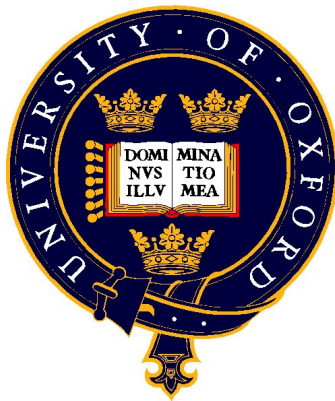

INVESTIGATING THE EFFECTS OF
VISUAL DEPRIVATION ON
SUBCORTICAL AND CORTICAL
STRUCTURES USING FUNCTIONAL
MRI AND MR SPECTROSCOPY



Gaëlle Simone Louise Coullon
ST. JOHN'S COLLEGE
UNIVERSITY OF OXFORD



A thesis submitted for the degree of
Doctor of Philosophy
Hilary 2015

Investigating the effects of visual deprivation on subcortical and cortical structures using functional MRI and MR spectroscopy

Gaëlle Simone Louise Coullon

St. John's College, Michaelmas 2014

A thesis submitted for the degree of Doctor of Philosophy

Abstract

Visual deprivation in early life causes widespread changes to the visual pathway. Structures normally dedicated to vision can be recruited for processing of the remaining senses (i.e. audition). This thesis used magnetic resonance imaging to explore how the 'visual' pathway reorganises in congenital bilateral anophthalmia, a condition where individuals are born without eyes. Anophthalmia provides a unique model of complete deprivation, since the 'visual' pathway has not experienced pre- or post-natal visual input.

Firstly, this thesis explored reorganisation of the anophthalmic 'visual' pathway for auditory processing, from subcortical structures responding to basic sounds (Chapters 3 and 4), to higher-order occipital areas extracting meaning from speech sounds (Chapter 7). Secondly, this thesis looked to better understand the neurochemical, neuroanatomical and behavioural changes that accompany reorganisation in anophthalmia (Chapters 5 and 6). Finally, this thesis investigated whether similar changes can take place in the sighted brain after a short period of visual deprivation (Chapter 8).

The experiments in this thesis provide some evidence that the lack of pre-natal visual experiences affects cross-modal reorganisation. Chapter 4 describes a unique subcortico-cortical route for auditory input in anophthalmia. Furthermore, Chapter 7 suggests that hierarchical processing of sensory information in the occipital cortex is maintained in anophthalmia, which may not be the case in congenital or early-onset blindness. However, this thesis also suggests that some reorganisation thought to be limited to anophthalmia can be found in early-onset blindness, for example with the subcortical functional changes described in Chapter 3. In addition, neurochemical, neuroanatomical and behavioural changes described in Chapters 5 and 6 are comparable to those reported in early-onset blindness, therefore demonstrating important similarities between these populations. Finally, this thesis describes how some of these functional and behavioural changes can also take place in sighted subjects after a short period of blindfolding, although this effect is extremely variable across subjects (Chapter 8).

The thesis concludes by highlighting the considerable contribution of individual differences in studies of cross-modal reorganisation, and emphasises the need for larger more homogenous groups when investigating subcortical and cortical plasticity in the absence of visual input.

Thesis word count: 43,801

Acknowledgements

I owe considerable thanks to my two fantastic supervisors, Holly Bridge and Kate Watkins. Their encouragement, advice, and enthusiasm have inspired me throughout this thesis, and I owe them a huge debt of gratitude. I would also like to thank Ione Fine and Fang Jiang for their help in shaping the ideas in this thesis. I also owe a special thank you to Danielle Kindree for inspiring me with her passion for all things biological.

Thank you to St. John's College for providing the funding I needed to undertake this DPhil, but also for becoming my second (or rather, seventh) home. I would also like to thank the many friends who have supported me through this thesis, but a special mention needs to go out to Madu Jayatunga, Ed Greening, Richard Lau, Marta Sarzynska, Elizabeth Ryznar, Emilie Lostis and Caz Woffindale. You have all contributed to my emotional well-being, and for that I am very grateful. I also need to thank Sara Ajina, for my DPhil certainly would not have been quite as manageable without her.

Un mot de remerciement est réservé pour Maman, Papa, et la famille Coullon-Léguistin. Les skype calls et les vacances en France ont beaucoup aidé à garder le calme (et le moral) pendant les moments de thèse difficiles!

Finally I would like to thank Ian, who has endured my constant complaining, laziness and general grumpiness over the past three years. Here's to many more adventures, and I promise to be considerably more cheerful when we are cycling across North America!

Contents

Abstract	i
Acknowledgments	iii
List of Abbreviations	xiii
List of Tables	xv
List of Figures	xviii
1 Introduction	1
1.1 Causes of blindness	2
1.2 Congenital bilateral anophthalmia	6
1.3 Human imaging allowed early demonstration of cross-modal plasticity	8
1.4 A ‘sensitive period’ for cross-modal plasticity?	9
1.5 Accompanying structural and neurochemical changes	12
1.6 How does auditory information reach the occipital cortex? . . .	14
1.7 Are auditory occipital responses functionally organised?	21
1.8 Thesis scope	24
2 General Methods	29
2.1 Anophthalmic participants	29
2.2 Magnetic resonance imaging (MRI)	31
2.3 Functional MRI	33

2.3.1	Sequences	33
2.3.2	Analysis	35
2.4	MR Spectroscopy	36
2.4.1	Sequences	37
2.4.2	Analysis	38

**PART I : FUNCTIONAL NEUROIMAGING OF
SUBCORTICAL STRUCTURES 39**

3	Subcortical functional reorganisation in anophthalmia and early blindness	41
3.1	Summary	41
3.2	Introduction	42
3.3	Methods	45
3.3.1	Participants	45
3.3.2	MR imaging acquisition	46
3.3.3	Auditory stimuli	47
3.3.4	Attentional task	49
3.3.5	MR imaging analysis	49
3.4	Results	53
3.4.1	Whole brain responses to sound in blind and sighted subjects	53
3.4.2	Recruitment of the superior colliculus for auditory processing in blind subjects	56
3.4.3	No auditory evoked responses in the LGN of blind or sighted subjects	58

3.4.4	Increased ipsilateral activity in the auditory thalamus of blind subjects	58
3.4.5	Inferior colliculus shows a mixed pattern of results	62
3.4.6	Cortical responses to sound in blind and sighted subjects	63
3.5	Discussion	65
3.5.1	Eliciting subcortical activity using a complex auditory stimulus	66
3.5.2	Recruitment of the superior colliculus for auditory processing in blind individuals	67
3.5.3	No evidence of recruitment of the LGN for auditory processing	68
3.5.4	Enhanced ipsilateral BOLD responses in blind individuals within the auditory thalamus	69
3.5.5	Anophthalmia as compared to early blindness	72
3.5.6	Conclusions	74
4	Subcortico-cortical connectivity in anophthalmia and early-onset blindness	75
4.1	Summary	75
4.2	Introduction	76
4.3	Methods	83
4.3.1	Participants	83
4.3.2	Auditory stimuli and MR imaging acquisition	84
4.3.3	MR imaging analysis	84
4.3.4	Dynamic causal modelling	85

4.4	Results	91
4.4.1	Model Space 1	91
4.4.2	Model Space 2	97
4.5	Discussion	98
4.5.1	Limited experimental power	99
4.5.2	Model Space 1 different from Klinge et al. (2010) . . .	100
4.5.3	MGN to A1 and V1 in Model Space 1	101
4.5.4	Superior colliculus to V1 in anophthalmia but not early-onset blindness	103
4.5.5	Anophthalmia as compared to early blindness	104
4.5.6	Conclusions	106

**PART II: NEUROCHEMICAL, NEUROANATOMICAL, AND
BEHAVIOURAL DATA 107**

**5 Neurochemical changes in the pericalcarine cortex in
anophthalmia 109**

5.1	Summary	109
5.2	Introduction	110
5.3	Methods	113
5.3.1	Participants	113
5.3.2	MR imaging acquisition	113
5.3.3	Data analysis	115
5.4	Results	117
5.4.1	¹ H magnetic resonance spectroscopy (MRS)	117

5.4.2	Cortical thickness and grey matter fraction	119
5.5	Discussion	123
5.5.1	Visual deprivation results in elevated choline levels . . .	124
5.5.2	Cortical thickness	125
5.5.3	GABA and the effects of grey matter content	126
5.5.4	Failure to see differences in total creatine and myo-Inositol	128
5.5.5	Conclusions	129
6	Auditory abilities in anophthalmia and correlations with occipital cortical thickness	131
6.1	Summary	131
6.2	Introduction	132
6.3	Methods	137
6.3.1	Participants	137
6.3.2	Auditory tasks	137
6.3.3	Data analysis	139
6.4	Results	139
6.5	Discussion	143
6.5.1	Superior pitch and melody discrimination in anophthalmia	143
6.5.2	Melody discrimination ability correlated with right occipital cortical thickness	145
6.5.3	Conclusions	147

**PART III: FUNCTIONAL NEUROIMAGING OF CORTICAL
STRUCTURES** **149**

7	Functional organisation of auditory-evoked occipital responses in anophthalmia	151
7.1	Summary	151
7.2	Introduction	152
7.3	Methods	157
7.3.1	Participants	157
7.3.2	Auditory setup	158
7.3.3	What-Where auditory task	158
7.3.4	Meaning-Syllable auditory task	159
7.3.5	MR imaging acquisition	161
7.3.6	MR imaging analysis	161
7.3.7	Region of interest (ROI) analysis	163
7.4	Results	164
7.4.1	What-Where task	165
7.4.2	Meaning-Syllable task	174
7.5	Discussion	183
7.5.1	Cortical responses to spatial tones in sighted subjects .	184
7.5.2	Occipital activations to spatial tones in anophthalmia .	187
7.5.3	Cortical responses to phonological and semantic sounds in sighted subjects	190
7.5.4	Occipital activations for phonological vs. semantic processing in anophthalmia	193

7.5.5	Auditory-evoked responses to language stimuli in the cerebellum	196
7.5.6	Conclusions	196
7.6	Appendix Figure	198
7.6.1	Appendix Figure 1	198
8	Behavioural and functional cortical changes after short-term visual deprivation	199
8.1	Summary	199
8.2	Introduction	200
8.3	Methods	205
8.3.1	Participants	205
8.3.2	Experimental design	205
8.3.3	Auditory tasks	206
8.3.4	MR imaging acquisition	207
8.3.5	MR imaging analysis	207
8.3.6	Region of interest (ROI) analysis	209
8.4	Results	210
8.4.1	Behavioural tasks	210
8.4.2	fMRI tasks	212
8.5	Discussion	224
8.5.1	Behavioural findings	225
8.5.2	Functional findings: increased occipital responses to sounds after blindfolding	227

8.5.3	Task-specific findings: experimental power concerns and between-subject variability	228
8.5.4	Task-specific lateralisation of occipital auditory-evoked responses after blindfolding	230
8.5.5	Short-term deprivation: rapid and reversible unmasking of existing connections?	231
8.5.6	Conclusions	233
8.6	Appendix Figures	234
8.6.1	Appendix Figure 1	234
8.6.2	Appendix Figure 2	235
8.6.3	Appendix Figure 3	236
8.6.4	Appendix Figure 4	237
9	General Discussion	239
9.1	Subcortical functional reorganisation in anophthalmia and early-onset blindness	242
9.2	Neurochemical, neuroanatomical and behavioural changes in anophthalmia	245
9.3	Cortical functional reorganisation in anophthalmia	248
9.4	Short-term visual deprivation in sighted adults	251
9.5	The importance of individual differences	253
9.6	Areas for future work	254
9.7	Final conclusions	257
	References	259

List of Abbreviations

A1	primary auditory cortex
BOLD	blood-oxygenation-level dependent
CSF	cerebrospinal fluid
DCM	Dynamic Causal Modelling
EPI	echo-planar imaging
FEAT	FMRI expert analysis tool
fMRI	functional magnetic resonance imaging
FMRIB	Functional Magnetic Resonance Imaging of the Brain Centre
FSL	FMRIB's Software Library
GLM	general linear model
IC	inferior colliculus
LGN	lateral geniculate nucleus
LOC	lateral occipital complex
MGN	medial geniculate nucleus
MNI	Montreal Neurological Institute
MPRAGE	magnetisation-prepared rapid acquisition gradient-echo sequence
MRI	magnetic resonance imaging
MRS	magnetic resonance spectroscopy
NAA	N-acetyl aspartate
ppm	parts per million
PRESS	Point resolved spectroscopy
SC	superior colliculus
SNR	signal to noise

SPECIAL SPin ECho full Intensity Acquired Localised spectroscopy

SPM Statistical Parametric Mapping

STEAM Stimulated-echo acquisition mode

TMS transcranial magnetic stimulation

V1 primary visual cortex

List of Tables

1	Brief description of anophthalmic cases	30
2	Brief description of early blind cases. All early blind participants were scanned at the University of Washington (UW).	46
3	Table of neurochemical concentrations in pericalcarine cortex (V1) in the anophthalmia and sighted groups	118
4	Table of whole-brain clusters in the <i>What-Where</i> task for sighted controls	168
5	Table of clusters from the <i>What-Where</i> task that include occipital regions for each anophthalmic case	170
6	Table of whole-brain clusters in the <i>Meaning-Syllable</i> task for sighted controls	176
7	Table of clusters from the <i>Meaning-Syllable</i> task that include occipital regions for each anophthalmic case	179
8	Table of LOC clusters from the contrast of <i>Meaning > Syllable</i> for each anophthalmic case	180
9	Schematic of each session of the blindfolding experiment	206
10	Table of <i>What-Where</i> blindfold and control session cluster coordinates	215
11	Table of <i>Meaning-Syllable</i> blindfold and control session cluster coordinates	221

List of Figures

1	World Health Organisation 2010 global causes of blindness	3
2	Timeline for age of blindness onset terminology	5
3	Human Visual Pathway	7

4	Cortico-cortical and thalamo-cortical pathways	15
5	Reverse Hierarchy theory	17
6	Possible thalamo-cortical pathway in anophthalmia	21
7	T1-weighted images of the five anophthalmic cases	30
8	Schematic of sparse sampling protocol	34
9	Example MRS spectra	36
10	MGN auditory stimuli	48
11	Whole brain example subjects	54
12	Whole brain groups	55
13	Superior colliculus activation to sound in blind groups	57
14	Superior colliculus % BOLD signal change	57
15	Auditory thalamus definitions compared to anatomical MGN and LGN	60
16	Auditory thalamus % BOLD signal change	61
17	Inferior colliculus % BOLD signal change	62
18	A1 and V1 % BOLD signal change	64
19	Human Auditory Pathway	70
20	Collignon et al. 2013 DCM results	82
21	Schematic of DCM models in Model Space 1	88
22	Schematic of DCM models in Model Space 2	89
23	Model Space 1 Bayesian Model Selection for all four subject groups	92
24	Model Space 1 Bayesian Model Selection for pooled sighted and blind groups	93

25	Model 4 MGN to A1 connections	94
26	Model 4 MGN to V1 connections	96
27	Model Space 2 Bayesian Model Selection	97
28	MRS voxel placement and spectra	114
29	Graph of neurochemical concentrations in pericalcarine cortex for each individual anophthalmic case normalised to sighted controls	118
30	Cortical thickness in the anophthalmia and sighted groups . . .	120
31	Neurochemical concentrations correlated with grey matter frac- tion	122
32	Anophthalmia and sighted groups behavioural results	141
33	Anophthalmia transposed melody scores correlated with corti- cal thickness	142
34	Schematic of the four <i>What-Where</i> sound locations	160
35	Schematic of the <i>What-Where</i> fMRI experimental design	160
36	Schematic of the <i>Meaning-Syllable</i> fMRI experimental design .	160
37	Image of whole-brain activations during the <i>What-Where</i> task for sighted controls and each anophthalmic case	167
38	Image 2 of whole-brain activations during the <i>What-Where</i> task for sighted controls and each anophthalmic case	169
39	Visual area ROI analysis for the <i>What-Where</i> task	172
40	ROI analysis of non-visual regions for <i>What-Where</i> task	173
41	Image of whole-brain activations during the <i>Meaning-Syllable</i> task for sighted controls only	175
42	Image of whole-brain activations during the <i>Meaning-Syllable</i> task for sighted controls and each anophthalmic case	178

43	Whole-brain contrast of <i>Meaning</i> > <i>Syllable</i> and <i>Syllable</i> > <i>Meaning</i> for sighted controls and each anophthalmic case . . .	180
44	Visual area ROI analysis for the <i>Meaning-Syllable</i> task	182
45	ROI analysis of non-visual regions for the <i>Meaning-Syllable</i> task	183
46	Appendix Figure: Meaning-Syllable cerebellum imaging	198
47	Blindfold and control session pitch and loudness thresholds . .	211
48	Blindfold and control session melody and phoneme task scores	211
49	Whole brain imaging of blindfolding > control session, all sounds combined	213
50	Whole brain imaging of blindfold and control session during the <i>What-Where</i> task	214
51	Active voxels difference between blindfold and control sessions during the <i>What-Where</i> task	218
52	Whole brain imaging of blindfold and control session during the <i>Meaning-Syllable</i> task	220
53	Active voxels difference between blindfold and control sessions during the <i>Meaning-Syllable</i> task	223
54	Blindfold Appendix Figure 1: <i>What-Where</i> percentage BOLD signal change	234
55	Blindfold Appendix Figure 2: <i>What-Where</i> active voxels analysis	235
56	Blindfold Appendix Figure 3: <i>Meaning-Syllable</i> percentage BOLD signal change analysis	236
57	Blindfold Appendix Figure 4: <i>Meaning-Syllable</i> active voxels analysis	237

1 Introduction

Organisation of the cerebral cortex into distinct visual cortical areas and pathways for visual function was first determined by investigating patients with brain damage (Holmes, 1918). The advent of functional neuroimaging, first PET and then functional MRI, led to further distinction of regions with specialisations within this sensory modality. However, with additional sensitivity and more sophisticated experiment design, functional MRI also revealed that brain regions, even those early in the sensory pathways, contribute to processing in multiple sensory modalities. The most convincing evidence for this ‘cross-modality’ or ‘multimodality’ comes from studies of sensory deprivation. When the cerebral cortex is deprived of a sense (such as vision) the cortical areas typically processing that sense can be recruited by the remaining modalities – this reorganisation is called ‘cross-modal plasticity’.

Blindness provides a unique model of sensory deprivation since vision is such a crucial component to human development and sensory perception; a larger proportion of the human cortex is dedicated to vision than in any other species (Van Essen, 2005) and the human visual system is much more highly developed at birth compared to other species. A study of visual deprivation

will therefore uncover the extent to which brain development depends on sensory input. Precisely how the brain changes to allow this plasticity, and the degree to which these changes are dependent on the nature and extent of the deprivation, is currently unclear. In the case of blindness, the age at which vision is lost is likely to play a critical role in determining where and how reorganisation takes place. The aim of this thesis is therefore to address whether the complete lack of visual input and the earliest age of blindness onset means that the 'visual' pathway completely reorganises its function and neurochemistry for auditory processing. Answering this question will help to understand the extent to which visual pathway development is driven by visual input in pre-natal and post-natal development. Furthermore, a greater understanding of how blindness in early life affects subcortical and cortical development may be important in the innovation of new sight restoration or improvement techniques. This introductory chapter reviews the current literature on cross-modal changes after visual deprivation, with focus placed on the auditory domain and how age of onset may influence this reorganisation.

1.1 Causes of blindness

In 2010, the World Health Organisation reported that there are approximately 39 million clinically blind individuals across the world (Pascolini and Mariotti, 2012). Of these, the single major cause of blindness is cataracts (51%), followed by glaucoma (8%) and age-related macular degeneration (5%)

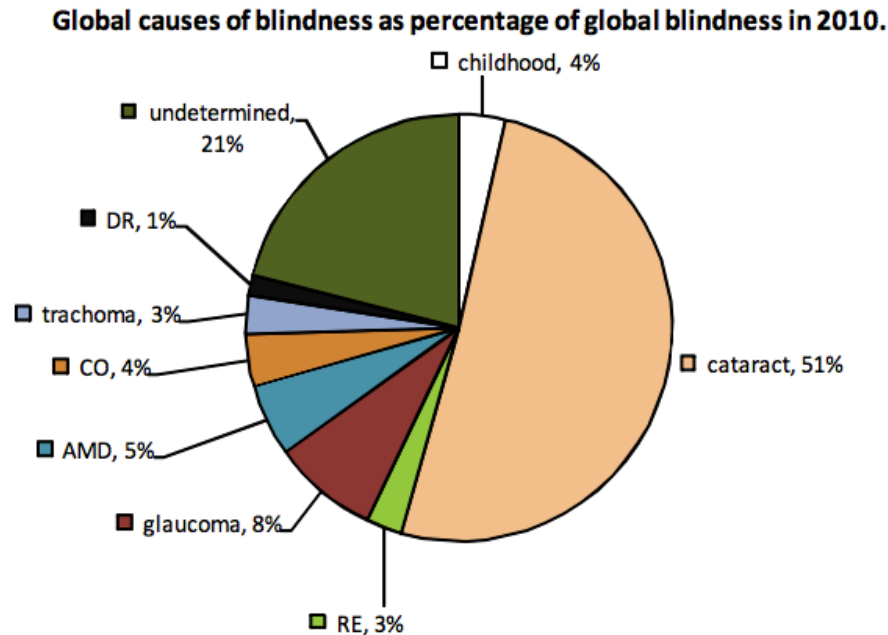


Figure 1: Adapted from Pascolini and Mariotti (2012). Causes of blindness, according to the World Health Organisation 2010 report on global visual impairments. DR = diabetic retinopathy; CO = corneal opacities; AMD = age-related macular degeneration; RE = uncorrected refractive errors.

(see **Figure 1**). Approximately 4% of individuals become blind in childhood; however, within this category there is also wide range of causes and aetiologies. In congenital glaucoma, incorrect eye development before birth increases pressure inside the eye, eventually leading to severe optic nerve damage at birth or in early life. Severe cases of congenital cataracts present from birth or in early life can also cause blindness in infants. Other causes have included retinopathy of prematurity (ROP), a condition resulting from the use of hyperbaric chambers to increase oxygen levels in infants, which can cause major retinal damage. However, the practice's dissolution in recent years has reduced the prevalence rate of ROP. Leber's congenital amaurosis, a rare

inherited disease of the retina, is linked to abnormal photoreceptor development and results in severe visual impairment and blindness. In addition to the wide range of blindness causes, another major source of variability is the amount of residual vision that individuals with these conditions have; this can range from total blindness to some light perception through to some colour and shape recognition.

Research on cross-modal plasticity samples a wide range of these causes of blindness. In order to understand the effect of blindness on neural development and allow comparison across studies, it is critical to have clear definitions of blindness categories as there is considerable variability in the literature as to what is defined as early-onset or late-onset blindness (Voss, 2013). Furthermore, some causes of acquired blindness may be gradual, thus making it difficult to establish the point of onset.

This introductory chapter will refer to age of blindness onset according to the following categories, and is designed to specifically highlight the most extreme type of blindness: bilateral congenital anophthalmia. **Congenital bilateral anophthalmia** is a condition in which the eyes do not develop, or eye formation is stopped in early development and the structure degenerates. Importantly, it is distinct from other causes of blindness as the lack of eyes means that the anophthalmic visual pathway has not experienced pre-natal or post-natal activity. **Congenital blindness** refers to an individual born blind with no residual vision, and therefore lacking any post-natal visual stimulation. As discussed above, causes can include congenital glaucoma, congenital cataracts, ROP and Leber's congenital amaurosis. **Early blind**

individuals are generally defined as blind within the first few years of life and usually prior to the age of 5 (e.g. Burton et al. (2002b)).

However, there are several studies in which this term has been used up to the age of 12 (Liu et al., 2007; Gougoux et al., 2005), even though this group is also classified as **late-onset blindness** in some cases (Burton et al., 2002b,a). Other studies have defined late blindness as occurring only after the start of puberty (age 12 years) (Voss, 2013). The variability in classification of early and late onset blindness, and consequently the proportion of life during which a person experiences normal vision, may lead to inconsistent results. Nonetheless, studies of acquired blindness can explore the different contribution of age of onset and duration of blindness on cross-modal plasticity. In this introductory chapter, early-onset blindness is considered as occurring in the first few years of life, and usually prior to the complete maturation of the visual pathway. Blindness occurring after 5 years but before the end of adolescence will be considered as **pre-adolescence late-onset blindness**, and blindness occurring after the end of adolescence will be classified as **post-adolescence late-onset blindness**. The categories are presented on a timeline in **Figure 2**.

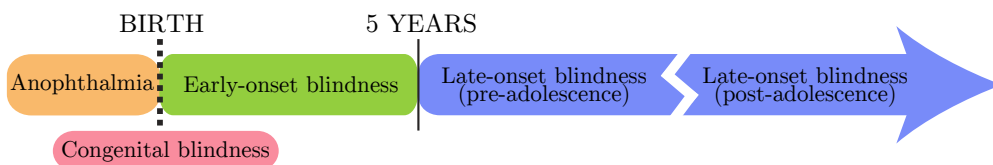


Figure 2: Timeline for age of blindness onset terminology

1.2 Congenital bilateral anophthalmia

The main blind population described in this thesis is congenital bilateral anophthalmia. This sub-type of congenitally blind individuals could be considered a model of extreme blindness; in bilateral anophthalmia, individuals are born without both eyes. This rare condition can be diagnosed using both CT and MR imaging in order to show the absence of a globe in the eye socket. Neural tissue from the visual pathway may be visible, although significantly reduced in size and volume (Albernaz et al., 1997).

Bilateral anophthalmia has a prevalence rate of approximately 1.8-4 in 100,000 (Källén and Tornqvist, 2005; Shaw et al., 2005; Verma and Fitzpatrick, 2007); it can be isolated, although in approximately a third of cases it is accompanied by co-varying disorders (Verma and Fitzpatrick, 2007). The precise cause of anophthalmia is largely unknown; it can be triggered in early development due to a failure to develop optic vesicles (primary anophthalmia), a failure to develop part of the neuronal tube (secondary anophthalmia), or the development of the optic vesicles stops and the structures degenerate (consecutive or degenerative anophthalmia). In such cases when eye development is aborted, the optic nerve, chiasm, tracts and a partially developed eye can be seen (FitzPatrick and Van Heyningen, 2005). Anophthalmia has also been linked to selected mutations of the SOX2, OTX2 and PAX6 genes, which may cause anophthalmia through retinal differentiation failures (FitzPatrick and Van Heyningen, 2005).

The main distinction between congenital bilateral anophthalmia and

other causes of blindness is the lack of eyes; as a result, it is assumed that the anophthalmic visual pathway has not experienced pre-natal activity. The neural circuits that make up the visual pathway (see **Figure 3**) are determined genetically during development. It is then thought that these connections are refined by neuronal activity in order to strengthen the pathway and prepare it for visual input (Katz and Shatz, 1996). This activity can take place before birth (pre-natal) or after birth (post-natal). Pre-natal sensory experiences include retinal waves, or correlated waves of retinal activity that occur spontaneously during very early development (Wong, 1999). They are thought to be instructive for the development of the visual pathway, for example they contribute to the development of layers in the lateral geniculate nucleus (LGN) (Stellwagen and Shatz, 2002) and retinotopic maps in the superior

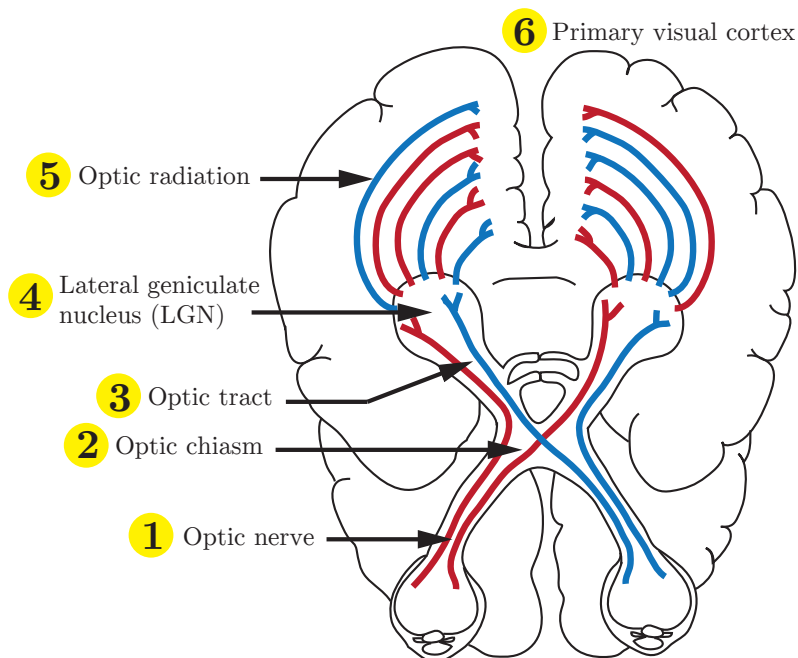


Figure 3: Schematic of the human visual pathway.

colliculus (Chandrasekaran et al., 2005). In anophthalmia, the absence of eyes in pre-natal development would mean this type of pre-natal sensory activity does not take place along the visual pathway.

1.3 Human imaging allowed early demonstration of cross-modal plasticity

Hubel and Wiesel's revolutionary work established that the lack of visual experience could affect normal development in the occipital 'visual' cortex. However, it was not until the advent of non-invasive human imaging that it became possible to understand the reorganisation occurring in blindness. The first imaging studies demonstrated that the occipital cortex can respond during auditory stimulation in blind humans (Buchel et al., 1998; Weeks et al., 2000; Arno et al., 2001; Burton et al., 2002b). Since then, the blind occipital cortex has been shown to respond during a range of auditory tasks, from sound localisation (Weeks et al., 2000; Gougoux et al., 2005), auditory motion (Poirier et al., 2006; Lewis et al., 2010), and detecting changes in sounds (Kujala et al., 2005), to more complex tasks involving language (Burton et al., 2002b, 2003; Bedny et al., 2010, 2011; Watkins et al., 2012), verbal memory (Amedi et al., 2003; Lambert et al., 2004), and episodic memory (Raz et al., 2005). These responses can be functionally relevant, as illustrated by the case study of a blind patient who lost her ability to read Braille following a bilateral stroke to the occipital cortex (Hamilton et al., 2000).

There is considerable evidence of blind individuals demonstrating equal

or improved performance on auditory tasks such as pitch discrimination (Gougoux et al., 2005; Voss and Zatorre, 2012), auditory spatial awareness (Collignon et al., 2009), verbal recall (Amedi et al., 2003), sensitivity to echo cues (Dufour et al., 2005), and auditory motion (Lewald, 2013). A number of studies have aimed to determine the relationship between auditory-evoked activity in the early blind occipital cortex and these improvements in auditory abilities. In particular, BOLD activity has been correlated with performance on spatial localisation tasks (Gougoux et al., 2005), verbal memory (Amedi et al., 2003) and episodic memory (Raz et al., 2005). Additionally, transcranial magnetic stimulation (TMS) to the occipital cortex in blind individuals can disrupt auditory processing, notably sound localisation (Collignon et al., 2007, 2009) and verb generation (Amedi et al., 2004).

1.4 A ‘sensitive period’ for cross-modal plasticity?

From the early literature, it was apparent that there was some degree of variation in the extent of cross-modal responses relative to age of blindness onset. The first evidence that age of onset is an important factor in occipital changes after deprivation came from a study on glucose metabolism. The authors showed that whilst occipital glucose levels in early blind subjects were comparable to sighted subjects with eyes open, glucose levels in late blind individuals were considerably lower (Veraart et al., 1990). Imaging studies during Braille reading found that occipital responses were not present in individuals blind after the ages of 14-16 years (Cohen et al., 1999; Sadato

et al., 2002). This implied there might be a limited time window in early development, or ‘critical age’, after which the occipital cortex cannot be functionally recruited for non-visual processing.

However, since comparable occipital responses to sounds were also reported in both early and late blind individuals (Kujala et al., 1997), this theory of a critical age was replaced by the idea of a ‘sensitive period’. While there are occipital responses to sounds in late blind individuals, the extent of activation appears less than in congenital or early blind populations, as demonstrated by Burton and colleagues in a series of functional imaging studies (Burton et al., 2002b,a, 2003; Burton, 2003). Here, aural and tactile semantic and phonological tasks activated ‘visual’ areas (defined retinotopically in sighted subjects) in both early and late blind groups; however, these responses were considerably more spatially extensive in early than late blind individuals. The theory of a ‘sensitive period’ suggests that lack of vision in early development allows for more extensive functional reorganisation of typically ‘visual’ cortical regions, as the brain is more sensitive to the available sensory input. In later life, visual experience has wired the occipital cortex for vision so it is perhaps less sensitive to change. This idea of a ‘sensitive period’ may also influence whether visual deprivation affects perceptual abilities in the remaining senses. Evidence for this comes from early blind individuals performing better at judging pitch changes than a group of both pre- and post-adolescence late blind individuals (Gougoux et al., 2004), and congenitally blind subjects performing slightly better on an auditory perception task than early blind subjects (Wan et al., 2010).

A number of studies provide evidence directly contradicting these findings mentioned above. Such work provides evidence that late-blind populations do not always show less cross-modal activations in comparison with early blind populations (Collignon et al., 2013). Furthermore, late blind individuals can demonstrate auditory abilities that are similar to those reported for early blind populations (Voss et al., 2004). This contradiction is made more complicated by the striking evidence that very short periods of visual deprivation can also induce similar functional cross-modal changes in healthy sighted adults. A series of experiments in which sighted adults were blindfolded for five days revealed that visual deprivation can increase brain activity to auditory and tactile stimulation in the occipital cortex (Pascual-Leone and Hamilton, 2001); furthermore, tactile discrimination performance in these individuals was impaired by TMS to the occipital cortex, suggesting that these responses can also be functionally relevant. Shorter periods of visual deprivation (90 minutes) have also increased occipital responses to tactile stimulation in sighted adults (Merabet et al., 2007) as well as improved tactile acuity (Facchini and Aglioti, 2003), auditory localisation (Lewald, 2007), and harmonicity thresholds (Landry et al., 2013). In summary, there is strong evidence for a sensitive period for cross-modal reorganisation in blindness. This needs to be reconciled with data in late blind populations and sighted ones that undergo short-term visual deprivation, which shows functional recruitment of occipital cortex for non-visual processing. It is possible that different mechanisms underpin cross-modal plasticity in these different groups. Further studies examining patterns of functional connectivity, high-resolution structural imaging and neurochemistry might shed light on this apparent

contradiction.

1.5 Accompanying structural and neurochemical changes

Whilst auditory-evoked responses tell us solely about functional changes in the absence of vision, changes in structure and neurochemistry can tell us about the underlying neural mechanisms. Anatomical and chemical markers provide clues as to how visual deprivation at different ages affects the development of the occipital cortex.

Extensive structural changes have been noted in subcortical 'visual' structures of anophthalmic, congenitally blind and early blind individuals; the lateral geniculate nucleus (Bridge et al., 2009), optic nerves, optic tracts and optic radiations (Noppeney et al., 2005; Shimony et al., 2006; Ptito et al., 2008; Bridge et al., 2009; Shu et al., 2009) have all shown signs of degeneration in these groups. However, this degeneration may be limited to early-onset blindness as these structures appeared structurally intact in late blind individuals (Schoth et al., 2006). At the cortical level, cortical thickness is increased in various 'visual' occipital areas including the pericalcarine region in anophthalmic (Bridge et al., 2009), congenitally blind (Voss and Zatorre, 2012; Qin et al., 2013), and early blind (Jiang et al., 2009) but not late blind individuals (Jiang et al., 2009; Park et al., 2009). Interestingly, increased occipital cortical thickness has been correlated with improved performance on pitch and melody tasks in early blind individuals, who were also significantly

better at these tasks than pre- and post-adolescence late blind and sighted subjects (Voss and Zatorre, 2012). A thicker occipital cortex in early-onset blindness could indicate a lack of cortical maturation, especially considering that the primary visual cortex undergoes substantial pruning (cortical thinning) during normal development following the onset of visual experience (Elston et al., 2009, 2010). Thicker occipital cortex would not be found in late-onset blindness, as visual experience in early life would have triggered this normal maturational process.

In addition to anatomical changes, various neurochemical changes have been noted in the animal and human literature on blindness. Animal models suggest that up-regulated excitatory and attenuated inhibitory pathways during occipital cortex development are the driving forces behind reorganisation. Cortical excitability could be increased via cholinergic pathways; increased levels of choline acetyltransferase, a cholinergic marker, were found in the primary and secondary visual areas of dark-reared kittens (Fosse et al., 1989). This could be combined with attenuated inhibitory circuits, potentially GABAergic, as demonstrated by lower GABA levels in the same cohort of dark-reared kittens (Fosse et al., 1989) and dark-reared rats (Benevento et al., 1995). GABA changes in the occipital cortex are thought to mark the end of sensitive or critical periods in development (Hensch et al., 1998), usually by an increase in occipital GABAergic inputs; however, this increase was not found in visually deprived animals (Morales et al., 2002). In humans, neurochemicals can be quantified in the occipital cortex using ^1H magnetic resonance spectroscopy (MRS). In early blind humans, increased levels of a

cholinergic marker and modest reductions in GABA (Weaver et al., 2013) seem to follow the theory of increased occipital cortex excitability in blindness. Another MRS study looking predominantly at acquired (late) blindness did not find such changes (Bernabeu et al., 2009), suggesting differences in ages of blindness onset may play a role in these neurochemical changes. However, it is difficult to make clear conclusions based on these limited sample sizes.

These findings suggest a lack of normal occipital cortex maturation in early-onset blindness, possibly because of the absence of visual input before the end of sensitive periods in development. As suggested by the structural and neurochemical evidence, the degree and extent of occipital changes could be explained at least partly by age of blindness onset. However, direct comparisons between groups that differ in ages of onset are required, especially considering the limited literature on neurochemical changes in human blindness.

1.6 How does auditory information reach the occipital cortex?

A key issue in the current literature is how non-visual information reaches the occipital cortex. New connections could be formed or, perhaps more plausible, existing projections between sensory or multisensory regions and the occipital cortex could be unmasked or strengthened by the absence of visual input (Pascual-Leone and Hamilton, 2001). During normal development, unused cortical connections are pruned in order to keep only efficient connections; in

the occipital cortex, this means a reduction in its connections with non-visual structures, including auditory cortical regions (Innocenti and Clarke, 1984; Dehay et al., 1988; Innocenti et al., 1988). However, visual deprivation early in life means there is no competition from visual inputs and these cross-modal projections could persist.

Two main pathways may be involved in carrying auditory information to the blind occipital cortex; cortico-cortical routes from auditory or multisensory regions, and thalamo-cortical routes from ‘visual’ or auditory subcortical structures (Bavelier and Neville, 2002) (**Figure 4**). The use of either or both of these pathways may depend on age of blindness onset. Support for cortico-cortical pathways comes from multiple approaches, including evidence for cross-modal connections in sighted subjects. Specifically, there is evidence

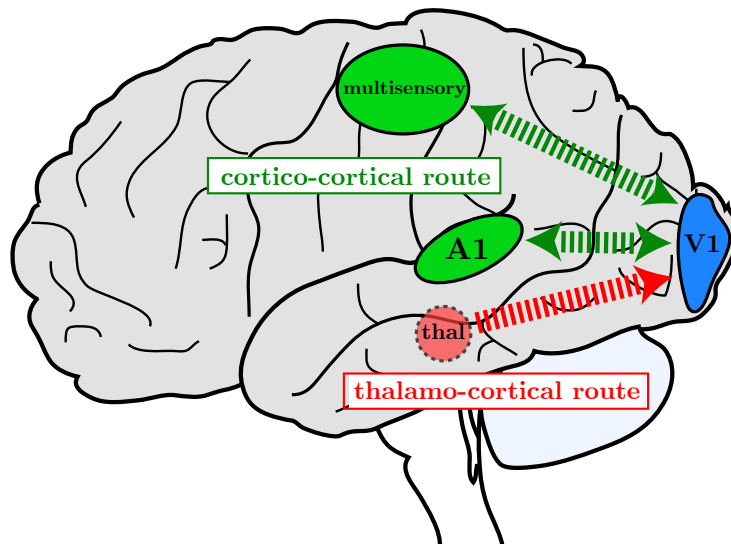


Figure 4: Schematic of the thalamo-cortical and cortico-cortical pathways for cross-modal inputs to the occipital cortex (V1). V1 receives feedforward input from thalamic structures such as the LGN and feedback information from auditory (A1) and multisensory regions.

that the different senses converge in early cortical regions, including the primary visual cortex (Laurienti et al., 2002; Schroeder et al., 2003; Driver and Noesselt, 2008; Liang et al., 2013). In sighted monkeys, retrograde and anterograde tracer injections have shown robust direct connections from auditory temporal and multisensory parietal regions to anterior (non-foveal) portions of primary and secondary visual areas (and vice-versa, see Falchier et al. (2002, 2010); Rockland and Ojima (2003); Clavagnier et al. (2004)). Similar anatomical connections between Heschl’s gyrus and the occipital cortex have been found in sighted humans using diffusion MRI (Beer et al., 2011), whilst resting state fMRI has shown a coupling of functional activity between Heschl’s gyrus and the anterior calcarine fissure (V1) in sighted individuals (Eckert et al., 2008).

If these multi-sensory connections are present in sighted individuals to facilitate multisensory integration, it may be that these pathways are used for cross-modal inputs in the blind, and perhaps strengthened by both long-term and short-term visual deprivation (Pascual-Leone and Hamilton, 2001). Indeed, auditory to visual cortex connections normally pruned during development (Innocenti et al., 1988) appear to be maintained in animals deprived of vision at birth (Berman, 1991; Yaka et al., 1999; Karlen et al., 2006). Similarly, human imaging data looking at connectivity between brain regions during an auditory fMRI task found that primary auditory (A1) to primary visual cortex (V1) connections are present in sighted individuals but the strength of these connections is greater in early blind individuals (Klinge et al., 2010). Furthermore, it may be that whilst early-onset blindness can

facilitate the use of normally pruned cross-modal connections, late-onset blindness may be constrained by the existing or established pathways. A recent imaging study found that whilst early blind individuals rely on direct A1 to V1 connections during an auditory task, auditory information to V1 in late blind individuals relies on feedback connections with multisensory parietal regions (Collignon et al., 2013).

Finally, cortico-cortical connections may be important in shaping the functional role of V1 in blind individuals. There is evidence in both early and congenitally blind people that V1 has a role in language. Amedi et al. (2003) reported V1 activations during a verbal memory task without sensory input. This finding led Büchel (2003) to suggest the existence of a “reverse hierarchy” in congenital blindness, in which V1 is the highest level of processing (**Figure 5**). Similarly, Bedny et al. (2011) showed that V1 activated more

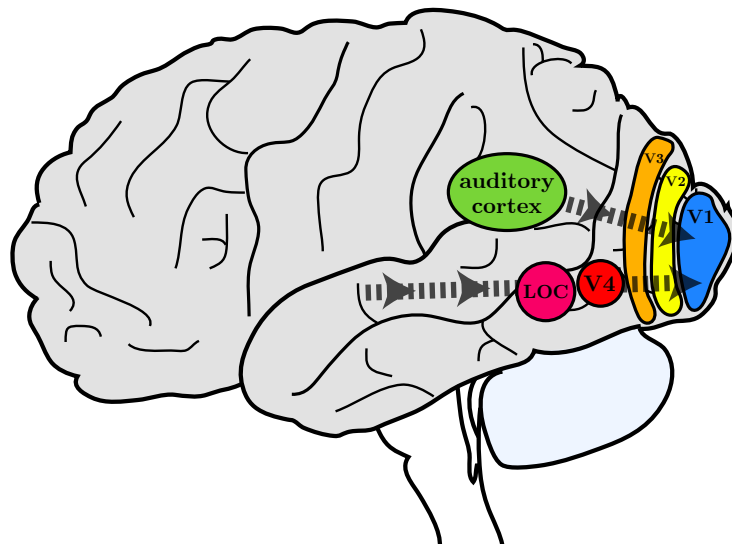


Figure 5: Schematic of the ‘reverse hierarchy’ theory in the blind occipital cortex. In this hypothesis, V1 is at the top of an auditory processing hierarchy, receiving input from auditory cortex and extrastriate ‘visual’ areas.

robustly to language than backwards speech, suggesting it is representing higher level auditory processing. This pattern of response seems unlikely if V1 input were primarily subcortical as in the normal visual system. It should be noted, however, that the hierarchy of processing for Braille in Amedi et al. (2003) was maintained; blind subjects showed greater activation in ‘higher’ visual areas than in V1. Pertinently, studies with anophthalmic cases show the same level of activity to both forward and reversed speech stimuli in V1 but specialisation for language in the lateral occipital complex (LOC), which is indicative of maintained hierarchy (see later; Watkins et al. (2012)). Whether this maintained hierarchy of language processing seen in anophthalmia is unique, and therefore a consequence of the very early disruption, remains to be determined, as does the functional relevance of this additional language processing.

There is some animal evidence to suggest that subcortical cross-modal projections could provide an alternative or perhaps complementary thalamo-cortical route for auditory inputs to the occipital cortex. The dorsal region of the lateral geniculate nucleus (LGN, a major thalamic visual nucleus), responds to auditory stimulation in several animal models of congenital blindness, including the anophthalmic (ZRDCT-an) mouse (Piché et al., 2004; Chabot et al., 2007), bilateral neonatally enucleated hamsters (Izraeli et al., 2002), and naturally blind rodents (Doron and Wollberg, 1994). Projections from the inferior colliculus, a subcortical structure for auditory processing, were found in all of these animals and could provide auditory input to the LGN. However, a direct comparison of anophthalmic and enucleated mice

revealed that this projection was only present in the anophthalmic mice (Chabot et al., 2008), suggesting this cross-modal input may be limited to blindness caused by very early disruption to the visual pathway. From the LGN, the optic radiations could provide auditory input to the primary visual cortex, which also responds to sound in these animals (Bronchti et al., 2002; Izraeli et al., 2002; Chabot et al., 2007). The evidence from human imaging studies for similar subcortical reorganisation is weakened, however, by the finding of reduced LGN volume in anophthalmic subjects (Bridge et al., 2009). While there is currently little information about LGN volume in early blindness, reduced LGN volume has also been found in monocularly enucleated patients (Kelly et al., 2014). Furthermore, studies in anophthalmic (Bridge et al., 2009) and early blind (Noppeney et al., 2005; Shimony et al., 2006; Ptito et al., 2008; Shu et al., 2009) subjects have shown that the organisation and structure of the optic radiations is abnormal compared to sighted subjects. It is assumed that if this pathway were used to convey auditory information to the cortex, it would show similar organisation and structure to the mature visual pathway, either due to maintenance or strengthening of existing connections. Thus, it seems unlikely that subcortical reorganisation involves the dominant thalamo-cortical pathway from LGN to V1.

An alternative ‘visual’ subcortical pathway to convey auditory information could be via the superior colliculus and pulvinar. While the superior colliculus is predominantly visual in sighted subjects, it has multisensory inputs and could redirect auditory information to the occipital cortex via its existing connections with extrastriate regions. The superior colliculus receives

non-visual subcortical inputs in sighted individuals (Meredith and Stein, 1986; Covey et al., 1987; Jiang et al., 1997; King et al., 1998), and it may be that these connections are strengthened by visual deprivation. Electrophysiological studies found that the number of auditory and somatic responding cells in the superior colliculus were increased in visually deprived animals (Vidyasagar, 1978; Rauschecker and Harris, 1983). The superior colliculus has projections to marmoset area V5/MT+ both via the pulvinar nucleus and directly (Warner et al., 2012); this pathway is potentially the basis for the phenomenon of ‘blindsight’ seen in patients with V1 damage (Covey, 2010). There is recent evidence to suggest that V5/MT+ may receive ‘early’ auditory information, particularly in anophthalmic subjects. Anophthalmic cases showed activity to pure tones of multiple frequencies in area V5/MT+ (Watkins et al., 2013); furthermore, this activity was tonotopically organised in three of the five cases studied. Since such a tonotopic organisation is only seen in auditory regions, this suggests processing of early information. It is also the case, however, that early blind populations show activation of V5/MT+ to auditory motion (Poirier et al., 2006; Bedny et al., 2010; Jiang et al., 2014). Such motion responses could also potentially have been received via projections from the superior colliculus and pulvinar (**Figure 6**) but this remains to be tested in early blind subjects. Similarly, there is currently no data to determine whether V5/MT+ responds to motion in addition to pure tones in anophthalmic subjects.

To summarise, evidence supports the existence of both cortico-cortical and thalamo-cortical pathways conveying auditory information to the occipi-

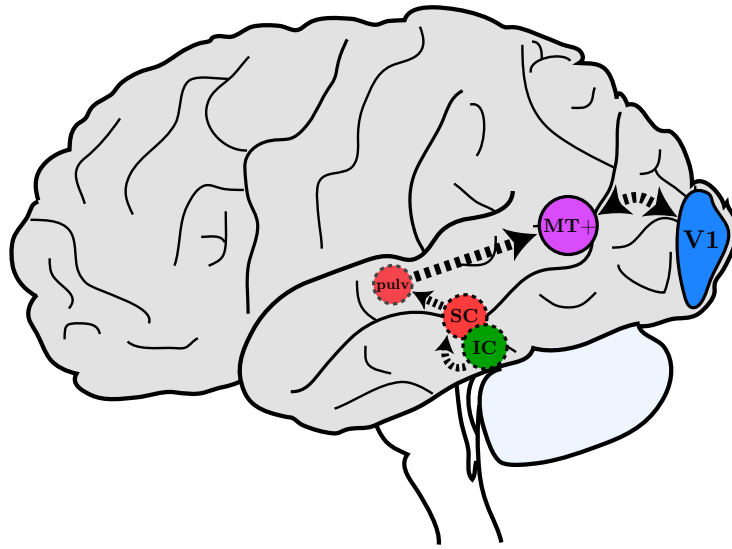


Figure 6: Suggested pathway for subcortical auditory inputs to the occipital cortex; auditory information from the inferior colliculus (IC) could project to the superior colliculus (SC) and then via the pulvinar to area V5/MT+.

tal cortex and, realistically, it is likely that a combination of such inputs is present particularly in anophthalmic, congenitally and early blind individuals. In late blind individuals or blindfolded healthy adults, it is difficult to imagine a recoding of subcortical structures to convey auditory information, and any auditory responses are likely to be along existing supra-modal connections that are unmasked by short as well as longer periods of visual deprivation.

1.7 Are auditory occipital responses functionally organised?

Once auditory information has reached the occipital cortex, precisely how these auditory responses are organised has become an important question in the current literature because it can determine whether functional spe-

cialisation in the cerebral cortex relies on specific sensory input. The visual system has a number of distinct functional modules that can be identified and respond to stimulus attributes such as faces, objects, colour or motion. Whether this modularity is specific to the visual modality or is a result of the occipital cortex organisation remains to be determined. One of the ways to test this modular theory is to investigate whether the dorsal and ventral streams are maintained in the absence of visual input. The dual stream hypothesis describes a ‘where’ pathway, in which dorsal occipital regions are dedicated to processing spatial information and global motion, and a ‘what’ pathway, in which ventral occipital regions are involved in stimulus identity processing such as object recognition (Ungerleider and Mishkin, 1982).

The maintained functional dissociation between dorsal and ventral regions in the absence of visual input has been demonstrated in several studies. Two studies investigating spatial and non-spatial pitch processing in early and congenitally blind individuals found a preference for spatial processing in the middle occipital gyrus (MOG), a dorsal occipital region (Renier et al., 2010; Collignon et al., 2011); this same region responded in sighted subjects during the visual equivalent of the spatial task (Renier et al., 2010). However, the ability of occipital subdivisions to be recruited for a similar function but with non-visual inputs may be limited by age of blindness onset; whilst congenital and late blind individuals showed occipital activation to sounds in general, only the congenital group showed a preference for spatial sounds in the right MOG (Collignon et al., 2013). The human motion area V5/MT+, also part of the dorsal visual stream, responds to auditory motion in early and

congenitally blind people as discussed earlier (Poirier et al., 2006; Saenz et al., 2008; Jiang et al., 2014). However, responses to auditory motion have also been found across the lateral occipital complex (Alink et al., 2012) as well as in both dorsal and ventral regions in early and late blind individuals (Lewald, 2013), suggesting that auditory motion processing may not be restricted to area V5/MT+ specifically.

It may be that some regions are perhaps more receptive to recruitment by other senses. The lateral occipital complex (LOC) in sighted people is a ventral visual area involved in the processing of objects (Grill-Spector et al., 2001); in both sighted and blind individuals, LOC has been shown to also respond to tactile objects (Amedi et al., 2007; Ptito et al., 2012) and auditory stimuli via a visual-to-auditory sensory substitution device (Kim and Zatorre, 2011). However, LOC may also have a higher-level role in congenital blindness; in congenitally blind (Bedny et al., 2011, 2012) and anophthalmic subjects (Watkins et al., 2012), LOC responds more to linguistic stimuli than to speech played backwards. In all cases, the activation was left-lateralised. Furthermore, this activation specific to LOC was not present in late blind individuals (Bedny et al., 2012). The dissociation between the tonotopic responses in area V5/MT+ and language in LOC suggests dorsal/ventral differences in anophthalmia as well as other causes of congenital blindness.

Very few of the other specialised areas in the occipital cortex have been characterised (particularly in the ventral stream), and it remains to be seen whether any further modules can be determined. Moreover, while this introductory chapter has concentrated on auditory function in the occipital

cortex, it may be that there is also some specialisation for tactile function (Ptito et al., 2012).

The role of V1 adds an interesting complication for the modular theory. According to its role in sighted individuals, the modular theory would expect this region to respond to all sounds in blind individuals. However, as previously discussed, the primary visual cortex in congenitally blind individuals is involved in a left lateralised language network and responds preferentially to words as opposed to non-words (Röder et al., 2002; Bedny et al., 2011, 2012). In the case of extreme blindness (anophthalmia), the pericalcarine region (V1) does not show this language preference and instead shows extensive activation to all sounds. This difference in the role of V1 could relate to different pathways for cross-modal inputs to the region. In anophthalmia, thalamo-cortical auditory connections (as suggested by the mouse model) could preserve the role of V1 for lower-level tasks. Cortico-cortical connections in congenital and early blindness would reverse the hierarchy of the occipital cortex (see **Figure 5**) and result in a higher-level function for V1.

1.8 Thesis scope

Based on the current literature, there appears to be a spectrum corresponding to age of blindness onset; the most extensive changes take place in the more extreme cases of congenital blindness, whilst the less extensive changes take place in late-onset blindness and perhaps even in sighted individuals after a short period of visual deprivation. The idea of a ‘sensitive period’ could be

relevant here; whilst late blind and sighted individuals can show some cross-modal plasticity, this is sometimes less extensive and perhaps less functionally relevant compared to congenitally and early blind groups. Age of blindness onset may also be important in determining whether auditory information is conveyed to the occipital cortex via cortical or subcortical pathways.

However, there are four questions that remain unresolved and therefore prevent a greater understanding the role of visual deprivation in cross-modal plasticity. The first question is how much reorganisation takes place in subcortical structures in blind individuals, and whether this is limited to the most extreme cause of blindness (congenital bilateral anophthalmia). This is important to answer because it may be that the absence of both endogenous (pre-natal) and exogenous (post-natal) visual experience is optimal for maximum plasticity. Most of the literature investigates occipital cortex plasticity in congenital and early blind individuals because it assumes no or little subcortical changes. If there is subcortical reorganisation in anophthalmia, as suggested in the animal literature, this could indicate that there is subcortical auditory input to occipital cortex.

The second question is whether the origin of cross-modal input to the occipital cortex determines how auditory information is processed in the occipital cortex, because differences in the origin of the input (subcortical or cortical) could explain whether the traditional hierarchy of the occipital cortex is maintained or reversed. This thesis hypothesises that hierarchical processing is preserved in anophthalmia because of maintained subcortico-cortical inputs to the occipital cortex, in contrast to reversed hierarchical

processing in congenital/early blindness driven by cortico-cortical inputs.

The third question relates to other changes that may have taken place in blind individuals and could explain the underlying mechanisms for reorganisation. Neurochemical, anatomical and behavioural changes in anophthalmia would provide important information about how the absence of pre-natal and post-natal visual experience results in reorganisation of the ‘visual’ pathway for audition. Answering this question is important because such changes may reflect altered development and maturation of the brain.

The fourth question relates to the other end of the ‘blind’ spectrum, and whether cross-modal changes can occur in sighted adults after a short period of visual deprivation. This is important because it would show that the adult brain can adapt to changes in sensory input, and that compensation for the lack of vision is not restricted to long periods of blindness.

Answering these four questions will be important when developing new sight restoration techniques. Current technologies primarily address retinal function and assume a normal early visual pathway. Sight restoration techniques may not be successful if these areas have reorganised extensively, as suggested by the history of cochlear implants. It may be that once the ‘visual’ pathway has reorganised for auditory processing, cross-modal changes are irreversible and these regions will be unable to process visual information. Studies with cochlear implants have shown that implants need to be in place before a critical age in order to allow for normal language acquisition (Voss 2013). Therefore, this thesis aims to quantify the effects of visual depriva-

tion on the 'visual' pathway. This will provide a clearer understanding of the time-scale and changes that occur, and allow clear assessment of target location and ages for future sight restoration procedures.

This thesis will address these four questions in the following way:

1. Firstly, this thesis asks whether cross-modal responses in anophthalmia are restricted to the cortical level, or whether they are also found subcortically, as suggested by the animal model of anophthalmia. Subcortical responses to sound will be compared to early blind individuals in order to investigate whether these changes are unique to anophthalmia (Chapters 3 and 4).

2. Altered occipital neurochemistry, changes in occipital neuroanatomy and improved auditory abilities have all been found in early and congenital blindness compared to sighted subjects. This thesis will address how these reported measures compare in anophthalmia (Chapters 5 and 6).

3. Thirdly, this thesis will look at how cross-modal responses are organised within the occipital cortex. Specifically, how auditory-evoked responses in this region in anophthalmia compare to other blind populations, and whether they mirror the hierarchy of the sighted occipital cortex. This question will be evaluated using fMRI by determining whether auditory-evoked responses to low-level and high-level stimuli are functionally organised in the anophthalmic occipital cortex (Chapter 7).

4. Finally, this thesis will address whether a short period of visual

deprivation can unmask similar changes in healthy sighted adults, either with improved auditory abilities or with increased cross-modal inputs to the occipital cortex (Chapter 8).

2 General Methods

This chapter will give an overview of the participants with congenital bilateral anophthalmia and the magnetic resonance imaging (MRI) methods used in this thesis.

2.1 Anophthalmic participants

Five individuals with congenital bilateral anophthalmia were recruited for this thesis (mean age 29 years, range 23-36, two females). **Table 1** provides a full account of participant age (at the start of data collection), gender, and basic clinical description. All had participated in at least one previous imaging study (Bridge et al., 2009; Watkins et al., 2012, 2013) and are referred to as cases 1, 2, 4, 5 and 6. The data presented in this thesis were acquired 4 to 7 years after the first study. Case 3 from that study was not scanned again. All anophthalmic participants except Case 1 read Braille and have no neurological history beyond the cause of their blindness.

Previous reports using structural MRI describe an absence of eyes in all of these participants, although presence of rudimentary eye-like structures

Table 1: Brief description of anophthalmic cases

Subject	Gender	Age	Clinical description
Case 1	M	33	Bilateral anophthalmia associated with OTX2 mutation, mother carrier, delayed speech and motor development.
Case 2	F	36	Isolated bilateral anophthalmia. No family history.
Case 4	F	23	Isolated bilateral anophthalmia, right orbital cyst. No family history.
Case 5	M	27	Isolated bilateral anophthalmia. No family history.
Case 6	M	28	Isolated bilateral anophthalmia. No family history.

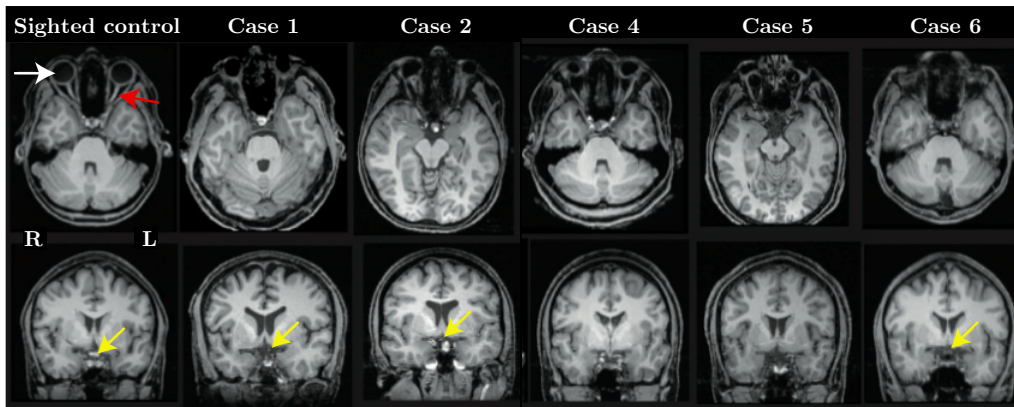


Figure 7: Figure adapted from Bridge et al. (2009). The red arrow shows a normal optic nerve, the white arrow shows a normal eye, and the yellow arrow shows the hypoplastic optic nerve in three anophthalmic cases.

were found in some cases (Bridge et al., 2009, 2012). In some cases, the optic nerve is hypoplastic but visible whilst in others it is absent (Bridge et al., 2009). **Figure 7** (adapted from Bridge et al. (2009)) shows the T1-weighted anatomical scans from one sighted control and the five anophthalmic cases included in this thesis. The top row of the figure shows a normal optic nerve (red arrow) and eye (white arrow) in the sighted control, but an absence of eyes in all anophthalmic cases. The bottom row shows a thin optic nerve (yellow arrow) visible in only three of the five anophthalmic cases. The oculomotor nerve is present in all cases and comparable in measurement to sighted controls (Bridge et al., 2012). The anophthalmic occipital cortex appears structurally normal without any notable abnormalities.

2.2 Magnetic resonance imaging (MRI)

MRI generates images of brain tissue by exposing the brain to a strong magnetic field (expressed in units of Tesla). Protons in a magnetic field will oscillate at a certain frequency depending on the strength of the field (resonance); in an MRI scanner, they will oscillate along the main magnetic field of the scanner (B_0). If these protons are then exposed to a second magnetic field at a specific frequency (a radiofrequency pulse emitted by the scanner), they will absorb the electromagnetic energy of this pulse (excitation). After absorbing this energy, protons will release it and return to their normal state of equilibrium, thus realigning to the main magnetic field B_0 (relaxation). This release or transmission of energy is the measured MRI signal. The amount

of time needed for protons to return to equilibrium varies according to brain tissue; differences in relaxation times can therefore be used to build images showing contrasts between grey matter, white matter, and cerebrospinal fluid (CSF).

MRI data presented in this thesis were acquired from 3 Tesla (3T) whole body MRI scanners. University of Oxford data in Chapters 3, 4 and 5 were acquired from a Siemens 3T Verio at the Functional MRI of the Brain (FMRIB) Centre. University of Washington data in Chapters 3 and 4 were acquired from a Phillips 3T MRI scanner at the Diagnostic Imaging Sciences Center (DISC). Finally, data in Chapters 7 and 8 were acquired from a Siemens 3T Trio at the University of Oxford Centre for Clinical Magnetic Resonance Research (OCMR, University of Oxford).

At all sites, T1-weighted MPRAGE structural images (1 mm isotropic) were acquired for registration purposes. In addition, these structural images were also processed in FreeSurfer using recon-all, the software's automated reconstruction tool (<http://surfer.nmr.mgh.harvard.edu/>). This produces grey matter, white matter and CSF segmentations within a standardised space. These segmentations were used to calculate cortical thickness within defined regions of interest.

2.3 Functional MRI

BOLD functional magnetic resonance imaging (fMRI) can be used to infer changes in brain activity over time in response to external stimulation. The basis of fMRI is the BOLD (blood-oxygenation-level dependent) signal, which relates to the amount of deoxygenated haemoglobin detected in an MRI image. Deoxygenated haemoglobin, or haemoglobin without attached oxygen, is attracted to magnetic fields. BOLD fMRI therefore measures the difference in signal on a T2*-weighted image according to the amount of detected deoxygenated haemoglobin. Changes in BOLD signal over time are indirect measures of neural activity as they assume that changes in blood volume and deoxygenated haemoglobin indicate brain activity. In this thesis, fMRI was used to investigate cortical and subcortical responses to a variety of auditory stimuli in sighted and visually deprived individuals.

2.3.1 Sequences

Echo-planar imaging (EPI) pulse sequences were used to acquire all fMRI data. EPI is a fast imaging sequence that can acquire a full volume (three dimensional image of the brain) every few seconds. Slices were positioned for maximal whole brain coverage (including the cerebellum), although superior portions of the parietal lobe were sometimes omitted due to head size. Sequence details can be found within the Methods section of each fMRI chapter.

In Chapter 3 and 4, fMRI was used to investigate subcortical responses to sounds using sparse or “silent” imaging. Sparse sampling is commonly used in auditory fMRI; to ensure minimal interference of acoustic scanner noise in the measured BOLD signal, volumes are acquired every 8-10 seconds. Due to haemodynamic delay in the BOLD signal (approximately 4 to 5 seconds for peak response in the auditory cortex), sparse sampling ensures that each acquired volume measures peak BOLD signal to the auditory stimuli with minimal interference from the haemodynamic response caused by the sound of the scanner (see **Figure 8**). The result is improved signal-to-noise for each individual volume (Hall et al., 1999).

In Chapters 7 and 8, fMRI was used to investigate cortical responses during an auditory localisation task and a language task. Continuous sampling was used for both tasks (volume acquisition every 3 seconds). Although this meant sacrificing the acoustic benefits of sparse sampling, it allowed for acquisition of a larger amount of data.

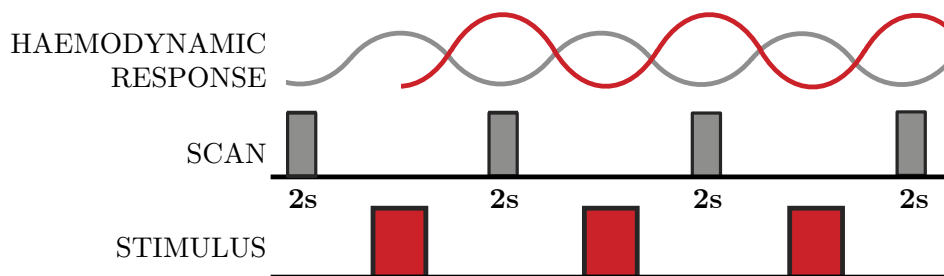


Figure 8: Schematic of a sparse sampling imaging protocol. Each volume samples the peak haemodynamic response to the auditory stimuli (red line) with minimal contribution from the haemodynamic response to scanner sounds (grey line).

2.3.2 Analysis

Statistical modelling of fMRI data was performed using the general linear model (GLM). Each voxel in the brain has a recorded timeseries, or BOLD signal over time. The GLM correlates these timeseries with the experimental design (a model of when stimulus presentation starts and stops) in order to identify voxels in the brain that are statistically related to, or more ‘active’ during, the stimulus presentation blocks than the rest blocks. The output is a series of statistical maps showing the statistical significance of each voxel in the brain to the stimuli. In order to match activity with anatomy, these maps can be overlaid on the subject’s own structural image or a ‘standard’ brain for a group analysis.

FMRI data was processed using FEAT (FMRI expert analysis tool) Version 6.00, part of FSL (FMRIB’s Software Library, www.fmrib.ox.ac.uk/fsl). Unless otherwise stated, standard space refers to normalisation of MRI data to Montreal Neurological Institute (MNI) space with 2 mm isotropic voxels. In Chapter 4, fMRI data was processed using SPM8 (Statistical Parametric Mapping, <http://www.fil.ion.ucl.ac.uk/spm/>). Detailed explanations of analysis protocols can be found within the Methods section of each fMRI chapter.

2.4 MR Spectroscopy

The chemical composition of human brain tissue within a selected region of interest can be measured in an MRI scanner using *in-vivo* ^1H magnetic resonance spectroscopy (MRS). MRS measures the radiofrequency signal emitted by hydrogen protons (^1H) spinning within different substances, or neurochemicals. The signals from protons in these different neurochemicals have their own unique frequency. This is because protons in certain substances differ in frequency (parts per million) from other substances; for example, protons in NAA (N-acetyl aspartate) and water differ by two parts per million (ppm), or approximately 250Hz in a 3T scanner. In MRS, proton signals are separated according to these differences in frequency, or chemical shift. The output is a spectrum of signal intensity (y-axis) vs. chemical shift (x-axis, in ppm) (see example spectra in **Figure 9**). The different peaks along this

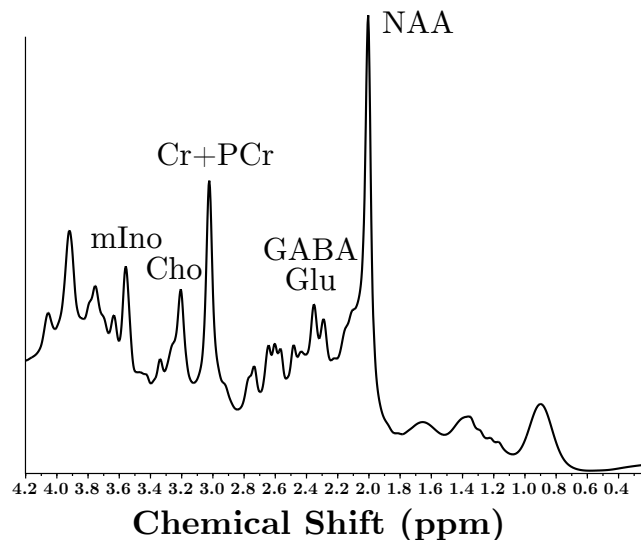


Figure 9: Example MRS spectra, with the main peaks identified for neurotransmitters myo-Inositol (mIno), choline (Cho), creatine and phosphocreatine (Cr+PCr), GABA, glutamate (Glu), and N-acetyl aspartate (NAA).

spectrum represent the different neurochemicals, and each neurochemical has one or more peaks. The total area under the peaks of each neurochemical is proportional to its concentration within the sampled brain tissue.

2.4.1 Sequences

MRS is performed in a defined region of interest, or voxel. Prior to data acquisition, shimming of the magnetic field is needed to correct for magnetic field inhomogeneity. Next, water signal must be suppressed; without this suppression, water content in the region of interest would mask signals from neurochemical protons at a ratio of approximately 10,000:1. Single voxel MRS can then be performed by exciting signals in the selected region of interest, using specifically designed acquisition sequences. As MRS is very susceptible to changes in magnetic field homogeneity within this region, acquisition time is short (approximately 5 minutes for a 2 x 2 x 2 cm voxel).

Traditionally, the two major MRS sequences are STEAM (stimulated-echo acquisition mode) and PRESS (point resolved spectroscopy). STEAM can acquire data using a short echo time (TE). Echo times shorter than 20 ms help to optimise the signal to noise ratio (SNR); reduced signal decay means neurochemical concentrations can be precisely quantified (Mekle et al., 2009). Furthermore, short echo times allow identification of neurochemicals beyond the three main resonances (NAA, creatine and choline) that may not be visible at longer echo times. Longer echo times lose information about certain neurochemicals and lipids that are thought to be important in clinical

MRS for detecting tumours (Kanowski et al., 2004). However, STEAM suffers considerable signal loss; the alternative, PRESS, uses a longer echo time and can acquire full signal intensity.

Data acquired for Chapter 5 used a SPECIAL sequence (SPin ECho full Intensity Acquired Localised spectroscopy). The SPECIAL sequence is designed to combine the benefits of both STEAM and PRESS; it takes advantage of the benefits of a short echo-time (like STEAM) but acquires signal from a full magnetisation (like PRESS) and therefore does not succumb to the signal loss usually found with other short echo-time sequences (Mekle et al., 2009).

2.4.2 Analysis

MRS data analysis was performed using an in-house implementation of LCmodel (Provencher, 1993). Using a “black box” approach to minimise user subjectivity, LCmodel fits the spectrum acquired by MRS to a ‘basis set’, or set of *in-vitro* spectra acquired under identical conditions. The identical protocol conditions between the MRS and *in-vitro* spectra mean that any methodological complications are accounted for. Compared to *in-vitro* measures, LCmodel produces good concentration estimates of a wide range of major and minor neurochemicals, and is robust to noise and baseline distortion.

PART I :

**FUNCTIONAL NEUROIMAGING OF
SUBCORTICAL STRUCTURES**

3 Subcortical functional reorganisation in anophthalmia and early blindness

3.1 Summary

The lack of visual input early in life results in occipital cortical responses to non-visual stimuli. However, it remains unclear whether this cross-modal plasticity also occurs in subcortical pathways. Using functional magnetic resonance imaging, auditory responses were compared between individuals with congenital anophthalmia (absence of eyes), those with early onset blindness (in the first few years of life) and normally sighted individuals. This chapter found that the superior colliculus, a ‘visual’ subcortical structure, was recruited by the auditory system in anophthalmia and early-onset blindness. Additionally, auditory subcortical responses to monaural stimuli were altered as a result of blindness. Specifically, responses in the medial geniculate nucleus were equally strong to contralateral and ipsilateral stimulation in both groups of blind subjects, whereas sighted controls showed stronger responses to contralateral stimulation. These findings suggest that early blindness results in substantial reorganisation of subcortical auditory responses.

3.2 Introduction

It is well established that the loss of a sense early in life results in brain areas normally associated with it being recruited for processing of the remaining senses (Bavelier and Neville, 2002; Merabet and Pascual-Leone, 2010). As discussed in Chapter 1, the occipital cortex of blind individuals responds during basic auditory tasks such as sound localisation (Gougoux et al., 2005; Lessard et al., 1998; Weeks et al., 2000), auditory motion (Bedny et al., 2010; Lewis et al., 2010; Poirier et al., 2006), and detecting changes in sounds (Kujala et al., 2005), as well as during more complex linguistic-based tasks requiring semantic processing and verbal memory (Amedi et al., 2003; Burton et al., 2002a,b; Röder et al., 2002).

In contrast, little is known about subcortical changes after visual deprivation. Although animal models suggest that substantial rewiring of subcortical connections can occur in response to developmental disruption of sensory pathways (Frost, 1981; Sur et al., 1988), few studies have addressed whether blindness leads to changes in the functional properties of subcortical pathways in humans. Previous imaging studies of blindness have not described differential activation of subcortical nuclei. Dynamic causal modeling of fMRI data obtained in congenitally blind humans during an auditory discrimination task did not indicate increased thalamo-cortical connectivity between the medial geniculate nucleus (MGN) and primary visual cortex (V1) (Klinge et al., 2010).

However, one possible reason that differences in subcortical responses

between blind and sighted individuals have not yet been observed is because it is relatively difficult to evoke activity in these small structures using functional MRI. The MGN serves as a “gateway” between subcortical auditory structures and the auditory cortex (Jones, 2003) and has a volume of approximately 90 mm^3 in humans (Winer, 1984). This small structure may be difficult to localise at the individual level using functional MRI, especially considering the pulsatile motion effects near the brainstem. However, the neighbouring lateral geniculate nucleus (LGN) has been extensively imaged (Chen et al., 1999; Schneider et al., 2004), therefore these confounds alone seem unlikely to prevent accurate imaging of this region. Alternatively, it may be that the traditional auditory stimuli of simple tones, noises and dynamic spectral ripples are not suited to eliciting robust responses in the MGN, especially considering the loud acoustics of the scanner. In non-human primates, neurons within the three subdivisions of the MGN (ventral, dorsal, and medial) have been shown to respond to a range of natural and artificial sounds with varying spectral and temporal features (Symmes et al., 1980; Alon and Yeshurun, 1985; Bartlett and Wang, 2011). In particular, the MGN appears to respond well to complex and speech-like stimuli with low predictability (von Kriegstein et al., 2008; Diaz et al., 2012). This chapter uses an auditory stimulus specifically designed to elicit robust auditory responses in the auditory thalamus/MGN (Jiang et al., 2013). The stimulus consists of speech and non-speech music scrambled into short segments; these segments ensure low predictability whilst sampling various spectro-temporally complex features found in speech. This stimulus has been shown to elicit stronger responses at an individual level compared to traditional auditory stimuli like

dynamic rippled (temporally and spectrally modulated) noise (Jiang et al., 2013). In addition, this ecologically valid stimulus is perhaps better suited to maintaining participant attention.

Another possibility is that subcortical functional reorganisation may be limited to anophthalmic individuals, whereas previous studies have focussed on mixed populations of blind subjects that have primarily consisted of individuals who became blind post-natally (i.e. early blind). Bilateral anophthalmia is an extreme example of visual deprivation; because both eyes fail to develop, the visual system never receives stimulation from the eyes. In the (ZRDCT-an) anophthalmic mouse, auditory stimulation elicited activity in the dorsal LGN and occipital cortex (Chabot et al., 2007; Piché et al., 2004) that was not observed in neonatally enucleated or sighted mice (Tucker et al., 2001).

In this chapter, subcortical auditory responses to both binaural and monaural stimulation were measured in individuals with anophthalmia as well as early blind subjects and sighted controls. It was hypothesised that subcortical 'visual' structures would be recruited for auditory processing in anophthalmia but not early blindness, as shown in the animal models of the two conditions. However, this chapter found evidence for subcortical reorganisation in both blind groups. The results in this chapter suggest that the lack of visual input early in life changes functional response properties of both the auditory and the 'visual' subcortical pathways.

3.3 Methods

3.3.1 Participants

Due to subject availability, the data used in this chapter were obtained using the same paradigm, but at two separate sites. To control for site differences, each group of blind people was compared to a group of sighted controls scanned at the same site.

University of Oxford The five bilateral anophthalmic subjects described in Chapter 2 participated in this imaging study (mean age 29 years, range 23-35, two females, for case descriptions see **Table 1** in Chapter 2). Ten age-matched controls with normal or corrected-to-normal vision were also recruited (mean age 26 years, range 23-37, seven females). This study was granted ethical approval by the Oxford University Central Ethical Committee and all subjects gave informed written consent prior to participation.

University of Washington Seven early blind subjects were recruited (mean age 51 years, range 31-63, three females). All subjects were blind at birth or within the first 5 years of life, and were left with no or very low light perception (see **Table 2**). Eight controls with normal or corrected-to-normal vision were also scanned at the same site (mean age 30 years, range 23-39, five females). All subjects gave written and informed consent prior to the experiment, following procedures approved by the University of Washington.

Table 2: Brief description of early blind cases. All early blind participants were scanned at the University of Washington (UW).

Subject	Gender	Age	Clinical description
EB 1	F	63	Ruptured right eye at 2 months, detached retina at 5 years; no residual light perception.
EB 2	F	59	Optic nerve virus infection at 1.5 years; low residual light perception.
EB 3	M	46	Congenital blindness caused by congenital glaucoma; low residual light perception
EB 4	M	60	Congenital blindness caused by retinopathy of prematurity; no residual light perception.
EB 5	F	61	Congenital blindness caused by cataracts; low residual light perception and colour in right eye.
EB 6	M	31	Congenital blindness caused by Leber’s congenital amaurosis; no residual light perception.
EB 7	M	39	Congenital blindness caused by congenital glaucoma; low residual light perception in right eye.

3.3.2 MR imaging acquisition

University of Oxford Images were acquired using a Siemens Verio 3-Tesla whole body MRI scanner and a 32-channel coil at the Functional Magnetic Resonance Imaging of the Brain Centre (University of Oxford). Structural images were acquired at 1-mm isotropic resolution using a T1-weighted MPRAGE sequence ($TR=2040$ ms, $TE=4.7$ ms, flip angle= 8° , 192

transverse slices, 1 mm isotropic voxels). A total of six functional runs were acquired using a sparse echo-planar imaging pulse sequence (TR=10 s, TA=2 s, TE=30 ms, flip angle=90°, 36 transverse slices, 3 mm isotropic voxels). Transverse slices were positioned to cover most of the brain (cerebellum, temporal and occipital lobes) although depending on head size, superior portions of the parietal lobe were sometimes omitted.

University of Washington Images were acquired using a Philips 3-Tesla whole body MRI scanner and an 8-channel coil at the University of Washington Diagnostic Imaging Sciences Center (DISC). Structural images were acquired at 1-mm isotropic resolution using a T1-weighted MPRAGE sequence (TR=2200 ms, TE=3.55 ms, flip angle=8°, 160 sagittal slices, 1 mm isotropic voxels). The six functional runs were acquired using a sparse echo-planer imaging pulse sequence (TR=10 s, TA=1.4 s, TE=16.5 ms, flip angle=76°, 32 transverse slices, 2.75 x 2.75 x 3 mm voxels). Again, slices covered as much of the brain as possible, but in some subjects superior portions of the parietal lobe were not scanned.

3.3.3 Auditory stimuli

Auditory stimuli were presented to participants via MRI-compatible ear-phones (Model S14, Sensimetrics) and sound levels adjusted to a comfortable listening level. Sighted controls were scanned in darkness with eyes closed. The stimuli consisted of scrambled musical segments presented binaurally (binaural), to the right ear (monaural right), or to the left ear (monaural

left). The intensity in the binaural condition was scaled by -6 dB in each ear relative to the monaural case to equate the total sound amplitude across monaural and binaural conditions. Equating the amplitude in this way reduces differences in loudness across conditions, but unfortunately did not allow measurement of binaural interactions.

In each 10 second trial, the scrambled segments were presented for 8 seconds followed by 2 seconds of silence to allow for MR volume acquisition. A fourth condition was also included, during which trials with no music were presented for 8 seconds (silence) followed by 2 seconds of MR volume acquisition (**Figure 10**). One advantage of this ‘sparse sampling’ method is that it minimises masking of the auditory stimulus by acoustic scanner noise. A second advantage is that, because of the haemodynamic delay in the BOLD signal (which is approximately 4-5 seconds to peak response in A1), each volume acquisition measures the BOLD response to auditory stimuli with minimal contribution of scanner acoustic noise to the BOLD response. As a

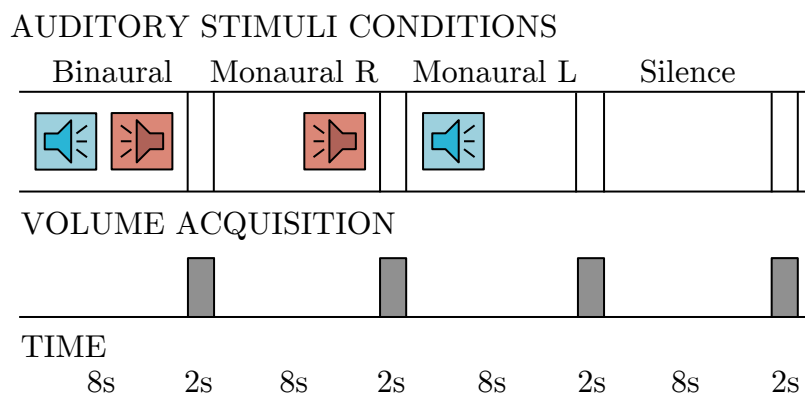


Figure 10: Auditory stimulation using sparse sampling to minimise scanner acoustical noise: 8 seconds auditory stimulus (binaural, monaural right, monaural left, silence) followed by 2 seconds for volume acquisitions.

result of reduced magnetic saturation, the signal-to-noise for each individual volume is higher than during continuous acquisition (Hall et al., 1999).

The presentation order of conditions was fixed for all subjects (binaural, monaural right, monaural left, silence). A total of 32 trials were presented in each of the 6 scans (each scan lasted approximately 6 minutes). The scrambled musical segments (1 second each) were extracted using MATLAB (Mathworks, MA) from three songs: God shuffled his feet (Crash Test Dummies), Will o' the wisp (Miles Davis), and Saeta (Miles Davis). The first song containing lyrics and the second two were music only. Each run contained scrambled segments from only one of the three songs. The order of songs was fixed for all participants: scans one and four sampled segments from the first song, scans two and five the second song, and scans three and six the third song.

3.3.4 Attentional task

During all music conditions, a 1 second musical segment was sometimes repeated consecutively. Participants were required to respond whenever this occurred (1-back task) and responses were recorded on a MRI-compatible response box. The task was only used to maintain participant attention.

3.3.5 MR imaging analysis

MR imaging analysis Functional MRI data processing was performed using FEAT (fMRI Expert Analysis Tool) Version 6.00, part of FSL (FMRIB's

Software Library, www.fmrib.ox.ac.uk/fsl). Pre-processing of functional images included motion correction using MCFLIRT (Jenkinson et al., 2002), non-brain removal using BET (Smith, 2002) and highpass temporal filtering (50s) to remove low-frequency fluctuations. No spatial smoothing was applied in order to prevent distortion in the small thalamic regions of interest. Time series statistical analysis was performed using a general linear model. The design matrix had 3 separate explanatory variables (EVs), one for each auditory stimulation condition (binaural, right-ear and left-ear stimulation). Haemodynamic response function (HRF) convolution was not applied; each condition was modelled separately as a boxcar function because of the long TR (10s), which meant there was only one estimate of the BOLD response for each stimulus presentation. Furthermore, in sparse sampling each estimate is taken at BOLD response peak and data from the rest of the HRF curve is not acquired, therefore convolution was not deemed necessary (Watkins et al., 2013). The limitation of this approach is that without HRF convolution and its first derivative, model error is not optimally accounted for.

Functional images were initially registered to each participant's T1-weighted structural image (BBR) for subject-specific analysis, and then registered to T1-weighted MNI-152 (Montreal Neurological Institute) 2 mm standard space using non-linear registration (FNIRT) for group analyses. Higher-level analyses were performed using fixed-effects analysis for an average of each participant's six runs and mixed-effects for group comparison. For whole-brain inspection, statistical maps showing BOLD activity during any of the three music conditions (binaural, monaural right and monaural

left) relative to baseline were thresholded at $z > 2.5$ (Gaussianised T/F) and projected onto either native T1-weighted 1 mm space (for single subject analyses) or MNI 2 mm standard space (for group analyses).

Region of interest (ROI) analysis To minimise distortion in the mid-brain region, all region of interest analyses were performed in subject space. This is because registration and warping images to MNI standard space seemed to affect correct alignment of subcortical functional activity to the anatomy; this was especially notable in the region of the inferior colliculus.

ROIs of the primary visual (V1) and auditory (A1) cortices were derived from the Juelich histological atlas as implemented in FSL with `fslview` (version 3.2.0). A1 was the combination of TE1.0, TE1.1 and TE1.2 (Morosan et al., 2001). Both of these probabilistic definitions were thresholded at 30%. Anatomical definitions of the lateral and medial geniculate nuclei were also derived from Juelich histological atlas, with the probabilistic maps thresholded at 15%.

Due to variability between participants and hemispheres (Rademacher et al., 2002), the auditory thalamus was defined for each participant in their native space based on BOLD activation to any of the three auditory conditions (binaural, monaural right, monaural left). The activation was in the expected location of the MGN (Juelich Histological Atlas, part of FSL), and was defined separately for the left and right sides by increasing statistical thresholds until reaching a volume of approximately 100 mm^3 , which is the approximate size of the MGN (Winer, 1984).

The inferior colliculus was not reliably activated in each subject and therefore individual functional masks could not be made. Instead, the superior and inferior colliculi were both defined anatomically based on each subject's tectum on their T1-weighted 1 mm structural scan. The tectum was divided into superior and inferior regions, and then divided at the midline into right and left regions of interest.

To determine the magnitude of activation evoked by the auditory stimulus, % blood oxygenation-level dependent (BOLD) signal change was extracted from these cortical and subcortical ROIs. Percentage BOLD signal change during each of the three auditory conditions relative to the silent baseline was calculated using Featquery (part of FSL), and statistical analyses were performed using SPSS (IBM, SPSS Version 20 for Mac). Repeated-measures ANOVAs and two-tailed Student t-tests (independent- and paired-samples) were performed to investigate differences in % BOLD signal change during the three auditory conditions (binaural, monaural contralateral and monaural ipsilateral) relative to baseline. A 4-way repeated-measures ANOVA was performed for each ROI separately. It included two between-group variables (group: sighted or blind; and scan site: Oxford or Seattle) and two within-subject variables (auditory conditions and hemisphere). Each ROI was treated separately and therefore corrections for multiple comparisons were not performed. Results were considered statistically significant at $p < 0.05$. Homogeneity of variance was assessed using Mauchly's test of sphericity; if significant, the Greenhouse-Geisser correction and adjusted degrees of freedom were reported.

3.4 Results

Firstly, whole brain responses to the auditory stimuli are shown for the blind and sighted subject groups. This is followed by ROI analyses of visual subcortical (superior colliculus and lateral geniculate nucleus) and auditory subcortical (auditory thalamus and inferior colliculus) structures. Finally, cortical responses within A1 and V1 are reported.

3.4.1 Whole brain responses to sound in blind and sighted subjects

The auditory stimuli activated auditory structures in both sighted and blind subjects. Two subjects (one sighted and one early blind) did not show significant activation in the auditory thalamus and were excluded from all further analyses. **Figure 11** shows examples of the responses in single subjects to all auditory stimulation conditions (binaural, monaural right and monaural left). The two sighted subjects (C: Oxford control; D; UW control) showed extensive, highly significant activation in the auditory cortex, auditory thalamus and inferior colliculus (IC). In the example anophthalmic (A) and early blind (B) subjects, there is additional, significant activation in the occipital cortex, including both pericalcarine and extrastriate regions.

Group activity maps revealed a pattern very similar to the example subjects described above. **Figure 12** shows the activation from a mixed-effects analysis performed separately for each group (A: anophthalmic; B:

early blind; C: Oxford controls; D: UW controls). These group statistical maps show clear activation in the auditory cortex, thalamus and colliculi across all subject groups. As predicted from previous studies, anophthalmic and early blind groups show additional occipital activation. This difference is highlighted later, in the contrast of blind>sighted (**Figure 13**) and the ROI analysis of the 'primary visual cortex' (defined using the Juelich probabilistic atlas, see **Figure 18**).

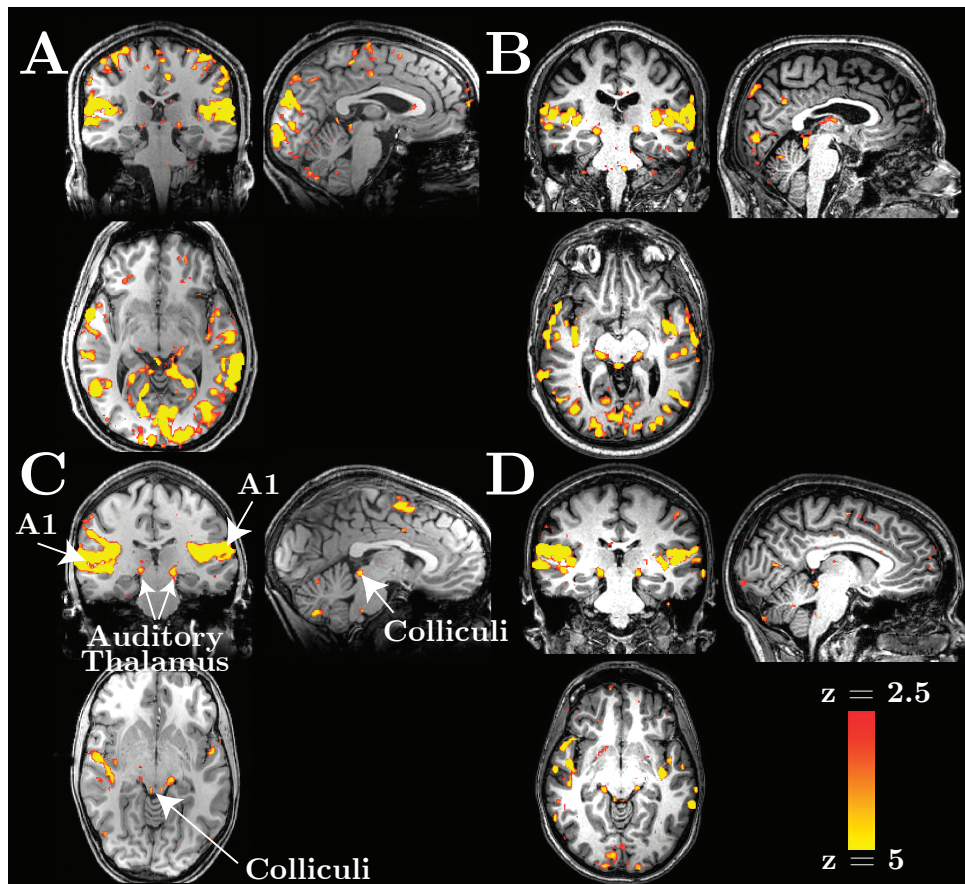


Figure 11: Example activation across all auditory stimulus conditions (binaural, monaural right and monaural left) for an anophthalmic (A), early blind (B), and sighted control subjects (C: Oxford site, D: UW site). Statistical maps are thresholded voxelwise at $z > 2.5$ for visualisation purposes.

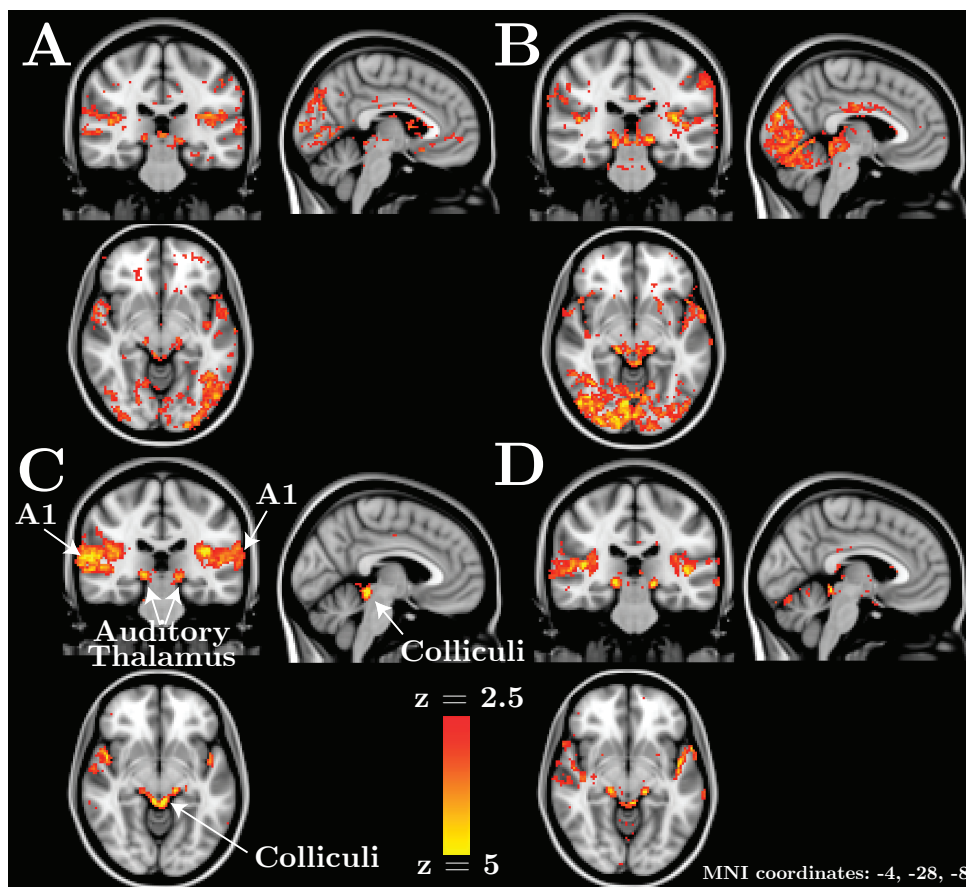


Figure 12: Group activation (in MNI 2 mm standard space) combined across all auditory stimulus conditions for anophthalmic (A), early blind (B), and sighted control subjects (C: Oxford site, D: UW site). Group statistical maps (mixed effects) are thresholded voxelwise at $z > 2.5$ for visualisation purposes.

3.4.2 Recruitment of the superior colliculus for auditory processing in blind subjects

Group data comparing responses within all four subject groups to all three auditory conditions within the region of the superior colliculus are shown in **Figure 13**. **Panel A** shows responses that are greater in the anophthalmic group compared to Oxford controls and **panel B** shows responses that are greater in the early blind group compared to UW controls. These contrasts reveal greater auditory activity in both blind groups compared to their respective sighted controls in the location of the superior colliculus, in addition to the expected greater occipital activity.

The superior colliculus was then defined anatomically for individual subjects using T1-weighted 1 mm structural scans, by dividing the tectum into a superior region of interest. Percentage BOLD signal change within this region during the three auditory stimulation conditions is shown across groups in **Figure 14** for anophthalmic subjects and their sighted controls (**panel A**) and early blind subjects and their sighted controls (**panel B**). A 4-way ANOVA (hemisphere x auditory condition x group (sighted and blind) x site) revealed that both blind groups showed significantly greater activity in the superior colliculus relative to the sighted control groups (main effect of group: $F(1, 24) = 5.08$, $p = 0.034$). The magnitude of the response was greatest in the binaural condition but differences among the three conditions were not significant (main effect of condition: $p = 0.053$). There were no significant differences in BOLD responses between the left and right superior

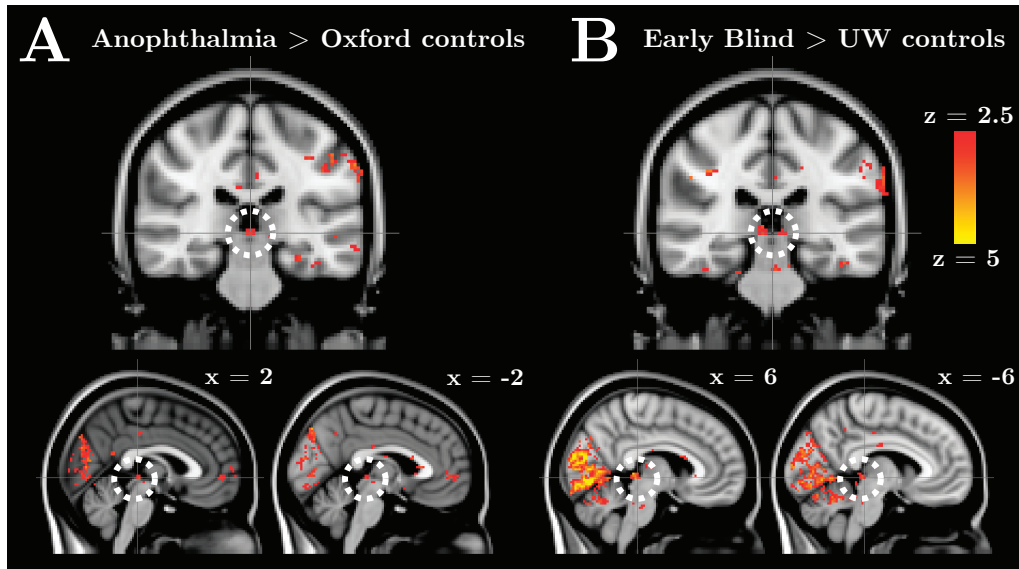


Figure 13: Contrasts of (A) Anophthalmia > Oxford sighted group and (B) Early Blind > UW sighted group in all three auditory conditions show auditory activity in the expected location of the superior colliculus in blind subjects. Group statistical maps (mixed effects) are thresholded at $z > 2.5$.

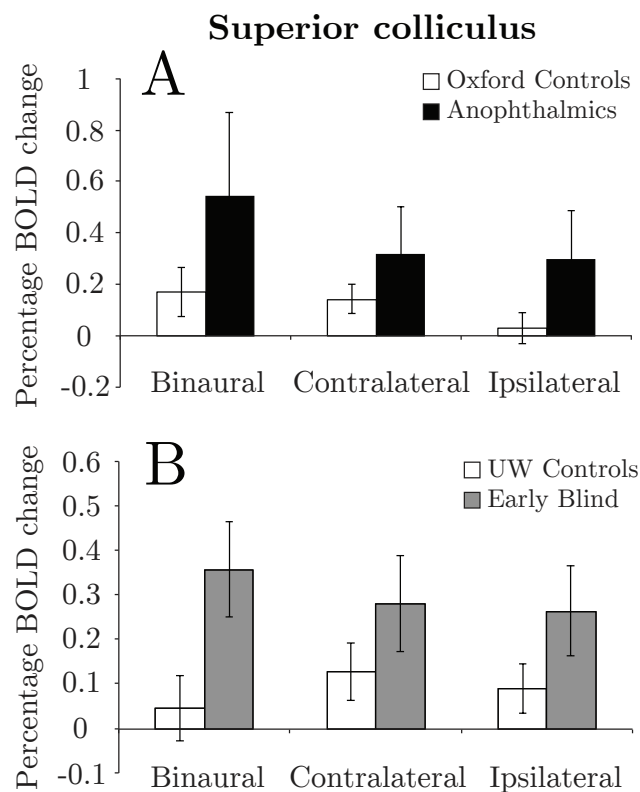


Figure 14: Mean % BOLD change within the superior colliculus during each of the auditory stimulation conditions (binaural, contralateral and ipsilateral). Results are separated by scan site (A: Oxford site; B: UW site). Note the y-axis scale difference between the two sites. Error bars represent the standard error of the mean.

colliculi or between scan sites (Oxford and UW), nor was there a significant interaction between group and condition.

3.4.3 No auditory evoked responses in the LGN of blind or sighted subjects

The anatomical definition of the LGN (Juelich histological atlas) was also used to determine whether there were any auditory responses in this structure in blind participants. There was no response in the LGN of any subject group. These data therefore provides some evidence that the LGN may not show cross-modal auditory plasticity, at least for the auditory stimuli used here.

3.4.4 Increased ipsilateral activity in the auditory thalamus of blind subjects

Using methods previously validated by Jiang et al. (2013)), the auditory thalamus was defined functionally in each subject's native space based on activation across all auditory stimulation conditions. When converted into MNI standard space, the mean coordinates (and standard deviation) for the central voxel within the auditory thalamus across all subjects were $x = -15$ (1.64), $y = -27$ (1.71), $z = -5$ (2.31) in the left hemisphere and $x = +16$ (1.59), $y = -27$ (1.82), $z = -5$ (2.29) in the right hemisphere. These match previous reports of MGN coordinates located with structural imaging (Rademacher et al., 2002; Devlin et al., 2006), functional imaging (Griffiths et al., 2001) and from post-mortem brains (Morel et al., 1997; Niemann et al., 2000). No

differences in these central coordinates were found among participant groups.

Furthermore, to ensure the auditory thalamus corresponds to location of MGN rather than the neighboring LGN, the functional definitions were overlaid with probabilistic anatomical definitions of the MGN and LGN from the Juelich histological atlas as implemented in FSL (thresholded at 15%, see **Figure 15**). Almost all of the functionally defined MGN (red) fell within the anatomically expected location of MGN (blue border) and very little fell within the anatomically expected location of neighboring LGN (green border). Thus, functionally defined auditory thalamus activity was centered on the anatomical definition of MGN for all subject groups.

The responses of the functionally defined auditory thalamus to the three auditory stimulation conditions are shown across groups in **Figure 16**. Data from participants scanned at Oxford and UW are presented in **panel A** and **panel B** respectively. A 4-way ANOVA (hemisphere x auditory condition x group (sighted and blind) x site) indicated significantly higher BOLD responses at the Oxford site compared to UW ($F(1, 24) = 12.46$, $p = 0.002$). There were no significant differences between binaural and contralateral auditory conditions in any group; sound amplitude was normalised to match loudness across binaural and monaural conditions so no differences related to loudness were expected.

In sighted subjects, the largest responses were to binaural and contralateral stimulation with significantly lower activation levels to ipsilateral stimulation (main effect of condition: $F(1.58, 37.9) = 16.52$, $p < 0.001$). This

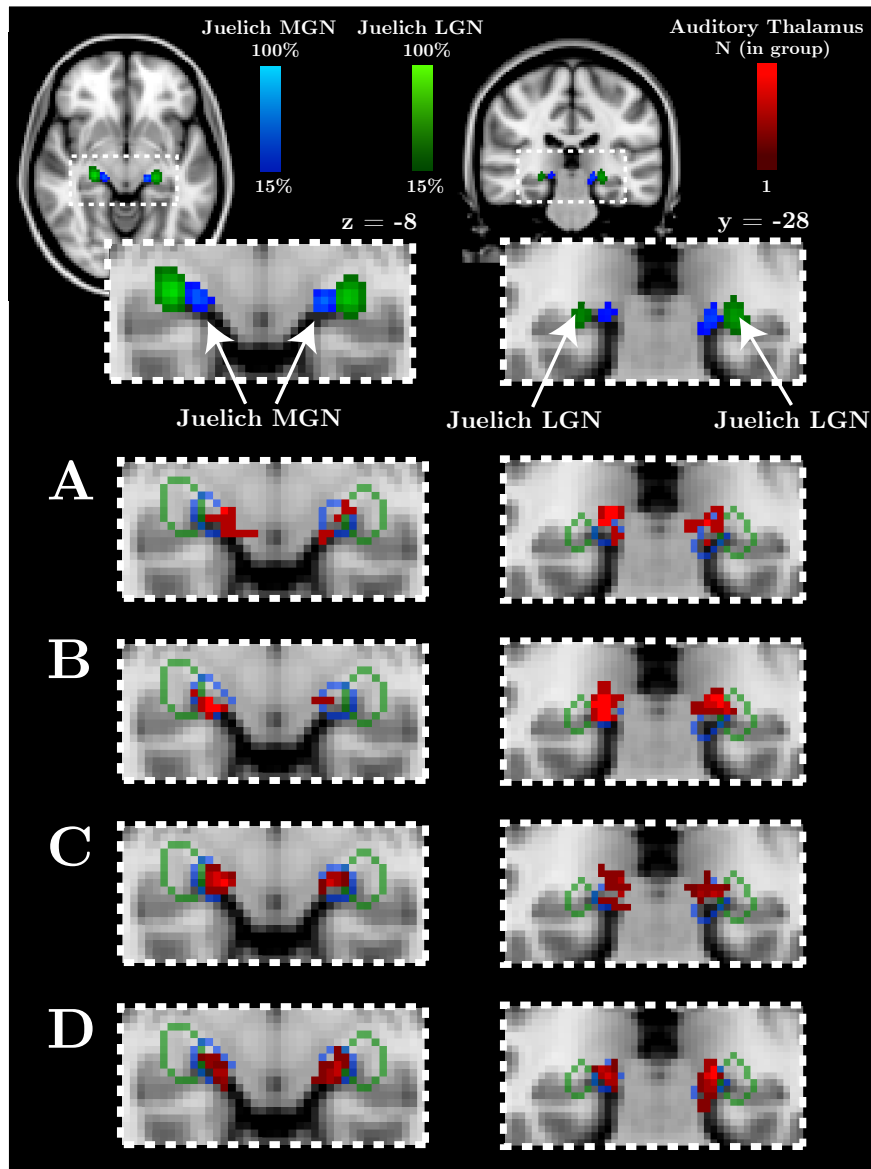


Figure 15: Functional definitions for all subjects (red) are superimposed on the location of anatomically-defined MGN (blue) and LGN (green). **Panel A** shows the anophthalmic group, **Panel B** the early blind group, **Panel C** the Oxford Control group and **Panel D** the UW control group. Despite some overlap with the anatomical definition of LGN (likely due to the close proximity of the two thalamic nuclei), auditory thalamus functional definitions are centered in the anatomical definition of MGN for all subject groups.

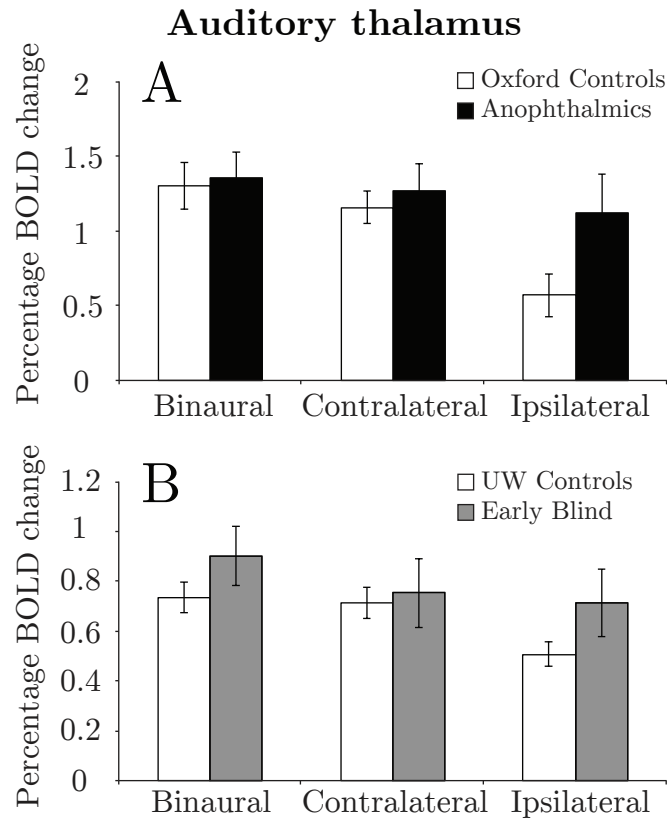


Figure 16: Mean % BOLD change extracted from the auditory thalamus (A: Oxford site; B: UW site) during each of the auditory stimulation conditions (binaural, contralateral and ipsilateral). Error bars represent the standard error of the mean. In the auditory thalamus, both control groups show an attenuated response to ipsilateral auditory stimulation, a pattern not found in either blind group. Note the y-axis scale difference between the two sites and thus the overall reduced response in the UW data.

pattern of responses is predicted from the known anatomical pathways, which are partially crossed at this stage in the auditory system. In contrast, neither blind group showed an attenuated response to the ipsilateral stimulation (group x condition interaction: $F(1.58, 37.9) = 3.53$, $p = 0.037$). Within-group paired t-tests revealed that contralateral activation was significantly higher than ipsilateral activation in the sighted groups (Oxford: $t(8) = 7.9$, $p < 0.001$; UW: $t(7) = 5.79$, $p < 0.001$) but responses to ipsilateral and

contralateral stimulation were not significantly different in the blind subject groups. Independent t-tests between conditions confirmed that the blind groups showed significantly higher activation than the sighted groups during ipsilateral stimulation only ($t(26) = 2.35$, $p = 0.027$). There was no difference between left and right auditory thalamus activation for any condition or group at either site, thus the effect is not due to functional ‘lateralisation’ of responses that may relate to the nature of the stimulus.

3.4.5 Inferior colliculus shows a mixed pattern of results

The inferior colliculus was defined anatomically for individual subjects using the T1-weighted 1 mm structural scan. Mean % BOLD signal changes are shown in **Figure 17**. The general pattern of response in the inferior colliculus (IC) is similar to the pattern seen in the auditory thalamus, in that the anophthalmic subjects show the same magnitude of responses for contralateral

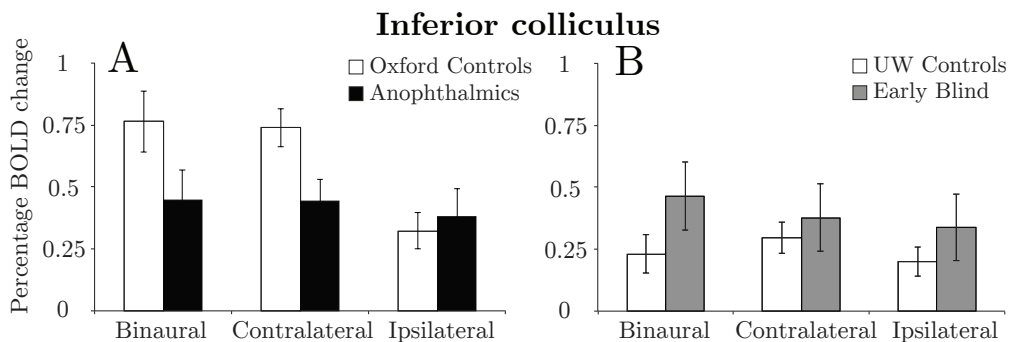


Figure 17: Mean % BOLD change extracted from the inferior colliculus (A: Oxford site; B: UW site) during each of the auditory stimulation conditions (binaural, contralateral and ipsilateral). Error bars represent the standard error of the mean.

and ipsilateral ear stimulation rather than the attenuated ipsilateral responses seen in sighted controls. The overall magnitude of BOLD responses was lower for anophthalmic subjects compared to Oxford controls, which may be due to a greater distribution of processing across the inferior and superior colliculi in the blind individuals (see Discussion). In addition, three sighted subjects from the UW site demonstrated very little activity in the IC, thus reducing the overall control means for the UW site.

3.4.6 Cortical responses to sound in blind and sighted subjects

Primary auditory (A1) and visual (V1) cortices were defined in MNI 2 mm standard space using the Juelich histological atlas as implemented in fslview. The responses of A1 and V1 to the auditory stimulation are shown in **Figure 18**.

For A1, the BOLD responses from the UW site were once again significantly lower than those from the Oxford site (main effect of site: $F(1,24) = 10.02$, $p = 0.004$). All groups showed the greatest A1 responses to binaural auditory stimulation, followed by contralateral monaural stimulation at a similar magnitude and lower responses to ipsilateral monaural stimulation (main effect of condition: $F(2,28) = 28.83$, $p < 0.001$). Blind groups again failed to show the control pattern of attenuated ipsilateral responses, but this effect was not as strong as in the auditory thalamus and did not quite reach significance (group x condition interaction: $p = 0.056$). Within-group paired-samples t-tests showed that the contralateral activation was signifi-

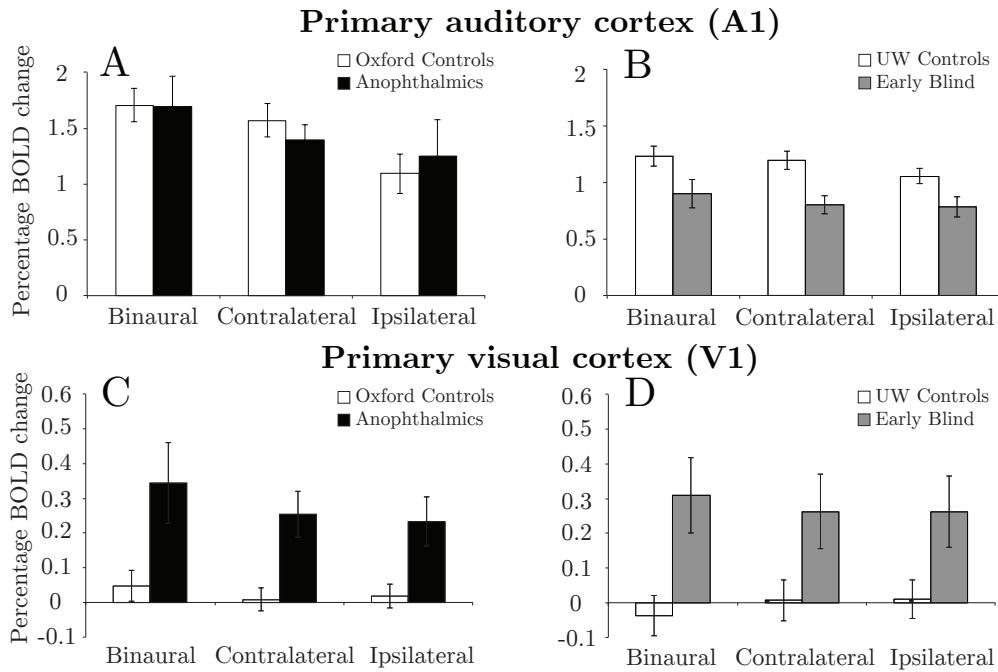


Figure 18: Mean % BOLD change within A1 (A: Oxford site; B: UW site) and V1 (C: Oxford site; D: UW site) during each of the auditory stimulation conditions (binaural, contralateral and ipsilateral). Error bars represent the standard error of the mean.

cantly higher than ipsilateral activation in the sighted groups (Oxford: $t(8) = 6.04$, $p < 0.001$; UW: $t(7) = 4.63$, $p = 0.002$) but the difference between ipsilateral and contralateral conditions was not significant in either of the blind groups (Anophthalmia: $t(4) = 0.6$, $p = 0.58$; Early Blind: $t(5) = 1.11$, $p = 0.32$). There was no difference between hemispheres for any condition or group at either scan site (Oxford and UW).

In the expected location of V1, sighted subjects did not show significant activation for any of the three auditory conditions, whereas the blind groups showed robust activation across all three conditions. Both blind groups had significantly greater BOLD signal change than sighted subjects (main effect

of group: $F(1,24) = 15.74$, $p < 0.001$). Interestingly, although there were no main effects of hemisphere or scan site on mean BOLD signal in V1, the activation in anophthalmic subjects was slightly left lateralised whereas in the early blind subjects it was slightly right lateralised resulting in a significant hemisphere by site interaction ($F(1,24) = 5.79$, $p = 0.024$). However, within each of these two blind groups the levels of activity in the right and left hemispheres were not significantly different.

3.5 Discussion

To date, most of the cross-modal plasticity literature has focussed on changes in the connections between occipital and other sensory or higher level cortices (for reviews Bavelier and Neville (2002); Noppeney et al. (2003); Lewis et al. (2010)). In the current study, a method for auditory thalamus functional localisation was used to show that the absence of visual input early in human development leads to changes at the subcortical level as well as in the cortex. Notably, this chapter provides evidence that the superior colliculus is recruited for auditory processing in anophthalmic and early blind individuals. Furthermore, compared to sighted controls, auditory-evoked responses in individuals lacking visual input were higher in subcortical structures ipsilateral to the ear that was stimulated. This increase resulted in attenuation of the contralateral-greater-than-ipsilateral responses to auditory stimulation that are evident in auditory subcortical structures of sighted people. These results are important because they suggest that blindness in early life affects the

functional properties of structures very early on in sensory processing pathways. This will be important to consider when developing sight restoration techniques. Furthermore, the superior colliculus result is important because this structure may then provide auditory input to the occipital cortex in anophthalmia and early-blindness. This subcortical input could determine how the blind occipital cortex responds to sound.

3.5.1 Eliciting subcortical activity using a complex auditory stimulus

The complex sound stimulus (scrambled music) used in this chapter was previously shown to reliably elicit responses within the auditory thalamus (Jiang et al., 2013). A variety of methods have been used to localise and measure functional responses within the MGN (Guimaraes et al., 1998; Giraud et al., 2000; Griffiths et al., 2001; Harms and Melcher, 2002; Krumbholz et al., 2005). However, this particular stimulus was chosen because it appears to elicit much stronger responses in the auditory thalamus at the individual level compared to dynamic rippled noise, as discussed in the Introduction. Furthermore, the sound vs. silent baseline contrast was chosen because the primary aim of this chapter was to elicit robust subcortical responses to auditory stimulation, rather than characterise more subtle functionally specific responses between different types of auditory stimuli. Using this stimulus, significant bilateral auditory thalamus activation was found in 26/28 individual participants.

A series of studies have suggested that pure tones (Devlin et al., 2003) and ‘speech like’ stimuli containing fast temporal modulations may be preferentially processed in left auditory structures (Zatorre and Belin, 2001; Schonwiesner et al., 2007), while musical stimuli, spatial or motion information may be preferentially processed in the right hemisphere (Zatorre et al., 2002; Krumbholz et al., 2005). However, this lateralisation may depend on context (Brechmann and Scheich, 2005; Shtyrov et al., 2005; Schonwiesner et al., 2007). In this chapter, similar to Jiang et al. (2013), consistently larger responses were found to contralateral as compared to ipsilateral stimuli in sighted subjects, but there was no evidence of any hemispheric specialisation. This may be because the stimuli used here contained a combination of auditory noise, music-like and speech-like features.

3.5.2 Recruitment of the superior colliculus for auditory processing in blind individuals

Electrophysiology studies with dark reared rats (Vidyasagar, 1978) and visually deprived cats (Rauschecker and Harris, 1983) have found significant increases in the mean number of somatic and auditory responsive cells within the superior colliculus. Consistent with these animal studies, the data presented in this chapter suggest recruitment of the superior colliculus for auditory processing in anophthalmic and early blind subjects. Blind groups showed significantly greater BOLD responses in the superior colliculus, defined anatomically, compared to the sighted groups.

The superior colliculus is known to have multimodal input even in sighted animals (Meredith and Stein, 1986; Covey et al., 1987; Jiang et al., 1997; King et al., 1998). These non-visual responses may become unmasked or more dominant in the absence of visual input. This type of unmasking of cross-modal projections has been reported in the cortex; connections between visual and auditory cortices are present in sighted animals but have been shown to be more abundant in neonatally enucleated animals (Innocenti et al., 1988; Karlen et al., 2006). Similarly, human imaging data shows that A1 to V1 connections are present in sighted individuals but that the strength of this connectivity is greater in early blind individuals (Klinge et al., 2010). It seems feasible that visual deprivation in early life (pre- and post-natal) could also unmask subcortical projections between visual and auditory structures.

3.5.3 No evidence of recruitment of the LGN for auditory processing

Based on the mouse model of anophthalmia (Piché et al., 2004; Laemle et al., 2006; Chabot et al., 2007, 2008), one might expect to see a recruitment of the lateral geniculate nucleus (LGN) for auditory processing. However, there was no significant modulation of neural activity within the anatomical location of LGN during any of the auditory stimulation conditions in any of the groups scanned. This could be due to a number of factors, including the possibility that humans differ from the mouse model and the LGN does not respond to auditory input, or the atrophy of the LGN in anophthalmia at least (Bridge et al., 2009) precludes detection of an auditory-evoked response.

Scanning this region at higher field strength may allow investigation of these alternatives.

If the LGN does not respond to sound in human early-onset blindness but the superior colliculus does, this has implications for the pathways by which cross-modal responses could reach the occipital cortex. It may be that the superior colliculus relays auditory input to and receives feedback from the occipital cortex via existing ‘visual’ pathways, for example with V1 (Nhan and Callaway, 2012) or extrastriate regions like area V5/MT+ (Fries, 1984). Several groups have reported ‘low-level’ auditory responses within the occipital cortex, including auditory motion (Poirier et al., 2006; Saenz et al., 2008; Bedny et al., 2010) and, more recently, a tonotopic map of auditory frequency in area V5/MT+ (Watkins et al., 2013). It is possible that these responses might be mediated by connections with the superior colliculus, either directly or via the pulvinar, as discussed extensively with relation to blindsight (Cowey, 2010).

3.5.4 Enhanced ipsilateral BOLD responses in blind individuals within the auditory thalamus

In the auditory pathway, inputs from the ear cross over to the contralateral brainstem from the level of the superior olivary nucleus (Langers et al., 2005). However, some information stays in the ipsilateral brainstem pathways whilst information reaching the contralateral side can cross back at the level of the inferior colliculus (**Figure 19**). As a consequence, subcortical and cor-

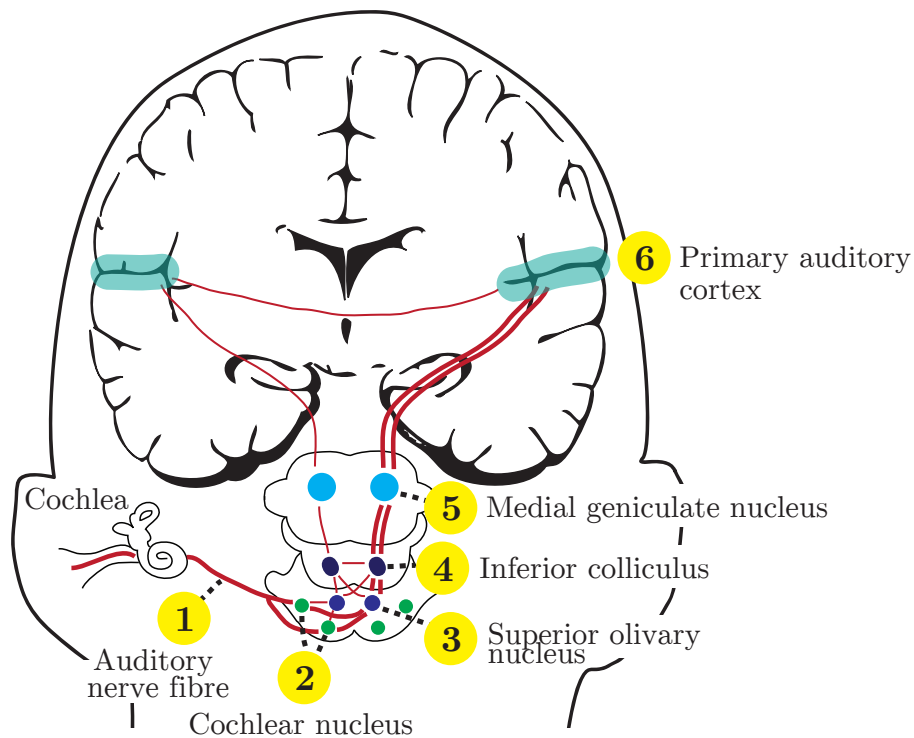


Figure 19: Schematic of the human auditory pathway, from the cochlea to the primary auditory cortex (A1).

tical auditory responses are stronger in the hemisphere contralateral to the stimulated ear in both animal models (Langers et al., 2005; Schnupp et al., 2011) and humans (subcortex: Langers et al. (2005); cortex: Woldorff et al. (1999); Suzuki et al. (2002)). This contralateral bias is clearly replicated in the sighted data presented in this chapter. Furthermore, at least in ferrets, this contralateral bias develops at the cortical level around one month after the onset of hearing, suggesting that it requires exogenous input, and consists of a boosting of the contralateral response rather than a suppression of the ipsilateral one (Mrsic-Flogel et al., 2006).

Based on the findings presented here, it appears that the absence of visual

input results in an increase (relative to sighted controls) of activity driven by the ipsilateral ear within subcortical structures. In sighted subjects, activation levels in the auditory thalamus were significantly higher during binaural and monaural contralateral stimulation than for monaural ipsilateral stimulation. In contrast to this normal activation pattern, blind subjects showed a similar magnitude of auditory thalamus BOLD responses to ipsilateral stimulation as for contralateral or binaural stimulation. This effect was found in both anophthalmic and early blind groups. Anatomical definitions of MGN and LGN confirmed that these activation levels were correctly localised to the MGN.

This reduction in the dominance of activity driven by the contralateral ear in the blind subcortical auditory pathway suggests that the visual system may have a role in shaping these responses. There are a number of possible reasons for this enhancement of ipsilateral responses in the auditory thalamus. The first is a bottom-up phenomenon. Given the considerable interaction between visual and auditory maps in the colliculi, and its role in orienting behaviour, one possibility is that the usual shaping of contralaterally driven responses is mediated by interactions between audition and vision in the colliculi. In the absence of vision, there may be a strengthening of inputs along the ipsilateral brainstem pathways or an increased crossing of inputs from the contralateral pathways at the level of the inferior colliculus or MGN. The second possible explanation is that an increase in top-down descending feedback from the cortex (either A1 or V1) may boost ipsilateral responses in the MGN. Although the enhancement of ipsilateral responses in blind sub-

jects compared to sighted subjects is considerably weaker in A1 than in the auditory thalamus, feedback from A1 could boost auditory thalamus ipsilateral responses. Furthermore, auditory responses in pericalcarine ‘visual’ areas (V1) in the blind groups did not show any evidence of being driven preferentially by stimulation of the contralateral ear, and could therefore contribute to the increased ipsilateral responses in auditory thalamus. Projections from the MGN to the primary visual cortex have been found in bilaterally enucleated opossums (Karlen et al., 2006), and it is possible that these projections are reciprocal. Although the results presented in this chapter cannot differentiate between these two possibilities (bottom-up or top-down), the finding of altered monaural responses in the auditory thalamus in either case is an interesting area for future work.

3.5.5 Anophthalmia as compared to early blindness

In human bilateral anophthalmia, both eyes fail to develop or development is arrested at a very early stage. Therefore, unlike other causes of congenital blindness, the anophthalmic visual pathway does not experience pre-natal retinal activity. Previous imaging work in the human brain suggests that reorganisation at the cortical level may differ between anophthalmic and early blind individuals; for example, in anophthalmia, the pericalcarine region (V1 in sighted subjects) appears to be a ‘low level’ auditory structure that does not distinguish between language and backwards speech (Watkins et al., 2012), whilst it does for early blind subjects (Bedny et al., 2011). The animal literature has also demonstrated that early ‘visual’ areas such as the LGN

and V1 have auditory c-Fos activity in anophthalmic, but not neonatally enucleated mice (Chabot et al., 2007).

Since the anophthalmic and early blind subjects in the current study differed in age and were scanned at different sites with different scanners and head coils, it is difficult to directly compare activation patterns. In addition, the small sample sizes, range of causes of blindness in the early blind group, and age differences between the early blind and controls at the UW site provide additional sources for variability. In the auditory cortex in particular, responses in the older early blind group showed an overall reduction in magnitude compared to the younger UW control group. This is consistent with evidence that age is correlated with reduced BOLD responses in the auditory cortex (Cliff et al., 2013). However, despite this general reduction in the response level in the older subjects scanned at the UW site, the main findings described above are unlikely to be due to age differences since they were always observed in anophthalmic (who were age-matched to their sighted controls) as well as early blind subjects.

One area for potential discrepancy is within the tectum (colliculi). In the inferior colliculus, the anophthalmic subjects appear to show reduced activation relative to the Oxford controls, whereas the early blind group do not show reduced activation relative to UW sighted controls. This result should be treated with caution, given the difficulty of eliciting robust activity in this small subcortical structure. However, whilst the experimental paradigm is identical and each group may be performing the same computations during the task, it could be that the metabolic expenditure is different in the anoph-

thalamic group (Poldrack, 2014). Higher resolution scanning targeting this structure could be used to confirm this finding and investigate any group differences further.

3.5.6 Conclusions

In conclusion, the data presented in this chapter describes for the first time subcortical reorganisation of function in the human brain as a result of absent visual input occurring early in development. Changes included an apparent recruitment of the superior colliculus for auditory processing and increased ipsilateral BOLD activity in the auditory thalamus. Future work is needed to determine the full extent of functional reorganisation within subcortical structures, and how these changes contribute to cross-modal reorganisation at the cortical level.

4 Subcortico-cortical connectivity in anophthalmia and early-onset blindness

4.1 Summary

The previous chapter presented the first human evidence of functional reorganisation in subcortical pathways due to early blindness. However, it remains unclear how these auditory responses influence cross-modal responses in the occipital cortex. Dynamic causal modelling (DCM) was performed on the same imaging dataset in order to investigate the effective connectivity underlying auditory responses in the pericalcarine cortex of both anophthalmic and early blind individuals (V1 in sighted subjects). Previous DCM in sighted and blind groups (Klinge et al., 2010) suggest that cortico-cortical connections between A1 and V1 are perhaps more important to carry auditory information to V1 in the absence of visual input than subcortico-cortical connections between MGN and V1. This chapter replicated the previous analysis using the same set of models from that previous study. The analysis revealed a best fit of the data in all sighted and blind groups to a model that does not contain direct connections between A1 and V1. Within this winning model,

sighted subjects showed a trend towards stronger MGN to A1 connections, whereas the blind participants showed significantly stronger MGN to V1 connections in both hemispheres. In a second more detailed analysis, the models were extended in the blind subjects only to include superior colliculus (shown to respond to sound in Chapter 3) and extrastriate regions. This analysis revealed that pericalcarine (V1) auditory responses in the early blind group relied on direct connections between V1 and A1 only. The same responses in the anophthalmia group were best explained by direct connections from A1 to V1 but also from the superior colliculus to V1. These results suggest that there may be some differences between anophthalmia and early blindness in how auditory information reaches the occipital cortex (via subcortical structures); however, a clear result could not be drawn from this small data set and therefore larger group sizes are needed before any further conclusions can be drawn from this chapter.

4.2 Introduction

The previous chapter presented the first human evidence for reorganisation of function in subcortical pathways as well as cortical structures due to early-onset blindness. The absence of eyes (anophthalmia) and loss of vision in the first few years of life (early blindness) changed the responses of both auditory (medial geniculate nucleus) and visual (superior colliculus) subcortical structures. However, it remains unclear to what extent these subcortical responses feed auditory information to the blind occipital cortex directly

via subcortico-cortical connections, or instead whether the occipital cortex receives auditory input solely via cortico-cortical connections with the auditory cortex. If subcortico-cortical 'visual' pathways become used for auditory innervation of the blind occipital cortex, this will have profound effects on whether sight restoration techniques can successfully restore their traditional role of carrying visual information.

Anatomical connections between low-level sensory areas (such as the primary visual cortex and primary auditory cortex) may provide a route for non-visual inputs to reach the occipital cortex in both sighted and blind individuals. Evidence of these direct pathways has been found in nonhuman primates with anatomical tracers and has contributed to the view that senses can converge in early stages of sensory processing (Schroeder et al., 2003). Retrograde tracer injections in monkey primary visual cortex (V1, or Brodmann area 17) revealed robust connections with several auditory cortical regions as well as the superior temporal polysensory region, a multisensory area in the temporal lobe. These connections were stronger to peripheral V1 than foveal V1, suggesting multi-sensory connectivity in early visual areas may be restricted to certain regions within the early visual cortex (Falchier et al., 2002). Feedback or reciprocal projections between peripheral secondary visual cortex (V2) and caudal regions of the auditory cortex have also been found in the macaque (Falchier et al., 2010). Additional studies using retrograde and anterograde tracer injections in monkeys have confirmed long distance connections between V1 and auditory or multisensory areas (Clavagnier et al., 2004), and from parietal and auditory association areas to

peripheral V1 and V2 (Rockland and Ojima, 2003).

Anatomical connections between auditory and visual cortices have also been found in humans. Diffusion weighted tensor MRI and probabilistic tractography in healthy participants have shown ipsilateral tracts seeded in Heschl's gyrus reaching occipital cortical regions, including the calcarine sulcus (Beer et al., 2011). Resting state fMRI in healthy humans has shown a coupling of functional activity between the medial portion of Heschl's gyrus and the anterior calcarine fissure (Eckert et al., 2008). Together, these studies suggest that direct connections between early visual and auditory cortices may facilitate multisensory integration in the early stages of sensory processing. Furthermore, it could be speculated that these existing connections are strengthened by visual deprivation and may provide a route for non-visual information to innervate the occipital cortex in the absence of visual input (Pascual-Leone and Hamilton, 2001). In support of this, retrograde and anterograde tracer injections to the primary visual cortex revealed direct projections with auditory, somatosensory, motor and association cortical areas in sighted, enucleated and anophthalmic (ZRDCT-an) mice (Charbonneau et al., 2012). Furthermore, some studies have found that these connections are slightly more abundant in neonatally enucleated animals than sighted animals (Innocenti et al., 1988; Karlen et al., 2006).

Connections between subcortical structures and subcortico-cortical pathways could provide an alternative or perhaps complementary route for non-visual inputs to innervate the occipital cortex. As discussed in previous chapters, dorsal LGN has been shown to activate to sound and receive projec-

tions from the inferior colliculus in anophthalmic (ZRDCT-an) mice (Chabot et al., 2007; Piché et al., 2004), bilateral neonatally enucleated hamsters (Izraeli et al., 2002), and naturally blind rodents (Doron and Wollberg, 1994). This projection would allow auditory information to reach the dorsal LGN, which could then innervate the occipital cortex via existing visual pathway projections. However, there is strong evidence that direct projections from LGN to V1 (the optic radiations) are atrophied in the blind humans, as is the LGN itself (Bridge et al., 2009; Noppeney et al., 2005). Furthermore, in Chapter 3 there was no evidence for auditory-evoked activity in the LGN of anophthalmic or early blind cases; it is therefore unlikely that the LGN provides subcortical auditory input to the occipital cortex in human early-onset blindness. It could be that other subcortical structures provide this input, possibly via the inferior colliculus, auditory thalamus, superior colliculus (which responds to sound in Chapter 3) or pulvinar. Whilst there is some evidence of direct cross-modal projections from the inferior colliculus to the primary visual cortex in the anophthalmic mice (Laemle et al., 2006), more sensitive tracing methods could not replicate these findings (Chabot et al., 2008). It is likely that if subcortico-cortical projections do play a role in carrying non-visual information to the occipital cortex, it would be in addition to cortico-cortical connections. In support of this, retrograde tracers injected in the primary visual cortex of bilaterally enucleated opossums revealed projections from subcortical non-visual nuclei (including the MGN) as well as auditory, somatosensory and multimodal cortices (Karlen et al., 2006). Precisely how these pathways may interact or vary according to the age of blindness onset remains unclear.

In recent years, MRI analyses have moved towards creating mechanistic models of brain function to address these questions of connectivity (Stephan et al., 2010). A typical example is dynamic causal modelling (DCM), which is a method that compares models and identifies the optimal model that fits to fMRI data or best explains how brain regions may influence each other during an fMRI task. DCM relies on the dynamic nature of Bayesian modelling in order to estimate and update the probability of a particular event given the available evidence. DCM assesses the effective connectivity, or coupling, between brain regions during a particular fMRI task (Friston et al., 2003). Effective connectivity in DCM is different from functional connectivity in that it explains how 'hidden' neuronal states can cause interactions between brain regions as a result of experimental interventions (in this case, the auditory input). These hidden states vary over time and cause noisy responses that cannot be observed directly. DCM therefore does not describe the interactions between fMRI responses themselves, but instead the interactions between these hidden noisy states. DCM is described by equations that explain two main causal properties: 1) how the state of one neuronal population changes the dynamics of another via connections, and 2) how these connections are affected by the external manipulation, for example the auditory stimulus used in this chapter. These equations are stored over time so that the state of a neuronal population at one time point will influence later time points (Stephan et al., 2010).

DCM can be a particularly useful tool to infer task-dependent connectivity across different human populations; in particular, how the influence

of specific brain areas on others may differ in clinical populations compared to healthy controls. DCM has been used to investigate effective connectivity in visually impaired individuals. Klinge et al. (2010), the first study to do this, investigated whether auditory fMRI responses in the blind pericalcarine cortex (V1 in sighted subjects) were due to cortico-cortical connections with the primary auditory cortex (A1) or subcortico-cortical connections with the medial geniculate nucleus (MGN). Using an auditory discrimination task containing emotional voices, they found that the data in both sighted and early blind groups best fit a DCM model that contained direct reciprocal connections between all three regions of interest (MGN, V1 and A1). Within this winning model, the strength of MGN to A1 and MGN to V1 connections did not differ significantly between the two groups but the connection between A1 and V1 was significantly stronger in the early blind group compared to the sighted group. This evidence for cortico-cortical connectivity was further investigated by Collignon et al. (2013), who compared A1 to V1 effective connectivity in 12 congenitally blind and 10 late-onset blind individuals whilst they performed a task discriminating the pitch and spatial location of sounds. In order to assess how auditory information reaches the occipital cortex in these two subject groups, the authors constructed a series of DCM models that connected V1 either directly with A1 ('feed-forward model') or indirectly via the intraparietal sulcus ('feed-back model'). In order to improve experimental power, models with unidirectional and reciprocal connections were grouped into families of 'feed-forward' or 'feed-back' models. They found that whilst the congenitally blind data best fit to a model that contained direct A1 to V1 connections, the late blind group best fit to a more

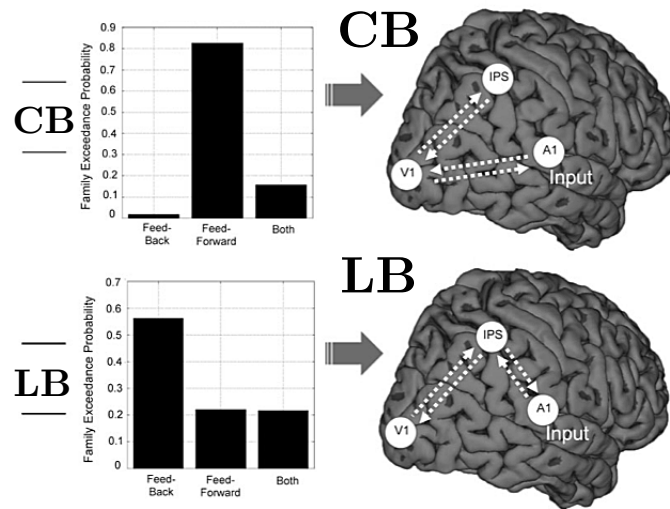


Figure 20: Results from Collignon et al (2013). Auditory fMRI data from the congenitally blind group (CB, top) best fit to a family of ‘feed-forward’ models, which included direct connections between A1 and V1 (top right). Data from the late-onset blind group (LB, bottom) best fit to a family of ‘feed-back’ models, which indirectly connected A1 to v1 via the intraparietal sulcus (IPS, bottom right).

indirect model that relayed the auditory information via the intraparietal sulcus (**Figure 20, adapted from Collignon et al. (2013)**).

Together, these studies suggest that cortico-cortical connections are the driving force underlying cross-modal auditory responses in the visually deprived occipital cortex, but that the precise route may depend on age of blindness onset. However, it is possible that subcortico-cortical connectivity is also at play but is perhaps undetected by lack of experimental power in subcortical regions. Alternatively, it may be that this connectivity is not present in populations of blind subjects who acquire blindness post-natally (i.e. early blind) but instead only in special cases of very early onset blindness, as suggested by data from the anophthalmic mouse model (ZRDCT-an) (Chabot et al., 2007; Laemle et al., 2006) and neonatally enucleated animals (Israeli

et al., 2002).

In this chapter, the fMRI dataset described in Chapter 3 was analysed using DCM in order to look at how subcortical auditory responses in the anophthalmic and early blind participants may supply auditory information to the occipital cortex. Firstly, the Klinge et al. (2010) study of effective connectivity in early blind individuals was replicated. Secondly, these DCM models were extended to include superior colliculus and extrastriate (area V5/MT+) regions in order to investigate the hierarchy of subcortico-cortical and cortico-cortical effective connectivity in early-onset blindness. It was hypothesised that whilst early-blindness may rely primarily on cortico-cortical connections to 'V1', as suggested by Klinge et al (2010), subcortico-cortical connections would provide an alternative route to 'V1' in anophthalmia, as suggested by the animal literature.

4.3 Methods

4.3.1 Participants

As described in the previous chapter, data was acquired at two scan sites (University of Oxford and University of Washington). Five bilaterally anophthalmic subjects (mean age 29 years, range 23-36, two females, see **Table 1** in Chapter 2) were scanned at the University of Oxford and seven early blind subjects (mean age 51 years, range 31-63, three females, see **Table 2** in Chapter 3) were scanned at the University of Washington. Data from

sighted control subjects was acquired at each site: ten sighted subjects at the University of Oxford (mean age 26 years, range 23-27, seven females) and eight sighted subjects at the University of Washington (mean age 30 years, range 23-39, five females). The study was granted ethical approval by the University of Oxford and the University of Washington, and all participants gave informed written consent prior to participation.

4.3.2 Auditory stimuli and MR imaging acquisition

This chapter used the same auditory stimulus and MRI data described in the Chapter 3 (see Methods section for more details).

4.3.3 MR imaging analysis

To perform dynamic causal modelling, functional MRI data were analysed using Statistical Parametric Mapping (SPM8, Wellcome Department of Imaging Neuroscience, London, UK). In order to facilitate dynamic causal modelling, the six functional runs were concatenated temporally for each participant. As these data were acquired using a sparse-sampling protocol, slice-timing correction was not required. Images were realigned using rigid body motion correction and spatially normalised to MNI 2 mm standard space. A spatial smoothing Gaussian kernel of 5 mm (full-width at half-maximum) was applied to aid region of interest selection for dynamic causal modelling, and a high-pass temporal filter cut off was set at 128 sec.

Statistical analysis was performed using a general linear model. All three auditory conditions (binaural, monaural right, monaural left) were pooled together into one regressor to use as the auditory input for dynamic causal modelling. To account for any differences between the six concatenated runs, extra regressors representing each individual run were included in the model (run regressors).

4.3.4 Dynamic causal modelling

Dynamic causal modelling (DCM) was used to investigate whether auditory cross-modal responses in the blind occipital cortex rely on direct subcortico-cortical connections with the MGN or superior colliculus, or cortico-cortical connections with the primary auditory cortex. DCM tests specific hypotheses (*a priori* knowledge) about how one brain area may influence another during an fMRI task (Friston et al., 2003). In DCM, the three model parameters are (1) extrinsic inputs to regions of interest, for example the direct influence of the auditory stimulus on a region's activity, (2) intrinsic coupling between regions, for example the direct connections between regions, and (3) changes in connectivity between regions due to the experimental paradigm, for example the auditory stimulus. In order to replicate the analysis of Klinge et al. (2010) and reduce model complexity, the models used in this chapter defined only the first two parameters.

Dynamic causal modelling was performed using DCM10 as implemented in SPM8. Timeseries were extracted from regions of interest, models were

fit to each participant's data, and the optimal model was identified for each subject group (four groups: Anophthalmics, Early Blind, Oxford controls and UW Controls). If the same model was optimal model for several groups, the strengths of the connections within this model were compared between these groups.

Timeseries extraction for regions of interest As described in the previous chapter, the brain regions that showed significant BOLD responses to the stimulus included the medial geniculate nucleus (MGN), inferior colliculus (IC) and auditory cortex (A1) for all subjects, and the superior colliculus and extensive occipital cortical regions in the blind groups only. In order to perform DCM, the timeseries of some of these regions of interest were extracted for each participant. To reduce model complexity, these were limited to the MGN, A1 and V1 for all subjects, and the superior colliculus (SC) and area V5/MT+ were added for blind subjects only. The first eigenvector of the timeseries was extracted, which is the first principal component of the timeseries for all voxels (above threshold) that lie within the defined region of interest. This timeseries was corrected for the covariates of no interest (motion and run regressors) and therefore only included voxels active above threshold for the three auditory conditions (binaural, monaural right, monaural left).

Timeseries were selected using criteria similar to those described by Klinge et al. (2010). Regions of interest were selected from areas showing activation to the auditory stimuli (binaural, monaural right, monaural left) at a significance level of $p < 0.05$ (uncorrected). Timeseries were extracted

from a sphere around the peak BOLD response in the expected coordinates of each region of interest (3 mm radius for MGN, SC and V5/MT+, 6 mm radius for A1 and V1). Anatomical location is considered useful information for finding timeseries coordinates in DCM (Stephan et al., 2010), therefore expected coordinates for the MGN were determined using a combination of anatomical location (Devlin et al., 2006; Morel et al., 1997; Niemann et al., 2000) and coordinates of individual auditory thalamus masks made in Chapter 3. Coordinates for the superior colliculus were determined by the anatomical location of the superior portion of the tectum, as described in the previous chapter. Expected coordinates for A1, V1 and V5/MT+ were based on the Juelich histological atlas as implemented in FSL with fslview (version 3.2.0). A1 was the combination of TE1.0, TE1.1 and TE1.2 (Morosan et al., 2001). A1 and V1 probabilistic definitions were thresholded at 30%, and V5/MT+ was thresholded at 15%.

If a participant did not show significant BOLD responses in a region of interest, a sphere around the central coordinate (centre of gravity) of the anatomical mask was used.

Model specification DCM can be used to identify one model (out of the range of proposed models) that best explains the fMRI dataset whilst maintaining model simplicity. Therefore, large and complex models are not necessarily better. It is assumed in DCM that models have been defined based on *a priori* knowledge, in that they provide plausible explanations for the fMRI data based on known anatomy and connectivity. With this in mind,

the two model spaces defined below were selected based on their simplicity and plausibility relative to the known anatomy of the visual and auditory pathways.

In the first model space, the four models defined in Klinge et al. (2010) were fit to each participant's data (**Figure 21**). As described in Klinge et al. (2010), the models all consisted of three regions of interest (MGN, A1 and V1) and the auditory stimulation (extrinsic input, or driving auditory input) always entered the model via the MGN. The models were defined separately for the left and right hemispheres and differed by one direct connection between two regions. Model 1 included all possible connections between regions (fully connected), model 2 lacked a connection between MGN and V1, model 3 lacked a connection between MGN and A1, and model 4 lacked a connection between A1 and V1. All models contained both 'forward' and 'backward' connections. Klinge et al. (2010) also included a set of models that replaced the MGN with the lateral geniculate nucleus (LGN), the visual

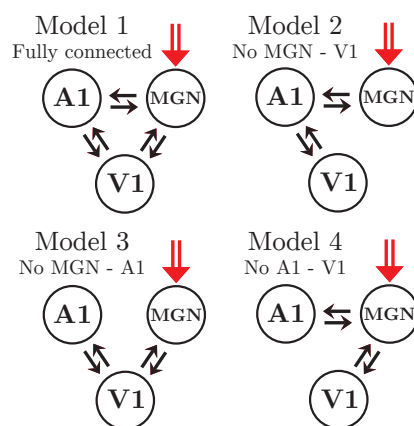


Figure 21: Schematic representation of model space 1. Auditory input always enters the models via MGN (red arrow). The black arrows represent the connections between regions. The models were defined separately for each hemisphere.

thalamic nucleus. However, as there was no evidence of LGN activity in either sighted or blind groups in this dataset (see Chapter 3), these models were not analysed.

The second model space extended the first by including the superior colliculus (SC) and area MT/V5+ as additional regions of interest. BOLD responses in the SC were found in anophthalmic and early blind groups only (see **Figure 14** in Chapter 3). This second model space investigated whether the SC could relay auditory information to the occipital cortex via existing 'visual' subcortico-cortical connections (either directly to V1 or via V5/MT+). DCM can only be performed using timeseries from regions of interest that contain significant BOLD responses, therefore this model space only included the blind subjects (**Figure 22**). Furthermore, in order to improve the power

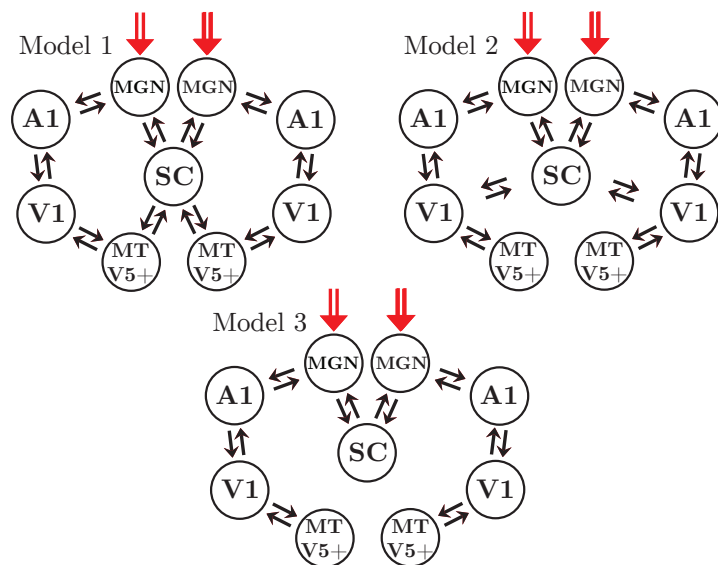


Figure 22: Schematic representation of model space 2, which includes the superior colliculus (SC) and area MT/V5+ in both hemispheres. Auditory input always enters the models via MGN (red arrow). The black arrows represent the connections between regions. This model space was defined in the blind subjects only.

of the models and feed as much available information into them as possible, each model contained both hemispheres. This was not done in the first model space because Klinge et al. (2010) analysed each hemisphere separately.

Bayesian model selection The optimal or most likely model to explain the data for each subject group was identified using random-effects Bayesian model selection (BMS), as implemented in SPM8 (Stephan et al., 2010). BMS is used to calculate an approximate model evidence for each model, or the likelihood of the model accurately representing the dataset in question. Models can then be compared according to these likelihood values in order to identify the optimal model for that particular dataset. In BMS, the optimal model is one that best explains the fMRI data (relative to all of the models defined in the model space), whilst avoiding unnecessary complexity; in other words, the best and simplest model will outperform the others. BMS results were plotted as exceedance probabilities for each model. Exceedance probability is the probability that model x is more likely to explain the data than all of the other models in the model space. An exceedance probability value is assigned to each model, and the values for all models in the model space are equal to 1 (or 100%). An exceedance probability value of greater than 0.85 (85%) is considered convincing evidence for that model (Stephan et al., 2010).

Inference on model parameters In cases when the same optimal model was identified for two or more subject groups, the parameter estimates of

that model (in other words, the strength of the connections between ROIs in that model) could be compared using a random-effects approach (Stephan et al., 2010). These parameter estimates are reported in Hertz (hz) because a strong connection in dynamic modelling corresponds to a fast effect or response. Two-tailed independent-samples t-tests were performed in order to compare differences in the strength of these connections between the subject groups. Bonferroni correction adjusted the p-value for the number of tests carried out (x number of tests adjusts the p-value to $0.05/x$).

4.4 Results

Whole brain analyses in SPM8 revealed very similar BOLD responses to those revealed by FSL, as described in Chapter 3 (see **Figure 11** and **Figure 12**). All subjects showed clear activation in the auditory cortex, auditory thalamus (MGN) and colliculus. Anophthalmic and early blind subjects showed additional auditory-evoked responses in the occipital cortex.

4.4.1 Model Space 1

A random-effects BMS was used within each group and hemisphere in order to identify which of the four models defined in Klinge et al. (2010) best explained the dataset in this chapter. **Figure 23** shows the results of this model comparison. In all groups and hemispheres, Model 4 (no A1 to V1 connections) had the largest exceedance probability, therefore indicating that

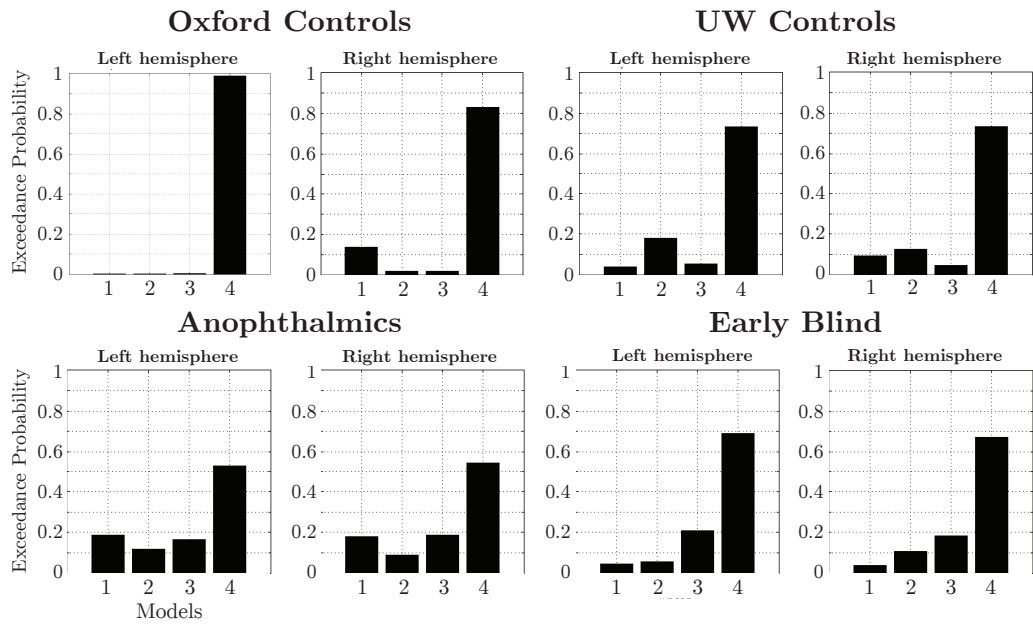


Figure 23: Model comparisons results (random-effects BMS) for the left and right hemisphere of each of the subject groups. The bars in each plot show the exceedance probability for each of the four models. The “winning” model (highest exceedance probability) in both hemispheres for each of the four groups was Model 4.

this model outperforms the others. Since this effect is found in all groups, it suggests some uniformity in the underlying connections between the blind and sighted groups in this particular dataset. However, exceedance probability did vary across the different groups, with the sighted groups reporting larger exceedance probability values for Model 4 than the blind groups. This may relate to the relatively large sample sizes in the sighted groups compared to the blind groups; outliers or between-subject variability in smaller groups would have a more profound effect on model evidence (measured here as exceedance probability).

Figure 24 shows model comparison results for the four subject groups pooled into ‘blind’ (anophthalmics and early blind) and ‘sighted’ (Oxford controls and UW controls) groups. Again, Model 4 outperforms the other

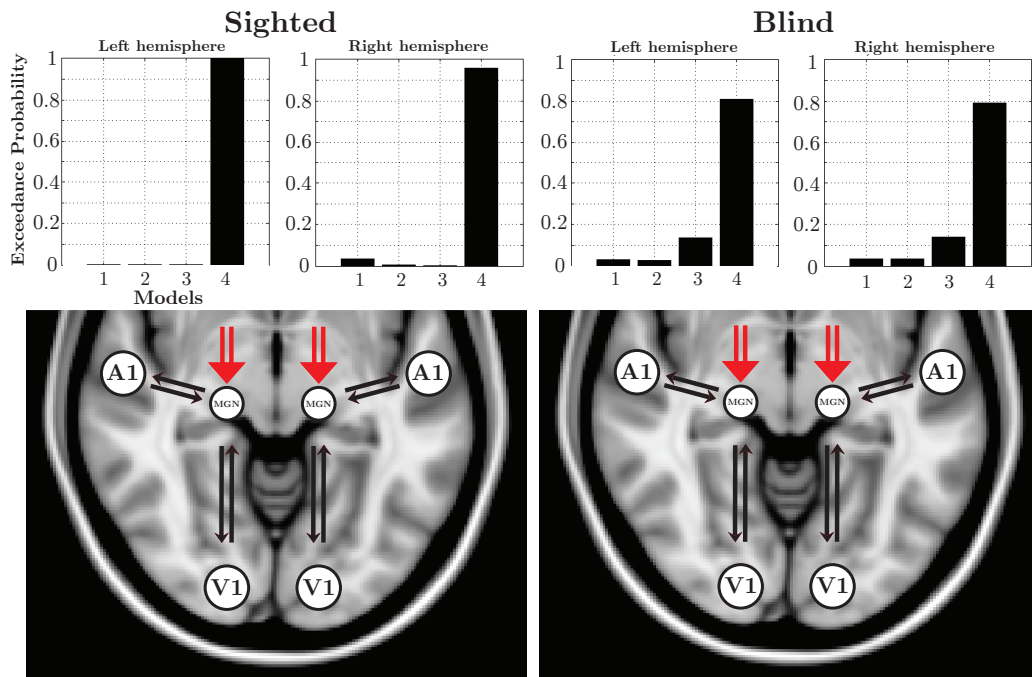


Figure 24: Model comparisons results (random-effects BMS) for the left and right hemisphere of the pooled "sighted" (left) and "blind" (right) groups. The bars in the plots show the exceedance probability for each of the four models. Below each plot is a schematic diagram of the winning model (Model 4 in both cases) on an axial slice of the MNI standard brain (at $z = -6$).

models in both hemispheres. It is interesting to note that the exceedance probability for Model 4 is higher when the groups are pooled together. Again, this may be due to the small sample size for each individual group being more affected by individual differences; in contrast, a larger group is more robust to these differences since one outlier subject will have less of a negative impact on Model 4 evidence.

The 'strength' of effective connections within Model 4 was then compared between groups for each hemisphere. One anophthalmic and two early blind participants were removed from this analysis as their data did not fit to any of the models. Within each hemisphere, Model 4 has one input connection

(auditory driving input to MGN) and two main ‘forward’ connections (MGN to A1 and MGN to V1). The strength of the auditory driving inputs to MGN did not differ between the four groups. Two-tailed independent-samples t-tests were performed in order to compare ‘forward’ connections from MGN to A1 and V1 between the different subject groups. The tests compared the strength of these connections between the ‘sighted’ and ‘blind’ groups, with Bonferonni correction for multiple comparisons setting the p-value to 0.025 (two tests carried out for each hemisphere). No significant differences were found between the Oxford and UW sighted controls, or between the anophthalmic and early blind subjects.

MGN to A1 connections in both hemispheres are shown in **Figure 25**,

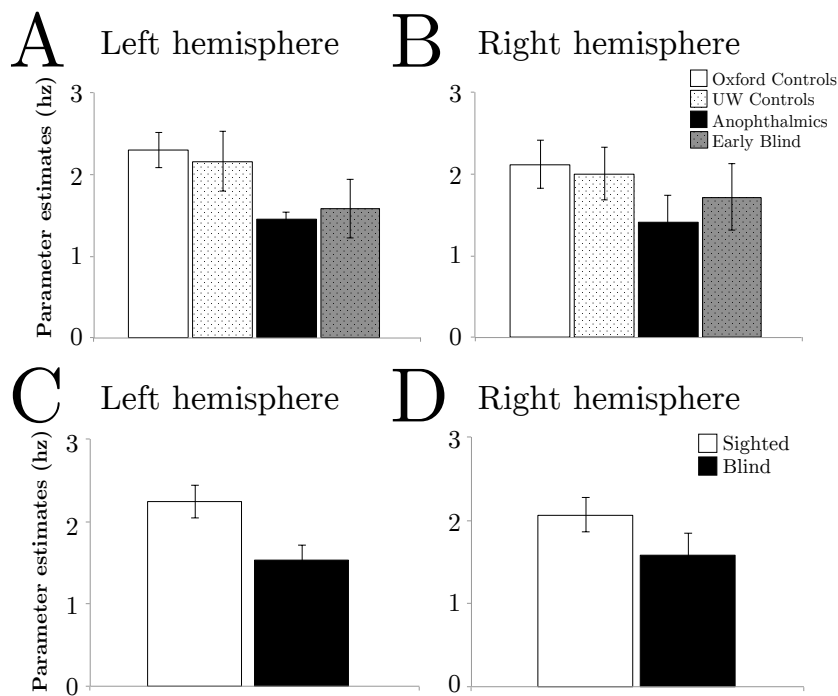


Figure 25: Connection from MGN to A1 in Model 4. **Panels A and B** show the left and right hemisphere connections for each subject group, and **panels C and D** show left and right hemisphere connections for the pooled ‘blind’ and ‘sighted’ groups. Error bars represent the standard error of the mean.

firstly for each group separately (**A** and **B**) and secondly for the pooled ‘sighted’ and ‘blind’ groups (**C** and **D**). This connection is the traditional subcortico-cortical route for auditory information to the primary auditory cortex and was robust in all subject groups. However, the strength of MGN to A1 connections was slightly reduced in the blind group compared to the sighted group, although this difference was not significant in the right hemisphere ($t(22) = 1.44$, $p = 0.164$) and did not survive Bonferonni correction for multiple comparisons in the left hemisphere ($t(22) = 2.39$, $p = 0.026$).

MGN to V1 connections in both hemispheres are shown in **Figure 26**, for each group separately (**A** and **B**) and for the pooled ‘sighted’ and ‘blind’ groups (**C** and **D**). This connection would not be expected to be robust in sighted groups, but may be in the blind subjects. Indeed, MGN to V1 connections were significantly higher in the blind group in both hemispheres (left hemisphere, $t(22) = -4.31$, $p = 0.0003$; right hemisphere, $t(22) = -2.68$, $p = 0.014$). In the right hemisphere, the anophthalmic MGN to V1 connection was affected by one negative value (a subject whose data did not fit as well to Model 4), therefore skewing the already small sample size.

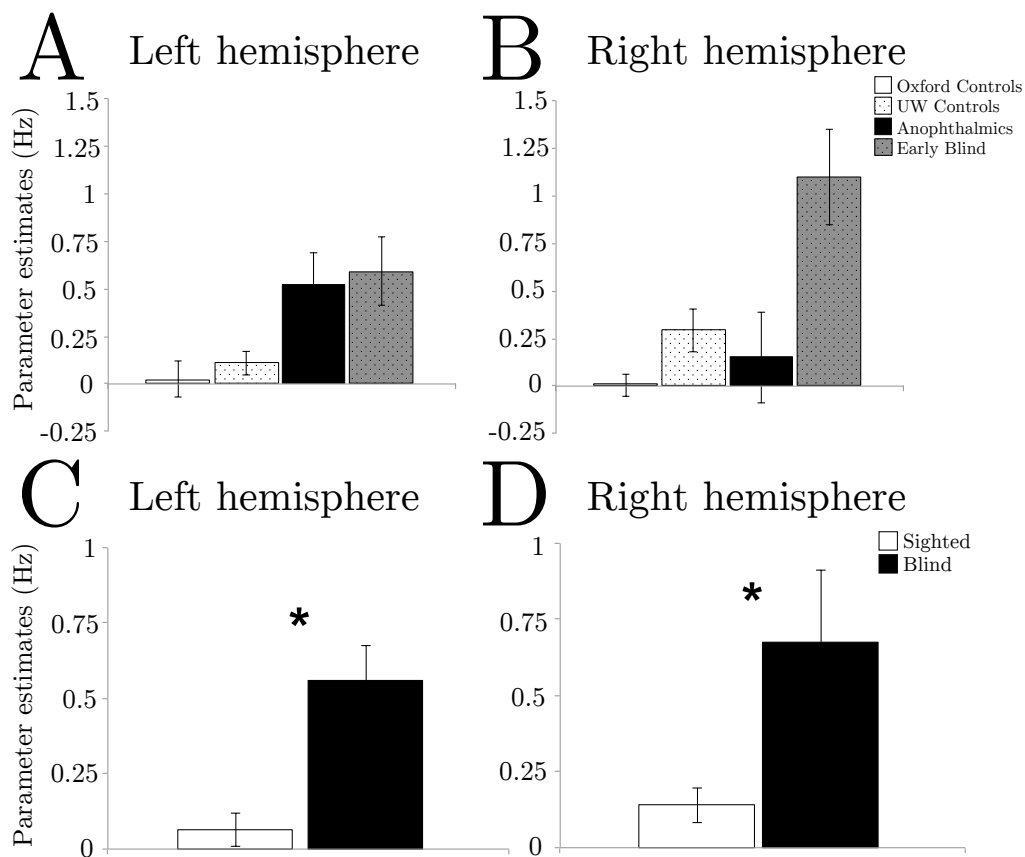


Figure 26: Connection from MGN to V1 in Model 4. **Panels A** and **B** show the left and right hemisphere connections for each subject group, and **panels C** and **D** show left and right hemisphere connections for the pooled 'blind' and 'sighted' groups. Error bars represent the standard error of the mean. Two-tailed independent-samples t-tests compared sighted and blind groups, and a star indicates statistical significance after Bonferonni correction for multiple tests. MGN to V1 connections were significantly stronger in the blind compared to the sighted group.

4.4.2 Model Space 2

Model comparison (random-effects BMS) of the three models containing the superior colliculus (SC) and area V5/MT+ was performed in the anophthalmic and early blind groups separately. Although limited by sample size (data from two anophthalmic and one early blind participant did not fit to any of the models), **Figure 27** shows that Model 2, with direct SC to pericalcarine cortex (V1) connections, best explained the anophthalmic data. The

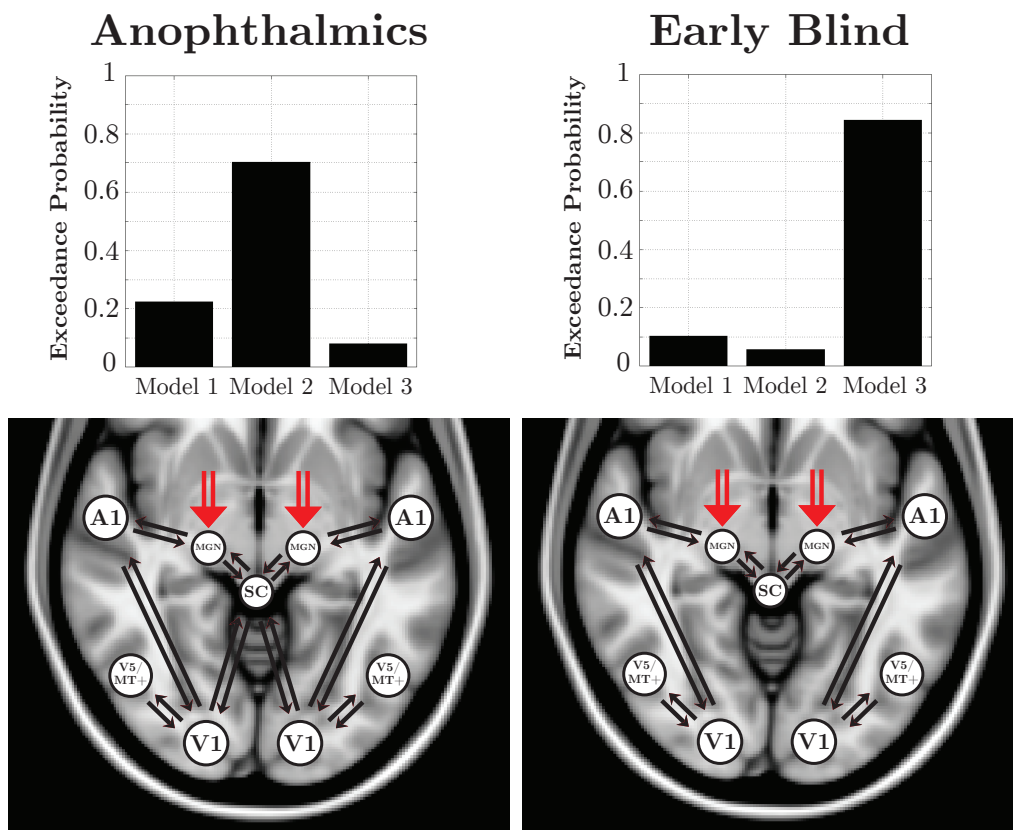


Figure 27: Results of model comparisons (random-effects BMS) in Model Space 2. The bars in each plot show the exceedance probability for the three models in the anophthalmic (left) and early blind (right) groups. Below each plot is a schematic diagram of the winning model on an axial slice of the MNI standard brain (at $z = -6$).

early blind data was best explained by Model 3, which did not contain direct subcortical connections to the occipital cortex and instead relies on cortical connections from the primary auditory cortex (A1).

4.5 Discussion

Using an fMRI task for auditory thalamus localisation, Chapter 3 revealed robust auditory responses in both auditory and visual subcortical structures in anophthalmic and early blind individuals. Dynamic causal modelling investigated the possible routes for these subcortical auditory responses to reach pericalcarine cortex (V1 in sighted subjects). In the first model space, the Klinge et al. (2010) model that did not contain A1 to V1 cortico-cortical connections (Model 4) provided the best fit to all sighted and blind data. Whilst MGN to A1 connections within this model were slightly stronger in sighted subjects, MGN to V1 connections in both hemispheres were significantly stronger in the blind compared to the sighted group. A second, more detailed model space was designed in order to include the superior colliculus, since this structure responds to sound in both blind groups (Chapter 3). In this second model space, the early blind data was best explained by a model that contained only cortico-cortical connections from A1 to V1 (Model 3), thus contradicting the findings in the first model space but in line with Klinge et al. (2010). In contrast, the anophthalmia data best fit to a model with additional subcortico-cortical connections between the superior colliculus and V1 (Model 2). DCM can only infer potential connections between regions

based on causality in fMRI data, and therefore does not necessarily describe the "real" underlying anatomy. Furthermore, with the small group sizes and low statistical power, it is difficult to draw meaningful conclusions from these results. The chapter's limitations, areas for future work, and a few speculative theories as to differences between anophthalmia and early blindness are discussed below.

4.5.1 Limited experimental power

In the first model space, data from one anophthalmic and two early blind participants did not fit to any of the defined models and were therefore excluded from any further analyses. In the second model space, data from two anophthalmic participants and one early blind participant did not fit to any of the models. The resulting small sample sizes introduce important concerns regarding the power of the modelling. It is also important to note that the results presented in Klinge et al. (2010) are drawn from a very large fMRI dataset acquired with continuous imaging. Although sparse sampling does provide several acoustical benefits (see Chapter 3) and has previously been applied to DCM (Kumar et al., 2007), the reduced experimental power and short runs used in this case (6 minutes each) are perhaps not ideal for this type of analysis. This limited experimental power may help to explain why the data from some anophthalmic and early blind participants did not fit to the models. However, across the small number of subjects included in the chapter, it is interesting that the evidence in favour of the winning models is consistent.

4.5.2 Model Space 1 different from Klinge et al. (2010)

In the first model space, Bayesian model selection revealed that Model 4 (lacking A1 to V1 connections) outperformed all of the other models, whilst the fully connected model (Model 1) was the clear winner in Klinge et al. (2010). This difference could be due to a number of factors which are discussed below.

Firstly, it is important to note that auditory stimuli and timeseries selection could be a source for variability between the present data and the data described in Klinge et al. (2010). The authors in that study found significant V1 activation in almost all sighted subjects; this may be because their auditory stimuli of emotional voices evoked imagery in sighted subjects. With this in mind, the A1 to V1 connectivity could be important in their sighted as well as blind data to explain these occipital auditory responses. Replicating the Klinge et al. (2010) paper has been problematic because whilst robust responses were found in MGN and A1 for all subjects, rather predictably there was very little significant occipital (V1) activation in sighted subjects during the auditory task used here. It could be argued that performing DCM on V1 coordinates primarily activated in blind subject groups could be biasing estimates of connectivity in this region. DCM is designed to explain responses that result from experimental manipulation, therefore timeseries should show significant activation in relation to the experimental paradigm (Stephan et al., 2010). However, model space 1 was intended to replicate the Klinge et al. (2010) models and therefore the sighted groups were included.

Furthermore, Model 4 outperformed the other models in both the sighted and blind groups, suggesting some uniformity and role of V1 across all subject groups.

Secondly, it could be that the simpler model 4 is more appropriate for the present data. Here, the MGN to A1 connections are robust in both sighted and blind subject groups, and MGN to V1 connections are robust in blind subjects. However, the A1 to V1 connection may not be consistent both within and between subjects, therefore this additional connectivity may be introducing too much variability and complexity to the model space.

4.5.3 MGN to A1 and V1 in Model Space 1

In the present data, anophthalmia and early blind connectivity values were not significantly different and were therefore combined into one blind group in order to improve power. The only possible difference between groups could be the strength of right hemisphere MGN to V1 connections (see **Figure 26 B**). However, this is likely driven by one outlier anophthalmic participant. Since only four of the five anophthalmic participants were included in this analysis, one outlier would have a considerable impact on the average.

In the “winning” Model 4, the strength of connections from MGN to A1 was greater in the sighted subjects compared to the blind subject groups. Although this difference was not significant after correction for multiple comparisons, it is interesting to note that this may be related to reduced A1 BOLD signal compared to sighted controls, as found by some studies in early

blind (Gougoux et al., 2009; Klinge et al., 2010) and anophthalmic (Watkins et al., 2013) subjects. It has been argued that this reduced auditory activity (and possibly weakened connections) within the auditory system of blind individuals could be due to the shift towards an auditory network which includes occipital areas (Röder et al., 1999).

In Klinge et al. (2010), the strength of connections between MGN and V1 was not significantly different between groups. Here, these connections were significantly stronger in both hemispheres of the blind compared to the sighted group. Although direct statistical comparisons across DCM model spaces cannot be made, this difference is interesting to note descriptively. It may be that the significant finding in the present data is because the auditory stimulus used here was designed for robust auditory thalamic responses at an individual subject level, and therefore may be better tailored for investigating subcortical connectivity. Perhaps there were significant differences in MGN to V1 connectivity in Klinge et al. (2010) but that these were masked by low signal in subcortical regions.

This finding of a strengthened MGN to V1 connection in early-onset blindness is in line with a tracing study demonstrating additional subcortico-cortical connections from non-visual thalamic nuclei (including the MGN) to the occipital cortex in enucleated animals (Karlen et al., 2006). Although several structural studies have noted degeneration of the LGN as well as the optic radiations in visually deprived subjects (Bridge et al., 2009; Noppeney et al., 2005; Shimony et al., 2006), it is unclear whether these degenerated connections can retain some functionality. If so, perhaps the MGN recruits

these connections from the neighbouring degenerated LGN in order to send auditory input to the pericalcarine cortex.

4.5.4 Superior colliculus to V1 in anophthalmia but not early-onset blindness

As described in the previous chapter, both anophthalmic and early blind groups showed significant auditory-evoked responses in the superior colliculus, a multimodal but predominantly visual subcortical structure. The second model space in this chapter was designed to test the blind data on extended DCM models, in order to determine whether more detailed models containing information about other structures responding to sound could reveal differences between the two blind groups. These models combined both hemispheres and contained the superior colliculus and V5/MT+ as additional regions of interest.

Interestingly, this model space showed a small difference between the anophthalmic and early blind groups. Data from the anophthalmia group best fit to a model that directly connected the superior colliculus with the occipital cortex (V1) in addition to cortico-cortical connections between A1 and V1. In contrast, data from the early blind group best fit to a model with only cortico-cortical connections between A1 and V1. Whilst this contradicts the optimal model selected in model space 1, it is in line with the strengthened A1 to V1 connection in early blind subjects in Klinge et al. (2010). It may be that extra information provided by the additional regions of interest help to better

explain the interactions between subcortical and cortical structures during auditory processing, and therefore differences between the two groups could be revealed. It may also be that whilst both blind groups utilise direct MGN to V1 connections, there are additional superior colliculus to V1 connections in anophthalmia specifically. However, it is important to note that DCM models containing different regions of interests cannot be compared directly (Stephan et al., 2010).

Exceedance probabilities for the winning models are not as high in the second model space, but this may be due to the small numbers in the two blind groups. Data from two anophthalmic and one early blind individual did not fit to any of the three defined models and were therefore excluded from Bayesian model selection. Whilst there was little inter-subject variability in the small subject groups and similar exceedance probability values have previously been reported (Collignon et al., 2013), small sample sizes and low statistical power prevent any further conclusions from being made regarding the implications of these results.

4.5.5 Anophthalmia as compared to early blindness

Whilst superior colliculi responses to auditory stimulation were found in both anophthalmic and early blind groups (see Chapter 3, **Figure 14**), typically 'visual' connections may be relaying these auditory responses directly to the pericalcarine cortex only in anophthalmia. This is based on anatomical evidence of remaining direct connections between the superior colliculus and

primary visual cortex in anophthalmic (ZRDCT/An) mice, despite not needing them for visual information (Chabot et al., 2008). In human bilateral anophthalmia, the absence of eyes means that the visual pathway does not experience prenatal retinal activity. Pre-natal influences likely include spontaneous retinal waves, which are thought to be instructive for the refinement of visual pathway connections. If this pre-natal activity is absent, subcortical visual structures and connections normally refined by this activity could be recruited for other sensory functions. It may be that superior colliculus to V1 connections have not been pruned in anophthalmia, possibly because the lack of eyes meant they were not refined in pre-natal development for visual input and could therefore be recruited instead for auditory information.

In contrast, auditory inputs in early blindness may rely on the traditional subcortico-cortical auditory route from MGN to A1 and then to V1 via cortico-cortical connections. This is based on the current literature on cortico-cortical effective connectivity in early blindness (Collignon et al., 2013; Klinge et al., 2010) and transcranial magnetic stimulation studies suggesting that cortico-cortical connections drive cross-modal auditory inputs to the blind occipital cortex (Collignon et al., 2007; Ptito et al., 2008). It may be that the superior colliculus responses to sound in the early-blind group feedback to the medial geniculate nucleus, or perhaps the neighbouring inferior colliculus, rather than directly projecting to the occipital cortex.

Previous work suggests that reorganisation at the level of the cortex may differ between anophthalmic and early blind individuals, and it may be that these differences are due to altered subcortical inputs to the cortex. For

example, in anophthalmic subjects the pericalcarine cortex (V1) appears to be performing low-level auditory processing and does not distinguish between language and backwards speech (Watkins et al., 2012), whilst it does for early blind subjects (Bedny et al., 2011). In early blindness, cortico-cortical connectivity with A1 could result in a reversed hierarchical organisation of auditory processing in the occipital cortex (Büchel, 2003). In anophthalmia however, perhaps subcortico-cortical auditory connections between the superior colliculus and the occipital cortex preserve a traditional processing hierarchy. Further investigations into the modular organisation of auditory processing within the anophthalmic occipital cortex could investigate this.

4.5.6 Conclusions

In conclusion, dynamic causal modelling has suggested some potential changes in the strength of subcortico-cortical connections in anophthalmia and early-onset blindness. However, due to limited statistical power and small group numbers, it is difficult to draw meaningful conclusions from these findings alone. Larger group sizes that replicate these results will be needed in order to show that auditory subcortico-cortical connections may be influencing cross-modal inputs to the visually deprived occipital cortex, either via the auditory thalamus or the superior colliculus.”

PART II:

**NEUROCHEMICAL,
NEUROANATOMICAL,
AND BEHAVIOURAL DATA**

5 Neurochemical changes in the pericalcarine cortex in anophthalmia

5.1 Summary

Congenital blindness is known to lead to large-scale functional and structural reorganisation in the occipital cortex, but relatively little is known about the neurochemical changes underlying this cross-modal plasticity. In order to investigate the effect of complete and early visual deafferentation on the concentration of metabolites in the pericalcarine cortex, ^1H magnetic resonance spectroscopy (MRS) was performed in five subjects with congenital bilateral anophthalmia and sixteen sighted subjects. In the pericalcarine cortex, where the primary visual cortex (V1) is normally located, choline was considerably elevated in all anophthalmic subjects relative to sighted controls. Consistent with previous studies, the pericalcarine cortex of the anophthalmic subjects was significantly thicker than that of sighted subjects, and a large proportion of the MRS voxel was grey matter. Increased choline and cortical thickness, which resembles the profile of the cortex at birth, suggests that the lack of visual input from the eyes may have affected the maturation of this cortical

region. Thus, the absence of the eyes in anophthalmia, and resulting lack of pre-natal sensory stimulation (e.g. spontaneous retinal waves) to the occipital cortex, may affect both the structure and neurochemistry of the occipital cortex and prevent the normal pattern of maturation of the pericalcarine cortex.

5.2 Introduction

As discussed in the previous chapters, there is considerable evidence of cross-modal reorganisation in the blind ‘visual’ pathway (Bavelier and Neville, 2002; Merabet and Pascual-Leone, 2010). Reorganisation of the occipital cortex for auditory and tactile processing has been demonstrated in a diverse range of neuroimaging and behavioural studies (for a review, see Voss (2013)), and is accompanied by structural (Bridge et al., 2009; Shimony et al., 2006) and metabolic (Gougoux et al., 2005; Goyal et al., 2006; Piovesan et al., 2002; De Volder et al., 1999) changes. However, while neurochemical changes have been well documented in animal models of visual deprivation, relatively little is known about such changes in the occipital cortex of blind humans.

Animal models provide a framework for understanding the neurochemical mechanisms that may mediate the extensive functional and structural reorganisation of the occipital cortex as a result of blindness. They suggest that reorganisation is driven by changes to the inhibitory and excitatory pathways that underlie the development of the occipital cortex. Occipital cortex excitability is thought to increase following visual deprivation because

of an up-regulation of cholinergic pathways; models of dark-reared kittens show increased choline acetyltransferase (a cholinergic marker) in primary and extrastriate visual areas (Fosse et al., 1989). This is combined with an attenuation of the inhibitory GABAergic circuits in dark-reared kittens (Fosse et al., 1989) and rats (Benevento et al., 1995). Thus, early-onset blindness seems to result in attenuated inhibitory circuits and strengthened cholinergic transmission; these alterations increase cortical excitability, and may also maintain the cortex in a more ‘plastic state’ (Bavelier and Hirshorn, 2010). However, it has not yet been investigated whether similar neurochemical changes occur in humans with congenital bilateral anophthalmia.

In humans, neurochemicals can be quantified within a localised region of tissue using ^1H magnetic resonance spectroscopy (MRS). Application of this method has allowed investigations of neurochemical differences in the occipital lobe of human subjects who are blind (Bernabeu et al., 2009; Boucard et al., 2007; Weaver et al., 2013). The earliest study by Boucard and colleagues (Boucard et al., 2007) found no difference in any measured metabolites when comparing patients with degenerative visual disorders (acquired glaucoma and age-related macular degeneration) with sighted subjects. In contrast, again investigating subjects with predominantly acquired blindness, Bernabeu et al. (2009) found an increase in concentrations of myo-inositol, a marker of glial cell activity, in the primary visual cortex. The only study to investigate neurochemical changes due to early blindness found increased levels of myo-inositol, but also choline and creatine+phosphocreatine (MRS measure of total creatine [tCr]) and decreased levels of GABA (although this difference

was not significant following correction for multiple comparisons) (Weaver et al., 2013). No significant changes were found in glutamate or NAA (N-Acetylaspartate). The inconsistencies among this previous body of work most likely reflect effects due to the variability in age at blindness onset and extent of vision loss.

This chapter used a combination of MRS and structural MRI to examine the neurochemical effects of blindness due to anophthalmia. As mentioned in earlier chapters, both eyes fail to develop in anophthalmia and thus there is no pre- or post-natal stimulation of the visual system. Given that there is no other neurological impairment in the anophthalmic cases presented in this thesis, they are an ideal population to study the effects of sensory deprivation on healthy brain tissue. It was hypothesised that in anophthalmia (unlike early blindness), neurochemical changes would reflect differences in cortical maturation due to the complete absence of input from the eyes. Using this unique population, this chapter aimed to correlate previously described structural differences (Bridge et al., 2009) with a novel investigation of neurochemical changes to help understand the considerable functional changes evident in these subjects (Watkins et al., 2012, 2013). Answering this question is important because it will provide direct evidence regarding the underlying mechanisms that allow the 'visual' pathway to reorganise for auditory processing in anophthalmia.

5.3 Methods

5.3.1 Participants

The five anophthalmic participants previously described in the General Methods chapter were included in this experiment (for case descriptions, see **Table 1** in Chapter 2), as well as sixteen age-matched controls with normal or corrected-to-normal vision (mean age 27.6 years, range 23-37). This study was granted ethical approval by the Oxford University Central Ethical Committee and all subjects gave informed written consent prior to participation.

5.3.2 MR imaging acquisition

All scans were performed using a Siemens Verio 3-Tesla whole body MRI scanner and a 32-channel coil at the Functional Magnetic Resonance Imaging of the Brain Centre (University of Oxford).

¹H magnetic resonance spectroscopy (MRS) was performed using a single voxel (2 x 2 x 2 cm) placed over the occipital midline of each subject, centered on the calcarine sulcus (primary visual cortex in sighted controls). The voxel was positioned medially and was large enough to cover as much of the V1 region as possible whilst avoiding signal contamination from fat and lipids of the skull (**Figure 28 A**). In 2 mm MNI standard space, the mean central coordinates (and standard deviation) across all subjects were $x = +0.8$ (3.6), $y = -79$ (4.03), $z = +13$ (16.1).

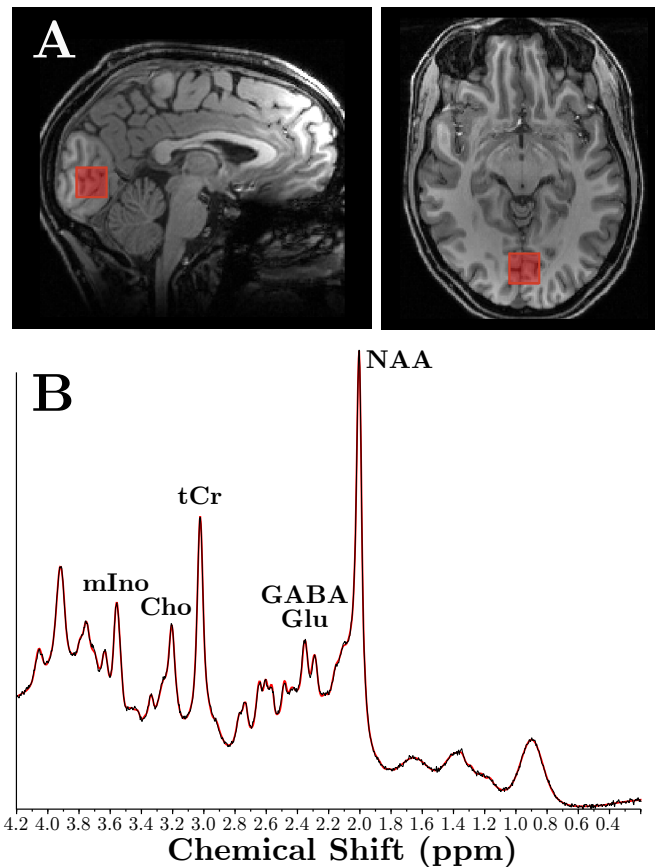


Figure 28: MRS voxel placement and spectra. **A** Example voxel placed over the occipital cortex midline in a sighted control subject. **B** Example spectra for the control subject, with the primary peaks for total creatine (tCr), choline (Cho), glutamate (Glu), GABA, myo-Inositol (mIno) and N-Acetyl-aspartate (NAA).

A SPECIAL sequence (SPin ECho full Intensity Acquired Localised spectroscopy) was employed ($TR=4$ s, $TE=8.5$ ms, flip angle= 90° , spectral width=2 kHz, 128 averages), as the short echo-time (TE) allows for an optimisation of the signal-to-noise ratio (SNR) whilst reducing signal attenuation. This enables identification of a wide range of neurochemicals, beyond the three main resonances (N-acetylaspartate, creatine and choline) which would otherwise be undetected with a longer echo-time (Kanowski et al., 2004). In addition, the SPECIAL sequence is designed to acquire signal from a full

magnetisation, thus taking advantage of these short echo-time benefits without the signal loss usually found with other short echo-time sequences (Mekle et al. (2009), see Chapter 2 for more details).

A high-resolution T1-weighted MPRAGE image was acquired for accurate MRS voxel placement and subsequent structural analyses (TR=2 s, TE=4.7 ms, flip angle=8°, 192 transverse slices, 1 mm isotropic voxels).

5.3.3 Data analysis

¹H magnetic resonance spectroscopy (MRS) MRS data were processed with LCmodel (Provencher, 1993) using a simulated basis set consisting of 22 individual metabolite basis spectra, as described elsewhere (Near et al., 2013). Spectra obtained from sequences with short echo-time are generally difficult to quantify, due to an overlap between neurochemical signals as well as potential interferences from lipids and macromolecules. However, the LC model employs a “black box” approach that accurately fits the spectra acquired *in-vivo* with MRS (within the frequency domain) based on spectra obtained *in-vitro* in identical conditions (Kanowski et al., 2004).

Absolute neurochemical concentrations were extracted from an average of 128 water-suppressed and drift-corrected runs (Near et al., 2014). Resonances were assigned according to their known ¹H chemical shift along the spectrum (x-axis, in parts per million); N-Acetylaspartate (NAA), gamma-aminobutyric acid (GABA), glutamate (Glu), total creatine (tCr), choline (Cho), and myo-inositol (mIno) (**Figure 28 B**). Neurochemical concentra-

tions are proportional to the total area under the curve of the peaks on the spectrum.

T1-weighted structural images were brain-extracted and tissue-type segmented using the FMRIB Software Library (FSL)'s Brain Extraction Tool (Smith, 2002) and FMRIB's Automated Segmentation Tool (Zhang et al., 2001). The percentage grey matter, white matter, and cerebrospinal fluid (CSF) within the MRS voxel were calculated from the resulting images to permit a correlation between GABA concentration and the grey matter fraction of the voxel, and to allow grey matter fraction to be used as a co-variate.

As customary, neurochemical values were reported as a ratio to total creatine (tCr). It is a standard practice to use simultaneously acquired metabolites, such as creatine, as references in order to reduce inter-subject variability and control for any problems with water suppression during data acquisition (Stagg, 2013). The blind and sighted groups did not differ in total creatine concentration, referenced to water (unlike Weaver et al. (2013)). Since all metabolites were normalised to tCr, no correction for CSF fraction was required.

Cortical thickness T1-weighted structural images were also analysed using Freesurfer (Dale et al., 1999) (<http://surfer.nmr.mgh.harvard.edu>). These images were segmented into tissue types (Fischl and Dale, 2000) and average cortical thickness values were calculated from those areas that can be reliably defined based on anatomical features (Brodmann area 17, extrastriate visual area MT, primary auditory cortex, primary somatosensory cortex (Brodmann

areas 3a and 3b) and primary motor cortex (Brodmann areas 4a and 4p)).

Statistical analysis Statistical analyses on all neurochemical and structural measurements were performed using SPSS (SPSS Version 20 for Mac). Two-tailed independent t-tests compared group neurochemical ratios and structural values, with results considered statistically significant at $p < 0.05$. Homogeneity of variance was confirmed by Levene's test for equality of variances.

5.4 Results

5.4.1 ^1H magnetic resonance spectroscopy (MRS)

Concentrations of the five neurochemicals of interest (myo-inositol, choline, glutamate, GABA and NAA) within the pericalcarine cortex were compared between the sighted and anophthalmia groups. As noted above, there were no significant differences between the controls and anophthalmia groups in total creatine (tCr) levels used as the reference metabolite ($t(19) = -0.11$, $p = 0.916$). **Table 3** shows mean concentrations (ratio to tCr) for the five metabolites of interest, standard errors, percentage difference between groups, and results of the independent t-tests before Bonferroni correction for the five comparisons made. To illustrate relative concentrations for the individual subjects with anophthalmia, anophthalmia data points were normalised to the control mean and presented in **Figure 29** as z-scores.

Table 3: Mean levels of the five neurochemicals of interest for the sighted and anophthalmia groups. Standard errors, percentage differences and independent t-test results are reported.

	Controls		Anophthalmia		% Difference	Independent t-tests	
	Mean	SEM	Mean	SEM		T-value	p-value
Choline/tCr	0.109	0.002	0.134	0.005	19.1 %	-5.658	0.00002*
NAA/ tCr	1.507	0.036	1.377	0.027	-9.5 %	1.955	0.066
GABA/ tCr	0.184	0.007	0.175	0.013	-5.0 %	0.575	0.572
Glutamate/ tCr	0.928	0.018	0.972	0.016	4.5 %	-1.278	0.217
Myo-Ins/ tCr	0.650	0.013	0.687	0.034	5.4 %	-1.263	0.222

* survives Bonferonni correction

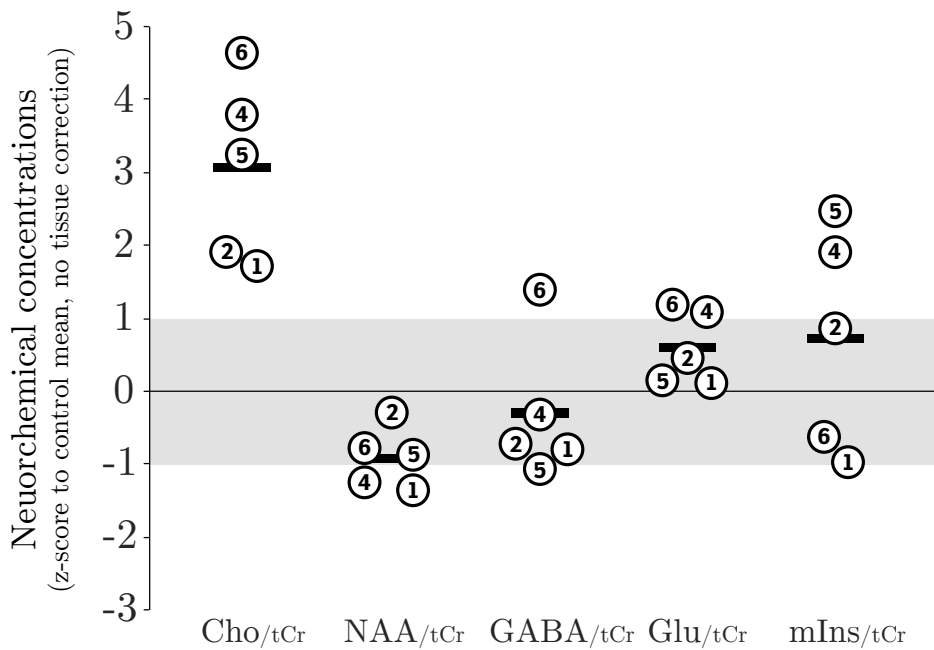


Figure 29: Neurochemical concentrations in pericalcarine cortex. For display purposes, z-scores for each anophthalmic participant (relative to sighted control) for the five neurochemicals of interest are presented here. The grey band indicates one standard deviation above and below the control mean.

The anophthalmia group showed significantly higher concentrations in choline/tCr compared to sighted controls ($p < 0.00005$) that survive Bonferroni correction. Indeed, all five anophthalmic subjects had choline/tCr concentrations that exceeded the mean + one standard deviation range of the sighted controls (see **Figure 29**). N-Acetylaspartate (NAA/tCr) was marginally lower in the anophthalmic subjects ($p = 0.066$), while there were no significant differences between groups for GABA/tCr, glutamate/tCr, or myo-inositol/tCr (see **Table 3**).

5.4.2 Cortical thickness and grey matter fraction

As previously shown (Bridge et al., 2009), the cortex in BA17 (representing V1) was significantly thicker in anophthalmic compared to sighted subjects (control mean = 1.65 mm^3 (SEM 0.03), anophthalmia mean = 1.99 mm^3 (SEM 0.09); $t(19) = 4.76$, $p < 0.0005$). In contrast, none of the other anatomically-defined primary sensory, primary motor or extrastriate (MT) regions showed any difference in cortical thickness between the anophthalmic and control subjects (**Figure 30 A**).

Given the difference in cortical thickness between the anophthalmic group and controls, it is not surprising that there was also an increase in the fraction of the MRS voxel contents assigned as grey matter (control mean = 0.55 (SEM 0.01); anophthalmia mean = 0.63 (SEM 0.01); $t(19) = 3.7$, $p < 0.005$). Since some metabolites may have different concentrations in grey and white matter, further analyses were designed to determine the effect of

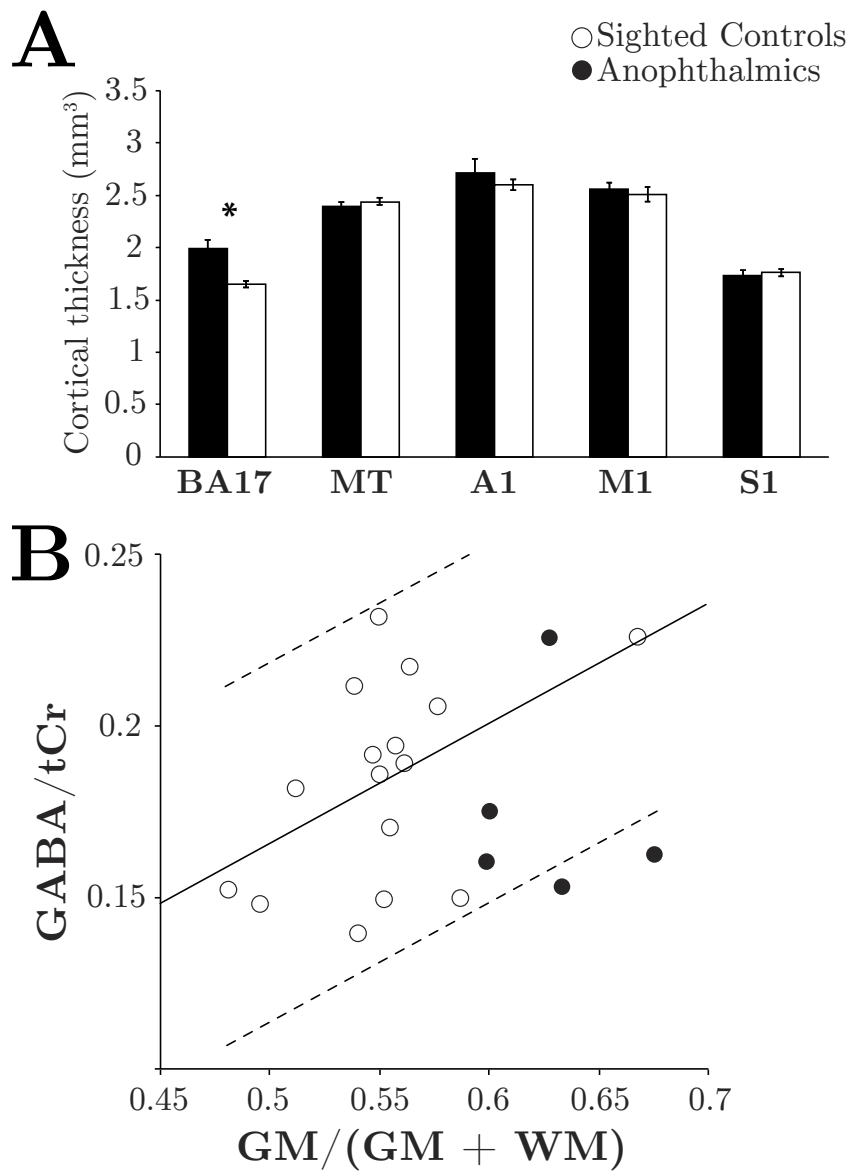


Figure 30: Cortical thickness. **(A)** Cortical thickness in Brodmann Area 17, extrastriate visual area MT, primary auditory cortex (A1), primary motor cortex (M1, according to Brodmann Areas 4a and 4p), and primary somatosensory cortex (S1, according to Brodmann Areas 3a and 3b). Error bars represent the standard error. A star between columns denotes a significant difference between groups. **(B)** GABA/tCr levels plotted against grey matter fraction for the sighted (white circles) and anophthalmic subjects (black circles). The solid line shows the positive correlation between grey matter fraction and GABA/tCr levels in the sighted control data and the dotted lines show +/- two standard deviations from the best fitting regression line.

different grey matter content. Firstly, to determine the effect of grey matter fraction on GABA content, the GABA/tCr levels are plotted against grey matter fraction in **Figure 30 B**. As suggested by the previous literature (Bhattacharyya et al., 2011), sighted subjects (white circles) show a non-significant positive correlation ($r = 0.49$; $p = 0.057$) between grey matter fraction and GABA/tCr levels. The values for the anophthalmic subjects are shown as black circles; two subjects fall below the dotted line representing two standard deviations below the best fitting regression line. One subject lies on the least squares line fit to the control data. This is consistent with the data shown in **Figure 29** where the same anophthalmic subject has considerably higher GABA/tCr levels than the other four. The correlation between grey matter fraction and the other metabolites was also plotted (see **Figure 31**).

In a second analysis, metabolite values were compared between the two groups while adding demeaned grey matter fraction as a co-variate. Choline remained significantly greater in the anophthalmic group ($F(2,18) = 15.87$, $p = 0.001$), NAA was significantly lower in the anophthalmic group ($F(2,18) = 8.08$, $p = 0.01$) and GABA was marginally lower in the anophthalmic group ($F(2,18) = 2.36$, $p = 0.14$). There were no differences between the groups for glutamate, myo-inositol or total creatine.

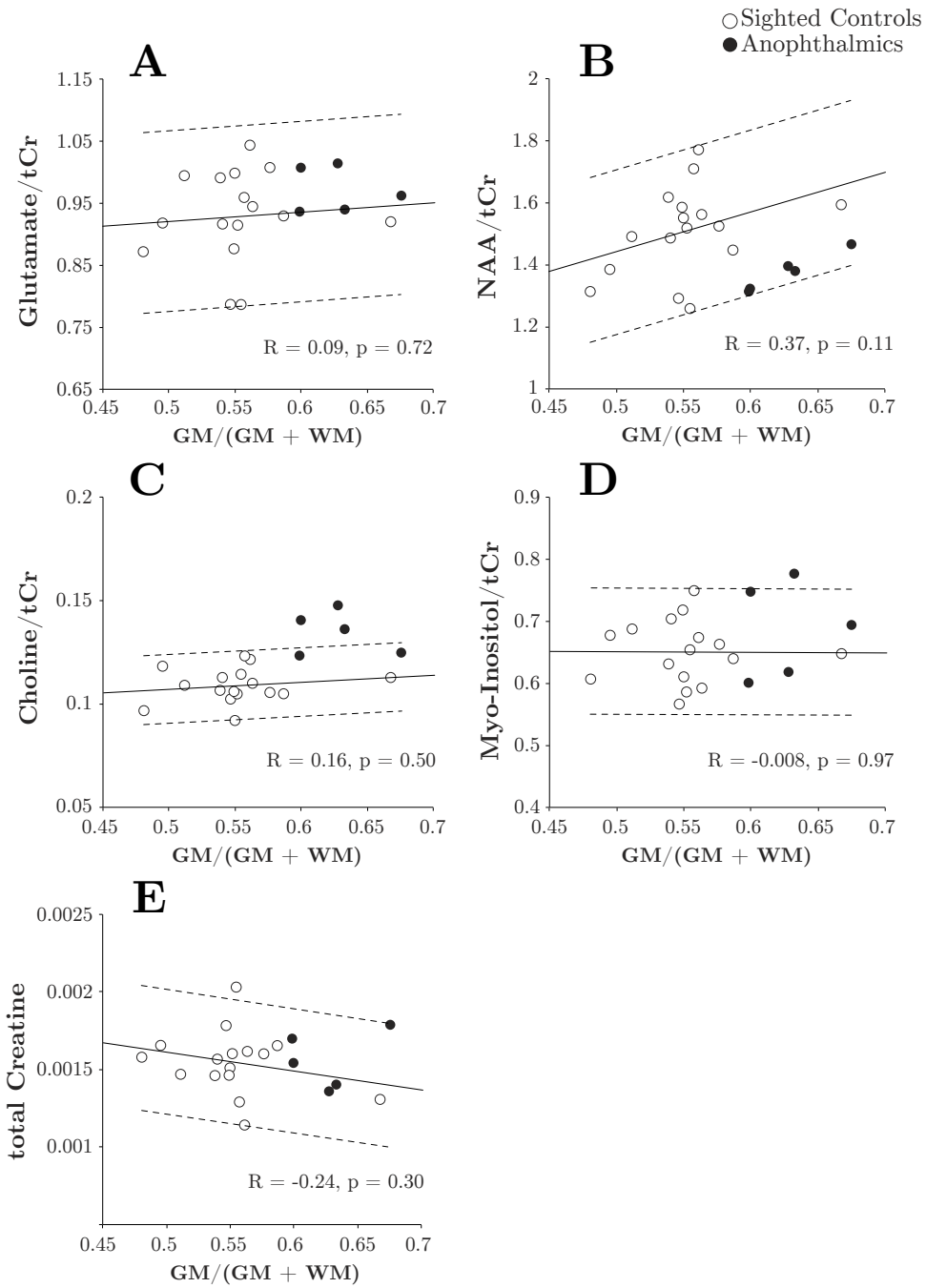


Figure 31: Metabolite levels plotted against grey matter fraction for the sighted (white circles) and anophthalmic subjects (black circles). The solid line shows the positive correlation between grey matter fraction and metabolite levels in the sighted control data, and the dotted lines show +/- two standard deviations from the best fitting regression line.

5.5 Discussion

In-vivo neurochemical assessment of the pericalcarine cortex in anophthalmia revealed significantly higher concentrations of choline compared to sighted controls. In contrast to individuals with acquired (Bernabeu et al., 2009) and some types of congenital (Weaver et al., 2013) blindness, the cortex of individuals with anophthalmia never receives retinal stimulation, and the findings in this chapter suggest that the neurochemistry of visual cortex may differ as a result. While the higher concentration of choline in anophthalmic subjects compared to sighted controls is consistent with Weaver et al., the data presented in this chapter did not show an increase in either total creatine or myo-inositol in the anophthalmia group, despite these chemicals being relatively easy to measure. In addition, structural analyses revealed a thicker pericalcarine cortex in anophthalmia compared to sighted controls; this increase was not found in any extrastriate regions or other primary sensory areas. The findings in this chapter from only a small sample of anophthalmic subjects further support earlier data that the lack of stimulation along the visual pathway significantly affects neurochemical circuits in the region of the occipital cortex where V1 is normally located. These results are important because they provide clues as to the altered developmental processes that may be taking place in the pericalcarine region in human bilateral congenital anophthalmia. Specifically, the results imply that pre-natal visual experiences are important for normal maturation of the occipital cortex. This functional reorganisation in anophthalmic occipital cortex could reflect “atypical” cross-modal plasticity (due to a lack of normal cortical maturation) rather than

adaptive plasticity (due to the absence of visual input).

5.5.1 Visual deprivation results in elevated choline levels

Consistent with reports from blind animals (Fosse et al., 1989; Dehay et al., 1996) and early blind individuals (Weaver et al., 2013), choline levels were elevated in the pericalcarine cortex of anophthalmic subjects. Choline is found in cell membranes and is usually considered a marker of membrane or structural integrity. In adulthood, increased choline is generally found in disease states as a marker of membrane breakdown, possibly due to demyelination. There are a variety of possible explanations for elevated choline in the anophthalmic cases described here (see also Weaver et al. (2013)). One possibility is that these elevated MRS choline concentrations represent cholinergic pathway activity. While acetylcholine is believed to be a very small component of the choline peak, it may provide a marker of cholinergic tone (Frederick et al., 1997; Satlin et al., 1997; Wang et al., 2008) since phospholipids play a key role in providing choline for acetylcholine synthesis (Wurtman et al., 1985; MacKay et al., 1996; Boulanger et al., 2000; Cantley, 2002; Suh and Hille, 2002; Belouèche-Babari et al., 2010). Cholinergic pathways are determined genetically, but their regulation and expression depends on whether there is visual input (Gu, 2003). Thus, these findings might reflect an up-regulation of activity in pericalcarine cholinergic circuits. Secondly, higher choline in the anophthalmic pericalcarine (V1) cortex could be explained by an increase in the number of cells, which would be consistent with the increased cortical thickness found in the same region.

Finally, elevated choline levels could represent some property of ‘immature’ cortex. Choline levels measured by MRS are high at birth and typically peak 3 months after birth. These levels gradually decrease following the onset of cortical maturation and pruning (Blüml et al., 2012). This period of maturation is also marked by a rapid increase in NAA in the first three months of development, followed by a gradual stabilisation in NAA levels (Blüml et al., 2012). This chapter found some evidence of lower levels of NAA in the anophthalmia group compared to sighted controls, although this is not as clear as the increase in choline.

5.5.2 Cortical thickness

As previously reported (Bridge et al., 2009), the pericalcarine cortex (defined here by Brodmann Area 17) was thicker in the anophthalmia group compared to sighted controls. This is also consistent with data from early-blind subjects (Jiang et al., 2009; Voss and Zatorre, 2012). The primary visual cortex is thought to undergo substantial pruning of inactive synapses during normal maturation; following the onset of visual experience, more spines are pruned than grow in V1 (Elston et al., 2009, 2010), resulting in a thinner cortex relative to the auditory and motor cortices (Fischl and Dale, 2000). This pruning process is thought to be controlled by sensory activity (Wong et al., 1993) in order to maintain and strengthen only functional or relevant connections. The findings in this chapter show that cortical thickness in the expected location for V1 was not reduced to the level of sighted controls. Cortical thickness was unaffected in anophthalmia extrastriate regions and

other sensory areas, suggesting that this effect is limited to the deafferented pericalcarine region where V1 is normally located. A thicker occipital cortex may be due to the lack of visual experience preventing the normal pruning or elimination of inefficient connections/synapses in this region (Jiang et al., 2009).

5.5.3 GABA and the effects of grey matter content

GABA has been shown to be lower in congenitally blind humans subjects (Weaver et al., 2013) and in dark reared animals (Fosse et al., 1989; Benevento et al., 1995). There is evidence that visually-deprived animals do not show the increase in occipital GABAergic inputs normally seen in sighted animals at the end of critical periods of development (Morales et al., 2002). As GABA is thought to play an important role in the timing of critical periods of development (Hensch et al., 1998), low levels of GABA in early blindness could reflect delayed or limited maturation or development of the visual cortex due to the lack of visual input (Pinto et al., 2010).

However, as described above, structural analyses revealed a thicker pericalcarine cortex in anophthalmia compared to sighted controls. There is considerable dispute over the relative concentration of some metabolites, including GABA and glutamate, in the grey and white matter. In particular, estimates of white matter/grey matter GABA concentrations range from 0.115 (Bhattacharyya et al., 2011) to 1.2 (Geramita et al., 2011), with a median of 0.24. Since the anophthalmic subjects studied here show significantly

greater grey matter content within the MRS voxel (related to increased BA17 cortical thickness), this makes it difficult to determine whether any subject differences were due to the different tissue composition or different metabolite concentration within the tissue. This particular issue was less of a concern for the study of Weaver et al. (2013) because that did not replicate the (well-established) finding of grey matter thickness in early blind individuals (Jiang et al., 2009). This is possibly because they used separate voxels for the left and right hemispheres, rather than a single voxel straddling the midline, which reduced the relative volume of V1 within their MRS voxels.

To investigate the effects of tissue composition, metabolite concentrations were plotted as a function of grey matter tissue fraction. For all metabolites, the correlation between metabolite concentration and grey matter fraction was non-significant in control subjects. For GABA/tCR, the correlation in control subjects was close to significant, and there was some indication of a trend towards anophthalmic subjects showing lower GABA/tCR per unit of grey matter volume (**Figure 30 B**).

Given the animal literature (Fosse et al., 1989; Benevento et al., 1995), it seems possible that the lack of a significant GABA effect in the current study and a small reduction in a previous study, which did not survive correction for multiple comparisons (Weaver et al., 2013), may be due to a combination of small subject numbers and the difficulty inherent in extracting reliable GABA concentrations. Indeed, the current study used a SPECIAL sequence that allowed quantification of a range of metabolites at the likely cost of reduced sensitivity for GABA (Mekle et al., 2009). Spectral editing sequences

such as MEGA-PRESS or MEGA-SPECIAL are more commonly used for measuring GABA *in-vivo* with MRS. Whilst the previous study by Weaver et al. (2013) did use a MEGA-PRESS sequence, their rest-retest reliability was low. However, it is also important to note recent evidence suggests that whilst spectral editing sequences like MEGA-PRESS may provide a more robust measure of GABA, GABA measured using the SPECIAL sequence is correlated with spectral edited GABA measures (Near et al., 2013).

5.5.4 Failure to see differences in total creatine and myo-Inositol

Unlike the previous study of the effects of early blindness on pericalcarine neurochemistry (Weaver et al., 2013), there were no group differences in either myo-Inositol or total creatine levels in anophthalmia. Myo-Inositol (the most common biological stereoisomer of inositol) is synthesised mainly within astrocytes, and heightened concentrations are generally interpreted as indicating increased glial number or size (Pellerin, 2005; Soares and Law, 2009). While this null result should be treated with caution (given the small anophthalmic sample size), one possible interpretation is that the up-regulation in metabolic processing which appears to occur in early blind subjects (Wanet-Defalque et al., 1988; Veraart et al., 1990; Uhl et al., 1993; De Volder et al., 1997) may be unaffected in anophthalmic individuals.

5.5.5 Conclusions

The combination of neurochemical and structural changes suggest that lack of eyes and stimulation along the visual pathway in anophthalmia has not triggered the normal pattern of maturation of the pericalcarine region where V1 is normally located, marked by cortical pruning and the end of the critical period. Such differences may underlie the substantial functional reorganisation found in this traditionally ‘visual’ region, in that the reorganisation reflects “atypical” cross-modal plasticity due to a lack of normal cortical maturation rather than adaptive plasticity due to the absence of visual input.

6 Auditory abilities in anophthalmia and correlations with occipital cortical thickness

6.1 Summary

This chapter investigates in more detail the auditory profile of bilateral congenital anophthalmia. In particular, how low-level auditory abilities may be affected by the loss of vision in very early development, and how these changes relate to reorganisation at the cortical level. Superior pitch and melody discrimination abilities were found in the five anophthalmic participants compared to eleven sighted controls. In addition, right pericalcarine cortical thickness was significantly correlated with performance on one of these melody discrimination tasks. These results replicate those previously reported in early blind individuals (Voss and Zatorre, 2012), and suggest that measures of neuroanatomical change after very early-onset blindness may indeed relate to some of the superior auditory abilities associated with visual deprivation.

6.2 Introduction

In addition to changes in structure, function and neurochemistry, early-onset blindness can be accompanied by superior non-visual abilities. How these changes relate to the functional and structural reorganisation of the occipital cortex is currently under investigation.

Superior abilities have been noted in several auditory domains, possibly as compensation for the absence of vision. On auditory tasks requiring low-level processing, for example pitch discrimination, early blind individuals have been shown to outperform sighted controls (Gougoux et al., 2004) and late blind individuals (Voss and Zatorre, 2012). One study has noted the higher number of blind compared to sighted musicians with absolute pitch (Hamilton et al., 2004), and recent evidence suggests that congenital and early blind individuals are better at detecting asynchronous beats compared to sighted individuals matched for musical experience (Lerens et al., 2014). There is also evidence demonstrating superior temporal order judgement (Stevens and Weaver, 2005), time interval discrimination (Muchnik et al., 1991), sensitivity to echo cues (Dufour et al., 2005) and auditory motion discrimination (Lewald, 2013) in blind individuals. Together, these types of changes in low-level auditory abilities may “translate” to higher-level auditory functions. Röder et al. (2000) recorded ERPs when congenitally blind and sighted subjects listened to semantically congruent and incongruent words. Interestingly, the typical wave elicited during semantic and lexical processing appeared sooner in the blind compared to the sighted subjects (Röder et al.,

2000). Furthermore, whilst blind and sighted subjects performed comparably on a word and pseudo-word task, the blind group had shorter reaction times (Röder et al., 2003). These results suggest that there may be a change in speech signal processing as a result of blindness, perhaps due to changes in low-level auditory perceptual skills described earlier being applied to higher-level tasks, rather than a “better” use of semantic information (Röder et al., 2003).

Additionally, some auditory abilities which are thought to be heavily reliant on visual calibration can appear unaffected by the lack of visual input. Lessard et al. (1998) found that early-blind subjects without residual vision could accurately map auditory space on the horizontal azimuth, and that half of these subjects were considerably better at monaural localisation than sighted subjects. Superior monaural localisation in blind subjects has been studied extensively (Leclerc et al., 2000; Doucet et al., 2005; Gougoux et al., 2005; Voss et al., 2004). However, it is possible that these results are dependent on specific task requirements and task difficulty, and that any changes to the stimuli or task may drastically affect performance. When tested in central space using a more complex task, Gori et al. (2014) found that early blind individuals were severely impaired at localising sounds. The authors tested the ability of these subjects to localise sounds relative to others in space using a spatial bisection task, during which participants had to judge the position of a sound relative to two others in central space (+ or - 25 degrees). Congenitally blind individuals were considerably worse than sighted controls, with some entirely unable to perform the task (Gori et al.,

2014). It may be that vision and multimodal integration is necessary to develop the topographic representations of space needed for this type of task (Schmid et al., 2007; Pasqualotto and Proulx, 2012).

There is some evidence that superior auditory abilities are linked to the occipital cortex's extensive reorganisation in the absence of visual input. Most of the literature has focussed on whether improved auditory abilities are related to recruitment of the occipital cortex for sound processing, either by correlating occipital activity with performance on auditory tasks or by measuring how auditory abilities are affected by temporary disruption of the occipital cortex. The early blind individuals that demonstrated superior monaural localisation in Lessard et al. (1998) also showed auditory ERPs in occipital regions during early stages of auditory processing (Leclerc et al., 2000). In addition, regional blood flow in the occipital cortex has been correlated with performance on an auditory localisation task in congenitally blind but not sighted subjects (Weeks et al., 2000). The magnitude of occipital BOLD responses in early blind subjects has also been correlated with overall accuracy during a monaural localisation task (Gougoux et al., 2005). Furthermore, repetitive TMS to the right dorsal extrastriate cortex in early blind participants significantly impaired sound localisation but not pitch or intensity discrimination (Collignon et al., 2007), suggesting that occipital responses to sound can contribute to specific auditory functions. In higher-level language tasks, occipital cortical activations have been shown to vary with syntactic and semantic content in congenitally blind individuals, for example when participants listened to semantically meaningful or

meaningless sentences (Röder et al., 2002; Bedny et al., 2011). Finally, there is evidence that auditory-evoked responses in the blind occipital cortex are functionally integrated into a larger auditory network. MEG performed during a cognitive task was used to characterise occipital activity in both sighted and congenitally blind subjects (Schepers et al., 2012). This revealed that auditory stimulation modulated oscillatory activity in the blind (but not sighted) occipital cortex, but also that auditory occipital responses in the blind group correlated with responses in the auditory cortex, and were similar to visual occipital responses in the sighted group. These results suggest that occipital circuits are maintained in the absence of vision in early life, and that auditory responses in this region appear to be functionally integrated into the normal auditory network. It should be noted, however, that improved verbal memory in a group of sighted musicians has also been shown to be accompanied by bilateral visual cortex activations during a memory retrieval task (Huang et al., 2010). This questions the extent to which auditory ability correlating with occipital activity is related to the lack of visual input rather than auditory training.

Considerably less is known about whether superior auditory abilities are related to other markers of cortical reorganisation following visual deprivation. Grey matter volume and cortical thickness have been linked to performance on various sensory tasks in sighted individuals; for example, spectral pitch perception is correlated with right auditory cortex (Heschl's gyrus) grey matter volume (Schneider et al., 2005), and melody recognition is correlated with right Heschl's sulcus cortical thickness (Foster and Zatorre,

2010). Occipital structural markers have also been linked to performance on visual tasks in sighted individuals (Schwarzkopf et al., 2011), thus suggesting that cortical anatomy may directly relate to cortical function. Voss and Zatorre (2012) investigated whether thicker occipital cortex in early blind individuals (Jiang et al., 2009; Park et al., 2009) is related to superior auditory abilities. They found that right hemisphere occipital cortical thickness was significantly correlated with pitch and melody discrimination performance in a study with early and late blind individuals. Thicker occipital cortex was matched with superior auditory abilities in the early blind group, whilst thinner cortex was matched with “normal” auditory abilities in the late blind group. This correlation suggests that thicker cortex in early-onset blindness may be a neuroanatomical marker of occipital functional change rather than an isolated effect of vision loss in early life.

This chapter will investigate auditory abilities in congenital bilateral anophthalmia using the series of musical tasks previously tested with early and late blind individuals (Voss and Zatorre, 2012). It was hypothesised that anophthalmic individuals would demonstrate superior auditory abilities compared to sighted controls, but also compared to early and late blind individuals. These results would be important to show that the extent of visual deprivation directly affects the remaining senses, specifically audition. Furthermore, performance on these tasks will be correlated with occipital cortical thickness. Chapter 5 discussed pericalcarine cortical thickness in anophthalmia as a potentially important marker of occipital cortex development in the absence of pre- and post-natal visual input; correlation with

auditory abilities would provide additional insights into the link between occipital neuroanatomy and the function of this region in anophthalmia.

6.3 Methods

6.3.1 Participants

The five anophthalmic participants described previously (see Chapter 2) were included in this experiment, as well as twelve neurologically healthy volunteers with normal vision and normal hearing (mean age 25.5 years, range 19-30 years, 7 females). This study was granted ethical approval by the Oxford University Central Ethical Committee and all subjects gave informed written consent prior to participation.

6.3.2 Auditory tasks

Auditory tasks consisted of two “lower-level” tasks (pitch and loudness discrimination), and three “higher-level” tasks (simple melody, transposed melody and phoneme discrimination) (Voss and Zatorre, 2012). The lower-level tasks were performed twice (and averaged), and the higher-level tasks were performed once. All tasks were run on a laptop with Presentation software (Neurobehavioural systems). Auditory stimuli were presented to participants via closed headphones (beyerdynamic DT 150). Sound levels were adjusted to comfortable listening level.

In the pitch discrimination task, participants heard two tones and responded verbally as to which tone was higher in pitch. Their response was recorded by the experimenter. The reference tone was set at 500 Hz and the initial difference in frequency was 7%. In the loudness discrimination task, participants heard two tones and responded verbally as to which tone was louder. The reference tone was set at 65 dB sound pressure level and the initial difference in loudness was 10 dB. Both tasks used a 2-down/1-up staircase procedure to identify discrimination threshold. The staircase procedure means that two correct responses are needed to step down and one incorrect response is needed to step up. Each run lasted approximately 3 minutes and consisted of 15 reversals. The threshold was calculated from the last 8 reversals. For more details see Voss and Zatorre (2012).

In the simple melody, transposed melody and phoneme discrimination tasks, participants heard two sequences of notes or speech sounds and responded verbally as to whether the two sequences were identical or different. Their response was recorded by the experimenter. Each sequence was made of between 5-13 notes or speech sounds, and lasted approximately 320 ms. Each task contained 30 trials and was preceded by example and practice trials. Half of the test trials were identical and half were different. In the simple melody task, the two sequential melodies were either identical or different (in pitch) by one note. The change in pitch in the 'different' trials was no more than 5 semitones. In the transposed melody task, the second melody sequence was transposed by 4 semitones (higher in pitch) in both identical and different trials, thus requiring judgement of the pattern of the melody. In

the different trials, one note was changed by 1 semitone. In the phoneme task, two sequential sequences of speech sounds were either identical or different by 1 phoneme. For more details, see Voss and Zatorre (2012).

6.3.3 Data analysis

Statistical analyses were performed using SPSS (SPSS Version 20 for Mac). Due to different variances in pitch thresholds across the two groups, non-parametric independent-samples Mann-Whitney U tests were performed to compare all behavioural scores between the two groups. Pearson's R was used to calculate correlations between behavioural scores and cortical thickness. Results were considered statistically significant at $p < 0.05$.

Cortical thickness was calculated from T1-weighted structural images analysed in the previous chapter (Chapter 5). These images were segmented using Freesurfer into tissue types (Fischl and Dale, 2000) and average cortical thickness values were calculated from Brodmann area 17 (location of primary visual cortex in sighted controls) as well as visual area V2 and extrastriate area MT.

6.4 Results

Performance on the five behavioural tasks was averaged across all 5 anophthalmic participants and 11 of the 12 sighted participants (data in one participant was excluded as this person could not consistently perform the tasks).

Raw loudness (A) and pitch (B) thresholds and overall percentage accuracy for the simple melody (C), transposed melody (D) and phoneme (E) discrimination tasks are presented in **Figure 32**.

Mann-Whitney tests were performed for each behavioural task to compare performance between the anophthalmia and control groups. No significant differences were observed between the two groups for the loudness ($p = 0.66$) or the phoneme discrimination tasks ($p = 0.32$). However, significant differences were found for the pitch ($U(14) = 1$, $p = 0.001$), simple melody ($U(14) = 8$, $p = 0.027$), and transformed melody ($U(14) = 6.5$, $p = 0.013$) tasks. For each of these tasks, the anophthalmia group performed better than the sighted controls.

Compared to results reported by Voss and Zatorre (2012), pitch thresholds in the anophthalmia group (mean = 0.25%, SEM = 0.07%) are lower (better) than the early blind (mean = 0.8%, SEM = 0.2%, $N = 14$) and late blind (mean = 2.8%, SEM = 0.6%, $N = 13$) groups. Accuracy scores on the simple melody task are comparable between the anophthalmia (mean = 83%, SEM = 3.2%) and early blind groups (mean = 78%, SEM = 3.3%), and both have higher scores than the late blind group (mean = 60%, SEM = 3.3%). Accuracy scores on the transposed melody task are also comparable between the anophthalmia (mean = 78%, SEM = 6.3%) and early blind (mean = 72%, SEM = 3%) groups, and reduced in the late blind group (mean = 60%, SEM = 2%).

As reported in the previous chapter (see **Figure 30** in Chapter 5), cor-

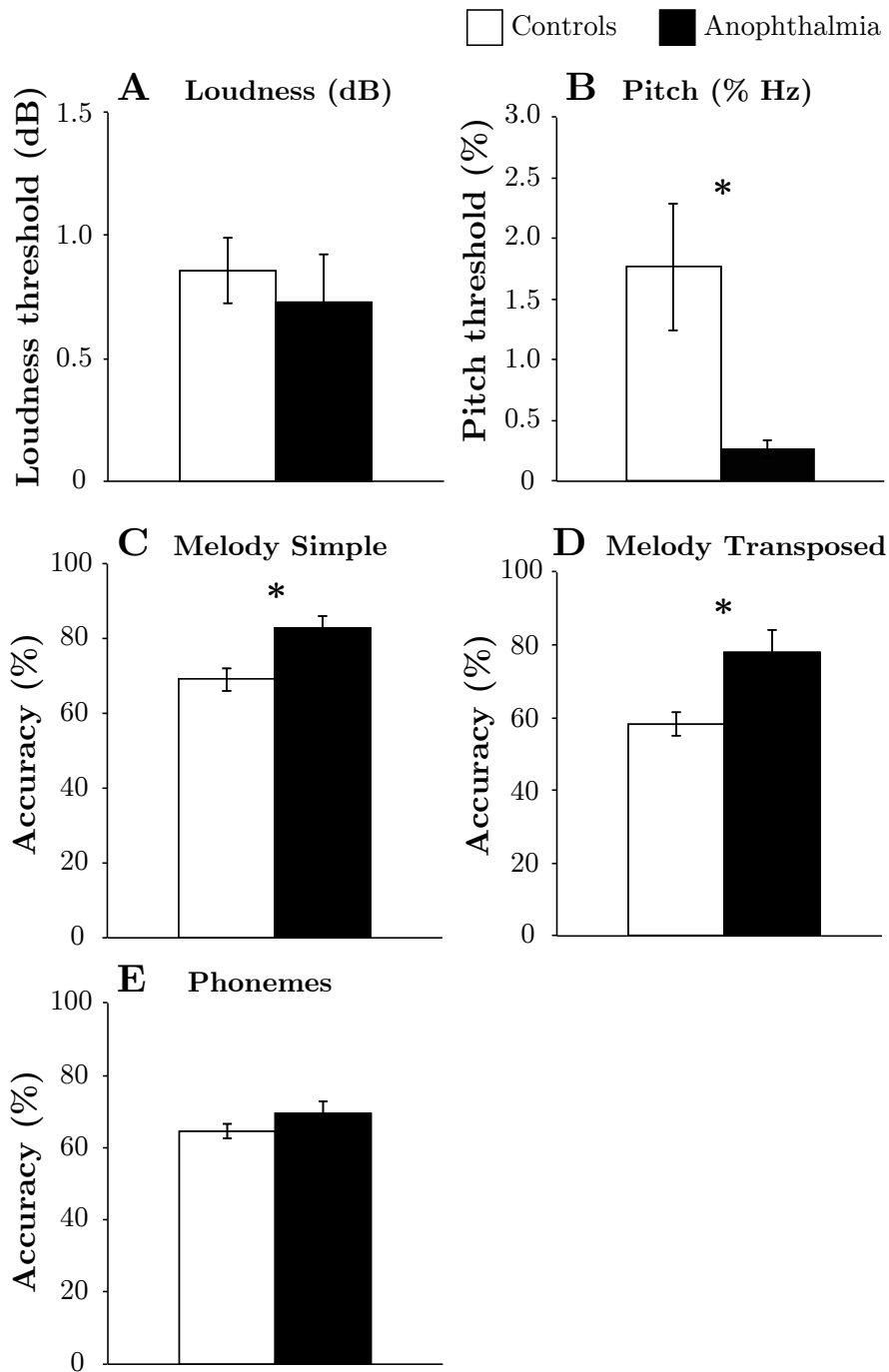


Figure 32: Group mean thresholds or accuracy scores on the loudness (A), pitch (B), simple melody (C), transposed melody (D) and phoneme (E) discrimination tasks (Voss and Zatorre, 2012). Pitch thresholds are significantly lower (better) in anophthalmia compared to sighted controls, and accuracy scores for both melody tasks are significantly better in anophthalmia. A star between columns represents a significant difference between groups (Mann-Whitney, $p < 0.05$). Error bars represent the standard error of the mean.

tical thickness in BA17 is significantly increased in anophthalmia compared to sighted controls. Voss and Zatorre (2012) reported significant correlations between increased right calcarine cortical thickness and pitch and transposed melody scores in their two blind groups. Therefore, the relationship between performance scores on the pitch/melody tasks and right BA17 cortical thickness measurements in the five anophthalmic participants was investigated. Pitch discrimination and accuracy on the simple melody task did not significantly correlate with cortical thickness (pitch $R = -0.62$, $p = 0.26$; simple melody $R = 0.58$, $p = 0.31$). However, accuracy on the transposed melody task was significantly positively correlated with cortical thickness ($R = 0.898$, $p = 0.038$;) (see **Figure 33**). Performance on these three tasks did not correlate with left BA17, bilateral V2, or bilateral MT cortical thickness.

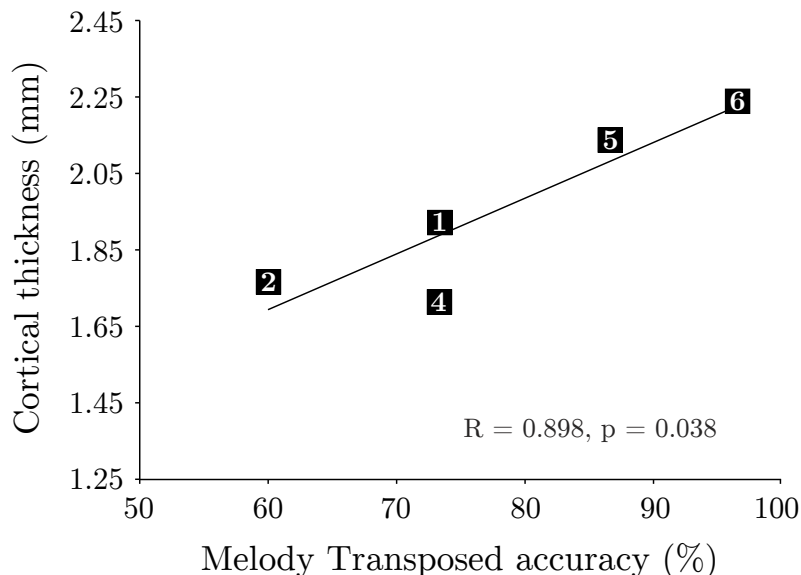


Figure 33: Individual performance on the transposed melody task correlated with right pericalcarine (BA17) cortical thickness in the five anophthalmia participants. Pearson's R and significance values are reported.

6.5 Discussion

This exploratory analysis of behavioural data suggests that anophthalmia is associated with superior pitch and melody discrimination abilities, and that these abilities are similar to those found in early blind but not late blind individuals (Voss and Zatorre, 2012). Whilst it wasn't clear if auditory abilities were better in anophthalmia compared to early blindness, these results are important because they further demonstrate that absence of vision affects the remaining senses. This is important in order to show that visual deprivation has a wide-spreading effect on cortical development and behaviour that goes beyond cross-modal reorganisation of the occipital cortex. Furthermore, there appears to be a link between right hemisphere occipital cortical thickness and performance on the transposed melody task. Together, these results suggest that increased occipital cortical thickness in anophthalmia may not be an isolated effect of lack of visual input. Instead, it may be that the changes in auditory abilities are intrinsically linked to the reorganisation taking place in the occipital cortex.

6.5.1 Superior pitch and melody discrimination in anophthalmia

Although limited by the small size of the anophthalmia group, these behavioural results are interesting in that they are consistent with the performance of early-blind individuals on the same tasks (Voss and Zatorre (2012), replicated in Voss et al. (2014)). The anophthalmia group demonstrated the same superior threshold for pitch discrimination (if slightly better), a finding

that is consistent with previous reports from early blind groups (Gougoux et al., 2005; Wan et al., 2010). Thresholds on the loudness task (which was used as a control for the pitch task) did not appear to differ between the anophthalmia and sighted groups; this is consistent with reports that blindness does not improve loudness discrimination abilities (Voss and Zatorre, 2012; Sakurabayashi et al., 1956; Starlinger and Niemeyer, 1981). In addition to pitch thresholds, accuracy scores on the simple and transposed melody tasks were significantly elevated in the anophthalmia group compared to sighted controls. Performance on the phoneme task did not differ between groups, thus confirming that superior abilities on the melody tasks are not due to differences in working memory, and are unique to musical stimuli since they do not generalise to linguistic stimuli. Whilst accuracy on the simple melody task was improved in both early and late blind groups, Voss and Zatorre (2012) noted that performance on the more complex transposed melody task was only elevated in the early blind group. Both melody tasks involve detecting differences in pitch; however, the transposed melody task requires more abstract perception of tonal pitch and therefore better pitch discrimination thresholds may be required for improved accuracy on this task.

There is some debate about whether low-level auditory abilities in blind individuals are beyond what one would expect from musically trained sighted individuals. Wan et al. (2010) claimed to be the first to account for musical training; early and congenitally blind subjects were still better on an auditory task than musically trained sighted subjects (Wan et al., 2010), but this does question the accuracy of previous reports of improved abilities if musical

ability has indeed not been properly accounted for. However, since then many studies have controlled for musical experience (Voss and Zatorre, 2012; Lerens et al., 2014; Voss et al., 2014) and found that differences in performance are maintained; thus, exposure or training cannot solely explain superior auditory abilities in blind individuals.

6.5.2 Melody discrimination ability correlated with right occipital cortical thickness

In addition to superior pitch and melody abilities in anophthalmia, the current data shows a positive correlation between performance on the transposed melody task and right pericalcarine thickness. This is consistent with correlations between early and late blind scores on the same task and cortical thickness in right hemisphere occipital regions (Voss and Zatorre, 2012). Voss and Zatorre (2012) also report a negative correlation with pitch thresholds (increased occipital cortical thickness correlating with lower/better thresholds); this negative correlation is present but not significant in the anophthalmia data, possibly due to the small group size. Voss et al. (2014) extended these findings by showing a correlation between performances on the same auditory tasks (as well as novel tactile tasks) and occipital grey matter concentration as well as a measure of myelin content (Voss et al., 2014).

The implications of a correlation between regional neuroanatomy and sensory abilities are interesting to discuss. In a previous study, a positive correlation was found in sighted subjects between performance on these same

tasks and cortical thickness in the intraparietal sulcus (IPS) and superior temporal gyrus (Foster and Zatorre, 2010); as both regions are intrinsically linked to auditory processing, this implies that cortical thickness could be used as an indirect report of regional functionality. The correlation here with right hemisphere occipital thickness is particularly interesting in the context of lateralisation of auditory functional responses. Whilst the left hemisphere is thought to specialise in rapid temporal processing, the right hemisphere appears more sensitive to spectral processing (Zatorre and Belin, 2001; Jamison et al., 2006). Furthermore, spectral pitch perception has been linked to grey matter volume in the right auditory cortex (Heschl's gyrus) of sighted adults (Schneider et al., 2005); the correlation in the present anophthalmia data could imply a similar spectral functionality for right hemisphere occipital cortex.

Voss and Zatorre (2012) argue that thicker occipital cortex in early blindness reflects occipital adaptive plasticity. This theory is supported by recent findings that occipital cortical thickness is also correlated with the magnitude of occipital functional responses to pitch and spatial sounds in a group of early blind individuals (Anurova et al., 2014). Increased cortical thickness in early-onset blindness (as discussed in Chapter 5; Jiang et al. (2009); Anurova et al. (2014); Voss and Zatorre (2012)) could be due to a reduction in the normal elimination of inactive synapses in the region during early life (pruning); this process is shaped by sensory experience (Wong et al., 1993) and therefore could be influenced by the absence of visual input. In this neurodevelopmental context, the link between thicker

occipital cortex and auditory abilities could be due to maintained cortico-cortical connections (possibly with the auditory cortex) that are normally pruned in sighted subjects when the visual pathway is strengthened by visual input. The maintenance of these connections in blindness could then facilitate recruitment of the occipital cortex for auditory processing. If this were the case, thicker occipital cortex would be restricted to early life visual deprivation and not found in late-onset blindness; this is consistent with reports of a negative correlation between cortical thickness and blindness onset, as well as evidence that increased occipital cortical thickness is limited to early-onset blindness (Voss and Zatorre, 2012). A similar pattern is also found in other congenital sensory disorders; increased cortical thickness and gray matter volume has been noted in olfactory cortical regions in individuals with congenital but not acquired anosmia (an inability to perceive odour, see Frasnelli et al. (2013)).

6.5.3 Conclusions

These exploratory analyses of behavioural results extend previous reports that loss of vision in very early life improves some low-level auditory abilities like pitch and melody discrimination. Furthermore, the data replicates previous findings that musical abilities may be related to a thicker occipital cortex. It could be speculated that the lack of vision prevents normal pruning of the occipital cortex, thus maintaining connections with auditory cortical regions and encouraging the recruitment of the occipital cortex for auditory processing.

PART III:

**FUNCTIONAL NEUROIMAGING OF
CORTICAL STRUCTURES**

7 Functional organisation of auditory-evoked occipital responses in anophthalmia

7.1 Summary

Previous studies with this group of anophthalmic subjects have demonstrated extensive auditory-evoked responses in the occipital cortex, with some evidence that different auditory tasks preferentially activate specific occipital regions (Watkins et al., 2012, 2013). This chapter further investigates how responses to sound are organised within the anophthalmic occipital cortex; specifically, whether auditory-evoked responses are functionally organised in a similar way to visually-evoked responses in the sighted occipital cortex. Low-level and higher-level auditory responses were assessed using a spatial task (What-Where) and a language task (Meaning-Syllable) in four anophthalmic cases and a group of sighted controls. This chapter outlines some preliminary findings in this small number of anophthalmic subjects, which demonstrate maintained occipital functional specialisation and preserved occipital hierarchy in congenital bilateral anophthalmia.

7.2 Introduction

The occipital cortex in sighted individuals is divided into distinct regions for specific functions. Studies on cross-modal reorganisation in blind individuals have investigated whether this modular organisation is maintained despite the occipital cortex being recruited for non-visual (i.e. auditory and tactile) processing. One of the ways to do this is to assess whether auditory responses demonstrate similar functional topography to visual responses and follow the normal hierarchy of processing observed in the sighted occipital cortex.

There is growing evidence that the blind occipital cortex mirrors the modular organisation of the sighted occipital cortex. This is rooted in the “neuronal recycling hypothesis” (Dehaene and Cohen, 2007), or the theory that auditory responses are distributed in regions or neuronal circuits intended for similar functions. For example, the visual pathway is thought to have a dorsal stream for object localisation (‘where’) and a ventral stream for object identification (‘what’) (Ungerleider and Mishkin, 1982; Zeki, 1978; Goodale and Milner, 1992). Many studies have tested whether these streams are maintained in the blind occipital cortex. Dorsal regions in the right occipital cortex have been associated with spatial processing of sounds in blind individuals, an area typically recruited for visuo-spatial processing (Haxby et al., 1991). In addition, responses to spatial sounds in right dorsal regions have been correlated with performance on auditory localisation tasks in blind subjects (Weeks et al., 2000; Gougoux et al., 2005; Collignon et al., 2007). Several studies have also shown a recruitment of the V5/MT+ complex

for auditory motion, an area typically involved in visual motion perception in the sighted occipital cortex (Poirier et al., 2006; Bedny et al., 2010; Lewis et al., 2010; Jiang et al., 2014). Considerably less work has looked at ventral regions, although there is evidence that the lateral occipital complex (LOC) is activated when blind individuals recognise objects by sound (Amedi et al., 2007). In addition, an early study using PET showed LOC activations when early blind subjects performed a pattern recognition task using a visual-to-auditory sensory substitution device (Arno et al., 2001). More recently, the ventral visual word form area in congenitally blind adults has been shown to respond selectively when processing letter “soundscapes”, or visual images of letters converted into topographical sounds using a sensory substitution device (Striem-Amit et al., 2012).

Spatial localisation in blind individuals has been extensively investigated as it is a fundamental ability for navigation in the absence of vision, and holds interesting implications regarding the theory that vision is needed for calibration of auditory space (Locke, 1954; Axelrod, 1959). As discussed in the previous chapter, in some cases early blind subjects have been shown to accurately map auditory space (Lessard et al., 1998), and half of the tested subjects were considerably better at monaural localisation than sighted subjects. Lewald (2002) looked to address the apparent contradiction between this evidence and that of visual input being required for calibration of auditory space (Zwiers et al., 2001). Whilst overall accuracy did not differ between early blind and sighted subjects, slightly different systematic errors were found when localising sounds in central space (0 to 40 degrees), sug-

gesting that blind individuals may utilise different mechanisms for assessing sound locations. These different mechanisms may relate to the cortical areas being recruited for auditory spatial processing. Medial parietal regions such as the precuneus are typically associated with multisensory spatial processing in sighted (Renier et al., 2009) and blind subjects (for a review, see Ricciardi et al. (2013)). In blind individuals, several studies have also noted additional preferential activation to spatial sounds (compared to pitch stimuli) in dorsal occipital regions, most notably the right cuneus and middle occipital gyrus (MOG) (Collignon et al., 2011; Renier et al., 2010). In sighted subjects, these dorsal stream regions are usually recruited for visuo-spatial processing; Renier et al. (2010) showed the same MOG region activated in sighted subjects during an equivalent visual spatial task, therefore providing strong evidence for maintained functional specialisation in the occipital cortex. However, it may be that this modular organisation is limited to early life visual deprivation, as preferential activation of these regions to spatial sounds was only noted in congenitally blind and not late blind subjects (Collignon et al., 2013). Finally, Renier et al. (2010) found a significant correlation between MOG activity during the sound localisation condition and task accuracy in early blind individuals. These dorsal occipital regions also appear to be integrated into a parietal (intraparietal sulcus) and frontal functional connectivity network, which is typically involved in spatial attention and sound localisation (Collignon et al., 2011). These two findings suggest that MOG responses may be functionally relevant for accurate sound localisation in early blind subjects.

Whilst there is considerable evidence of preserved modular organisation for low-level tasks in the blind occipital cortex, the organisation of areas typically for “higher-level” processing in sighted occipital cortex appears to be more complex. Various extrastriate regions including the lateral occipital complex (LOC) have been shown to activate in blind individuals during semantic processing (Röder et al., 2002; Bedny et al., 2011), verb generation (Burton et al., 2002b; Amedi et al., 2003), phonological and semantic processing (Burton et al., 2003), as well as semantic decision-making based on heard nouns (Noppeney et al., 2003). Furthermore, some of this activation is left-lateralised (Noppeney et al., 2003; Bedny et al., 2011) and integrated into a functional connectivity network with cortical regions typically involved in semantic processing (Noppeney et al., 2003). However, there is considerable evidence that early occipital areas (where V1 is located in sighted subjects) are also involved in language processing. V1 preferentially activates to language and verbal memory in congenitally blind individuals (Amedi et al., 2003), and TMS to this region in blind subjects (but not sighted controls) disrupts accuracy scores on a verb generation task by inducing semantic (rather than phonological) errors (Amedi et al., 2004). Additionally, V1 responds to language but not reversed speech in early blind subjects and appears to be involved in a functional connectivity network with language areas in the left frontal cortex and thalamus (Bedny et al., 2011). It therefore seems that both low-level and higher-order occipital regions are involved in semantic processing in these blind subjects, thus apparently contradicting the theory that occipital modular organisation is maintained in the absence of vision.

However, it may be that at least in anophthalmia (the most extreme case of congenital blindness), the hierarchy of the occipital cortex for auditory language processing is maintained. Watkins et al. (2012) investigated BOLD responses during an auditory naming task in which anophthalmic and sighted subjects covertly retrieved words described by heard sentences. In anophthalmia, the authors found that V1 activated equally to reversed speech and auditory naming; however, BOLD responses in extrastriate regions such as the lateral occipital complex (LOC) and area V3a were greater in the language task. In particular, LOC activated less when the language stimulus was meaningless (reversed speech) than when it was semantically meaningful (auditory naming). Furthermore, left LOC (but not V1) appeared to be included in a left-lateralised resting-state network with frontal and temporal regions typically involved in language processing (Watkins et al., 2012). Whilst it is unclear from this dataset whether occipital activations to language stimuli represent phonological or semantic processing, it does suggest that higher-level occipital regions like V3a and LOC are recruited for higher-level functions in this case of very early-onset blindness.

This chapter further investigates the functional organisation of auditory responses within the anophthalmic occipital cortex. Firstly, a lower-level auditory identification and spatial localisation task was used (What-Where task), which is similar to what has been tested in early blind subjects (Renier et al., 2010; Anurova et al., 2014). It was hypothesised that these stimuli would activate lower-order ‘visual’ areas and show some preferential activation for processing spatial sounds in dorsal areas like the right cuneus or MOG.

Secondly, a language task (Meaning-Syllable task) was designed to dissociate phonological from semantic processing using previously validated stimuli (Gough et al., 2005). Based on the results from Watkins et al. (2012), the speech stimuli were expected to activate all occipital regions but that there would be preferential (and perhaps lateralised) activation in V3a during phonological processing and in LOC during semantic processing. These findings will be important in order to show that functional modules and hierarchical processing are characteristic features of the occipital cortex, and that the absence of pre-natal visual experiences means that the hierarchy of the occipital cortex can be recruited for auditory processing.

7.3 Methods

7.3.1 Participants

Four of the five anophthalmic participants described previously (see Chapter 2) were included in this experiment, as well as twelve neurologically healthy volunteers with normal vision and normal hearing (mean age 25.5 years, range 19-30 years, 7 females). Case 4 was unable to be scanned at this time. This study was granted ethical approval by the Oxford University Central Ethical Committee and all subjects gave informed written consent prior to participation.

7.3.2 Auditory setup

All tasks were carried out on a laptop with Presentation software (Neurobehavioural systems). Auditory stimuli were presented to participants via MRI-compatible earphones (Nordic NeuroLabs), and sound levels were adjusted to comfortable listening level. Button presses were recorded on a MRI-compatible response box.

7.3.3 What-Where auditory task

The What-Where task was designed to evoke BOLD responses during an auditory identification and localisation 1-back task. The design and stimuli used is similar to other tests of auditory spatial processing (Renier et al., 2010; Anurova et al., 2014). Participants heard a series of piano chords coming from different spatial locations. There were four possible piano chords and four possible spatial locations, all on the horizontal azimuth (relative to head position when lying down in the scanner). The four piano chords were A major, C major, D major and E major. The four locations were -90° (far left), -30° (front left), $+30^\circ$ (front right) and $+90^\circ$ (far right) (see **Figure 34**). The stimuli were made in Garage Band '11 (Version 6.0.5, Apple Inc. 2012) on a MacBook Pro laptop (Mac OS X 10.9.4).

In identification blocks ('what'), participants responded by pressing a button when they heard the same chord repeated in succession. In localisation blocks ('where'), participants responded when the chord they heard came

from the same location in succession. Each block lasted 25 seconds (a series of 1 second stimuli followed by 1.5 second silent pause) and was preceded by a 5 second silent pause and a spoken cue (“what” or “where”). A rest period (15 seconds of silence) separated the blocks (**Figure 35**). The blocks (13 for each condition) were organised in a pseudo-random order. Each block contained between two and three target pairs, and the total number of target pairs across ‘what’ and ‘where’ blocks was controlled for consistency.

7.3.4 Meaning-Syllable auditory task

The Meaning-Syllable task was designed to evoke BOLD responses during semantic and phonological processing using a 1-back task. Participants heard a series of words (one word presented every 2.5 seconds). Words of one to five syllables were selected based on similar ratings of concreteness, imageability and familiarity (Gough et al., 2005). They were recorded in-house and audio files were normalised and filtered for background noise using the software Audacity (Version 2.0.3, www.audacity.sourceforge.net).

In the semantic blocks (‘meaning’), participants responded when they heard successive words with the same meaning. In the phonological blocks (‘syllable’), participants responded when they heard successive words with the same number of syllables. Each block lasted 25 seconds and was preceded by a 5 second interval during which a spoken cue was presented (“meaning” or “syllable”). A rest period (15 seconds of silence) separated the blocks (**Figure 36**). The blocks (13 for each condition) were organised in a pseudo-

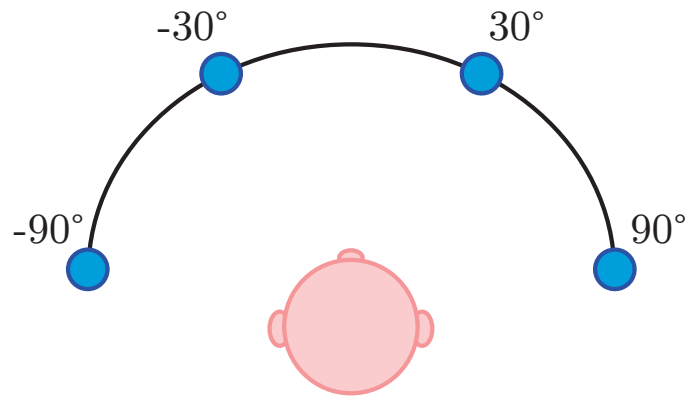


Figure 34: Schematic of the location of the four positions relative to head position on the horizontal azimuth for the What-Where task.

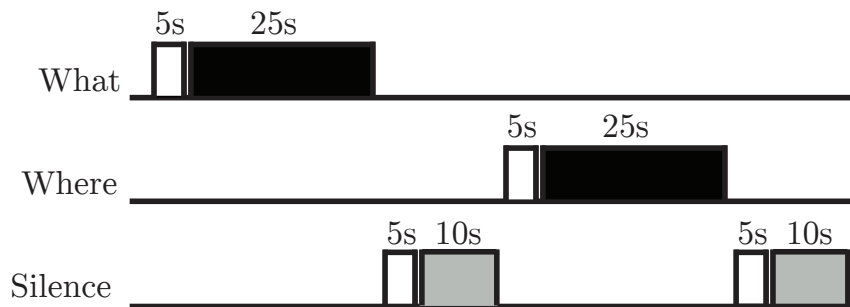


Figure 35: Schematic of the experimental design for the What-Where task. Each stimuli block (black) is 30 seconds (including 5 seconds cue, in white) followed by 15 seconds of rest (grey).

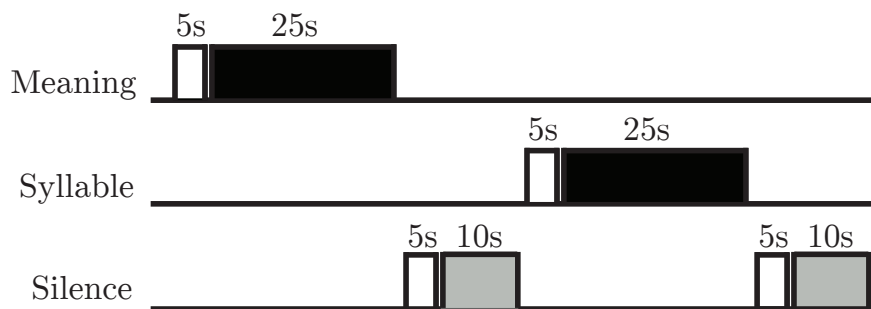


Figure 36: Schematic of the experimental design for the Meaning-Syllable task. Each stimuli block (black) is 30 seconds (including 5 seconds cue, in white) followed by 15 seconds of rest (grey).

random order. Each block contained between two and three target pairs, and the total number of target pairs across the meaning and syllable blocks was controlled for consistency.

7.3.5 MR imaging acquisition

All images were acquired using a Siemens Trio 3-Tesla whole body MRI scanner and a 12-channel coil at the Oxford Centre for Clinical Magnetic Resonance Research (OCMR, University of Oxford). Structural images were acquired at 1 mm isotropic resolution using a T1-weighted MPRAGE sequence (TR=2040 ms, TE=4.7 ms, flip angle=8°, 192 transverse slices, 1 mm isotropic voxels). The two fMRI scans were acquired using an echo-planar imaging pulse sequence (TR=3 s, TE=30 ms, flip angle=87°, 3 mm isotropic voxels, 45 transverse slices, 390 volumes). Transverse slices were positioned to cover the entire brain.

7.3.6 MR imaging analysis

Functional MRI data processing was performed using FEAT (FMRI Expert Analysis Tool) Version 6.00, part of FSL (FMRIB's Software Library, www.fmrib.ox.ac.uk/fsl). Pre-processing of images included motion correction using MCFLIRT (Jenkinson et al., 2002), non-brain removal using BET (Smith, 2002) and prewhitening using FILM. In addition, a highpass temporal filter cut-off of 100s was applied to remove low-frequency fluctuations. Spatial smoothing was also applied using a Gaussian kernel of 6 mm (full width half

maximum).

A general linear model was applied using a design matrix with a double-gamma haemodynamic response function and its first derivative. Explanatory variables (EVs) were generated for each condition ('what' and 'where' or 'meaning' and 'syllable'). In addition, motion correction parameters (translations and rotations in x, y and z) as well as the timeseries of white matter and CSF BOLD signal were included as covariates of no interest and thus removed potential motion and physiological noise artefacts from the data. Timeseries data were extracted from a 3-mm radius sphere within CSF in the anterior lateral ventricle (MNI coordinates: $x = +2$, $y = +10$, $z = +8$) and white matter in the dorsal posterior frontal lobe (MNI coordinates: $x = -26$, $y = -22$, $z = +28$) (Leech et al., 2012). In cases of extreme head motion (more than 1 mm absolute motion in either fMRI session), motion outlier volumes were identified using FSL's motion outlier script and included as regressors in the model.

Functional images were initially registered to each participant's T1-weighted structural image (BBR) for subject-specific analysis, and then registered to T1-weighted MNI-152 (Montreal Neurological Institute) 2 mm standard space using non-linear registration (FNIRT) for group comparisons. Group analyses for the sighted controls were performed using FLAME (FM-RIB's Local Analysis of Mixed Effects). However, as only four of the anophthalmic cases were included in this dataset, each participant was presented individually. All statistical maps were thresholded at $z > 2.6$ (cluster corrected, $p < 0.05$) for visualisation purposes and projected onto MNI 2 mm standard

space.

Peak coordinates (and selected sub-peaks) for all major clusters in the control group are reported in tables, as are clusters that included occipital activity in the four anophthalmic cases. Results for the basic contrasts with rest (i.e. ‘what’, ‘where’, ‘meaning’ or ‘syllable’ vs. baseline rest) are reported using a cluster forming threshold of $z > 3.1$ ($p < 0.05$ corrected). For contrasts of the different sound conditions (i.e. ‘syllable’ > ‘meaning’ or ‘meaning’ > ‘syllable’), results are thresholded at $z > 2.6$ ($p < 0.05$ corrected). It is important to note here that due to anophthalmic case 5’s extensive activation in all sound conditions, and therefore the difficulty in extracting meaningful clusters, the threshold when reporting cluster sizes for this subject was increased to $z > 5$ ($p < 0.05$ corrected).

7.3.7 Region of interest (ROI) analysis

To examine the pattern of occipital cortex activation to the different auditory stimuli, mean percentage signal change was extracted from a number of visual cortex ROIs that have previously been used with this group of anophthalmic participants (Watkins et al., 2012). These included visual areas V1, V2, V3, V3a, V4 and LOC, and were derived from a probabilistic atlas based on retinotopic mapping in 18 sighted controls (Bridge, 2011). In addition, visual area V5/MT+ (V5) was derived from the Juelich histological atlas as implemented in FSL with `fslview` (version 3.2.0). Primary auditory cortex (A1) and inferior frontal gyrus (IFG) ROIs were selected as control areas, and

were also derived from the Juelich histological atlas. A1 was the combination of TE1.0, TE1.1 and TE1.2 (Morosan et al., 2001). Probabilistic definitions of A1 and IFG were thresholded at 30%, and V5 at 15%.

Percentage BOLD signal change during each of the four auditory conditions ('what', 'where', 'meaning' and 'syllable') relative to the silent baseline was calculated using Featquery. The limited number of anophthalmic subjects in this chapter ($n = 4$) precluded the use of statistics (i.e. repeated-measures ANOVA) to compare these measurements with the group of sighted controls. Instead, the sighted and anophthalmic group means were compared descriptively.

7.4 Results

In order to ensure attention was maintained throughout the two fMRI tasks, participants needed to correctly identify at least 70% of the target pairs in each condition during the two tasks. Using these criteria, data from three sighted controls and two sighted controls were excluded from the What-Where and Meaning-Syllable tasks respectively. After these exclusions, mean accuracy scores (correctly identifying target pairs) on the What-Where task were 95.3% (SD = 3.8%) for the anophthalmia group and 90.2% (SD = 9.8%) for the control group. Mean accuracy scores on the Meaning-Syllable task were 95.3% (SD = 3.8%) for the anophthalmia group and 93.8% (SD = 5.2%) for the control group. Performance on either task was not significantly different between the anophthalmia and control groups, and there were no

significant differences between the What-Where and Meaning-Syllable tasks in either group.

Whole-brain images and ROI analyses for the What-Where and Meaning-Syllable tasks are presented below. Whole brain images and tables compare BOLD responses versus silent baseline in the sighted group and each of the four anophthalmic cases. Additionally, contrasts of the two conditions (relative to each other) are presented for the Meaning-Syllable task.

7.4.1 What-Where task

Whole-brain imaging The contrast of each auditory condition (‘what’ and ‘where’) versus silent baseline revealed bilateral activations in auditory cortical regions in the sighted group and anophthalmic subjects, including the superior temporal gyrus and anterior insula. Group maps for the nine sighted subjects are shown in the top rows of **Figure 37** and **Figure 38**, and activations in similar slices for each anophthalmia case are shown below. **Table 4** reports all major clusters in the sighted group for both ‘what’ and ‘where’ conditions (thresholded at $z > 3.1$), as well as selected sub-peaks of interest located within the larger clusters.

The top row in **Figure 37** shows bilateral parietal responses (superior parietal lobule, intraparietal sulcus and some precuneus) in sighted subjects during the ‘where’ condition. The white circles in the figure highlight some of this activity, and coordinates of the peak responses within these circles are reported in **Table 4**. This same region responds to both ‘what’ and ‘where’

conditions in each anophthalmia case.

In addition, all anophthalmic cases (but not sighted subjects) show dorsal occipital responses in the region of the cuneus. The green circles in **Figure 37** highlight this occipital activity, and coordinates of the peak activity within these circles are reported in **Table 5** for each anophthalmic case. These anophthalmic occipital responses are bilateral and present during both conditions, although in some cases they are more extensive in the right hemisphere (Case 1, Case 2, Case 6) and in the ‘where’ condition (Case 1 and Case 2). However, a contrast of ‘what’ > ‘where’ and ‘where’ > ‘what’ did not reveal a consistent pattern of preferential activation in this region, or elsewhere in the occipital cortex.

The top row in **Figure 38** shows bilateral temporal and frontal responses in sighted subjects during the ‘what’ and ‘where’ conditions. In both conditions, anophthalmic cases show additional responses in early occipital regions (except Case 2). Auditory-evoked responses are also found in the right middle occipital temporal cortex, and Case 5 shows bilateral activations in this region. These responses are highlighted by the purple circles in **Figure 38**, and coordinates of the peak activity within these circles are reported in **Table 5** for each anophthalmic case.

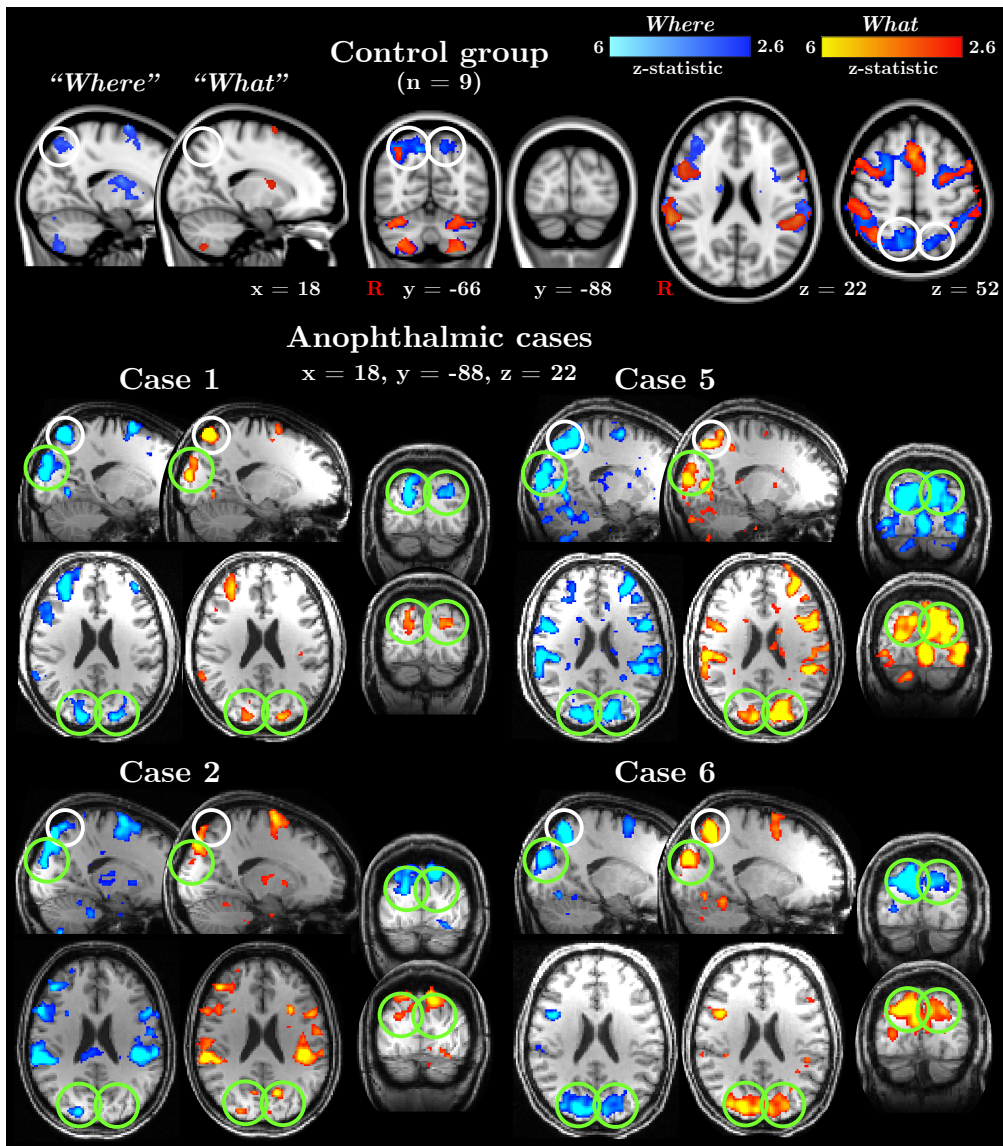


Figure 37: Functional activation (in MNI 2-mm standard space) during the What-Where task for the 9 sighted controls (top row) and each anophthalmic case. Statistical maps are thresholded at $z > 2.6$ (cluster corrected, $p < 0.05$) for visualisation purposes. In addition to bilateral parietal activations in both groups (white circles), anophthalmic but not control subjects show bilateral (right dominant in some cases) dorsal occipital responses (shown in the green circles). Peak coordinates for activity in these green circles are reported in Table 5.

Control Mean – ‘What’	Cluster size	Z (peak)	x (mm)	y (mm)	z (mm)
Right STG to frontal cortex	3299	5.81	52	-8	0
Right insular cortex		5.02	34	22	4
Right IFG to MFG		4.91	52	12	36
Left STG to parietal cortex	2118	6.18	-40	-30	12
Left IPS		3.96	-40	-46	42
Midline frontal cortex; paracingulate	588	5.23	0	14	50
Right SMG	310	5.15	50	-38	44
Right superior parietal cortex; IPS	167	4.62	36	-60	44
Left insular cortex	152	4.52	-30	22	6
Left putamen	40	3.70	-24	6	8
Control Mean – ‘Where’	Cluster size	Z (peak)	x (mm)	y (mm)	z (mm)
Right insular and frontal cortex	4396	5.96	34	20	4
IFG to MFG		5.67	46	16	4
Right SMG to STG	4306	6.51	48	-40	48
Right precuneus (white circle)		5.01	12	-66	50
Right IPS		5.56	38	-44	42
Left STG to parietal and frontal cortices	3534	5.67	-40	-32	12
Left SMG/IPS		5.21	-34	-44	42
Left precuneus (white circle)		4.43	-12	-72	48
Left insular cortex		5.04	-30	24	0
Left premotor & motor cortices	807	5.52	-26	-6	52
Right putamen	60	4.17	22	4	0
Left putamen	34	3.84	-22	-4	6

Table 4: Size and peak coordinates of major clusters during the What-Where task for the sighted control group. Selected sub-peaks within large clusters are also reported. Coordinates of maximal activity in the white circles in **Figure 37** are reported as sub-peaks within the right SMG to STG ‘where’ cluster and the left STG to parietal and frontal cortices ‘where’ cluster. Results for these basic contrasts (‘what’ and ‘where’ vs. rest) are thresholded at $z > 3.1$ ($p < 0.05$ corrected). STG = superior temporal gyrus; SMG = supramarginal gyrus; IPS = intraparietal sulcus; IFG = inferior frontal gyrus; MFG = middle frontal gyrus.

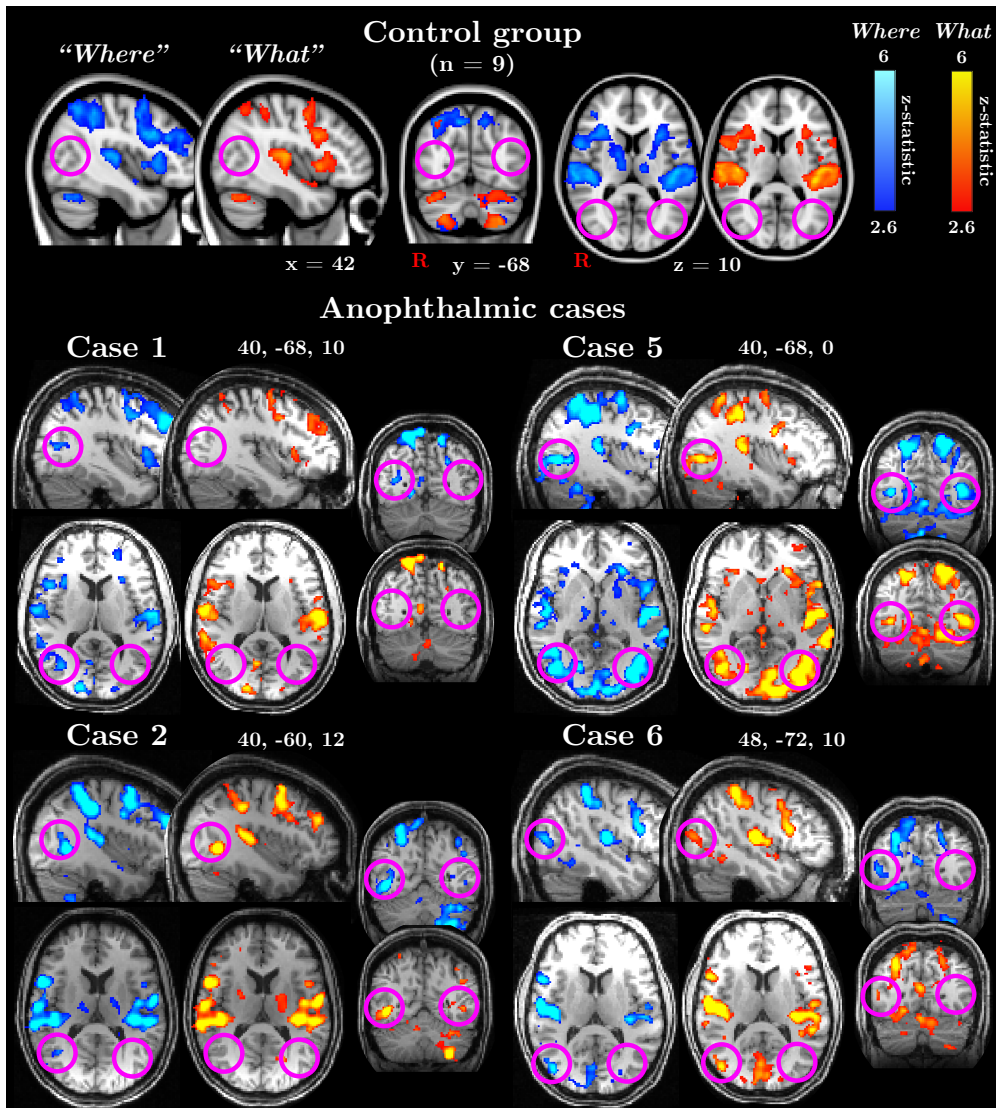


Figure 38: Functional activation (in MNI 2-mm standard space) during the What-Where task for the 9 sighted controls (top row) and each anophthalmic case. Statistical maps are thresholded at $z > 2.6$ (cluster corrected, $p < 0.05$) for visualisation purposes. Anophthalmic subjects but not sighted controls show activations in right middle occipital gyrus (purple circles). Case 5 shows extensive bilateral responses in this region. Coordinates of peak activity in these purple circles are reported in **Table 5**.

Case 1 – ‘What’		Cluster size	Z (peak)	x (mm)	y (mm)	z (mm)	Case 1 – ‘Where’		Cluster size	Z (peak)	x (mm)	y (mm)	z (mm)
Right dorsal occipital cortex (green circle)	336	6.99	18	-94	14	14	Right dorsal occipital cortex (green circle)	989	9.11	16	-94	18	18
Left dorsal occipital cortex (green circle)	208	5.77	-24	-92	18	18	Middle occipital gyrus (purple circle)		5.28	34	-70	12	12
							Left superior parietal to occipital cortex	954	9.66	-16	-66	58	58
							Left dorsal occipital (green circle)		6.61	-16	-90	22	22
Case 2 – ‘What’													
Left precuneus and occipital cortex (green circle)	999	10.0	-4	-82	46	46	Right SMG; right STG; occipital cortex	14489	14.6	32	-32	40	40
Right middle occipital temporal cortex (purple circle)	453	10.3	42	-56	-2	-2	Right dorsal occipital cortex (green)		6.88	18	-88	22	22
Right dorsal occipital cortex (green circle)	28	4.77	24	-90	22	22	Right middle occipital temporal cortex (purple circle)	608	10.7	44	-58	-2	-2
Left middle occipital temporal cortex (purple circle)	21	4.59	-46	-60	2	2							
Case 5 – ‘What’													
Left temporal cortex to bilateral occipital cortex	6646	13.1	-32	-54	52	52	Left STG to bilateral occipital cortex	8139	15.0	-44	-30	8	8
Right dorsal occipital (green)		7.97	16	-94	12	12	Right dorsal occipital (green)		10.9	16	-94	12	12
Left dorsal occipital (green)		11.4	-14	-96	10	10	Left dorsal occipital (green)		9.92	-14	-96	12	12
Left middle occipital (purple)		8.98	-36	-72	4	4	Left middle occipital (purple)		9.32	-36	-80	2	2
Right middle occipital cortex (purple circle)	93	8.19	42	-70	0	0	Right STG to right parietal and occipital cortices	4573	15.0	-48	-24	8	8
							Right middle occipital (purple)		10.2	42	-70	0	0
Case 6 – ‘What’													
Right superior parietal cortex to bilateral occipital cortex	5471	11.8	22	-62	58	58	Right superior parietal lobule; SMG; bilateral occipital cortex	5600	11.5	22	-62	58	58
Right dorsal occipital (green)		8.84	8	-88	28	28	Right dorsal occipital (green)		9.91	18	-88	26	26
Left dorsal occipital (green)		6.17	-8	-88	24	24	Left dorsal occipital (green)		6.11	-10	-88	24	24
Right middle occipital (purple)		7.09	44	-80	12	12	Right middle occipital (purple)		6.73	44	-80	12	12

Table 5: Size and peak coordinates of clusters that include occipital activity in the What-Where task for each anophthalmic case. Coordinates of maximal activity in the green circles in **Figure 37** and the purple circles in **Figure 38** are reported as sub-peaks within the larger clusters. All cases are thresholded at $z > 3.1$ ($p < 0.05$ corrected), except Case 5 ($z > 5$ ($p < 0.05$)).

ROI analyses The magnitude of auditory-evoked activation in visual and control cortical regions during the two conditions was compared between the sighted and anophthalmia groups. Percentage BOLD signal change is plotted in visual areas (**Figure 39**) and two control regions (**Figure 40**) in both subject groups.

In visual areas during the ‘what’ condition (**Figure 39, panel A**), inspection of the means for the two groups showed considerably higher BOLD responses to sound in the anophthalmia group. It is also interesting to note the robust bilateral V3a responses in the anophthalmia group. There were no clear differences between hemispheres during the ‘what’ condition. During the ‘where’ condition (**Figure 39, panel B**), BOLD responses appear significantly higher in the anophthalmia group in right hemisphere visual areas, but not in most left visual areas. Again, there are robust auditory responses in bilateral V3a in the anophthalmia group, although it is interesting that this response is higher in right V3a. Right V3a responses in the anophthalmia group during the ‘where’ condition also appear slightly elevated compared to the ‘what’ condition.

In A1 and IFG (**Figure 40**), BOLD signal change during the ‘what’ and ‘where’ conditions were similar across the sighted and anophthalmia groups. It is interesting to note in **Figure 40 (panel B)** that both groups show increased responses in right compared to left IFG during the ‘where’ condition.

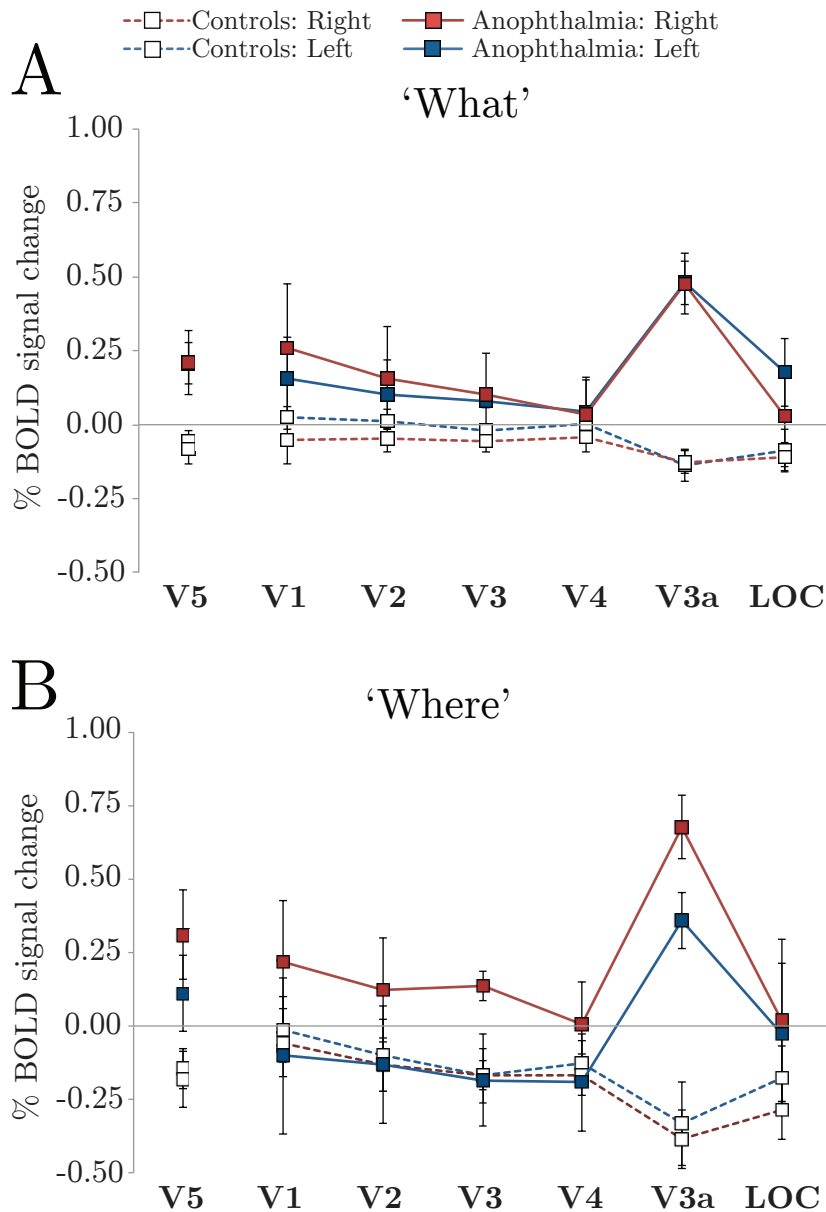


Figure 39: Mean % BOLD change extracted from primary and extrastriate visual areas during the ‘what’ (**A**) and ‘where’ (**B**) auditory conditions. Mean values for the anophthalmia group (n=4) are shown as red (right hemisphere) and blue (left hemisphere) squares with solid lines, and means for the control group (n=9) are shown as white squares with dotted red (right hemisphere) and blue (left hemisphere) lines. Error bars represent the standard error of the mean.

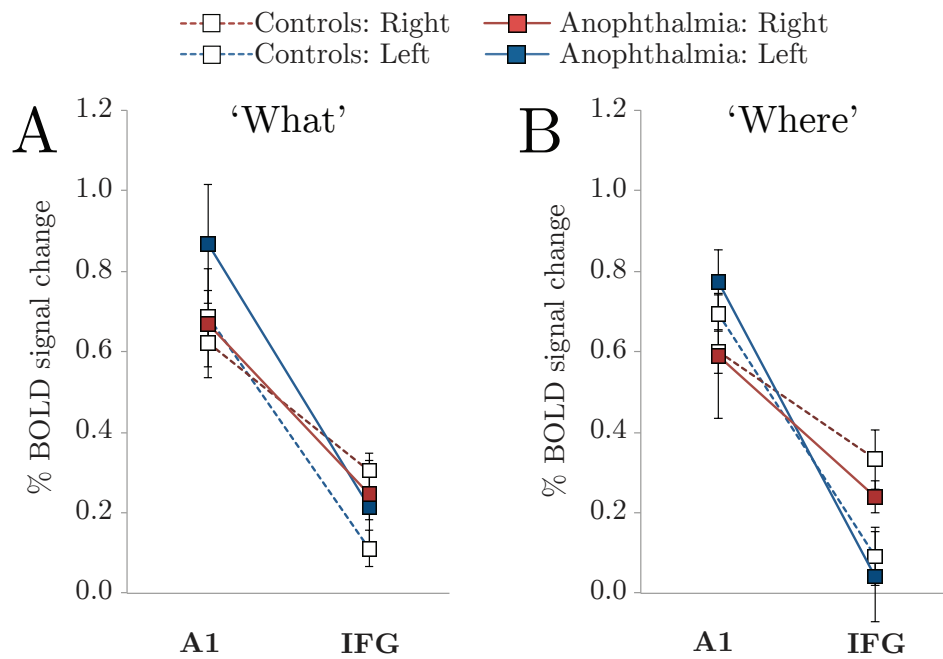


Figure 40: Mean % BOLD change extracted from primary auditory cortex (A1) and inferior frontal gyrus (IFG) during the 'what' (A) and 'where' (B) conditions. Mean values for the anophthalmia group (n=4) are shown as red (right hemisphere) and blue (left hemisphere) squares with solid lines, and means for the control group (n=9) are shown as white squares with dotted red (right hemisphere) and blue (left hemisphere) lines. Error bars represent the standard error of the mean.

7.4.2 Meaning-Syllable task

Whole-brain imaging In sighted subjects, a contrast of each language condition ('meaning' and 'syllable') versus silent baseline revealed extensive bilateral activations in auditory temporal and frontal regions (**Figure 41 panel A**). Frontal auditory responses during the 'meaning' condition (blue-light blue) were more anterior and appear to correspond with IFG's pars triangularis division (anterior dotted circle). In the 'syllable' condition (red-yellow), there were additional responses that correspond with the pars opercularis division of IFG (posterior dotted circle). Responses during the 'syllable' condition were also found in the parietal cortex (**panel B**) and early visual areas (**panel A**). Finally, a contrast of 'syllable' > 'meaning' and 'meaning' > 'syllable' (**panel C**) illustrates the difference in IFG activation loci between the two conditions. This contrast also shows extensive responses in the supramarginal gyrus for the 'syllable' condition. Coordinates of peak activity for all major clusters (and selected sub-peaks within these clusters) are reported in **Table 6**.

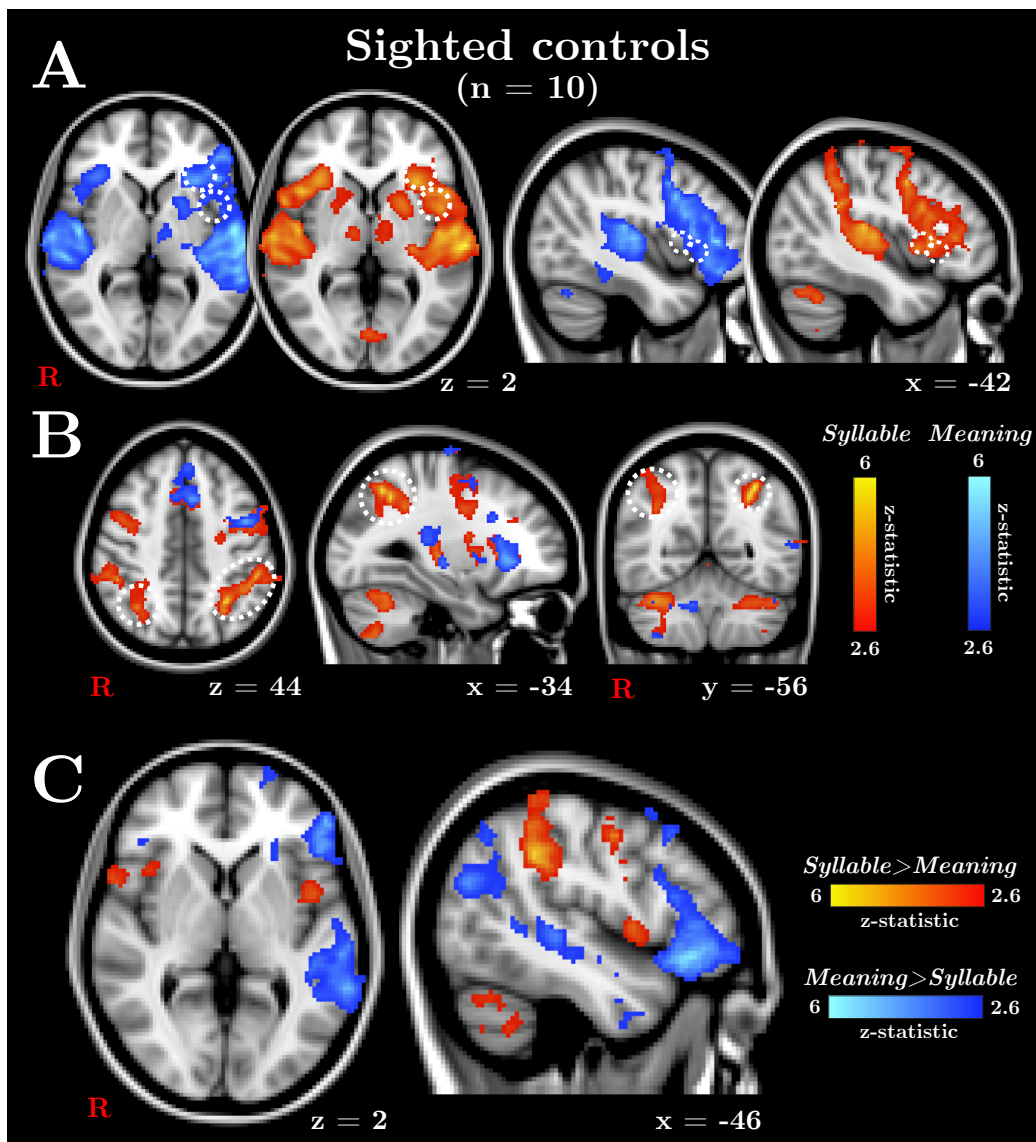


Figure 41: Group functional activation (in MNI 2-mm standard space) during the Meaning-Syllable task for the 10 sighted controls. Statistical maps are thresholded at $z > 2.6$ (cluster corrected, $p < 0.05$) for visualisation purposes. **Panel A** shows the different loci of activation for ‘meaning’ (anterior IFG in the anterior dotted circle) and ‘syllable’ (additional posterior IFG in the posterior dotted circle). **Panel B** shows a dorsal parietal cluster for the ‘syllable’ condition (highlighted by the dotted circle). **Panel C** shows contrasts of the two conditions (‘meaning’ > ‘syllable’ in blue to light blue, ‘syllable’ > ‘meaning’ in red to yellow) and highlights the dissociation of these two conditions in IFG as well as the increased supramarginal gyrus responses in the ‘syllable’ condition.

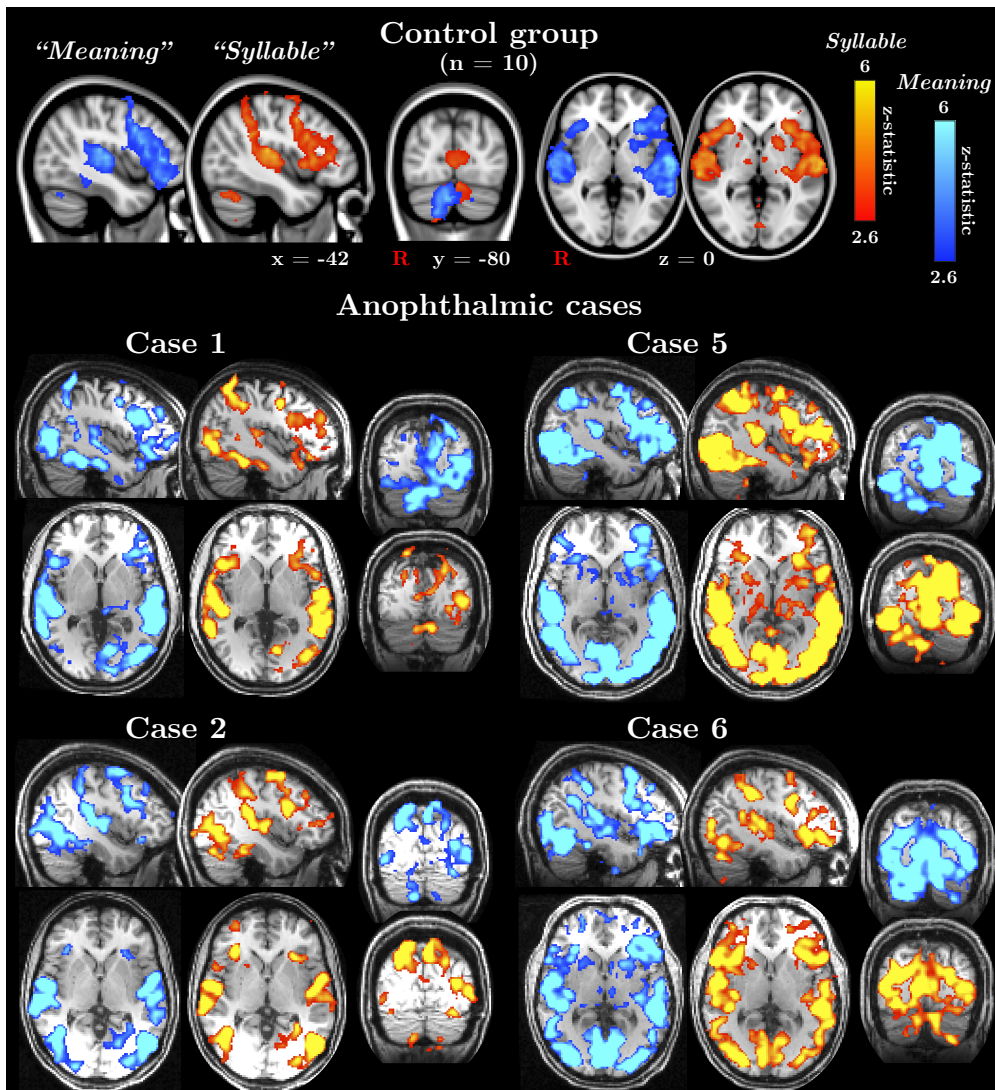
'Syllable'	Cluster size	Z (peak)	x (mm)	y (mm)	z (mm)	'Syllable' > 'Meaning'	Cluster size	Z (peak)	x (mm)	y (mm)	z (mm)
Left STG; frontal and parietal cortices	7412	6.39	-64	-20	4	Right superior parietal cortex	4372	5.66	36	-42	40
Left IFG		5.22	-30	24	6	Right SMG		5.55	50	-32	54
Left superior parietal cortex		5.73	-32	-54	48						
Right IFG to temporal cortex	3233	5.62	46	16	4	Left superior parietal cortex	2737	5.59	-40	-44	42
Right STG		5.49	66	-18	6	Left SMG		5.53	-54	-34	46
Right superior parietal cortex	246	4.25	36	-60	42	Left frontal cortex; left; posterior IFG	1039	4.87	-60	6	18
Right SMG	272	5.52	48	-40	48						
Bilateral paracingulate	873	5.45	-4	8	52						
Right precentral gyrus	195	4.34	44	2	46						
Bilateral primary visual cortex	367	3.93	0	-72	10						

'Meaning'	Cluster size	Z (peak)	x (mm)	y (mm)	z (mm)	'Meaning' > 'Syllable'	Cluster size	Z (peak)	x (mm)	y (mm)	z (mm)
Left STG; left frontal cortex	7537	6.17	-48	-36	16	Left anterior IFG; temporal cortex	9524	6.25	-44	28	-10
Left IFG		5.52	-42	32	6	Left STG		5.43	-56	-6	-10
Right STG	2323	6.22	50	-28	10	Left lateral occipitoparietal cortex	1283	4.79	-56	-70	24
Bilateral paracingulate	506	5.64	-6	18	48	Right frontal cortex	340	4.04	48	36	-8
Right IFG	486	4.60	44	20	8						
Left caudate; left putamen	262	4.37	-18	6	12						

Table 6: Size and peak coordinates of major clusters for the sighted control group during the Meaning-Syllable task. Selected sub-peaks within larger clusters are also reported. Results for the basic contrasts vs. rest ('syllable' and 'meaning') are thresholded at $z > 3.1$ ($p < 0.05$ cluster corrected). Results for the 'syllable' > 'meaning' and 'meaning' > 'syllable' contrasts are thresholded at $z > 2.6$ ($p < 0.05$). STG = superior temporal gyrus; IFG = inferior frontal gyrus.

Whole-brain comparisons of the control group and the four anophthalmic cases are shown in **Figure 42** and **Figure 43**. **Figure 42** shows extensive occipital responses in all anophthalmic cases to both conditions. These responses are located in the pericalcarine cortex (for all subjects except Case 2) as well as extrastriate regions. In some subjects, these occipital responses appear greater in the left hemisphere (Case 1 and Case 2, and to a lesser extent Case 5). Selected coordinates of peak activity in the occipital cortex are reported in **Table 7**.

A contrast of ‘syllable’ > ‘meaning’ and ‘meaning’ > ‘syllable’ is presented in **Figure 43**. This shows that in at least some anophthalmic cases, there appears to be more activation in the left lateral occipital complex (LOC, white outline) during the ‘meaning’ compared to ‘syllable’ condition. Case 6 shows LOC activation in both hemispheres. Coordinates of peak activity for each anophthalmic case that shows this pattern of preferential activation are reported in **Table 8**.



Case 1 – ‘Syllable’		Case 1 – ‘Meaning’		Cluster size	Z (peak)	x (mm)	y (mm)	z (mm)	
Left STG; left frontal cortices; bilateral occipital cortex (left-lateralised)	13908	13.1	-52	-46	10	14.2	-52	-46	10
Pericalcarine cortex	7.36	-4	-86	14	8.83	-12	-74	-2	
Left lateral occipital cortex	7.68	-42	-72	-6	9.74	-40	-74	-8	
Case 2 – ‘Syllable’		Case 2 – ‘Meaning’		Cluster size	Z (peak)	x (mm)	y (mm)	z (mm)	
Bilateral superior parietal cortex; bilateral occipital cortex	10109	13.7	-4	-82	48	16337	62	-8	-6
Left lateral occipital cortex	12.8	-46	-64	-10	9.67	-14	-90	34	
Dorsal occipital parietal cortex	11.1	-14	-90	34	12.88	-46	-64	-10	
Case 5 – ‘Syllable’		Case 5 – ‘Meaning’		Cluster size	Z (peak)	x (mm)	y (mm)	z (mm)	
Left superior parietal cortex; bilateral STG; left frontal cortex; bilateral occipital cortex	37848	17.4	-34	-58	54	25443	48	-78	-10
Pericalcarine cortex	12.2	0	-84	12	12.2	2	-82	10	
Left lateral occipital cortex	15.0	-52	-70	-8	14.1	-36	-82	-2	
Right lateral occipital cortex	16.0	48	-78	-10					
Dorsal occipital cortex	16.1	-12	-88	28					
Case 6 – ‘Syllable’		Case 6 – ‘Meaning’		Cluster size	Z (peak)	x (mm)	y (mm)	z (mm)	
Right superior parietal cortex; bilateral parietal and occipital cortices; bilateral STG; right frontal cortex	44742	14.8	22	-60	56	54216	-56	-30	-2
Pericalcarine cortex	10.0	10	-80	6	11.7	12	-80	6	
Right lateral occipital cortex	11.6	44	-80	10	12.9	26	-86	26	
Right dorsal occipital cortex	13.2	20	-90	26	11.7	42	-56	-12	
					12.3	-40	-68	-12	

Table 7: Size and peak coordinates of clusters that include occipital activity in the Meaning-Syllable task for each anaphthalmic case (as shown in **Figure 42**). Coordinates of selected sub-peaks in the occipital cortex are also reported. All cases are thresholded at $z > 3.1$ ($p < 0.05$ corrected), except Case 5 ($z > 5$ ($p < 0.05$)).

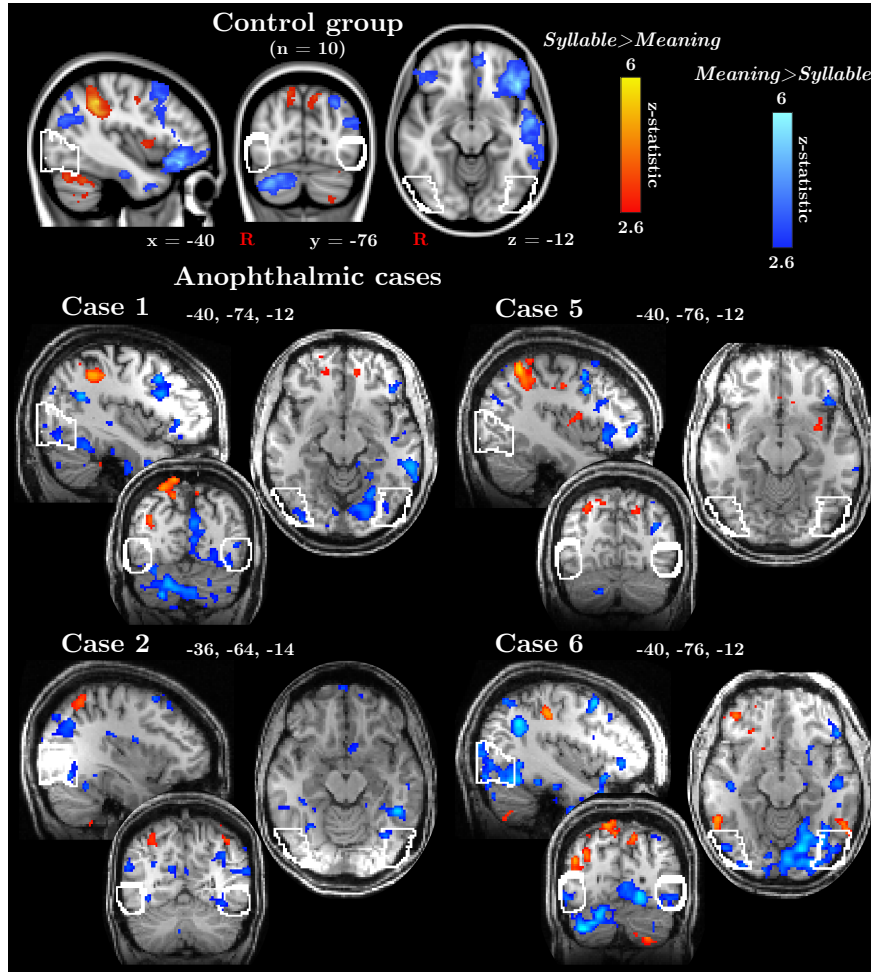


Figure 43: A contrast of ‘meaning’ > ‘syllable’ (blue to light blue) and ‘syllable’ > ‘meaning’ (red to yellow) in the control group (top row) and the four anophthalmic cases. Statistical maps are thresholded at $z > 2.6$ (cluster corrected, $p < 0.05$) for visualisation purposes. This contrast reveals a cluster of higher responses in the ‘meaning’ condition in some anophthalmic cases (but not sighted controls) in the left lateral occipital complex (outlined in white). This activation is bilateral in Case 6.

	Cluster size	Z (peak)	x (mm)	y (mm)	z (mm)
Case 1 – ‘Meaning’ > ‘Syllable’					
Cerebellum; occipital cortex	7984	6.35	0	-62	-50
Left LOC		3.48	-40	-74	-16
Right LOC		3.76	38	-88	-12
Case 2 – ‘Meaning’ > ‘Syllable’					
Left LOC	42	4.13	-36	-66	-14
Case 6 – ‘Meaning’ > ‘Syllable’					
Cerebellum; occipital cortex	5682	7.71	26	-82	-38
Left LOC		5.38	-34	-70	-14
Right LOC		4.10	52	-76	-12

Table 8: Anophthalmic cases. Size (in voxels) and peak coordinates for ‘meaning’ > ‘syllable’ clusters that include LOC activity (as shown in **Figure 43**). Results for all cases are thresholded at $z > 2.6$ ($p < 0.05$ corrected).

ROI analyses The magnitude of auditory-evoked BOLD responses in visual and control regions during the ‘syllable’ and ‘meaning’ conditions was compared between the sighted and anophthalmia groups. Percentage BOLD signal change is plotted in visual regions (**Figure 44**) and two control regions (**Figure 45**).

In visual areas, the anophthalmic group shows considerably higher BOLD responses during both conditions compared to the sighted group (**Figure 44**). The magnitude of auditory-evoked responses in the anophthalmia group during both conditions appears to increase in “higher-order” areas like V3a and LOC compared to “lower-level” areas like V1 and V2. Furthermore, auditory responses during the ‘meaning’ condition are largely left-lateralised across these ‘visual’ areas. It is also interesting to note that BOLD responses in LOC appear to be greatest in the left hemisphere during the ‘meaning’ condition. Finally, there appears to be a slight dissociation between V3a and LOC responses in the two conditions; whilst V3a responses are slightly more elevated than LOC in the ‘syllable’ condition, LOC responses appear slightly higher than V3a in the ‘meaning’ condition.

In A1 and IFG (**Figure 45**), auditory-evoked responses during the two conditions are similar across the two groups. As expected from the linguistic demands of the task, left IFG responses are considerably greater than right IFG in the ‘meaning’ but not ‘syllable’ condition. However, it is interesting to note that left and right IFG responses during both the ‘syllable’ (**panel A**) and ‘meaning’ (**panel B**) are higher in the anophthalmia group compared to sighted controls. This could be due to a low magnitude of responses in

the control group, possibly because activity in IFG is being diluted by an averaging of BA 45 and BA 44 to make up this ROI.

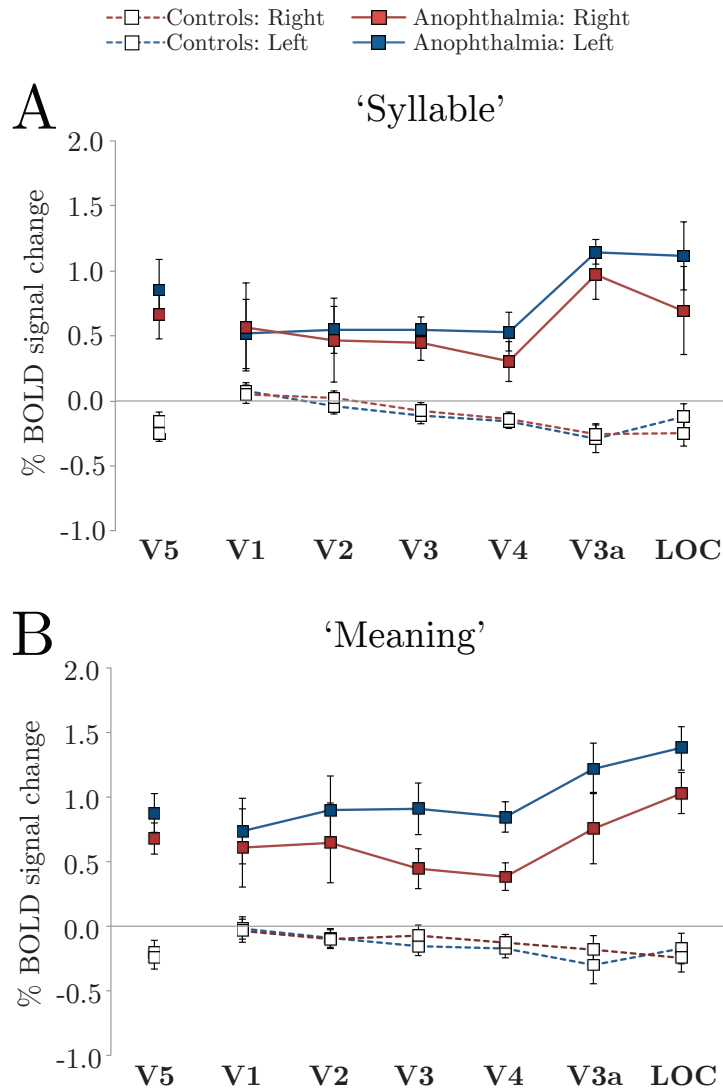


Figure 44: Mean % BOLD change extracted from primary and extrastriate visual areas during the 'syllable' (A) and 'meaning' (B) auditory conditions. Mean values for the anophthalmia group (n=4) are shown as red (right hemisphere) and blue (left hemisphere) squares with solid lines, and means for the control group (n=9) are shown as white squares with dotted red (right hemisphere) and blue (left hemisphere) lines. Error bars represent the standard error of the mean.

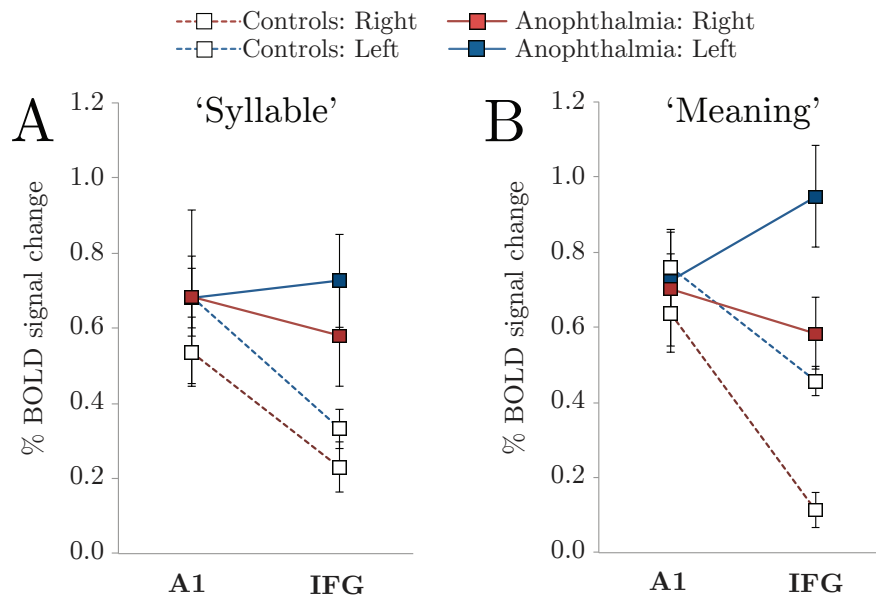


Figure 45: Mean % BOLD change extracted from primary auditory cortex (A1) and inferior frontal gyrus (IFG) during the ‘meaning’ (A) and ‘syllable’ (B) conditions. Error bars represent the standard error of the mean.

7.5 Discussion

There is growing evidence that cross-modal responses in the early blind occipital cortex mirror the functional organisation of visually-evoked responses in the sighted occipital cortex. This chapter used fMRI to clarify this theory in congenital bilateral anophthalmia, using a low-level auditory task (pitch identification and sound localisation) and a higher-level auditory language task (phonological and semantic processing). Both tasks elicited expected activations in temporal, parietal, and frontal cortical regions for auditory processing in sighted and anophthalmic subjects. In anophthalmia, additional robust responses were found in early (V1/V2) and higher-order (V4, V3a,

LOC) ‘visual’ areas. Occipital responses to spatial tones were localised to regions typically associated with visuospatial processing in sighted subjects (cuneus and middle occipital regions). Furthermore, these preliminary findings provide some evidence of preserved hierarchy in anophthalmia; analysis of percentage BOLD responses in ‘visual’ ROIs during the language task showed a stronger magnitude of activation in left compared to right higher-order areas (V3a, LOC), whilst responses were bilateral in earlier occipital regions. These preliminary results are important because they suggest that functional modules and hierarchical processing are innate features of the occipital cortex, and that the absence of pre-natal visual experiences allows this hierarchy to be recruited for auditory processing. These results provide important insights into how the cortex develops according to sensory input.

7.5.1 Cortical responses to spatial tones in sighted subjects

The What-Where task is similar to a previously validated paradigm of low-level auditory spatial processing. Renier et al. (2010) and Anurova et al. (2014) both used a comparable task with early blind individuals; four piano chords were presented in four possible locations on the horizontal azimuth and subjects performed a 1-back task for either sound frequency (pitch identification) or spatial location (localisation).

In the task used in this chapter, ‘what’ and ‘where’ conditions elicited BOLD responses in temporal and frontal regions in the sighted group and the four anophthalmic cases. The ‘where’ condition elicited stronger activations

than the ‘what’ condition in superior and medial parietal regions typically associated with spatial attention (Corbetta et al., 2000; Andersen et al., 1997; Szczepanski et al., 2010). Renier et al. (2010) found comparable responses in their blind and sighted groups, including specialisation of superior and medial parietal regions (intraparietal sulcus and precuneus) for sound localisation. Collignon et al. (2011) also noted similar parietal responses in both blind and sighted subjects during a comparable auditory spatial task. There is some evidence that different regions of the auditory cortex specialise in sound localisation and identification; posterior auditory cortex is thought to be involved in sound localisation whilst anterior auditory cortex specialises in identity processing (Ahveninen et al., 2013). However, the task used here did not reveal such differences. This may be because the ‘what’ and ‘where’ conditions use identical stimuli; the required change in attention to either the pitch or location of the sounds may not elicit responses strong enough to reveal subtle differences in activation foci in the extensively activated auditory cortex.

Mean percentage BOLD change in the ‘where’ condition was higher in the right inferior frontal gyrus in both sighted and anophthalmia groups. In both conditions, auditory-evoked activity in temporal, frontal, and parietal regions was more extensive in the right than left hemisphere (as indicated by cluster sizes reported in **Table 4**). Whilst this chapter does not statistically compare right and left hemispheres due to the small subject numbers, preference for musical processing in the right hemisphere has been extensively studied. It was initially noted with lesion studies showing that pitch perception was

impaired in patients with lesions to right but not left Heschl's gyrus, as well as lesions to the anterior temporal lobe (Zatorre, 1988). Similarly, right (but not left) temporal lobe lesions in Heschl's gyrus significantly impaired thresholds for judging the direction of pitch change (Johnsrude et al., 2000). The advent of functional neuroimaging helped to clarify the role of right hemisphere auditory cortex for tonal pitch perception; Zatorre et al. (1994) used PET and MRI to localise responses to tones and found that listening to melodies (vs. acoustic noise) increased cerebral blood flow (CBF) to the right superior temporal cortex in sighted subjects. Furthermore, comparing pitch tones in melodies (vs. passive listening) increased CBF in the right frontal lobe and decreased CBF in the left primary auditory cortex. Zatorre and Belin (2001) tested the theory stemming from this literature that the two hemispheres have separate auditory functions. Whilst sighted subjects listened to tones, PET showed that discriminating spectral features and sound frequencies was right-lateralised. In contrast, the left hemisphere appeared to specialise in rapid temporal processing, which may be important for characterising speech sounds. Jamison et al. (2006) used fMRI to confirm this dissociation of "temporal" and "spectral" processing between the two hemispheres; the authors found that tones with varying temporal features activated bilateral Heschl's gyrus, but that this activity was left-lateralised in primary auditory areas. In contrast, spectrally varying sounds elicited responses in bilateral superior temporal gyrus although responses were largely right-lateralised.

7.5.2 Occipital activations to spatial tones in anophthalmia

The What-Where task elicited additional auditory responses in the occipital cortex of the four anophthalmic cases. In particular, all cases showed bilateral activation in the cuneus (dorsal occipital cortex), possibly due to an extension of activity in parietal and temporal areas. Activity in the cuneus appeared more extensive in the right hemisphere and the ‘where’ condition (**Figure 37**). Similar right hemisphere activations have been found in early blind subjects attending to spatial sounds (compared to pitch identification) (Collignon et al., 2011, 2013). The coordinates of the right hemisphere activity reported in Collignon et al (2011) ($x = 22, y = -80, z = 22$) are comparable to those of the four anophthalmic cases described in this chapter (peak coordinates for activity in the green circles of **Figure 37** are reported in **Table 5**).

This dorsal region was identified in this chapter as equivalent to the location of V3a in sighted subjects (Tootell et al., 1997). Indeed, the plots of % BOLD signal change during the ‘what’ and ‘where’ conditions show a similar magnitude of activation across the different occipital regions in the anophthalmia group; however, activation was maximal in V3a. As this area in sighted subjects is thought to be included in a visuospatial network with the parietal cortex (Tootell et al., 1997), it is interesting to note a similar response profile in the anophthalmic subjects for an audio-spatial task. TMS over this region (right hemisphere) interfered with sound localisation but not pitch discrimination in congenitally blind subjects but not sighted subjects (Collignon et al., 2007), thereby demonstrating that activation of this region

in blind individuals can be functionally integrated into a larger audio-spatial processing network.

The What-Where task also revealed auditory-evoked responses in an area of the middle occipital cortex near the temporal cortex (potentially identifiable as the middle occipital gyrus, see **Figure 38**). This activity was primarily in the right hemisphere for three cases and bilateral in Case 5. Responses to auditory localisation and not pitch identification have previously been found in the middle occipital gyrus (MOG) and middle occipital temporal gyrus of blind subjects (Collignon et al., 2011; Renier et al., 2010). The coordinates of these regions as reported by Collignon et al. (2011) (MOG: $x = 48$, $y = -76$, $z = 6$; MO-Temp Gyrus: $x = 40$, $y = -56$, $z = 12$) are comparable to peak activity in the purple circles shown in **Figure 38** (coordinates for each anophthalmic case are reported in **Table 5**). Whilst Case 2 and Case 5 show comparable responses in this region for the two auditory conditions, Case 1 and Case 6 show activity in the ‘where’ condition only. However, a contrast of the two auditory conditions did not reveal clear differences between the two conditions. Regardless, the preliminary anophthalmic data discussed in this chapter add to the existing literature of maintained functional specialisation of middle occipito-temporal regions in blind subjects (Renier et al., 2010; Collignon et al., 2011, 2013).

It is interesting that occipital auditory-evoked responses during the What-Where task was slightly greater in the right hemisphere in anophthalmia, as shown in the plot of % BOLD signal change during the ‘where’ condition. These responses could suggest that the profile of auditory re-

sponses in the anophthalmic occipital cortex is comparable to traditional auditory processing regions, as previously discussed. It is also interesting in relation to the behavioural findings reported in the previous chapter, notably the correlation between performance on a musical task and right pericalcarine cortical thickness in the anophthalmic cases.

Finally, it is important to note that V5/MT+ was plotted separately in the % BOLD signal graphs. A previous study suggested that this region is recruited for low-level auditory processing in at least some of the anophthalmic cases (Cases 1 and 2 included in this chapter as well as Case 4; Watkins et al. (2013)); therefore, V5 in anophthalmia may not fit its traditional role in the occipital hierarchy as a higher-order area. There is also some evidence in sighted primates that this extrastriate region develops like an “early” visual area, possibly because of its direct connections with subcortical visual structures (Bourne and Rosa, 2006; Warner et al., 2012). Similar mechanisms and pathways may allow area V5/MT+ to develop as an “early” area for auditory processing in anophthalmia. In the What-Where task, auditory responses in bilateral V5 were similar to those found in early visual areas (V1, V2) in terms of magnitude and the lack of discernable hemispheric differences. It may be that connections from the thalamus or pulvinar to the V5/MT+ complex are maintained in these anophthalmic cases and allow early auditory processing in this region (this theory is discussed more extensively in previous chapters).

7.5.3 Cortical responses to phonological and semantic sounds in sighted subjects

The Meaning-Syllable task was based on a paradigm previously validated by Gough et al. (2005) for semantic and phonological processing. Whilst sighted subjects read the same words used in this chapter, TMS applied to the anterior portion (pars triangularis) of the left inferior frontal gyrus (IFG) disrupted semantic processing (meaning of words). In contrast, TMS to the posterior portion (pars opercularis) of left IFG disrupted phonological processing (word rhyming) (Gough et al., 2005). In this chapter, the phonological condition was changed to syllable counting in order to increase task difficulty during auditory processing, as rhyme detection of stimuli presented through the auditory modality was considered too easy.

In the sighted group, the ‘meaning’ and ‘syllable’ conditions elicited robust BOLD responses in bilateral temporal and frontal regions. Responses in the ‘syllable’ condition extended to bilateral parietal regions (**Figure 41**). In the left IFG, the data presented in this chapter confirm the different activation patterns reported by Gough et al. (2005); activity during the ‘meaning’ condition was largely in anterior left IFG whilst activity in the ‘syllable’ condition extended to posterior left IFG. This is consistent with extensive evidence of IFG being anatomically subdivided for different linguistic functions. Poldrack et al. (1999) used visually presented words in an fMRI task to show that dorsal posterior regions of the left inferior prefrontal cortex (corresponding to BA 44, or the pars opercularis division of IFG) activated to syllable

counting, whilst ventral anterior regions (BA 45, or the pars triangularis division of IFG) activated more when extracting the meaning of words. Similar results have been reported in sighted subjects with other visually presented words (McDermott et al., 2003; Gitelman et al., 2005) and regardless of task difficulty (Gabrieli et al., 1998), as well as with auditory words in sighted and blind subjects (Burton et al., 2003).

Additional bilateral responses were also found in the parietal cortex during phonological processing; activity in the superior parietal lobule and supramarginal gyrus was noted in the ‘syllable’ condition alone (**Figure 41 panel B**) and in a contrast of ‘syllable’ > ‘meaning’ (**Figure 41 panel C**). Previous studies have found similar activations during phonological but not semantic processing; in addition to the different activation foci in IFG (as discussed above), McDermott et al. (2003) noted preferential activation of bilateral parietal regions in the phonological condition. These activations were also localised to the supramarginal gyrus (SMG; BA 40) and the pre-cuneus (BA 7). In a similar study, TMS to the SMG during a reading task slowed reaction tasks during phonological word processing but not semantic processing, thus supporting the selective role of this parietal region for phonological tasks (Sliwinska et al., 2012). Finally, Burton et al. (2003) also showed bilateral parietal activations (including SMG) to phonological auditory stimuli (rhyming), thus corroborating that parietal regions are involved in phonological processing irrespective of modality.

Together, these findings are in line with the theory of a ventral and dorsal stream for different language functions (Hickok and Poeppel, 2000, 2004,

2007). Auditory-presented speech is initially processed in bilateral superior temporal gyrus, but then separates into a ventral stream to access lexical information and extract meaning, and a dorsal stream for speech perception at a sub-lexical level. In the ventral stream, speech sounds are matched for meaning (semantic processing) in superior and middle regions of the temporal lobe. This stream is thought to involve multiple parallel and bilateral processes; this is possibly because speech signals have multiple complex cues that need to be processed at the same time. Evidence for this comes from patients with bilateral temporal lobe lesions who have severe speech recognition deficits, whilst patients with unilateral temporal damage maintain these abilities (Hickok and Poeppel, 2007). Conversely, the dorsal stream is thought to be involved in mapping the acoustics of speech sounds to the frontal lobe for speech production and articulation (phonological processing). This stream does not need to access lexical information, and instead maintains sub-lexical information by recruiting working memory and executive control networks of the frontal lobe. The dorsal stream is also thought to include posterior dorsal temporal regions and the parietal cortex for auditory-motor integration (Warren et al., 2005). Both ventral and dorsal streams then converge in their respective IFG subdivisions. Similar theories about ‘what’ and ‘where’ processing streams have been reported elsewhere for non-linguistic auditory processing (Rauschecker, 1998; Rauschecker and Tian, 2000). Furthermore, the similarities between these streams and those hypothesised in the visual cortex (as discussed earlier) suggest that dual streams may be a feature of how sensory systems are organised more generally.

7.5.4 Occipital activations for phonological vs. semantic processing in anophthalmia

As discussed above, the language stimuli used in this chapter were validated by eliciting BOLD responses in known language areas, in particular the left anterior IFG for semantic processing and the left posterior IFG as well as the parietal cortex for phonological processing. Therefore, it follows that any occipital responses in the anophthalmic subjects could also be reflecting semantic and phonological processing.

The Meaning-Syllable task elicited extensive responses in the occipital cortex of all anophthalmic cases, from lower level areas around the calcarine sulcus (except Case 2) to dorsal and ventral higher-order areas like V3a and LOC (see **Figure 42**). Indeed, the magnitude of BOLD responses plotted in **Figure 44** showed robust responses in all ‘visual’ areas in the anophthalmia group compared to sighted controls. This is consistent with previous findings of extensive occipital activity in early blind individuals on a comparable linguistic task (Burton et al., 2003). However, the authors of that study noted that the magnitude and extent of occipital responses was reduced in the phonological compared to the semantic condition. This contrasts with the data presented in this chapter, where occipital responses were comparable across the two conditions. The difference between this chapter and the Burton study may be due to the choice of syllable counting rather than rhyming in order to increase task difficulty, which may in turn influence the magnitude of BOLD responses. Alternatively, it could be that anophthalmia differs from

early-onset blindness, and that phonological and semantic auditory processing networks equally recruit the occipital cortex in anophthalmia. It is also important to note that, as shown in **Figure 41 (panel A)** and **Table 6**, some early visual area responses were also found in the sighted control group during the ‘syllable’ condition. This is also shown in **Figure 44 (panel A)**, with percentage BOLD responses in V1 for the control group just above 0%. These responses could be driven by a small number of control subjects showing occipital responses to the sounds, possibly due to visual imagery or audio-visual associations during phonological processing.

Whilst auditory-evoked responses during the Meaning-Syllable task were found throughout the anophthalmic occipital cortex, the magnitude of responses appeared greater in higher-order visual areas (V3a and LOC) than early areas (V1, V2) (see **Figure 44**). In particular, BOLD responses in LOC were considerably greater during this linguistic task compared to the lower-level What-Where task. This is consistent with a previous study of the same anophthalmic cases (Watkins et al., 2012), which showed higher BOLD responses in left LOC for meaningful speech compared to non-meaningful reversed speech. It is also interesting that early areas (V1, V2, and possibly V5) in both ‘syllable’ and ‘meaning’ conditions demonstrate comparable BOLD responses across the two hemispheres. In contrast, responses in higher-order areas are higher in the left hemisphere, in particular during the ‘meaning’ condition. However, statistics were not carried out to confirm this due to the small anophthalmia group size. The left hemisphere is thought to be involved in processing temporal features of sounds (Zatorre and Belin, 2001; Jamison

et al., 2006); as language requires good temporal processing, responses to linguistic stimuli tend to be left-lateralised in sighted subjects (Belin et al, 1998). In this chapter, contrasts of ‘meaning’ > ‘syllable’ revealed increased activation in left LOC in the ‘meaning’ condition in at least some anophthalmic cases (**Figure 43**, coordinates reported in **Table 8**). This is reflected in a slightly elevated anophthalmic mean response in left LOC during the ‘meaning’ compared to ‘syllable’ condition (**Figure 44**). It could be that left LOC responses in anophthalmia during the ‘meaning’ condition indicates semantic processing of the heard words. However, with a small group, it is possible that the anophthalmia mean is driven by one or two participants, and therefore a larger sample size would be required to further investigate this effect.

Based on Watkins et al. (2012), the role of dorsal stream V3a was hypothesised for phonological processing and ventral stream LOC for semantic processing, in support of the theory of preserved hierarchy in the anophthalmic occipital cortex. Whilst the data in this chapter appeared to show slightly higher responses in LOC compared to V3a during the ‘meaning’ condition (and slightly higher responses in V3a compared to LOC in the ‘syllable’ condition), the implications of this slight dissociation cannot be speculated without acquiring data from a larger number of anophthalmic participants.

7.5.5 Auditory-evoked responses to language stimuli in the cerebellum

Finally, although not reported in the results section of this chapter, robust auditory-evoked responses were found in the cerebellum during both ‘meaning’ and ‘syllable’ conditions in the sighted group. Examples of these responses are shown at the end of this chapter in **Appendix Figure 1 (panel A)**. Whilst responses are bilateral in the ‘syllable’ condition, they are almost exclusively located in the right cerebellum in the ‘meaning’ condition. This is consistent with findings from a meta-analysis of cerebellum functionality that reports a right-lateralisation of linguistic responses (Stoodley and Schmahmann, 2009). The paper also notes similar clusters (right lobule VI and right crus I/II) to those shown in **panel A**. Buckner et al. (2011) used functional connectivity to create parcellations of the cerebellum according to their cortical projections (Yeo et al., 2011). An example of one of these maps is shown in **panel B**. Auditory-evoked responses to the ‘meaning’ and ‘syllable’ conditions shown in **panel A** match onto the cerebral parcellation that maintains connections with a frontoparietal control network (**panel B**), thus suggesting the functional involvement of the cerebellum in this linguistic task.

7.5.6 Conclusions

Using two auditory fMRI tasks, this chapter confirms the extensive recruitment of the anophthalmic occipital cortex for both low-level and higher-level auditory processing. Whilst the “low-level” musical task (What-Where) re-

vealed largely dorsal auditory-evoked responses in the anophthalmic occipital cortex, the “higher-level” language task (Meaning-Syllable) elicited a combination of both ventral (LOC) and dorsal (V3a) auditory-evoked responses. Together, these findings partially fulfil this chapter’s hypotheses of maintained ventral and dorsal streams in the anophthalmic occipital cortex. The preliminary data suggest that despite the lack of pre- and post-natal visual input in anophthalmia, there is (i) preserved functional specialisation in some occipital regions, such as V3a and middle occipito-temporal cortex for spatial processing, and (ii) an overall preservation of the traditional hierarchy found in the sighted occipital cortex, with early areas (like V1 and V2) for bilateral processing of all sounds, whilst higher-order areas like V3a and LOC may specialise in higher-order auditory processing. However, a considerably larger anophthalmic group is required to confirm and further investigate this theory.

7.6 Appendix Figure

7.6.1 Appendix Figure 1

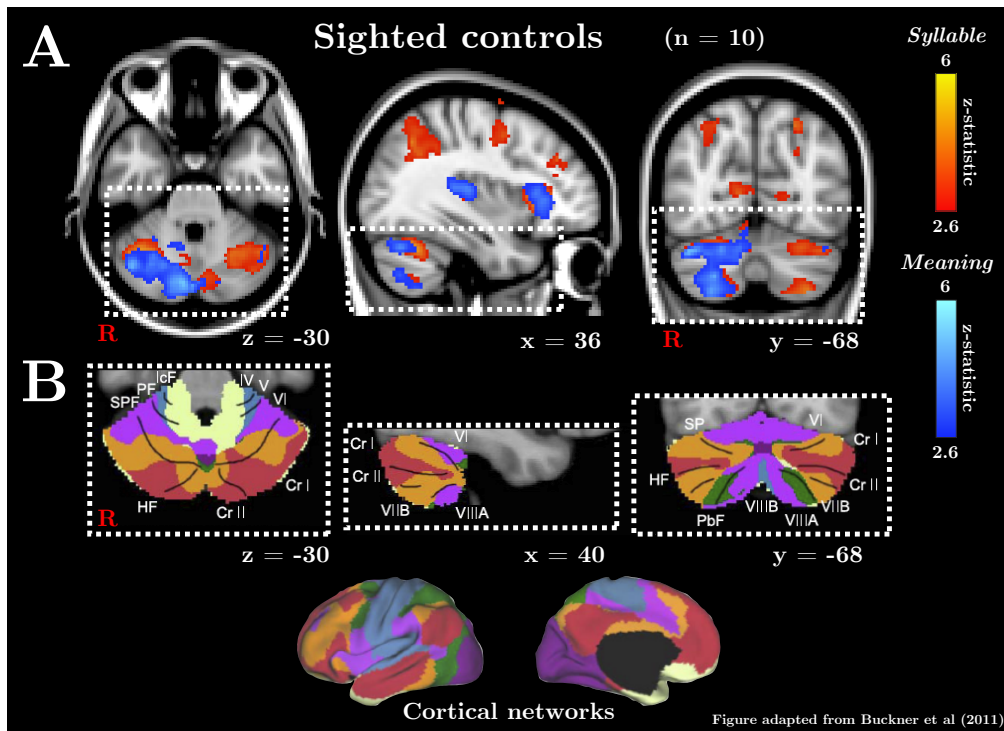


Figure 46: **Panel A** shows group functional activation (in MNI 2-mm standard space) during the Meaning-Syllable task for 10 sighted controls (mixed-effects group analysis). Statistical maps are thresholded at $z > 2.6$ (cluster corrected, $p < 0.05$) for visualisation purposes. **Panel B** shows cerebellum parcellation (in comparable slices) according to functional connectivity cortical networks, taken from Buckner et al. (2011). ‘Syllable’ (red – yellow) and ‘meaning’ (blue – light blue) clusters in the cerebellum match well with divisions of the cerebellum that (according to Buckner et al. (2011)) are functionally connected with a frontoparietal cortical network (orange network)

8 Behavioural and functional cortical changes after short-term visual deprivation

8.1 Summary

The literature discussed in the previous chapters on congenital and early blindness demonstrates the multisensory nature of the ‘visual’ cortex, and the significant improvements in auditory abilities that can be induced by long-term visual deprivation. However, the timeline for these changes remains unclear. In particular, whether similar changes can occur in the developed visual cortex of sighted individuals after shorter periods of visual deprivation. In this chapter, sighted adults took part in two experimental sessions: a control session and a blindfold session. Behavioural abilities (measured using the tasks from Chapter 6) and auditory-evoked BOLD responses (using the What-Where and Meaning-Syllable tasks from Chapter 7) were compared within-subjects between their control and blindfold session. Pitch discrimination abilities were significantly improved after 80 minutes of visual deprivation, and there was some evidence of increased auditory-evoked responses in the occipital cortex after 160 minutes of visual deprivation. How-

ever, due to considerable between-subject variability and low experimental power, additional subjects are required to further investigate these findings.

8.2 Introduction

Short-term visual deprivation of healthy sighted adults (from minutes to days) is thought to temporarily improve non-visual abilities, and perhaps unmask tactile- or auditory-evoked responses in the occipital cortex in a similar way to what has been recorded in blind individuals. Perhaps the most well known are the blindfolding experiments carried out by Pascual-Leone and colleagues (Schlaug et al., 2000; Pascual-Leone and Hamilton, 2001). Over a five-day period, fMRI was used to assess occipital cortex responses to tactile and auditory stimuli in blindfolded and non-blindfolded adults. By the fifth day, the authors found increased primary and extrastriate occipital activation during both Braille and auditory tone discrimination tasks in the blindfolded but not control subjects, an effect that disappeared once the blindfolding period ended. In addition, TMS to the occipital cortex interfered with tactile Braille discrimination in the blindfolded subjects (Schlaug et al., 2000; Pascual-Leone and Hamilton, 2001). This effect, which was not found in controls or after the blindfold was removed, has also been observed in early blind individuals (Cohen et al., 1999).

Since these 5-day experiments, most of the literature has looked at the effects of shorter periods of visual deprivation on tactile stimulation. As little as 90 minutes of visual deprivation improved tactile acuity thresholds

in sighted adults compared to non-deprived control subjects (within-subject comparisons were not made). This effect was reversed 130 minutes after the end of the blindfolding period (Facchini and Aglioti, 2003). Merabet et al. (2007) used fMRI to investigate how 90 minutes of blindfolding could affect BOLD responses to tactile stimulation in retinotopically defined visual areas. In addition to bilateral intraparietal sulcus (IPS) activations during a raised-dot pattern task, the authors noted significant early occipital activations (V1) combined with suppressed BOLD signal (deactivation) in extrastriate regions (V2, V3, V3a, MT and V4) (Merabet et al., 2007).

Whilst the effects of blindfolding on tactile performance and BOLD responses evoked by tactile stimuli have been explored in various studies (Kauffman et al., 2002; Facchini and Aglioti, 2003; Weisser et al., 2005; Merabet et al., 2007), there is little work in the auditory domain. Beyond the occipital activations noted after 5 days of blindfolding, the small number of previous studies that have examined auditory processing have used shorter periods of visual deprivation and focussed on behavioural changes only. Gibby and colleagues found increased sensitivity to pitch and loudness discrimination in adults after 3 hours of near total blindness (Gibby et al., 1970). More recently, Lewald (2007) looked at whether improvements in auditory spatial abilities could be found in visually deprived sighted subjects, in a similar way to what has been noted in blind individuals (Lessard et al., 1998; Röder et al., 1999). In a task requiring subjects to point their head towards the location of a sound on the horizontal azimuth, Lewald found that 90 minutes of blindfolding led to a reversible improvement in head pointing accuracy.

Whilst overall accuracy was not affected, the distance or deviation of head pointing from the target's correct location (i.e. the size of the error) was reduced in central space (0 to 40 degrees) (Lewald, 2007). This result is similar, albeit weaker, to what has been recorded in congenital and early blind individuals (Lewald, 2002). The effects of short-term visual deprivation on more complex spectral cues have also been investigated. As harmonic sounds are important components in our auditory environment (Micheyl and Oxenham, 2010), in particular for speech and music perception, Landry and colleagues (2013) investigated the effects of 90 minutes of visual deprivation on a harmonicity discrimination task. In this task, blindfolded and control subjects were asked to judge whether a tone within a sequence was tuned or mistuned. The authors found significant improvements in harmonicity thresholds after 90 minutes (but not 60 minutes) of blindfolding, an effect which took approximately 30 minutes to return to baseline after blindfold removal (Landry et al., 2013). These studies suggest that short-term visual deprivation, even late in life, can influence existing circuits and lead to small but significant plastic changes in auditory perception. Importantly, these subtle changes may not necessarily relate to overall performance, as suggested by Lewald's spatial localisation study (Lewald, 2007); this could explain why some studies have not noted improvements on more passive tactile spatial acuity tasks after blindfolding (Wong et al., 2011).

In addition to these changes in auditory abilities, short-term deprivation has also been noted to affect the functional properties of the visual cortex. Using MEG, Lazzouni et al. (2012) looked at the effects of deprivation on

auditory steady state responses (ASSRs) to tones. They compared ASSRs during a monaural and binaural auditory detection task at the onset of blindfolding and after 2 hours, 4 hours, and 6 hours of visual deprivation. After 6 hours of blindfolding, the occipital cortex of half of the subjects showed two spectral peaks that are typically found in the auditory cortex (Lazzouni et al., 2012). Not only does this study highlight the importance of individual differences, it also suggests that the occipital cortex may become functionally responsive to typical auditory features after visual deprivation. Short-term deprivation has also been shown to influence occipital cortex excitability. Transcranial magnetic stimulation (TMS) to the occipital cortex induces phosphenes, and can be used as a measure of cortical excitability. Boroojerdi and colleagues applied single pulses of TMS to the occipital cortex of sighted adults after visual deprivation to find the minimum intensity needed to elicit phosphenes. They found that 45 minutes of blindfolding significantly reduced this threshold, which suggests increased occipital cortex excitability. This effect continued for the 180 minutes of deprivation but returned to baseline once sight was restored (Boroojerdi et al., 2000).

Finally, some important changes have been noted in the auditory cortex as a result of visual deprivation, for example with an expansion of tonotopic areas in the auditory cortex of blind individuals (Elbert et al., 2002). A recent study has shown that short-term visual deprivation in adult animals can also induce auditory cortex changes. Petrus and colleagues measured primary auditory cortex (A1) responses to pure tones in mice exposed to a dark environment for 6-8 days. They found that A1 neurons in the deprived

animals showed improved sensitivity to different auditory frequencies as well as increased frequency discrimination compared to control animals. In addition, thalamo-cortical inputs from MGN to A1 were strengthened in the deprived animals, an effect which was not noted after deafening (Petrus et al., 2014). Together, these results suggest an enhancement of feedforward sensory processing after short-term sensory deprivation even in the remaining senses.

This chapter further investigates the effects of short-term visual deprivation on auditory abilities and auditory-evoked cortical responses in healthy sighted adults. Following a period of 80 minutes of visual deprivation, changes in performance on the series of auditory behavioural tasks (Voss and Zatorre, 2012) used in Chapter 6 were measured. fMRI was also used to assess how BOLD responses can be altered after 160 minutes of visual deprivation in sighted adults, using the two auditory fMRI tasks discussed in Chapter 7. It was hypothesised that blindfolding would increase auditory-evoked activity in bilateral early visual areas. Furthermore, it was hypothesised that later visual areas would respond preferentially for the different auditory tasks and may show lateralised responses. These results would provide important evidence that the occipital cortex can adapt and reorganise, even in adulthood, based on the available sensory input.

8.3 Methods

8.3.1 Participants

Twelve neurologically healthy volunteers with normal vision and normal hearing participated in two sessions of this blindfolding experiment (mean age 25.3 years, range 19-30 years, 7 females). These were the same subjects used as the sighted control group in Chapters 6 and 7. This study was granted ethical approval by the Oxford University Central Ethical Committee and all subjects gave informed written consent prior to participation.

8.3.2 Experimental design

Each volunteer participated in two sessions: one control session and one blindfolded session. Data from the control session was used as the sighted control group in Chapters 6 and 7. Each session lasted approximately 210 minutes (3.5 hours) and consisted of pre-scan behavioural testing followed by an MRI scan. Both sessions were identical with the exception that participants were blindfolded for the entirety of one session (blindfolded session) using a Mindfold Relaxation Mask (www.mindfold.com). In the other control session, participants were only blindfolded during the MRI scan. In the blindfolding sessions, participants were visually deprived for approximately 80 minutes prior to pre-scan behavioural testing and at least 160 minutes prior to the MRI scan (see **Table 9**). During this waiting time, participants practiced the two fMRI tasks and were helped to walk around the building.

Table 9: Schematic of each session of the blindfolding experiment

Time	Description of Tasks
0 mins to 80 mins	Practice What-Where and Meaning-Syllable tasks. Rest and walk around the building.
80 mins to 120 mins	Pre-scan behavioural testing. Loudness discrimination (x2), Pitch discrimination (x2), Simple melody discrimination, Transposed melody discrimination, Phoneme discrimination.
120 mins to 160 mins	Setup MRI equipment and acquire MPRAGE. Acquire other sequences (not included in this thesis).
160 mins to 210 mins	fMRI tasks. What-Where task, Meaning-Syllable task.

This was designed to encourage exploration of the auditory environment and accommodation to the lack of visual input. The order of the two sessions was counterbalanced across the twelve participants. The two sessions were carried out four weeks apart and at the same time of day.

8.3.3 Auditory tasks

Auditory tasks were grouped into two sessions; the first was the series of pre-scan behavioural tests of pitch, loudness, melody, and phoneme discrimination (Voss and Zatorre, 2012) used in Chapter 6. The second session consisted of the two fMRI tasks used in Chapter 7 (What-Where and Meaning-Syllable tasks). The tasks are described in detail in Chapters 6 and 7.

All tasks were run on a laptop with Presentation software (Neurobehavioural systems). Auditory stimuli were presented to participants via closed headphones (beyerdynamic DT 150, <http://europ.beyerdynamic.com>) during the pre-scan behavioural testing and MRI-compatible earphones (Nordic NeuroLabs) during the fMRI tasks. Sound levels were adjusted to a comfortable listening level. Button presses during the fMRI tasks were recorded on a MRI-compatible response box.

8.3.4 MR imaging acquisition

All images were acquired using a Siemens Trio 3-Tesla whole body MRI scanner and a 12-channel coil at the Oxford Centre for Clinical Magnetic Resonance Research (OCMR, University of Oxford). Structural images were acquired at 1 mm isotropic resolution using a T1-weighted MPRAGE sequence (TR=2040 ms, TE=4.7 ms, flip angle=8°, 192 transverse slices, 1 mm isotropic voxels). The two fMRI scans were acquired using an echo-planar imaging pulse sequence (TR=3 s, TE=30 ms, flip angle=87°, 3 mm isotropic voxels, 45 transverse slices, 390 volumes). Transverse slices were positioned to cover the entire brain.

8.3.5 MR imaging analysis

Functional MRI data processing was performed using FEAT (FMRI Expert Analysis Tool) Version 6.00, part of FSL (FMRIB's Software Library, www.fmrib.ox.ac.uk/fsl). Pre-processing of images included motion correc-

tion using MCFLIRT (Jenkinson et al., 2002), non-brain removal using BET (Smith, 2002) and prewhitening using FILM. In addition, a highpass temporal filter cut-off of 100s was applied to remove low-frequency fluctuations. Spatial smoothing was also applied using a Gaussian kernel of 6 mm (full width half maximum).

A general linear model was applied using a design matrix with a double-gamma haemodynamic response function and its first derivative. Explanatory variables (EVs) were generated for each condition ('what', 'where', 'meaning', 'syllable'). In addition, motion correction parameters (translations and rotations in x, y and z) as well as the timeseries of white matter and CSF BOLD signal were included as covariates of no interest and thus removed potential motion and physiological noise artefacts from the data. Timeseries data were extracted from a 3 mm radius sphere within CSF in the anterior lateral ventricle (MNI coordinates: $x = +2$, $y = +10$, $z = +8$) and white matter in the dorsal posterior frontal lobe (MNI coordinates: $x = -26$, $y = -22$, $z = +28$) (Leech et al., 2012). In cases of extreme head motion (more than 1 mm absolute motion in either fMRI session), motion outlier volumes were identified using FSL's motion outlier script and included as regressors in the model.

Functional images were initially registered to each participant's T1-weighted structural image (BBR) for subject-specific analysis, and then registered to T1-weighted MNI-152 (Montreal Neurological Institute) 2 mm standard space using non-linear registration (FNIRT) for group analyses. For within-subject group comparisons of control and blindfolded sessions, second-

level analyses were performed using FLAME (FMRIB's Local Analysis of Mixed Effects) with a subject variable for each subject. Firstly, a group analysis of all auditory conditions ('what', 'where', 'meaning' and 'syllable') was performed. Secondly, group analyses were performed for each task separately (What-Where and Meaning-Syllable). Statistical maps were thresholded at $z > 2.6$ (cluster corrected at $p < 0.05$) for visualisation purposes and projected onto MNI 2 mm standard space.

Peak coordinates for all major clusters in the group average of the control and blindfold sessions are reported in tables. Results for the basic contrasts with rest ('what', 'where', 'meaning' or 'syllable' vs. baseline rest) are reported using a cluster forming threshold of $z > 3.1$ ($p < 0.05$ corrected). For contrasts of the two sessions (i.e. 'blindfold' > 'control'), clusters are thresholded at $z > 2.6$ ($p < 0.05$ corrected, unless otherwise stated).

8.3.6 Region of interest (ROI) analysis

The pattern of occipital cortex activation to the different auditory stimuli was examined in a number of visual cortex ROIs and two control ROIs. The primary visual cortex (V1), extrastriate visual areas (V2, V3v, V4, V5), primary auditory cortex (A1), and inferior frontal gyrus (IFG) were derived from the Juelich histological atlas as implemented in FSL with `fslview` (version 3.2.0). A1 was the combination of TE1.0, TE1.1 and TE1.2 (Morosan et al. 2001). Probabilistic definitions of V1, V2, V3v, V4, A1, and IFG were thresholded at 30%, and V5 at 15%.

Activation during each of the four auditory conditions ('what' and 'where', 'meaning' and 'syllable') relative to the silent baseline was calculated in two ways. Firstly, by measuring the mean percentage BOLD signal change (using Featquery). Secondly, by calculating the "active" tissue volume (number of voxels with activity above a certain statistical threshold) as a proportion of the total volume of each ROI (Devlin et al., 2003). Active tissue volume was calculated at two thresholds: $z > 1.645$ (which is a p-value of 0.05 and therefore measures how many voxels are "active" above noise level), as well as $z > 2.3$ to assess whether the pattern of responses is maintained regardless of threshold choice. All statistical analyses of these measurements were performed using SPSS software (IBM, SPSS Version 20 for Mac).

8.4 Results

8.4.1 Behavioural tasks

Performance on the Voss and Zatorre (2012) behavioural tasks in the control and blindfold session was averaged across 11 of the 12 sighted participants (as mentioned in Chapter 6, data from one participant was excluded as they could not consistently perform the tasks). Behavioural testing started after 80 minutes of blindfolding in the blindfold session. Raw loudness (**A**) and pitch (**B**) thresholds for the control and blindfold sessions are plotted in **Figure 47**, with error bars showing within-subject standard error of the mean (SEM). Whilst there was no significant difference in loudness thresholds between sessions (paired-samples $t(10) = -0.146$, $p = 0.887$), pitch thresholds were

significantly lower after blindfolding compared to the control session (paired-samples $t(10) = 2.584$, $p < 0.05$). Overall percentage accuracy for the simple melody, transposed melody and phoneme discrimination tasks are reported in **Figure 48**, with error bars representing within-subject SEM. There were no significant differences between sessions in these three tasks (Melody Simple $p = 0.929$; Melody Transposed $p = 0.286$; Phonemes $p = 0.341$).

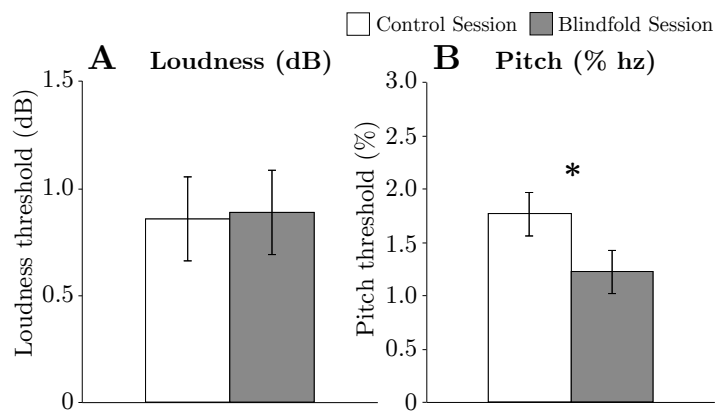


Figure 47: Group mean thresholds for the loudness (**A**) and pitch (**B**) discrimination tasks (Voss and Zatorre, 2012) show that blindfolding significantly improves pitch but not loudness discrimination. A star between columns represents a significant paired difference between sessions ($p < 0.05$). Error bars represent within-subject standard error of the mean.

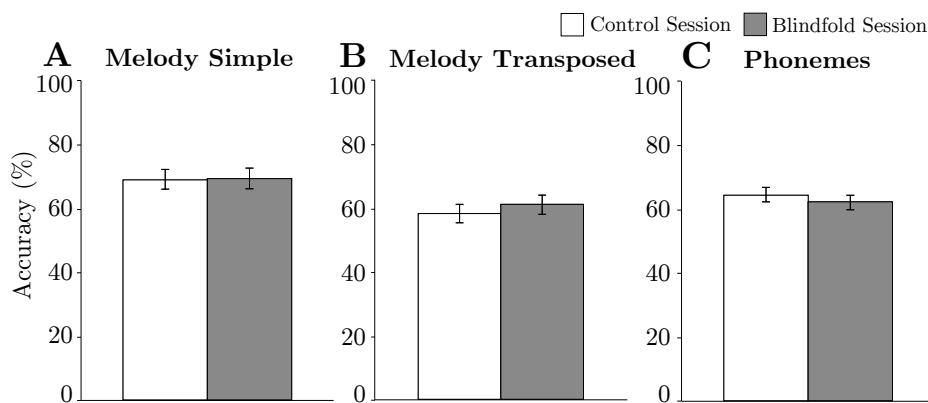


Figure 48: Group mean accuracy scores for the simple melody (**A**), transposed melody (**B**), and phoneme (**C**) discrimination tasks (Voss and Zatorre, 2012). These show no significant group differences between sessions. Error bars represent within-subject standard error of the mean.

8.4.2 fMRI tasks

The fMRI scans were acquired after a minimum of 160 minutes of visual deprivation in the blindfold session. In order to ensure attention was correctly maintained throughout each of the fMRI tasks, participants needed to correctly identify at least 70% of the target pairs. As outlined in Chapter 7, data from three participants were excluded from the What-Where task and data from two participants were excluded from the Meaning-Syllable task. These exclusions resulted in a total of nine participants included in the What-Where task and ten participants in the Meaning-Syllable task. Mean accuracy scores (correctly identifying target pairs) for the control session are reported in Chapter 7. No significant differences were found between the two tasks or between the control and blindfold sessions.

All auditory conditions All sound conditions ('what', 'where', 'meaning', 'syllable') were averaged for the nine subjects that performed both tasks, and whole brain responses were compared between the control and blindfold sessions. The resulting contrast of blindfold > control (**Figure 49**) revealed robust clusters of auditory-evoked activity in the striate and extrastriate cortex. These occipital responses to sound map onto the location of bilateral V1 (blue), right V3a (yellow), and left V3 (pink). Right hemisphere occipital cortex includes a cluster that extends from V1 to V3a (356 voxels, peak at $x=24$, $y=-92$, $z=16$); left hemisphere occipital cortex includes a small V1 cluster (13 voxels, peak at $x=-16$, $y=-82$, $z=12$) and a larger cluster that extends from anterior V1/V2 to V3 (833 voxels, peak at $x=-6$, $y=-58$, $z=-2$).

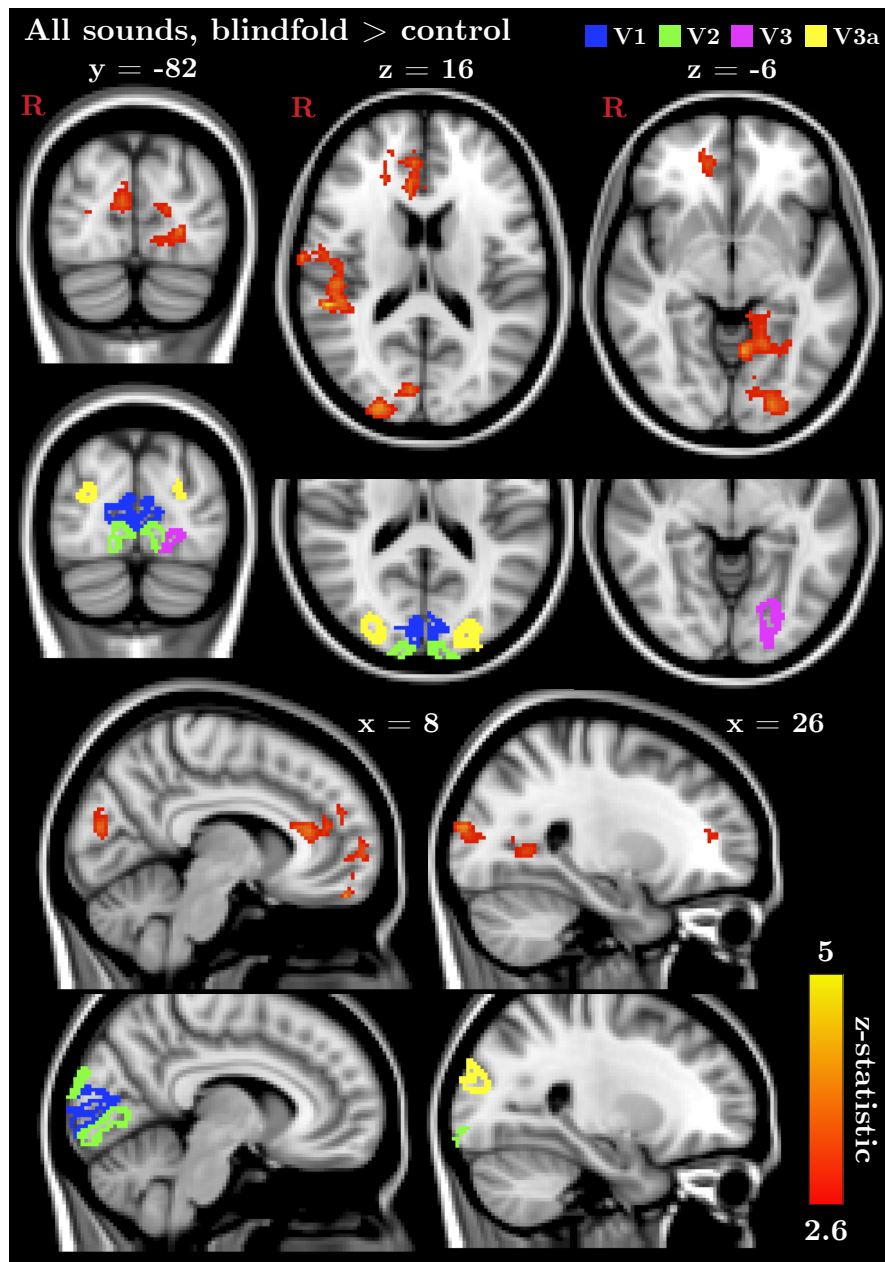


Figure 49: Group average contrast of blindfold > control sessions for all sound conditions ('what', 'where', 'meaning' and 'syllable'). Statistical maps (9 subjects, mixed effects) are thresholded at $z > 2.6$ (cluster corrected, $p < 0.05$) for visualisation purposes. Auditory-evoked activity increased in early (V1, V2) and later (V3, V3a) visual areas after blindfolding. Visual area ROIs depicted in this figure are the same as those used in Chapter 7.

What-Where task Group whole-brain responses during the ‘what’ (sound identification) and ‘where’ (sound localisation) conditions are shown in **Figure 50**. **Table 10** compares all major clusters in the control session (also previously reported in Chapter 7) and the blindfold session (thresholded at $z > 3.1$), as well as selected sub-peaks of interest located within these larger clusters. The auditory stimuli evoked robust responses in the superior temporal gyrus, anterior insula and putamen bilaterally during both sessions. In the ‘where’ condition, there was also activation of medial parietal areas and thalamus. In the blindfold session, additional auditory-evoked responses were found in early visual areas during both ‘what’ and ‘where’ conditions

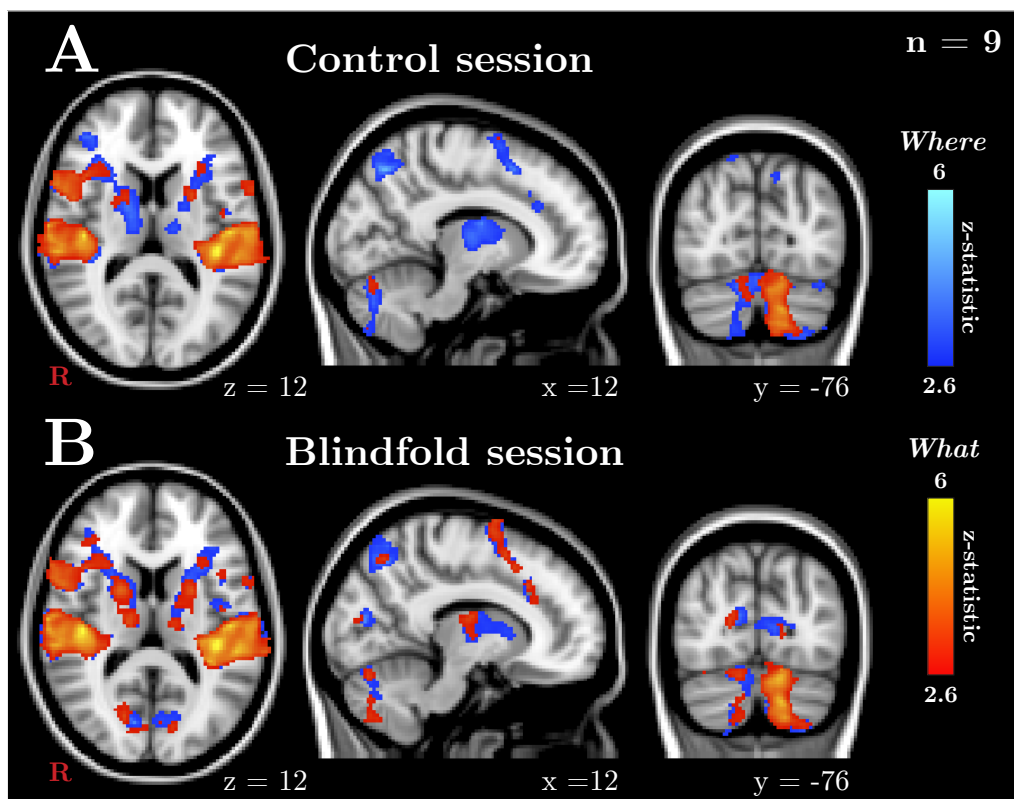


Figure 50: Group activation (in MNI 2-mm standard space) in the ‘what’ and ‘where’ auditory conditions for the control (top) and blindfold (bottom) sessions. Group statistical maps (mixed effects, 9 subjects) are thresholded at $z > 2.6$ (cluster corrected, $p < 0.05$) for visualisation purposes.

Control Mean – ‘What’	Cluster size	Z (peak)	x (mm)	y (mm)	z (mm)	Blindfold Mean – ‘What’	Cluster size	Z (peak)	x (mm)	y (mm)	z (mm)
Right STG to frontal cortex	3299	5.81	52	-8	0	Right STG to frontal cortex	4418	6.29	44	-20	12
Right insular cortex	5.02	34	22	4	4	Right insular cortex	5.19	32	20	20	4
Right IFG to MFG	4.91	52	12	36	36	Right IFG to MFG	5.56	48	10	34	34
Left STG to parietal cortex	2118	6.18	-40	-30	12	Left STG to parietal cortex	2602	6.21	-40	-30	12
Left IPS	3.96	-40	-46	42	42	Left IPS	4.60	-38	-44	42	42
Midline frontal cortex; paracingulate	588	5.23	0	14	50	Midline frontal cortex; paracingulate	869	5.26	0	14	50
Right SMG	310	5.15	50	-38	44	Right SMG	1043	5.49	50	-38	44
Right superior parietal cortex; IPS	167	4.62	36	-60	44	Left precentral gyrus	422	4.53	-36	0	44
Left insular cortex	152	4.52	-30	22	6	Left premotor and motor cortices	143	4.09	-24	4	10
Left putamen	40	3.70	-24	6	8						
						<i>Right primary visual cortex</i>	<i>16</i>	<i>3.5</i>	<i>18</i>	<i>-74</i>	<i>12</i>
						<i>Left primary visual cortex</i>	<i>8</i>	<i>3.17</i>	<i>-12</i>	<i>-80</i>	<i>12</i>
Control Mean – ‘Where’	Cluster size	Z (peak)	x (mm)	y (mm)	z (mm)	Blindfold Mean – ‘Where’	Cluster size	Z (peak)	x (mm)	y (mm)	z (mm)
Right insular and frontal cortex	4396	5.96	34	20	4	Right insular cortex and frontal cortex	5316	5.78	34	20	4
Right SMG to STG	4306	6.51	48	-40	48	Right SMG to STG	4006	6.50	48	-40	48
Right precuneus	5.01	12	-66	50	50	Right STG	5.90	62	-30	14	14
Right IPS	5.56	38	-44	42	42	Right IPS	5.75	36	-60	44	44
Left STG to parietal and frontal cortices	3534	5.67	-40	-32	12	Left STG to parietal and frontal cortices	4788	5.76	-40	-32	12
Left SMG/IPS	5.21	-34	-44	42	42	Left SMG/IPS	5.25	-36	-46	40	40
Left precuneus	4.43	-12	-72	48	48	Left insular cortex	5.29	-30	24	0	0
Left insular cortex	5.04	-30	24	0	0						
Left premotor & motor cortices	807	5.52	-26	-6	52	Right precuneus	279	4.61	12	-66	50
Right putamen	60	4.17	22	4	0	Left precuneus	161	4.46	-12	-72	48
Left putamen	34	3.84	-22	-4	6	Left primary visual cortex	62	3.91	-10	-78	8
						Right primary visual cortex	45	4.34	12	-78	12

Table 10: Size and peak coordinates of major clusters during the What-Where task for control and blindfold sessions. Selected sub-peaks within large clusters are also reported. Results for these basic contrasts (‘what’ and ‘where’ vs. rest) are thresholded at $z > 3.1$ (cluster corrected $p < 0.05$). STG = superior temporal gyrus; SMG = supramarginal gyrus; IPS = intraparietal sulcus; IFG = inferior frontal gyrus; MFG = middle frontal gyrus.

(**Figure 50, panel B**). The coordinates of these clusters (thresholded at $z > 3.1$) are reported in **Table 10**. However, in the ‘what’ condition these clusters do not survive the increased threshold (as shown by the very small clusters reported in italics in **Table 10**). Furthermore, a paired contrast of blindfold > control session did not reveal any auditory-evoked responses in the occipital cortex for either auditory condition, suggesting this may be an artefact of thresholding.

Auditory-evoked BOLD responses during the ‘what’ and ‘where’ auditory conditions (relative to the silent baseline) were calculated for occipital visual areas and compared between each subject’s control and blindfold session. However, mean percentage BOLD signal change (as calculated in Chapter 7 with the control and anophthalmia groups) meant that small ‘what’/‘where’ responses averaged over large ROI sizes yielded mostly “negative” mean percentage BOLD change (see **Appendix Figure 1** at the end of this chapter). As an alternative, the extent of activation in occipital areas was calculated as the number of active voxels in each ROI (Devlin et al., 2003). Voxels were defined as “active” at two thresholds: $z > 1.645$ (noise level) and $z > 2.3$. The average number of active voxels (relative to total ROI volume) in the control and blindfold sessions are plotted in **Appendix Figure 2**. This figure shows considerable activated tissue volume in visual areas during both the control and blindfold session. Statistical analyses (3-way ANOVA of session x visual area x hemisphere) on these measurements did not find a significant difference between the blindfold and control sessions in either the ‘what’ or ‘where’ conditions.

As this null result could be due to large between-subject variability, within-subject differences were plotted instead (**Figure 51**). This figure shows the difference in number of active voxels between each subject's blindfolded and control session (number in the blindfold session – number in the control session, divided by total number of active voxels in both sessions). This difference index therefore accounts for between-subject variability in number of active voxels and ROI sizes. The group average difference index (with SEM error bars) is plotted for the 'what' and 'where' conditions at each threshold in **Figure 51 (panels A-D)**. Difference indices for each individual subject are plotted for two sample ROIs in **panels E and F**. At the group level, there is a mean positive index for the 'what' condition (**A**), especially in right early visual areas. This is similar to the higher threshold (**C**). The pattern is less consistent in the 'where' condition (**B**), although there is a clearer separation between hemispheres at the higher threshold (**D**) in V4, favouring the right hemisphere. However, as demonstrated by large error bars in **panels A-D** and the individual plots for two sample ROIs in **panels E-F**, there is considerable variability across the subjects. Whilst some participants show an increase in activity following blindfolding, a subgroup shows the opposite effect. The composition of this second group of subjects is relatively consistent for both 'what' and 'where' conditions (subjects 2, 3 and 9 in particular).

In order to assess whether improvements in pitch thresholds after blindfolding (shown in the pre-scan behavioural tests) are related to occipital responses to sound, demeaned changes in pitch thresholds were correlated

LEGEND Difference in # active voxels = $\frac{\text{blindfold} - \text{control}}{\text{blindfold} + \text{control}}$ $\cdots\blacksquare\cdots$ Left $\cdots\blacksquare\cdots$ Right

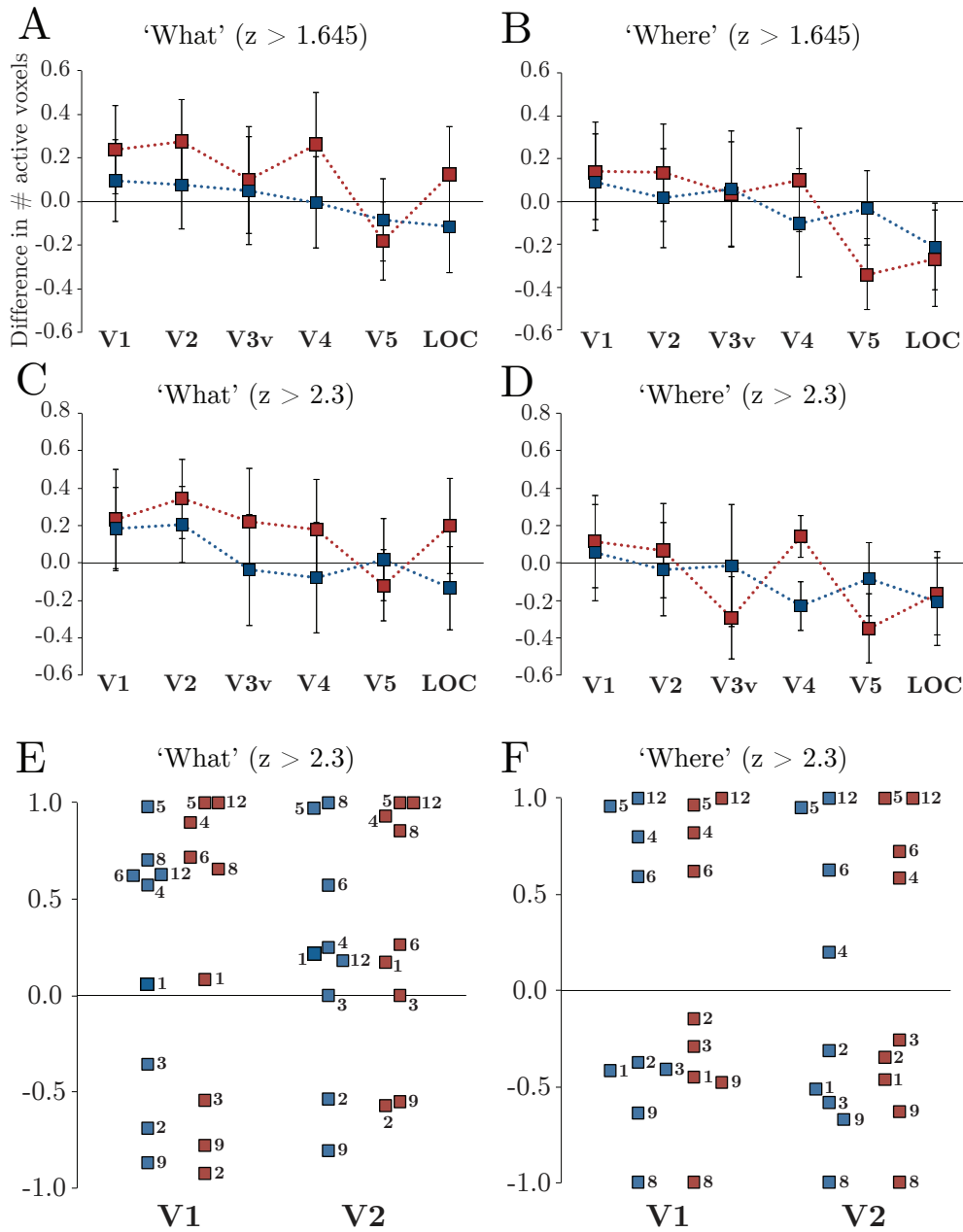


Figure 51: Difference between blindfold and control sessions in the number of “active” visual area voxels during the ‘what’ (left column) and ‘where’ (right column) auditory conditions. Difference is calculated for each subject as $(\text{blindfold} + \text{control}) / (\text{blindfold} - \text{control})$, so that values above zero indicate an increase in the number of voxels in the blindfold session compared to the control session. Average differences (SEM error bars) for the two hemispheres are plotted in A-D at two different thresholds: $z > 1.645$ (A, B) and $z > 2.3$ (C, D). Differences for each individual subject in two sample ROIs (V1 and V2) are plotted in E and F ($z > 2.3$).

with changes in activated tissue volume during the ‘what’ condition (also a pitch discrimination task). However, a significant correlation between these two measures was not found.

Meaning-Syllable task Group whole brain responses to the ‘meaning’ (semantic) and ‘syllable’ (phonological) conditions are shown in **Figure 52 (panels A and B)**. **Table 11** compares all major clusters in the control session (also previously reported in Chapter 7) and the blindfold session (thresholded at $z > 3.1$), as well as selected sub-peaks of interest located within these larger clusters. The stimuli evoked robust responses in the superior temporal cortex, anterior insular cortex, medial frontal cortex and putamen bilaterally in both sessions and both conditions (**Figure 52, panels A and B**, left column). The ‘syllable’ condition evoked robust responses in dorsal parietal regions (**Figure 52, panels A and B**, right columns) as well as early visual areas in both the control and the blindfold session. Whilst group occipital responses in the ‘meaning’ condition were found in the blindfold session only (peak coordinates for these clusters are reported in **Table 11**), a paired-subject contrast of blindfold $>$ control session did not confirm this (**Figure 52 (panel C)**). This contrast revealed some clusters of auditory-evoked responses during the ‘syllable’ condition in several left hemisphere visual areas (see **Table 11** for peak coordinates), although these have low statistical power. Blindfold $>$ control session auditory responses during the ‘meaning’ condition did not reveal any clusters of voxels at this uncorrected threshold with an extent of >30 voxels.

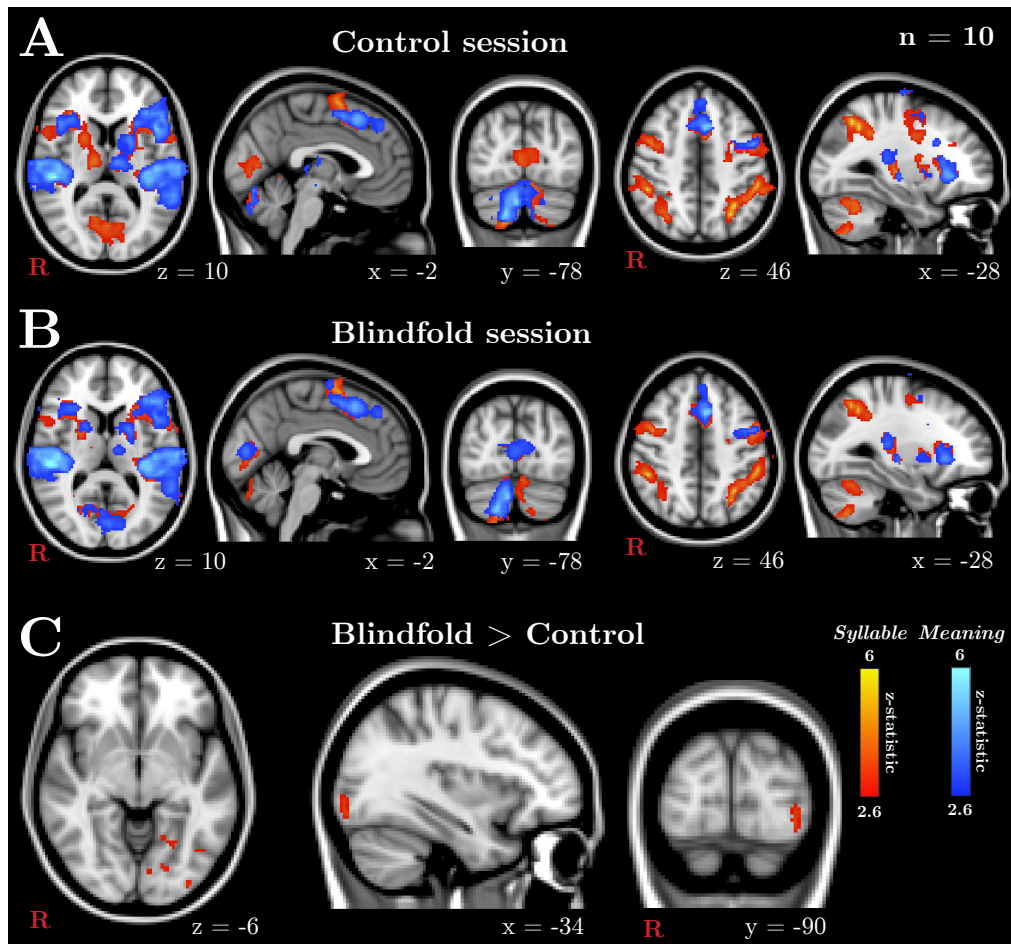


Figure 52: Group activation (in MNI 2-mm standard space) in the ‘meaning’ and ‘syllable’ auditory conditions for the control (top) and blindfold (bottom) sessions. Group statistical maps (10 subjects, mixed effects) are thresholded at $z > 2.6$ (cluster corrected, $p < 0.05$) for visualisation purposes. Panel C shows a paired contrast of blindfold > control session in the ‘meaning’ and ‘syllable’ conditions. Group statistical maps here are thresholded at $z > 2.6$ uncorrected but with a cluster size of minimum 30 voxels.

‘Syllable’	Cluster size	Z (peak)	x (mm)	y (mm)	z (mm)	Blindfold Mean – ‘Syllable’	Cluster size	Z (peak)	x (mm)	y (mm)	z (mm)
Left STG; frontal and parietal cortices	7412	6.39	-64	-20	4	Left STG; frontal and parietal cortices	6229	6.46	-64	-20	4
Left IFG		5.22	-30	24	6	Left IFG (pars opercularis)		4.80	-46	16	2
Left superior parietal cortex		5.73	-32	-54	48	Left SMG/superior parietal cortex		5.59	-32	-56	50
Right IFG to temporal cortex	3233	5.62	46	16	4	Right STG; right frontal cortex	2707	5.82	56	-28	12
Right STG		5.49	66	-18	6						
Right superior parietal cortex	246	4.25	36	-60	42	Right SMG	272	5.58	48	-40	48
Right SMG	272	5.52	48	-40	48	Right IFG (pars opercularis)	424	4.94	52	12	30
Bilateral paracingulate	873	5.45	-4	8	52	Bilateral paracingulate	914	5.28	-2	8	52
Right precentral gyrus	195	4.34	44	2	46	Right precentral gyrus	176	4.41	44	2	46
Bilateral primary visual cortex	367	3.93	0	-72	10	Left putamen	340	4.72	-22	6	4
						Bilateral primary visual cortex	124	4.03	2	-74	8
						Right occipital cortex	90	3.96	14	-66	4
‘Meaning’	Cluster size	Z (peak)	x (mm)	y (mm)	z (mm)	Blindfold Mean – ‘Meaning’	Cluster size	Z (peak)	x (mm)	y (mm)	z (mm)
Left STG; left frontal cortex	7537	6.17	-48	-36	16	Left STG; left frontal cortex	7187	6.53	-48	-36	16
Left IFG (pars triangularis)		5.52	-42	32	6	Left IFG (pars triangularis)		5.27	-42	30	14
Right STG	2323	6.22	50	-28	10	Right STG	2515	6.49	50	-28	10
Bilateral paracingulate	506	5.64	-6	18	48	Bilateral paracingulate	609	5.55	-6	18	48
Right IFG (pars triangularis)	486	4.60	44	20	8	Right IFG (pars triangularis)	352	4.08	44	20	6
Left caudate; left putamen	262	4.37	-18	6	12	Left putamen	293	4.49	-22	8	2
						Bilateral primary auditory cortex	262	4.02	-2	-82	10
Blindfold > Control – ‘Syllable’	Cluster size	Z (peak)	x (mm)	y (mm)	z (mm)						
Left early visual areas (V1, V2, V3)	58	3.34	-22	-78	2						
Left anterior primary visual cortex	52	3.37	-24	-60	-2						
Left extrastriate cortex (V4, LOC)	38	3.32	-34	-88	-12						
Left lateral occipital cortex	31	3.31	-44	-70	-16						

Table 11: Size and peak coordinates of major clusters during the Meaning-Syllable task for control and blindfold sessions. Selected sub-peaks within large clusters are also reported. Results for the basic contrasts (‘syllable’ and ‘meaning’ vs. rest) are thresholded at $z > 3.1$ (cluster corrected $p < 0.05$). Contrasts between sessions (‘blindfold’ > ‘control’) are thresholded at $z > 2.6$ (minimum cluster size of 30 voxels).

As with the What-Where task, auditory-evoked BOLD responses during the ‘meaning’ and ‘syllable’ auditory conditions were calculated in occipital visual areas and compared between each subject’s control and blindfold sessions. Mean percentage BOLD signal change also yielded largely negative results, again most likely due to small responses averaged over large ROIs (see **Appendix Figure 3** at the end of this chapter). Instead, the number of active voxels (relative to total ROI volume) was calculated for each subject’s blindfold and control session and plotted in **Appendix Figure 4**. Similarly to the What-Where task, this figure shows considerable activated tissue volume in visual areas during both the control and blindfold session. Statistical analyses (3-way ANOVA of session x visual area x hemisphere) on these measurements did not find a significant difference between the blindfold and control sessions in either the ‘syllable’ or ‘meaning’ conditions.

In order to account for between-subject variability, the difference in number of active voxels between each subject’s blindfold and control session was calculated for the two conditions (blindfold session - control session, divided by total of both sessions). Group averages (and SEM error bars) are shown in **Figure 53 (panels A-D)**. Difference indices for each individual subject are plotted for two sample ROIs in **panels E and F**. At the group level, there is a mean positive difference index for both conditions (**panels A and B**); this pattern is maintained at a higher threshold (**panels C and D**). Whilst difference indices in the early visual areas are similar across the two hemispheres, there appears to be a larger difference in number of active voxels in left extrastriate visual areas in the blindfold compared to control

LEGEND Difference in # active voxels = $\frac{\text{blindfold} - \text{control}}{\text{blindfold} + \text{control}}$ $\cdots\blacksquare\cdots$ Left $\cdots\blacksquare\cdots$ Right

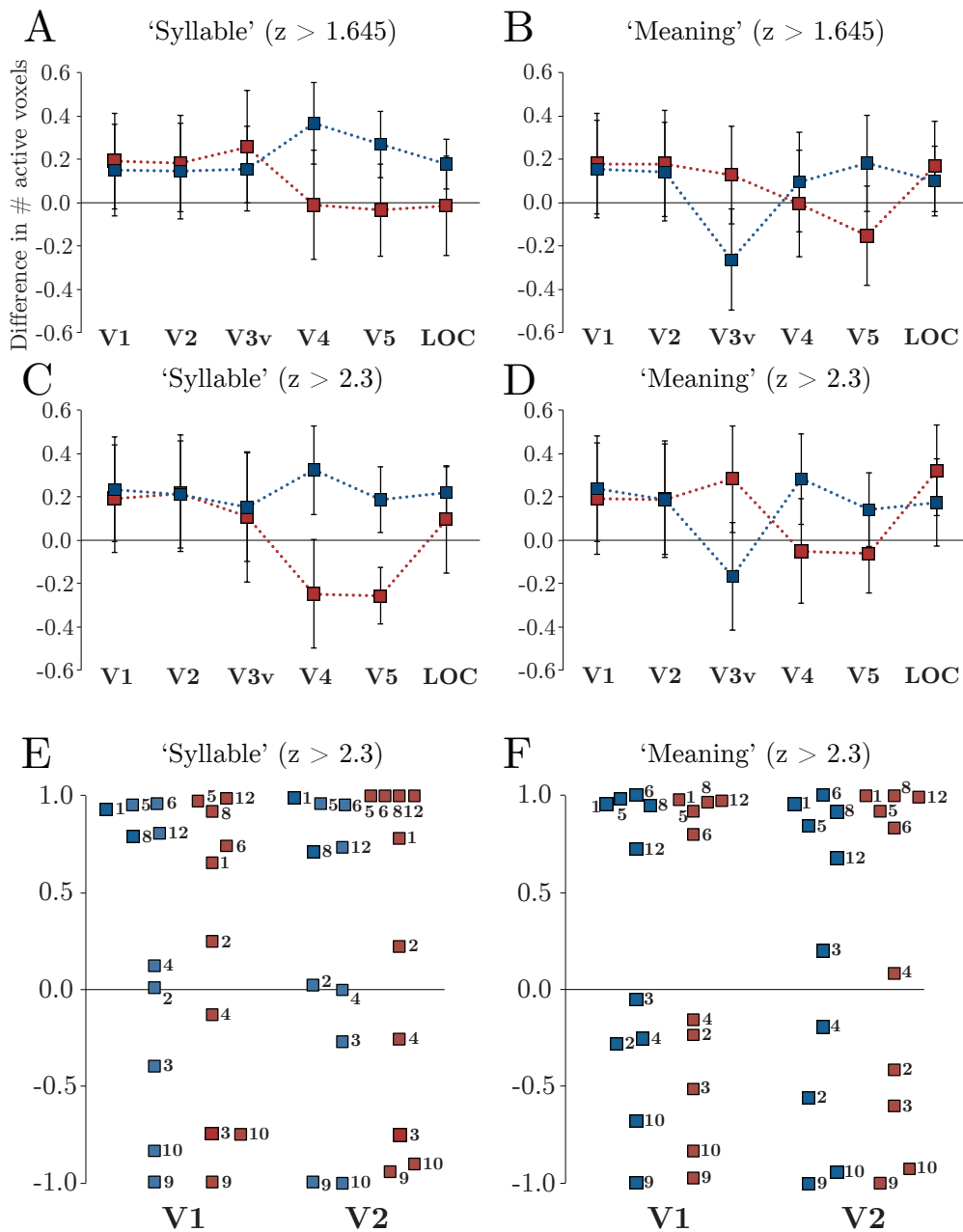


Figure 53: Difference between blindfold and control sessions in the number of “active” visual area voxels during the ‘syllable’ (left column) and ‘meaning’ (right column) auditory conditions. Difference is calculated for each subject as (blindfold – control) / (blindfold + control). Average differences (SEM error bars) for the two hemispheres are plotted in A-D at two different thresholds: $z > 1.645$ (A, B) and $z > 2.3$ (C, D). Differences for each individual subject in two sample ROIs (V1 and V2) are plotted in E and F ($z > 2.3$).

session. This is more robust in the ‘syllable’ condition and is consistent with the left extrastriate clusters shown in **Figure 52 (panel C)**. However, as demonstrated in **panels E and F**, there is considerable variability among subjects and no statistical tests were carried out to test this pattern. The same five subjects (2, 3, 4, 9 and 10) have negative difference indices in both the ‘syllable’ and ‘meaning’ condition. It is interesting to note that three subjects (2, 3 and 9) with negative difference indices in the What-Where task (see **Figure 51, panels E and F**) again show a similar pattern in the Meaning-Syllable task.

8.5 Discussion

A within-subject design was used to investigate whether short-term visual deprivation in sighted adults can induce auditory behavioural changes as well as cross-modal responses in the occipital visual cortex. Using behavioural measures of tonal and musical performance, this chapter shows that 80 minutes of visual deprivation can significantly improve pitch discrimination thresholds in sighted individuals. This chapter also notes an increase in occipital cortex activity during a combination of four tonal and speech sound conditions after 160 minutes of visual deprivation. This cross-modal change could mean that even in adulthood, the cortex can reorganise according to the available sensory input. This will be important for individuals who become blind later in life and need to adapt to their new sensory environment. However, within the individual sound conditions, this effect was very variable across

individuals and a larger sample size is needed to investigate whether this effect is robust. Nevertheless, the between-subject variability seems in part due to auditory-evoked BOLD responses in occipital areas during the control session in about half of the participants, which is a potentially interesting inter-individual difference.

8.5.1 Behavioural findings

Consistently lower (better) pitch thresholds were found in the sighted participants after 80 minutes of blindfolding. This means that temporary visual deprivation increased the ability of participants to resolve smaller pitch differences than when not visually deprived. This improvement in pitch discrimination abilities is consistent with Voss and Zatorre (2012) findings of lower pitch thresholds in early blind individuals. However, as noted in previous studies (Gougoux et al., 2004; Wan et al., 2010), pitch thresholds for late blind participants in the Voss and Zatorre study did not differ from those of sighted controls. Voss and Zatorre drew the logical conclusion that improvements in pitch performance could develop only as a consequence of early onset blindness. The findings in this chapter suggest that this may not be the case, and that short periods of visual deprivation can induce comparable changes to those seen in individuals who have been blind for a long time due to early-onset blindness. It is not known how long the changes observed in sighted participants will persist or whether they would return to baseline after a longer period of deprivation, as suggested by data from late blind participants.

It is possible that the heightening of pitch abilities after blindfolding is related to the recruitment of occipital cortex when performing the task. As mentioned in the results section, occipital BOLD responses during a pitch identification task (the ‘what’ condition) were seen in some of the sighted participants during the blindfold session, but the extent of occipital activation did not correlate significantly with individual improvements at pitch discrimination. Gougoux et al. (2005) found that blind individuals who demonstrate superior sound localisation abilities also showed occipital cortex activation (measured with PET) when presented with spatial sounds. However, additional subjects and a clear and significant correlation between pitch change and increased occipital BOLD responses after blindfolding will be needed in order to assess whether a similar effect is present after short-term visual deprivation.

Loudness thresholds appear unaffected by short-term visual deprivation, which is consistent with Voss and Zatorre’s findings for both blind groups. Performances on the melody and phoneme discrimination tasks were also unaffected by short-term visual deprivation (80 minutes duration). Based on the Landry et al. (2013) findings that harmonicity thresholds are improved after 90 minutes of blindfolding, it was expected that performance on either the simple or transposed melody task would improve. However, Landry and colleagues found this effect was not unmasked after 60 minutes of blindfolding, therefore it is possible that a slightly longer period of deprivation than the one used in this chapter is required.

8.5.2 Functional findings: increased occipital responses to sounds after blindfolding

A contrast of blindfold > control sessions for the group of subjects that performed all four fMRI auditory conditions ('what', 'where', 'syllable' and 'meaning') revealed a significant increase in occipital responses to all sounds after 160 minutes of blindfolding (**Figure 49**). Clusters of auditory-evoked BOLD responses were found bilaterally in early visual areas like V1 and V2, as well as left V3 and right V3a. It is unlikely that visual imagery induced by visual deprivation is responsible for these increased auditory-evoked BOLD responses, since subjects were blindfolded during both control and blindfold scans. Occipital responses reported in the blindfold session are therefore additional to any found in the control session.

Interestingly, the large left hemisphere cluster of voxels in the blindfold > control contrast that extends to V3 also includes anterior portions of V1 and V2. Similar anterior occipital regions have previously been reported to receive and send projections to auditory and multisensory cortical regions. Retrograde tracer injections in peripheral (anterior) V1 of sighted monkeys revealed robust connections with primary and secondary auditory cortices as well as the superior temporal polysensory region (Falchier et al., 2002). Similar pathways have been found between peripheral V2 and caudal auditory cortex (Falchier et al., 2010). In sighted humans, resting state fMRI has shown a significant coupling of activity between medial Heschl's gyrus and anterior portions of the calcarine fissure (Eckert et al., 2008). Auditory input to the

occipital cortex as a result of visual deprivation may therefore utilise these pathways.

8.5.3 Task-specific findings: experimental power concerns and between-subject variability

Images of group averages for each session and task revealed auditory-evoked activity in bilateral primary visual cortex in the blindfold sessions. This was in addition to the expected whole-brain auditory activity found in the control session (see **Figure 50** and **Table 10** for the What-Where task; **Figure 52** and **Table 11** for the Meaning-Syllable task). However, contrasts of blindfold > control for each task did not show the same robust responses revealed by the contrast of all sound conditions combined (**Figure 49**). This is likely an indication of lack of experimental power, despite the use of a within-subject design with identical task demands for both the control and blindfold sessions.

The lack of power is likely worsened by considerable between-subject variability, as indicated by ROI analyses of the two tasks (**Figure 51** and **Figure 53**). Approximately half of the participants consistently show increased auditory-evoked responses in visual areas after blindfolding (notably subjects 5, 6, 8 and 12) in both the What-Where and Meaning-Syllable tasks. However, in the ‘what’ and ‘where’ conditions, three subjects showed no effect (no difference between sessions) and even a negative difference index (higher number of active voxels in the control than in the blindfold session). These same three subjects comprise the subgroup of half of the subjects in

the ‘meaning’ and ‘syllable’ conditions that showed no effect or a negative difference index. A negative index indicates there were considerably greater auditory-evoked responses in visual areas during the control session in these subjects. At a group level, it is therefore difficult to differentiate these sources of between-subject variability from the effects of blindfolding, especially considering the small sample of subjects and that the effects of interest are likely to be small.

This variability amongst individuals is not uncommon in the literature on both short- and long-term visual deprivation. Previous studies have noted large variability in the pattern of responses amongst blindfolded participants (Merabet et al., 2004). In addition, half of a group of blindfolded adults showed a posterior shift in the source of auditory steady-state response waveforms (measured by MEG) after 6 hours of visual deprivation, suggesting that in these subjects (but perhaps not in the others) the occipital cortex was recruited for auditory responses (Lazzouni et al., 2012). Similar variability is also documented amongst blind individuals (Gougoux et al., 2005; Lessard et al., 1998; Voss et al., 2008). The variability amongst the sighted subjects in this chapter, combined with low experimental power, makes it difficult to clearly establish whether there is a significant effect of blindfolding on occipital BOLD responses to sounds.

8.5.4 Task-specific lateralisation of occipital auditory-evoked responses after blindfolding

Nevertheless, increased visual area BOLD responses to all sounds (at a group level) and to specific sound conditions (in at least a subset of participants) after blindfolding is worth pursuing further. It may be that the occipital cortex's existing but perhaps latent role in auditory processing can be unmasked by visual deprivation in these subjects. Lewald et al. (2004) found that repetitive TMS to the sighted occipital cortex can modulate spatial hearing abilities, which suggests that the occipital cortex is cross-modal or “multimodal” by nature.

Chapter 7 proposed that auditory-evoked responses in the anophthalmic occipital cortex mirror the hierarchy of the sighted occipital cortex. If there are increased auditory-evoked responses in visual areas after blindfolding in sighted subjects, it is unclear precisely how these may be organised. However, there are some clues in the active voxel plots during the Meaning-Syllable task (**Figure 53**). As discussed in Chapter 7, occipital responses in anophthalmia to this language stimulus are bilateral in early ‘visual’ areas, but become left-lateralised in higher order areas. In sighted adults after 160 minutes of blindfolding, responses in early visual areas appear to be bilateral. However, increases in activated tissue volume in visual areas after blindfolding are left-lateralised in higher-order regions (V4, V5, LOC) (**Figure 53**). This is most notable in the ‘syllable’ condition, and confirmed in the contrast of blindfold > control (**Figure 52, panel C**). As discussed in Chapter 7, lateralisation

of responses is usually indicative of higher-order sensory processing. Rather than the hypothesised “reverse hierarchy theory” for cross-modal changes in the visually deprived occipital cortex (as discussed in Chapter 1, see Büchel (2003)), these lateralised auditory responses after short-term visual deprivation are more in line with the theory of maintained hierarchy. However, additional subjects are required to investigate this further.

8.5.5 Short-term deprivation: rapid and reversible unmasking of existing connections?

One would assume that any changes after short-term visual deprivation would resemble the profile of late-onset blindness. However, whilst a heightening of auditory abilities (such as pitch discrimination) has sometimes been noted in early-onset and not late-onset blindness (Voss and Zatorre, 2012; Gougoux et al., 2004; Wan et al., 2010), this chapter describes how rapid behavioural improvements can be found after a short period of visual deprivation in sighted adults. This is consistent with previous reports of improved abilities after short-term visual deprivation on various auditory tasks (Lewald, 2007; Landry et al., 2013), which are also similar to performances reported in congenital and early-blind individuals (Lewald, 2002). This chapter also provides some evidence of increased occipital BOLD responses to tones and speech sounds after 160 minutes of short-term visual deprivation, which is in line with previous reports of increased tactile-evoked occipital responses after five days of blindfolding (Pascual-Leone and Hamilton, 2001; Merabet et al., 2007). These responses in the Pascual-Leone blindfolding study were

disrupted by TMS to the occipital cortex, an effect which has also been found in early blind but not late-blind individuals (Cohen et al., 1997, 1999), thus further supporting the possibility that cross-modal changes after short-term deprivation appear different from changes noted after late-onset blindness.

It is unclear how these rapid changes are mediated in sighted adults over such a short period of time, and why these changes are not observed in late-blind individuals. Due to their rapid nature, it is likely that any increases in non-visual responses in the occipital cortex use pre-existing connections between sensory cortical areas. It has been postulated that short-term visual deprivation rapidly unmasks or releases the inhibition of these existing pathways (Pascual-Leone and Hamilton, 2001). Similar mechanisms and pathways should also be available to individuals with late-onset blindness, but perhaps these unmasking effects weaken or change in some way over time. Pitskel et al. (2007) found that the threshold for TMS-induced phosphenes in sighted adults over 5 days of blindfolding was reduced after 48 hours of blindfolding (indicating a transient increase in occipital cortex excitability), but then returned to baseline before the end of the blindfolding period. These findings suggest that the short-term effects of visual deprivation are only temporary and may normalise over time.

There is clear evidence for pre-existing connections between sensory cortices even in adulthood; it is therefore likely that these are the connections being used for cross-modal input to the occipital cortex. As discussed earlier, direct anatomical projections between primary auditory and visual cortices have been found in sighted non-human primates (Falchier et al., 2002;

Rockland and Ojima, 2003; Clavagnier et al., 2004). Moreover, connectivity between these two regions has also been noted in sighted humans using probabilistic tractography (Beer et al., 2011) and resting state fMRI (Eckert et al., 2008). The direct connection between primary auditory and primary visual cortex has been used to explain auditory spatial BOLD responses in the ‘primary visual cortex’ of early blind individuals using dynamic causal modelling (Collignon et al., 2013). Alternatively, auditory input could feed to the occipital cortex via existing connections from parietal or auditory association areas to the occipital cortex. Similar projections have been found in sighted non-human primates (Rockland and Ojima, 2003) and may be used in late-onset blindness to feed auditory spatial information to the occipital cortex (Collignon et al., 2013). Either of these pathways could be unmasked by short-term deprivation.

8.5.6 Conclusions

In conclusion, this chapter shows that 80 minutes of short-term visual deprivation can improve pitch discrimination abilities in sighted adults. Furthermore, 160 minutes of visual deprivation can also increase BOLD responses to tones and speech sound in the occipital cortex. However, there is also considerable between-subject variability, which may influence this result. Nevertheless, these findings suggest that subtle changes may be taking place after even short periods of visual deprivation, although the pathways that enable these rapid changes are yet to be investigated.

8.6 Appendix Figures

8.6.1 Appendix Figure 1

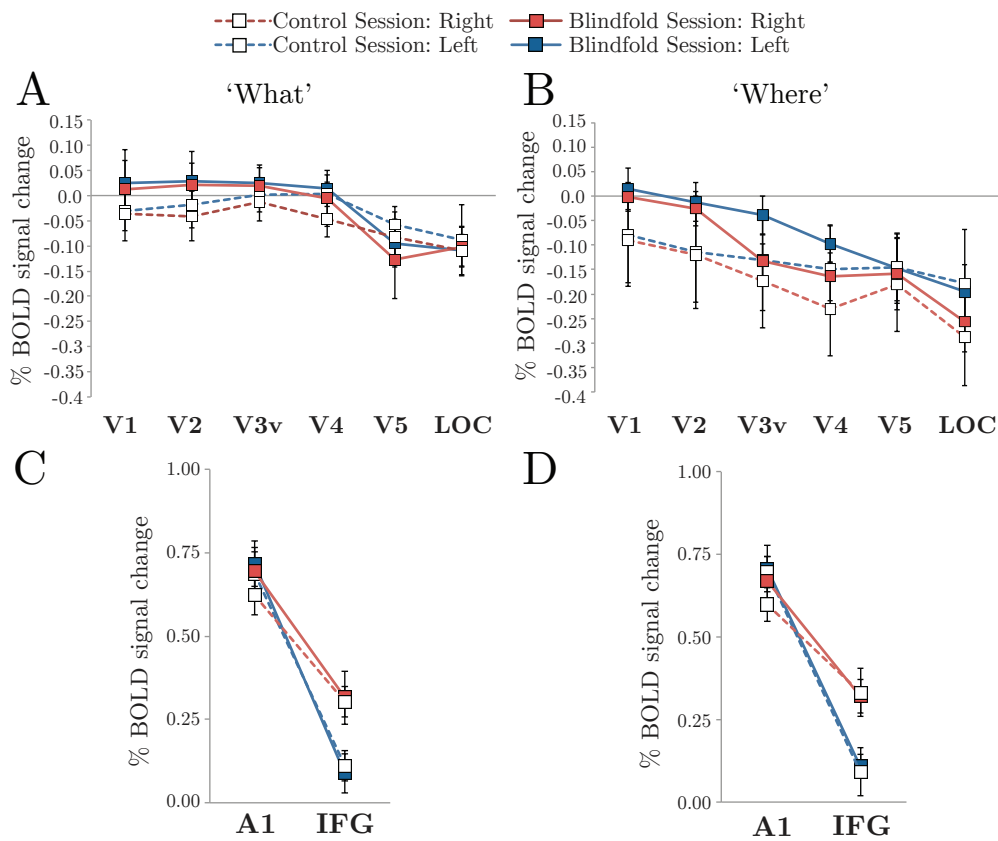


Figure 54: Group plots of percentage BOLD signal change during the 'what' and 'where' conditions in visual (A-B) and control (C-D) regions of interest. Error bars represent the standard error of the mean.

8.6.2 Appendix Figure 2

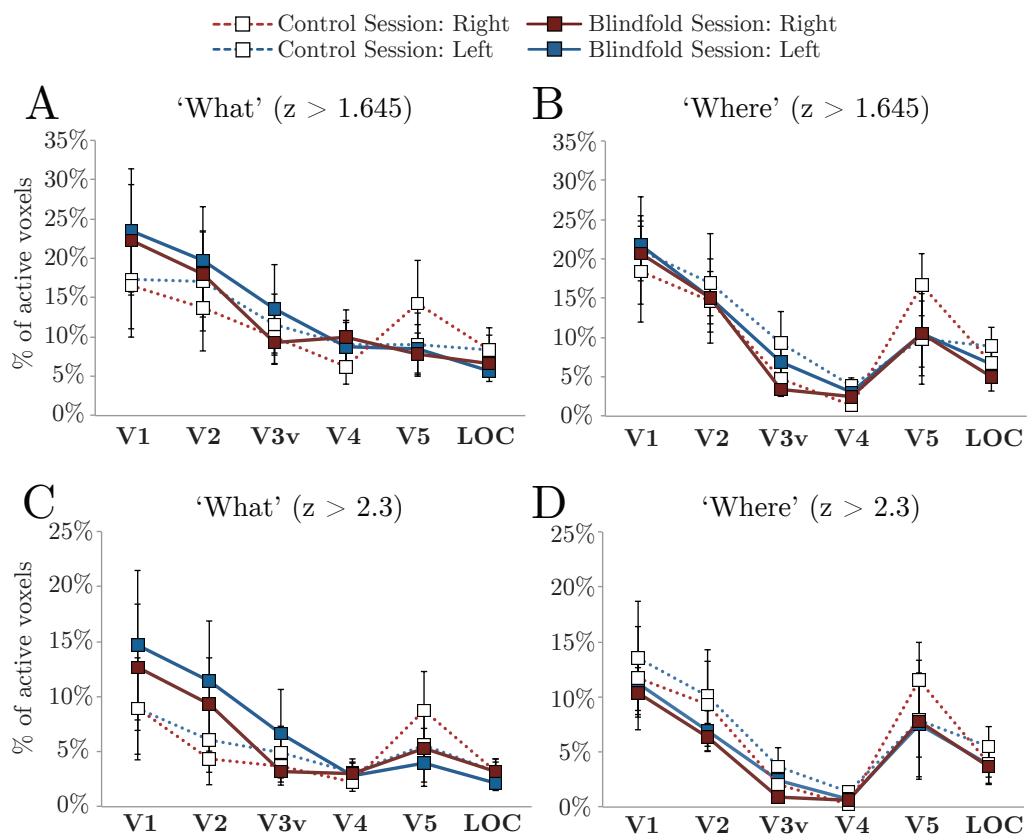


Figure 55: Number of active voxels (at two thresholds) relative to total ROI volume during the 'what' and 'where' conditions. Error bars represent the standard error of the mean.

8.6.3 Appendix Figure 3

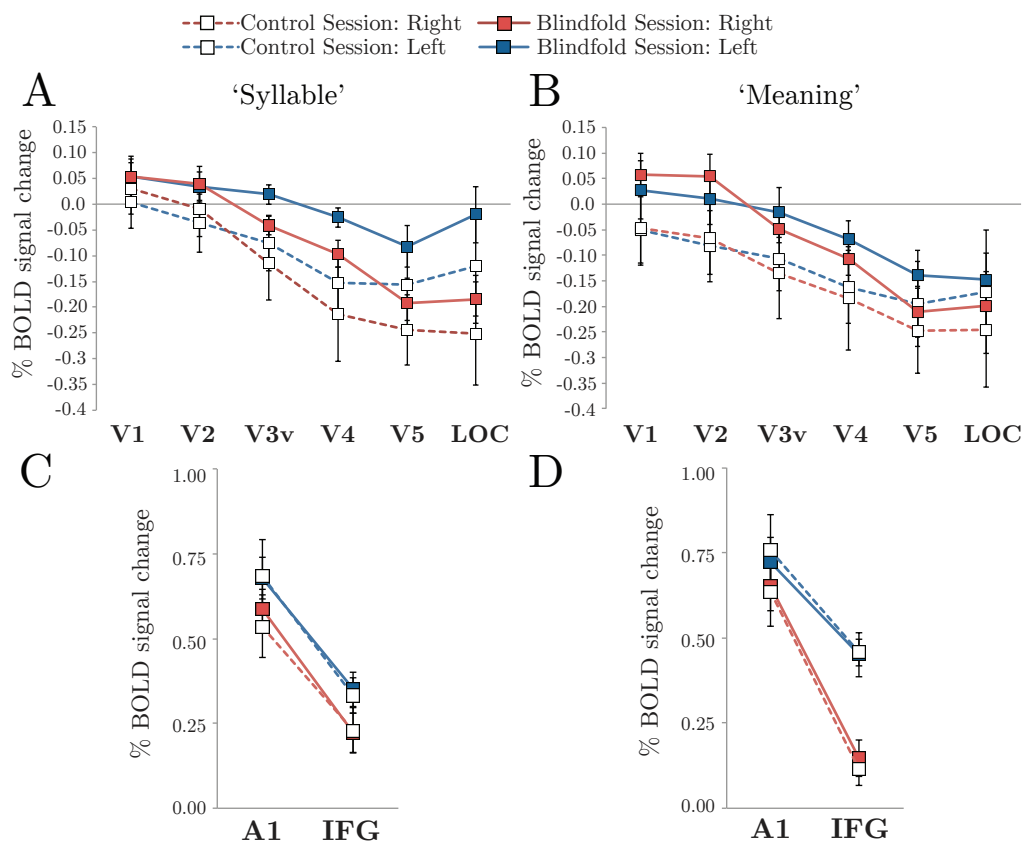


Figure 56: Group plots of percentage BOLD signal change during the 'syllable' and 'meaning' conditions in visual (A-B) and control (C-D) regions of interest. Error bars represent the standard error of the mean.

8.6.4 Appendix Figure 4

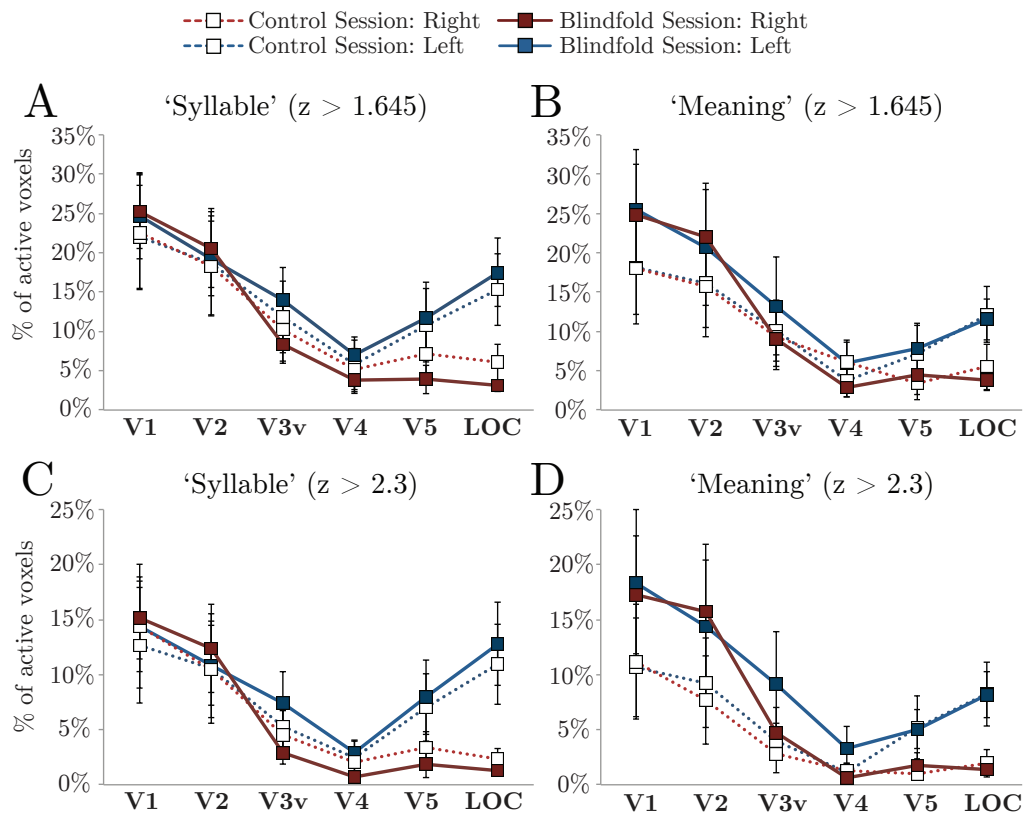


Figure 57: Number of active voxels (at two thresholds) relative to total ROI volume during the 'syllable' and 'meaning' conditions. Error bars represent the standard error of the mean.

9 General Discussion

The overall aim of this thesis was to determine how the absence of pre-natal visual experiences in anophthalmia affects the mechanisms, pathways, and organisation of cross-modal responses in ‘visual’ subcortical and cortical structures. This is important in order to determine the extent to which ‘visual’ pathway development relies on visual input in pre-natal and post-natal development. In particular, the thesis focused on how reorganisation of the ‘visual’ pathway in anophthalmia compares to other visually deprived populations. This was largely motivated by the body of work arguing that the most extensive changes in the ‘visual’ pathway happen with the earliest onset of visual deprivation.

The thesis addressed four questions in order to allow for a better understanding of the role of visual deprivation in cross-modal plasticity. The first was whether reorganisation takes place in subcortical structures, since subcortical inputs may provide a pathway for cross-modal innervation of the occipital cortex. The second was whether the traditional hierarchy of the occipital cortex is maintained in the absence of input, since this organisation may depend on pre-natal and post-natal visual experience. The third was

whether cross-modal reorganisation in anophthalmia is explained by changes in other properties of the blind cerebral cortex, either by its neurochemical content or by the effect of visual deprivation on the remaining senses. The fourth concerned the other end of the ‘blind’ timeline, and whether cross-modal changes can occur in sighted adults after very short periods of visual deprivation. Answering these four questions is important for the development of more appropriate sight restoration methods. These currently focus on restoring retinal function and assume normal functioning of cortical and subcortical areas. However, it is possible that once the ‘visual’ pathway has reorganised for auditory processing, cross-modal changes are irreversible and these regions will be unable to process visual information. By understanding how visual input influences development, new sight restoration techniques (such as prosthetic implants, gene therapies or stem cell replacements) can adapt their targets according to age of blindness onset.

The chapters in this thesis were designed to address the following research aims:

1. Test whether cross-modal responses to sound are found subcortically in anophthalmia, as suggested by the animal model of the condition. Furthermore, ask whether subcortical reorganisation is unique to anophthalmia by comparing their responses to a group of early blind individuals (Chapter 3 and Chapter 4). The results in these chapters show that the functional properties of subcortical sensory structures can reorganise in both anophthalmia and early blindness. These results are important because subcortical reorganisation may then affect how auditory input reaches the occipital cortex,

and therefore how the occipital cortex reorganises for auditory processing.

2. Characterise the neurochemical, neuroanatomical, and behavioural changes that may accompany long-term visual deprivation in anophthalmia. Occipital cortex neurochemistry and neuroanatomy are explored in Chapter 5, and auditory behavioural abilities (in relation to neuroanatomy) in Chapter 6. The results in these chapters are important because they suggest that reorganisation in anophthalmia may be due to atypical maturation of the 'visual' pathway. Furthermore, they illustrate that visual deprivation has a wide-spreading effect on cortical development and behaviour.

3. Explore how auditory responses are organised once they reach the occipital cortex in anophthalmia. In particular, assess whether functional specialisation and hierarchical processing in the sighted occipital cortex is maintained in anophthalmia when processing auditory stimuli (Chapter 7). The preliminary results in this chapter are important because they show that functional modules and hierarchical processing are present even in the absence of pre-natal and post-natal visual input. This illustrates that some characteristic features of the occipital cortex do not rely on visual input in order to develop.

4. Finally, investigate whether short periods of visual deprivation in sighted adults induce behavioural and cross-modal changes comparable to those characterised in blind populations (Chapter 8). Whilst the results in this chapter were variable between individuals, there was some evidence that the brain can adapt to the available sensory input, even in adulthood. If

replicated on a larger scale, these results will be important for individuals who become blind later in life and need to adapt to their new sensory environment.

The following chapter will summarise the conclusions drawn from these four research aims, and highlight some limitations and potential areas for future work.

9.1 Subcortical functional reorganisation in anophthalmia and early-onset blindness

The first part of this thesis looked at the organisation of the early ‘visual’ pathway in anophthalmia. Evidence obtained from animal models suggests that reorganisation of the ‘visual’ pathway for auditory processing in anophthalmia may differ from other causes of congenital or early blindness, especially in subcortical structures. In the anophthalmic mouse model (but not other blind populations), auditory responses as well as increased connections with auditory subcortical structures (like the inferior colliculus) have been found in dorsal portions of the ‘visual’ thalamic nucleus (LGN) (Piché et al., 2004; Chabot et al., 2008; Tucker et al., 2001). There is also some evidence of increased connectivity between subcortical structures, like the auditory thalamic nucleus (MGN), and the striate cortex in enucleated animals (Karlen et al., 2006). These findings provided motivation to study the human condition of anophthalmia in more detail, firstly by investigating subcortical reorganisation.

Chapter 3 explored subcortical responses to sound in anophthalmia using sparse sampling fMRI, and compared these to sighted subjects as well as a group of early blind individuals. The auditory stimulus was previously designed for robust auditory thalamus localisation (Jiang et al., 2013). Indeed, auditory-evoked responses were found in the region of the thalamus that matched the location of MGN in all subject groups. In contrast to auditory-evoked responses during the two fMRI tasks in Chapters 7 and 8 (What-Where and Meaning-Syllable), responses in this region using the stimulus from Chapter 3 were robust at an individual level. Whilst this difference could be due to the use of sparse vs. continuous sampling, previous work with the anophthalmic cases have also used sparse sampling fMRI and yet have not reported robust thalamic activations (Watkins et al., 2013).

Furthermore, responses to the stimulus revealed changes in how both auditory and ‘visual’ subcortical structures respond to sound in early-onset blindness. Firstly, the superior colliculus (a structure typically involved in visual processing in sighted subjects) was recruited for auditory processing in the anophthalmic and early blind groups. This structure has multimodal properties in sighted subjects (Meredith and Stein, 1986; Covey et al., 1987; Jiang et al., 1997; King et al., 1998), therefore it is feasible that it is more amenable for auditory processing in the absence of visual input. It would be interesting to find out whether this change also takes place after acquired blindness, or whether it is limited to early-onset blindness. Secondly, ipsilateral responses in the auditory thalamus of both anophthalmic and early blind groups were greater than their respective sighted control groups. This

suggests that the typical contralateral-greater-than-ipsilateral responses in the sighted auditory thalamus are not found in early-onset blindness. Some evidence for attenuated contralateral ear bias was also found in the anophthalmic inferior colliculus. Based on these data alone, it is not clear if this effect is bottom-up (possibly a strengthening of ipsilateral brainstem pathways, or crossing over from subcortical contralateral inputs) or top-down (increased descending feedback from A1 or V1). Both alternatives are possible; further investigations would therefore be needed to differentiate between them. Finally, contrary to the animal literature discussed earlier, this chapter did not provide evidence for the ‘visual’ thalamic nucleus (LGN) responding to sound in either blind group. Instead, auditory thalamic responses were localised to the region of the MGN. Whilst the animal model of anophthalmia suggests a recruitment of dorsal LGN for subcortical auditory processing, it may be that the human condition does not, possibly due to degeneration of this structure (Bridge et al., 2009). Scanning at higher field strengths may be able to address this question.

Surprisingly, Chapter 3 did not find differences between subcortical functional responses in anophthalmia and early-onset blindness. In order to look for more subtle or “hidden” differences between these two groups, Chapter 4 investigated effective connectivity between subcortical and cortical structures in this fMRI dataset. Dynamic causal modelling (DCM) has previously examined possible auditory pathways to V1 in early blind subjects (Klinge et al., 2010) and looked for differences between congenital and late-blind subjects (Collignon et al., 2013). Chapter 4 used some of these previously validated

DCM models (Klinge et al., 2010) to reveal a strengthening of MGN to V1 connections in both blind groups (separately and combined) compared to sighted controls. However, when tested with more complex DCM models that included the superior colliculus (since this region was shown to respond to sound in Chapter 3), the superior colliculus seemed to provide an alternative auditory subcortico-cortical route to V1 in anophthalmia only. In the early blind group, auditory inputs to V1 were limited to cortico-cortical routes from A1; this is in line with Klinge et al. (2010) showing that the pathway to V1 in early blind subjects are cortico-cortical (from A1) rather than subcortico-cortical (from MGN). This difference between anophthalmia and early blindness is interesting but would require additional data in order to boost experimental power and validate with a larger sample size.

9.2 Neurochemical, neuroanatomical and behavioural changes in anophthalmia

The second part of this thesis looked at other changes in anophthalmia that may reflect reorganisation of the visual pathway and its underlying neural mechanisms, in order to better understand functional changes taking place in subcortical and cortical structures.

In addition to recruitment for auditory processing, there is evidence of neurochemical (Weaver et al., 2013; Bernabeu et al., 2009) and anatomical (Shimony et al., 2006; Bridge et al., 2009; Jiang et al., 2009) reorganisation in the visually deprived occipital cortex. Chapter 5 used magnetic resonance

spectroscopy (MRS) and structural MRI to characterise the neurochemical content of the anophthalmic pericalcarine cortex (V1), and correlate this with previously reported anatomical changes (Bridge et al., 2009). Significant and robust increases in choline measures were found in anophthalmic V1 compared to sighted subjects. This is consistent with early blind subjects (Weaver et al., 2013) and animal models of visual deprivation (Fosse et al., 1989; Dehay et al., 1996). Choline measured by MRS could indicate increased activity in cholinergic pathways, which in turn could reflect increased cell numbers in this occipital region. Furthermore, choline measured by MRS is reported to be high at birth and decrease as the cortex matures (Blüml et al., 2012). Combined with increased cortical thickness in anophthalmic V1, which suggests a lack of pruning (Fischl and Dale, 2000), this chapter hypothesised that the lack of visual input in anophthalmia has affected the development of ‘visual’ pathway circuits. In particular, it may be that the lack of vision from birth has not triggered the normal patterns of neuronal maturation in the occipital cortex (Goldshmit et al., 2010).

Interestingly, this chapter did not replicate the differences in creatine or myo-inositol found in the pericalcarine cortex of early blind subjects (Weaver et al., 2013). This may be due to differences between the two blind groups, but the small anophthalmic sample size prevents any further speculation. In addition to a larger group size, the MRS data presented in Chapter 4 could be improved by obtaining a control measurement, for example in motor cortex, in order to ascertain that neurochemical changes are restricted to the ‘visual’ occipital areas. Finally, it is important to note that Chapter 4 did not

show a robust reduction in anophthalmic GABA measurements, which has been reported in early blind individuals (Weaver et al, 2013) and dark reared animals (Fosse et al., 1989; Benevento et al., 1995). However, this may be masked by changes in grey matter in the anophthalmic pericalcarine cortex where the MRS voxel was placed; when accounting for this, there was a trend for lower GABA per unit of grey matter in anophthalmia. However, this assumes that GABA is found only in grey matter; whilst there is evidence that this is largely the case, some GABA may be located within white matter (Bhattacharyya et al., 2011; Geramita et al., 2011). In order to clarify GABA content in anophthalmic pericalcarine cortex, an alternative MRS sequence may be required, for example one that uses spectral editing (for a review, see Puts and Edden (2012)).

In addition to cross-modal reorganisation of the occipital cortex, there is also evidence of improved auditory abilities in congenital and early blind subjects, such as musical and spatial processing (Gougoux et al. (2004); Lerens et al. (2014); Lewald (2013) to name a few). Furthermore, these improvements can be correlated with auditory-evoked responses in the occipital cortex (Gougoux et al. (2005); Collignon et al. (2007) to name a few) as well as anatomical changes in the blind occipital cortex (Voss and Zatorre, 2012; Voss et al., 2014). Chapter 6 looked to characterise some auditory abilities that may be enhanced in anophthalmia compared to sighted subjects. This chapter used auditory tasks previously tested with early and late blind individuals (Voss and Zatorre, 2012). Anophthalmic subjects demonstrated similar superior abilities on a pitch discrimination task to the early blind

subjects performing the same task (if not slightly better), as well as similar superior performance on two melody discrimination tasks. Moreover, there was a correlation between performance scores on one of these melody tasks (transposed melody discrimination) and right hemisphere V1 cortical thickness in anophthalmia. This correlation, which was also reported in early blind subjects (Voss and Zatorre, 2012), suggests a link between improved auditory abilities in anophthalmia and reorganisation of the occipital cortex. The right hemisphere correlation is also interesting in relation to the typical right lateralisation of auditory spectral responses in sighted subjects (Zatorre and Belin, 2001; Jamison et al., 2006), as it further implies functionality of the right occipital cortex in anophthalmia for processing spectral information.

9.3 Cortical functional reorganisation in anophthalmia

The third part of this thesis looked to determine how the occipital cortex is recruited for auditory processing in the absence of visual input. A previous imaging study with the anophthalmic cases included in this thesis (Watkins et al., 2012) suggested that traditional hierarchical processing of sensory information is maintained in the anophthalmic occipital cortex, with ‘early’ areas (like V1) responding to a range of sounds and higher-order areas specialising in high-level tasks like auditory language. This is contrary to evidence that various occipital areas (including V1) in congenital and early blindness can respond preferentially to semantically meaningful speech stimuli (Amedi et al., 2003; Röder et al., 2002; Bedny et al., 2011).

Chapter 7 used continuous sampling fMRI to address these differences, by exploring how different anophthalmic occipital ‘visual’ areas may be functionally specialised for processing low-level (spatial tones) and high-level (speech sounds) auditory stimuli. Preliminary data were obtained from four of the five anophthalmic cases discussed in this thesis. The data showed some evidence of functional organisation and hierarchical processing of sounds in the occipital cortex. Firstly, occipital responses in anophthalmia appeared to imitate the lateralisation of auditory responses typically found in sighted subjects (Zatorre and Belin, 2001; Jamison et al., 2006). The audio-spatial task (What-Where) elicited largely right-lateralised occipital responses, most notably in the ‘where’ condition, whilst auditory-evoked responses during the speech task (Meaning-Syllable) were greater in left occipital regions, especially in the ‘meaning’ condition.

Secondly, some auditory responses were localised to occipital regions that perform similar functions in sighted subjects. In the What-Where task, spatial sounds elicited robust responses in cuneus and middle occipito-temporal regions usually associated with visuo-spatial processing in sighted subjects (Renier et al., 2010). However, whilst responses in the ‘where’ condition appeared slightly elevated in right V3a (cuneus) compared to the ‘what’ condition, there was otherwise no clear dissociation between spatial localisation (‘where’) and sound localisation (‘what’). This could be due to the small sample size; a larger number of anophthalmic cases and a group analysis may be required to reveal preferential activity for spatial processing in these regions, as suggested by previous studies with congenital and early blind

subjects (Collignon et al., 2011, 2013; Renier et al., 2010).

Finally, there was some evidence of hierarchical auditory processing in the anophthalmic occipital cortex. During the Meaning-Syllable task, responses in early ‘visual’ areas (V1, V2 and possibly V5) were bilateral, whilst those in higher-order areas (V4, V3a, LOC) were largely left-lateralised. Furthermore, as suggested by Watkins et al. (2012), LOC appears to specialise for semantic processing in anophthalmia. Whilst LOC auditory-evoked responses in the anophthalmic cases did not differ from sighted controls in the low-level What-Where task, they were quite robust during the Meaning-Syllable task. Furthermore, in three of the four anophthalmic cases, LOC auditory responses appeared greater in the ‘meaning’ than ‘syllable’ condition, and were left-lateralised in the ‘meaning’ condition. Together, these findings suggest a hierarchical processing of auditory stimuli in the anophthalmic cortex, one that mirrors that of sighted occipital cortex for visual processing. This would mean that anophthalmia differs from other causes of congenital and early-onset blindness, because in these groups there appears to be no clear preferential activation for linguistic auditory stimuli in higher-order areas only, and instead perhaps some evidence for a “reversed hierarchy” (as discussed in Chapter 1).

However, it is important to note that Chapter 7 outlines preliminary findings. A larger anophthalmic group would be required in order to draw conclusions regarding the functional organisation of anophthalmic occipital cortex, and how this may differ from other causes of blindness. It is also interesting that V3a in anophthalmia appears to respond robustly to a range

of auditory stimuli, from spatial tones to speech sounds. Based on the data shown in Chapter 7, it cannot be concluded what features of sound this area selectively responds to. Additional stimuli could be designed to further investigate this.

9.4 Short-term visual deprivation in sighted adults

Finally, Chapter 8 looked to better understand cross-modal reorganisation after visual deprivation by investigating the timeline for these changes. In this chapter, sighted adults completed two experimental sessions, one in which they were blindfolded and the only in which they were not. Performance on the auditory tasks from Chapter 6 was compared between the two sessions, as were auditory-evoked fMRI responses using the two tasks from Chapter 7 (What-Where and Meaning-Syllable).

Pitch discrimination thresholds were significantly improved after 80 minutes of blindfolding, whilst 160 minutes appeared to increase BOLD responses to a combination of spatial tones and speech sounds in the occipital cortex of these sighted subjects. This is in line with evidence that short-term visual deprivation can improve various auditory abilities, including pitch (Gibby et al., 1970) and harmonicity (Landry et al., 2013) thresholds, as well as induce changes in how sighted subjects spatially locate sounds in a similar way to early blind subjects (Lewald, 2007). Furthermore, there is some evidence of increased auditory and tactile evoked responses in early visual areas of sighted subjects after short-term visual deprivation (see Pascual-Leone

and Hamilton (2001)). Interestingly, some of these changes have not been noted in late-blind subjects (Voss and Zatorre, 2012), so it is possible that temporary and reversible reorganisation normalises over time (Pitskel et al., 2007). Whilst the neural mechanisms for these changes are largely unclear, they could be due to an unmasking of existing pathways between primary visual and primary auditory cortex. It could be interesting to use resting state fMRI to further investigate these pathways and how they may be affected by short-term visual deprivation.

However, possibly one of the most substantial findings from Chapter 8 is the considerable between-subject variability in the sighted group. Whilst a combination of all sound conditions revealed increased occipital responses to sound after blindfolding, this effect was not robust for each individual task (What-Where and Meaning-Syllable). This is most likely due to limited experimental power as well as between-subject variability. Whilst some sighted subjects demonstrated increased auditory-evoked responses after blindfolding, a subgroup of subjects showed considerable occipital responses to sounds in the control session. This resulted in a negative difference between the two sessions, or a larger amount of auditory occipital activity in the control compared to blindfold session. It is interesting that the subjects comprising this subgroup were generally the same across the different task conditions ('what', 'where', 'meaning' and 'syllable'). Whilst it is possible that these differences are simply due to noise, between-subject variability has also been observed in other blindfolding studies (Lazzouni et al., 2012; Merabet et al., 2004); it is therefore likely that the effects of short-term visual deprivation

vary naturally across individuals. This holds important implications for all studies of visual deprivation, as discussed in below.

9.5 The importance of individual differences

One of the main conclusions that can be drawn from the work presented in this thesis is that individual differences are very important to the study of visual deprivation. The anophthalmia cases presented a unique opportunity to study a homogenous group of blind individuals who have never experienced pre- or post-natal visual input. Indeed, some interesting results were found relating to subcortico-cortical sensory pathways, changes in neurochemistry and neuroanatomy, and hierarchical processing of auditory stimuli in the occipital cortex. However, even within this homogenous group, there were considerable individual differences between these five cases (four in Chapter 7). This may account for the difficulty extracting robust differences between anophthalmia and early blindness in Chapters 3 and 4. Whilst homogenous groups are important to account for confounding differences between aetiology and age of blindness onset, this thesis highlights the importance of obtaining large groups in order to account for between-subject variability.

Additionally, Chapter 8 could be used as an example of how between-subject variability in sighted subjects could be confounding studies of cross-modal plasticity in blind populations. If, as shown in Chapter 8, some sighted adults show considerable occipital responses during auditory tasks (even under non-visually deprived conditions), these responses may not necessarily reflect

the same cross-modal processes taking place in the occipital cortex of blind individuals. For example, occipital responses to sound in sighted adults could be indicative of experience-dependent plasticity such as musical training or other auditory experience that might involve a recruitment of the visual cortex for auditory processing. Indeed, Huang et al. (2010) found increased auditory-evoked responses in bilateral occipital cortex when sighted musicians performed a memory retrieval task (Huang et al., 2010). When sighted adults are used as controls for studies of cross-modal reorganisation in blindness, occipital responses to sound in this group could end up masking occipital responses in the blind subject groups, especially if the cross-modal effects of interest are small. This brings to light some concerns about how blind groups should be compared to sighted control subjects, whether alternative methods should be used, or at least a more in-depth consideration of the implications.

9.6 Areas for future work

Some potential avenues for future work are outlined below. Firstly, the subcortical changes discussed in Chapters 3 and 4 could be interesting to investigate in the context of spatial navigation; there is a wide literature showing alterations in auditory spatial processing in blind individuals, but the underlying mechanisms are unclear. Gori et al. (2014) recently reported that binaural auditory localisation in central space was severely impaired in early blind individuals when localising a target sound relative to the location of two other sounds. The deficit appears to be unique to this complex spatial

bisection task in central space, as performance was unaffected in simpler localisation tasks and previous studies have reported normal peripheral auditory localisation in early blind individuals (Röder et al., 1999; Voss et al., 2004). During monaural sound location, some early blind individuals have shown superior performance which correlated with occipital auditory-evoked responses (Gougoux et al., 2005). The superior performance was characterised by a weaker tendency to localise monaural stimulus towards the unobstructed ear. This is consistent with the idea that blind subjects may rely less on interaural amplitude or response differences, and may instead rely more heavily on cues like Doppler, interaural time differences, and spectral cues. As the superior colliculus is thought to be important for spatial attention (for a review, see Krauzlis et al. (2013)), recruitment of this structure for auditory processing in early-onset blindness (Chapter 3) could be important for auditory spatial navigation. Furthermore, the enhancement of ipsilateral ear responses in the auditory thalamus (Chapter 3) could also affect spatial representations in blind individuals, since these representations rely on input from the two ears. A spatial navigation task could be designed to investigate how these two changes in early-onset blindness may contribute to spatial orientation.

Secondly, it would be interesting to further investigate how the anophthalmic occipital cortex interacts with other cortical and subcortical areas, in particular in relation to its role in auditory processing. This thesis provided some clues as to altered auditory processing in non-visual cortical areas in anophthalmia, for example in the auditory thalamus in Chapter 3. It has been postulated that the inclusion of occipital areas in the auditory network

in early blind subjects may affect how other cortical areas process sounds (Röder et al., 1999). For example, there is some evidence of increased functional connectivity between the occipital cortex and frontal cortex in blind subjects (Bedny et al., 2011; Watkins et al., 2012; Noppeney et al., 2003; Liu et al., 2007). It would be interesting to further investigate this connectivity by temporarily disrupting the anophthalmic occipital cortex with TMS and then use resting state neuroimaging to investigate the effects of this disruption on whole brain functional connectivity. TMS to the anophthalmic occipital cortex could also be used to investigate the theory postulated in Chapter 7 of maintained hierarchical processing. Temporary disruption of V1 could be used to confirm that this ‘early’ area carries out general auditory processing in anophthalmia, and is not selective to language processing. TMS over left LOC could then test the role of this ‘higher-order’ area in semantic processing of speech sounds, whilst stimulation of V3a could be used to further understand its role in auditory processing.

Finally, it is possible that auditory responses to sound in ‘visual’ areas in anophthalmia are not due to typical cross-modal plasticity. As discussed earlier, the neurochemical and neuroanatomical changes found in anophthalmia (Chapter 5) may be indicative of atypical occipital cortex maturation due to the complete absence of visual input. It follows that this atypical maturation will have influenced not only the neurochemical and anatomical properties of the occipital cortex, but also how it reorganises to respond to auditory stimuli (Chapter 7). Furthermore, atypical maturation could also have occurred at the subcortical level in anophthalmia, thus affecting the functional profile of

subcortical structures and how these respond to sound (Chapter 3), as well their connections with the occipital cortex. Cross-modal recruitment of these subcortical and cortical regions for auditory processing in anophthalmia may therefore reflect atypical development rather than adaptive cross-modal plasticity. Any future work with anophthalmia should consider this possibility when discussing reorganisation of the 'visual' pathway, as what is considered 'plasticity' in anophthalmia may be very different from typical cross-modal plasticity observed after normal development.

9.7 Final conclusions

The experiments outlined in this thesis explored how the anophthalmic 'visual' pathway reorganises for auditory processing, from subcortical structures responding to basic sounds, to higher-order occipital areas extracting meaning from speech sounds. This thesis was motivated by evidence that the most extensive changes in the 'visual' pathway happen with the earliest visual deprivation onset (i.e. congenital bilateral anophthalmia). The thesis also looked to better understand the neurochemical, neuroanatomical and behavioural changes that accompany this reorganisation. Finally, preliminary findings were presented on whether similar changes can take place in the sighted brain after short periods of visual deprivation.

The findings presented here provide some evidence that the lack of prenatal visual experiences affects cross-modal reorganisation in anophthalmia, and that this phenomenon differs from other causes of early-onset blindness.

For example, the thesis shows a possibly unique subcortico-cortical route for auditory input to V1 from the superior colliculus, as well as maintained hierarchical processing of auditory stimuli in occipital cortex. However, this thesis also suggests that some reorganisation thought to be limited to anophthalmia can also be found in early blind subjects, for example with the subcortical changes described in Chapter 3. In addition, neurochemical, neuroanatomical and behavioural changes described in Chapters 5 and 6 are comparable to those reported in early-blind groups, therefore demonstrating considerable similarities between these populations. Finally, this thesis highlights the considerable contribution of individual differences in studies of cross-modal responses, and emphasises the need for larger more homogenous groups when investigating subcortical and cortical reorganisation in the absence of visual input.

References

- Ahveninen, J., Huang, S., Nummenmaa, A., Belliveau, J. W., Hung, A.-Y., Jääskeläinen, I. P., Rauschecker, J. P., Rossi, S., Tiitinen, H., and Raij, T. (2013). Evidence for distinct human auditory cortex regions for sound location versus identity processing. *Nature Communications*, 4:2585.
- Albernaz, V. S., Castillo, M., Hudgins, P. a., and Mukherji, S. K. (1997). Imaging findings in patients with clinical anophthalmos. *American Journal of Neuroradiology*, 18:555–61.
- Alink, A., Euler, F., Kriegeskorte, N., Singer, W., and Kohler, A. (2012). Auditory motion direction encoding in auditory cortex and high-level visual cortex. *Human Brain Mapping*, 33:969–78.
- Allon, N. and Yeshurun, Y. (1985). Functional organization of the medial geniculate body's subdivisions of the awake squirrel monkey. *Brain Research*, 360:75–82.
- Amedi, A., Floel, A., Knecht, S., Zohary, E., and Cohen, L. G. (2004). Transcranial magnetic stimulation of the occipital pole interferes with verbal processing in blind subjects. *Nature Neuroscience*, 7:1266–1270.
- Amedi, A., Raz, N., Pianka, P., Malach, R., and Zohary, E. (2003). Early 'visual' cortex activation correlates with superior verbal memory performance in the blind. *Nature Neuroscience*, 6(7):758–66.
- Amedi, A., Stern, W. M., Camprodon, J. A., Bermpohl, F., Merabet, L., Rotman, S., Hemond, C., Meijer, P., and Pascual-Leone, A. (2007). Shape conveyed by visual-to-auditory sensory substitution activates the lateral occipital complex. *Nature Neuroscience*, 10:687–689.
- Andersen, R. A., Snyder, L. H., Bradley, D. C., and Xing, J. (1997). Multi-modal representation of space in the posterior parietal cortex and its use in planning movements. *Annual Review of Neuroscience*, 20:303–330.
- Anurova, I., Renier, L. a., De Volder, A. G., Carlson, S., and Rauschecker, J. P. (2014). Relationship Between Cortical Thickness and Functional Activation in the Early Blind. *Cerebral Cortex*.
- Arno, P., De Volder, A. G., Vanlierde, A., Wanet-Defalque, M. C., Streel, E., Robert, A., Sanabria-Bohórquez, S., and Veraart, C. (2001). Occipital activation by pattern recognition in the early blind using auditory substitution for vision. *NeuroImage*, 13:632–645.

- Axelrod, S. (1959). Effect of early blindness: performance of blind and sighted children on tactile and auditory tasks. *American Foundation for the Blind, New York*.
- Bartlett, E. L. and Wang, X. (2011). Correlation of neural response properties with auditory thalamus subdivisions in the awake marmoset. *Journal of Neurophysiology*, 105:2647–2667.
- Bavelier, D. and Hirshorn, E. A. (2010). I see where you're hearing: how cross-modal plasticity may exploit homologous brain structures. *Nature Neuroscience*, 13:1309–1311.
- Bavelier, D. and Neville, H. J. (2002). Cross-modal plasticity: where and how? *Nature reviews. Neuroscience*, 3:443–452.
- Bedny, M., Konkle, T., Pelphrey, K., Saxe, R., and Pascual-Leone, A. (2010). Sensitive period for a multimodal response in human visual motion area MT/MST. *Current Biology*, 20:1900–1906.
- Bedny, M., Pascual-Leone, A., Dodell-Feder, D., Fedorenko, E., and Saxe, R. (2011). Language processing in the occipital cortex of congenitally blind adults. *Proceedings of the National Academy of Sciences of the United States of America*, 108(11):4429–34.
- Bedny, M., Pascual-Leone, A., Dravida, S., and Saxe, R. (2012). A sensitive period for language in the visual cortex: Distinct patterns of plasticity in congenitally versus late blind adults. *Brain and Language*, 122:162–170.
- Beer, A. L., Plank, T., and Greenlee, M. W. (2011). Diffusion tensor imaging shows white matter tracts between human auditory and visual cortex. *Experimental Brain Research*, 213:299–308.
- Belouèche-Babari, M., Chung, Y.-L., Al-Saffar, N. M. S., Falck-Miniotis, M., and Leach, M. O. (2010). Metabolic assessment of the action of targeted cancer therapeutics using magnetic resonance spectroscopy. *British Journal of Cancer*, 102:1–7.
- Benevento, L. A., Bakkum, B. W., and Cohen, R. S. (1995). gamma-Aminobutyric acid and somatostatin immunoreactivity in the visual cortex of normal and dark-reared rats. *Brain Research*, 689:172–182.
- Berman, N. E. J. (1991). Alterations of visual cortical connections in cats following early removal of retinal input. *Developmental Brain Research*, 63:163–180.

- Bernabeu, A., Alfaro, A., García, M., and Fernández, E. (2009). Proton magnetic resonance spectroscopy (1H-MRS) reveals the presence of elevated myo-inositol in the occipital cortex of blind subjects. *NeuroImage*, 47:1172–1176.
- Bhattacharyya, P. K., Phillips, M. D., Stone, L. A., and Lowe, M. J. (2011). In vivo magnetic resonance spectroscopy measurement of gray-matter and white-matter gamma-aminobutyric acid concentration in sensorimotor cortex using a motion-controlled MEGA point-resolved spectroscopy sequence. *Magnetic Resonance Imaging*, 29:374–379.
- Blüml, S., Wisnowski, J. L., Nelson, M. D., Paquette, L., Gilles, F. H., Kinney, H. C., and Panigrahy, A. (2012). Metabolic Maturation of the Human Brain From Birth Through Adolescence: Insights From In Vivo Magnetic Resonance Spectroscopy. *Cerebral Cortex*, pages 2944–2955.
- Boroojerdi, B., Bushara, K. O., Corwell, B., Immisch, I., Battaglia, F., Muellbacher, W., and Cohen, L. G. (2000). Enhanced excitability of the human visual cortex induced by short-term light deprivation. *Cerebral Cortex*, 10:529–534.
- Boucard, C. C., Hoogduin, J. M., van der Grond, J., and Cornelissen, F. W. (2007). Occipital proton magnetic resonance spectroscopy (1H-MRS) reveals normal metabolite concentrations in retinal visual field defects. *PLoS ONE*, 2:e222.
- Boulanger, Y., Labelle, M., and Khiat, A. (2000). Role of phospholipase A2 on the variations of the choline signal intensity observed by 1H magnetic resonance spectroscopy in brain diseases. *Brain Research Reviews*, 33:380–389.
- Bourne, J. A. and Rosa, M. G. P. (2006). Hierarchical development of the primate visual cortex, as revealed by neurofilament immunoreactivity: Early maturation of the middle temporal area (MT). *Cerebral Cortex*, 16:405–414.
- Brechmann, A. and Scheich, H. (2005). Hemispheric shifts of sound representation in auditory cortex with conceptual listening. *Cerebral Cortex*, 15:578–587.
- Bridge, H. (2011). Mapping the visual brain: how and why. *Eye (London, England)*, 25:291–296.

- Bridge, H., Cowey, A., Ragge, N., and Watkins, K. (2009). Imaging studies in congenital anophthalmia reveal preservation of brain architecture in 'visual' cortex. *Brain : a journal of neurology*, 132(Pt 12):3467–80.
- Bridge, H., Ragge, N., Jenkinson, N., Cowey, A., and Watkins, K. E. (2012). The fate of the oculomotor system in clinical bilateral anophthalmia. *Visual Neuroscience*, 29:193–202.
- Bronchti, G., Heil, P., Sadka, R., Hess, A., Scheich, H., and Wollberg, Z. (2002). Auditory activation of "visual" cortical areas in the blind mole rat (*Spalax ehrenbergi*). *European Journal of Neuroscience*, 16:311–329.
- Büchel, C. (2003). Cortical hierarchy turned on its head. *Nature Neuroscience*, 6(7):657–8.
- Buchel, C., Price, C., Frackowiak, R. S. J., and Friston, K. (1998). Different activation patterns in the visual cortex of late and congenitally blind subjects. *Brain : a journal of neurology*, 121:409–419.
- Buckner, R. L., Krienen, F. M., Castellanos, A., Diaz, J. C., and Yeo, B. T. T. (2011). The organization of the human cerebellum estimated by intrinsic functional connectivity. *Journal of Neurophysiology*, 106:2322–2345.
- Burton, H. (2003). Visual Cortex Activity in Early and Late Blind People. *Journal of Neuroscience*, 23:4005–4011.
- Burton, H., Diamond, J. B., and McDermott, K. B. (2003). Dissociating cortical regions activated by semantic and phonological tasks: a fMRI study in blind and sighted people. *Journal of Neurophysiology*, 90:1965–1982.
- Burton, H., Snyder, A. Z., Conturo, T. E., Akbudak, E., Ollinger, J. M., and Raichle, M. E. (2002a). Adaptive changes in early and late blind: a fMRI study of Braille reading. *Journal of Neurophysiology*, 87:589–607.
- Burton, H., Snyder, A. Z., Diamond, J. B., and Raichle, M. E. (2002b). Adaptive changes in early and late blind: a fMRI study of verb generation to heard nouns. *Journal of Neurophysiology*, 88:3359–3371.
- Cantley, L. C. (2002). The phosphoinositide 3-kinase pathway. *Science*, 296:1655–1657.
- Chabot, N., Charbonneau, V., Laramée, M.-E., Tremblay, R., Boire, D., and Bronchti, G. (2008). Subcortical auditory input to the primary visual cortex in anophthalmic mice. *Neuroscience Letters*, 433:129–134.

- Chabot, N., Robert, S., Tremblay, R., Miceli, D., Boire, D., and Bronchti, G. (2007). Audition differently activates the visual system in neonatally enucleated mice compared with anophthalmic mutants. *European Journal of Neuroscience*, 26:2334–2348.
- Chandrasekaran, A. R., Plas, D. T., Gonzalez, E., and Crair, M. C. (2005). Evidence for an instructive role of retinal activity in retinotopic map refinement in the superior colliculus of the mouse. *Journal of Neuroscience*, 25:6929–6938.
- Charbonneau, V., Laramée, M.-E., Boucher, V., Bronchti, G., and Boire, D. (2012). Cortical and subcortical projections to primary visual cortex in anophthalmic, enucleated and sighted mice. *European Journal of Neuroscience*, 36:2949–63.
- Chen, W., Zhu, X. H., Thulborn, K. R., and Ugurbil, K. (1999). Retinotopic mapping of lateral geniculate nucleus in humans using functional magnetic resonance imaging. *Proceedings of the National Academy of Sciences of the United States of America*, 96:2430–2434.
- Clavagnier, S., Falchier, A., and Kennedy, H. (2004). Long-distance feedback projections to area V1: implications for multisensory integration, spatial awareness, and visual consciousness. *Cognitive, Affective & Behavioral Neuroscience*, 4:117–126.
- Cliff, M., Joyce, D. W., Lamar, M., Dannhauser, T., Tracy, D. K., and Shergill, S. S. (2013). Aging effects on functional auditory and visual processing using fMRI with variable sensory loading. *Cortex*, 49:1304–1313.
- Cohen, L. G., Celnik, P., Pascual-Leone, A., Corwell, B., Falz, L., Dambrosia, J., Honda, M., Sadato, N., Gerloff, C., Catalá, M. D., and Hallett, M. (1997). Functional relevance of cross-modal plasticity in blind humans. *Nature*, 389:180–183.
- Cohen, L. G., Weeks, R. A., Sadato, N., Celnik, P., Ishii, K., and Hallett, M. (1999). Period of susceptibility for cross-modal plasticity in the blind. *Annals of neurology*, 45:451–460.
- Collignon, O., Dormal, G., Albouy, G., Vandewalle, G., Voss, P., Phillips, C., and Lepore, F. (2013). Impact of blindness onset on the functional organization and the connectivity of the occipital cortex. *Brain : a journal of neurology*, 136:2769–83.

- Collignon, O., Lassonde, M., Lepore, F., Bastien, D., and Veraart, C. (2007). Functional cerebral reorganization for auditory spatial processing and auditory substitution of vision in early blind subjects. *Cerebral Cortex*, 17:457–465.
- Collignon, O., Vandewalle, G., Voss, P., Albouy, G., Charbonneau, G., Lassonde, M., and Lepore, F. (2011). Functional specialization for auditory-spatial processing in the occipital cortex of congenitally blind humans. *Proceedings of the National Academy of Sciences of the United States of America*, 108:4435–4440.
- Collignon, O., Voss, P., Lassonde, M., and Lepore, F. (2009). Cross-modal plasticity for the spatial processing of sounds in visually deprived subjects. *Experimental Brain Research*, 192:343–358.
- Corbetta, M., Kincade, J. M., Ollinger, J. M., McAvooy, M. P., and Shulman, G. L. (2000). Voluntary orienting is dissociated from target detection in human posterior parietal cortex. *Nature Neuroscience*, 3:292–297.
- Covey, E., Hall, W. C., and Kobler, J. B. (1987). Subcortical connections of the superior colliculus in the mustache bat, *Pteronotus parnellii*. *Journal of Comparative Neurology*, 263:179–197.
- Cowey, A. (2010). The blindsight saga. *Experimental Brain Research*, 200:3–24.
- Dale, A. M., Fischl, B., and Sereno, M. I. (1999). Cortical surface-based analysis. I. Segmentation and surface reconstruction. *NeuroImage*, 9:179–194.
- De Volder, A. G., Bol, A., Blin, J., Robert, A., Arno, P., Grandin, C., Michel, C., and Veraart, C. (1997). Brain energy metabolism in early blind subjects: Neural activity in the visual cortex. *Brain Research*, 750:235–244.
- De Volder, A. G., Catalan-Ahumada, M., Robert, A., Bol, A., Labar, D., Coppens, A., Michel, C., and Veraart, C. (1999). Changes in occipital cortex activity in early blind humans using a sensory substitution device. *Brain Research*, 826:128–134.
- Dehaene, S. and Cohen, L. (2007). Cultural recycling of cortical maps. *Neuron*, 56:384–398.
- Dehay, C., Giroud, P., Berland, M., Killackey, H., and Kennedy, H. (1996). Contribution of thalamic input to the specification of cytoarchitectonic

- cortical fields in the primate: effects of bilateral enucleation in the fetal monkey on the boundaries, dimensions, and gyrification of striate and extrastriate cortex. *Journal of Comparative Neurology*, 367(1):70–89.
- Dehay, C., Kennedy, H., and Bullier, J. (1988). Characterization of transient cortical projections from auditory, somatosensory, and motor cortices to visual areas 17, 18, and 19 in the kitten. *Journal of Comparative Neurology*, 272:68–89.
- Devlin, J. T., Raley, J., Tunbridge, E., Lanary, K., Floyer-Lea, A., Narain, C., Cohen, I., Behrens, T., Jezzard, P., Matthews, P. M., and Moore, D. R. (2003). Functional asymmetry for auditory processing in human primary auditory cortex. *Journal of Neuroscience*, 23:11516–11522.
- Devlin, J. T., Sillery, E. L., Hall, D. A., Hobden, P., Behrens, T. E. J., Nunes, R. G., Clare, S., Matthews, P. M., Moore, D. R., and Johansen-Berg, H. (2006). Reliable identification of the auditory thalamus using multi-modal structural analyses. *NeuroImage*, 30:1112–1120.
- Diaz, B., Hintz, F., Kiebel, S. J., and von Kriegstein, K. (2012). Dysfunction of the auditory thalamus in developmental dyslexia. *Proceedings of the National Academy of Sciences of the United States of America*, 109:13841–13846.
- Doron, N. and Wollberg, Z. (1994). Cross-modal neuroplasticity in the blind mole rat *Spalax ehrenbergi*: a WGA-HRP tracing study. *Neuroreport*, 5:2697–2701.
- Doucet, M.-E., Guillemot, J.-P., Lassonde, M., Gagné, J.-P., Leclerc, C., and Lepore, F. (2005). Blind subjects process auditory spectral cues more efficiently than sighted individuals. *Experimental Brain Research*, 160:194–202.
- Driver, J. and Noesselt, T. (2008). Multisensory interplay reveals crossmodal influences on 'sensory-specific' brain regions, neural responses, and judgments. *Neuron*, 57:11–23.
- Dufour, A., Després, O., and Candas, V. (2005). Enhanced sensitivity to echo cues in blind subjects. *Experimental Brain Research*, 165:515–519.
- Eckert, M. A., Kamdar, N. V., Chang, C. E., Beckmann, C. F., Greicius, M. D., and Menon, V. (2008). A cross-modal system linking primary auditory and visual cortices: evidence from intrinsic fMRI connectivity analysis. *Human Brain Mapping*, 29:848–857.

- Elbert, T., Sterr, A., Rockstroh, B., Pantev, C., Müller, M. M., and Taub, E. (2002). Expansion of the tonotopic area in the auditory cortex of the blind. *Journal of Neuroscience*, 22:9941–9944.
- Elston, G. N., Oga, T., and Fujita, I. (2009). Spinogenesis and pruning scales across functional hierarchies. *Journal of Neuroscience*, 29:3271–3275.
- Elston, G. N., Oga, T., Okamoto, T., and Fujita, I. (2010). Spinogenesis and pruning from early visual onset to adulthood: an intracellular injection study of layer III pyramidal cells in the ventral visual cortical pathway of the macaque monkey. *Cerebral Cortex*, 20:1398–1408.
- Facchini, S. and Aglioti, S. M. (2003). Short term light deprivation increases tactile spatial acuity in humans. *Neurology*, 60:1998–1999.
- Falchier, A., Clavagnier, S., Barone, P., and Kennedy, H. (2002). Anatomical evidence of multimodal integration in primate striate cortex. *Journal of Neuroscience*, 22:5749–5759.
- Falchier, A., Schroeder, C. E., Hackett, T. A., Lakatos, P., Nascimento-Silva, S., Ulbert, I., Karmos, G., and Smiley, J. F. (2010). Projection from visual areas V2 and prostriata to caudal auditory cortex in the monkey. *Cerebral Cortex*, 20:1529–1538.
- Fischl, B. and Dale, A. M. (2000). Measuring the thickness of the human cerebral cortex from magnetic resonance images. *Proceedings of the National Academy of Sciences of the United States of America*, 97:11050–11055.
- FitzPatrick, D. R. and Van Heyningen, V. (2005). Developmental eye disorders. *Current Opinion in Genetics and Development*, 15:348–353.
- Fosse, V. M., Heggelund, P., and Fonnum, F. (1989). Postnatal development of glutamatergic, GABAergic, and cholinergic neurotransmitter phenotypes in the visual cortex, lateral geniculate nucleus, pulvinar, and superior colliculus in cats. *Journal of Neuroscience*, 9:426–435.
- Foster, N. E. V. and Zatorre, R. J. (2010). Cortical structure predicts success in performing musical transformation judgments. *NeuroImage*, 53:26–36.
- Frasnelli, J., Fark, T., Lehmann, J., Gerber, J., and Hummel, T. (2013). Brain structure is changed in congenital anosmia. *NeuroImage*, 83:1074–80.
- Frederick, B., Satlin, A., Wald, L. L., Hennen, J., Bodick, N., and Renshaw, P. F. (1997). Brain proton magnetic resonance spectroscopy in Alzheimer

- disease: changes after treatment with xanomeline. *American Journal of Geriatric Psychiatry*, 10:81–8.
- Fries, W. (1984). Cortical projections to the superior colliculus in the macaque monkey: a retrograde study using horseradish peroxidase. *Journal of Comparative Neurology*, 230:55–76.
- Friston, K. J., Harrison, L., and Penny, W. (2003). Dynamic causal modelling. *NeuroImage*, 19:1273–1302.
- Frost, D. O. (1981). Orderly anomalous retinal projections to the medial geniculate, ventrobasal, and lateral posterior nuclei of the hamster. *Journal of Comparative Neurology*, 203:227–256.
- Gabrieli, J. D., Poldrack, R. A., and Desmond, J. E. (1998). The role of left prefrontal cortex in language and memory. *Proceedings of the National Academy of Sciences of the United States of America*, 95:906–913.
- Geramita, M., van der Veen, J. W., Barnett, A. S., Savostyanova, A. A., Shen, J., Weinberger, D. R., and Marenco, S. (2011). Reproducibility of prefrontal ??-aminobutyric acid measurements with J-edited spectroscopy. *NMR in Biomedicine*, 24:1089–1098.
- Gibby, R. G. J., Gibby, R. G. S., and Townsend, J. C. (1970). Short-term visual restriction in visual and auditory discrimination. *Perceptual and Motor Skills*, 30(1970):15–21.
- Giraud, A. L., Lorenzi, C., Ashburner, J., Wable, J., Johnsrude, I., Frackowiak, R., and Kleinschmidt, A. (2000). Representation of the temporal envelope of sounds in the human brain. *Journal of Neurophysiology*, 84:1588–1598.
- Gitelman, D. R., Nobre, A. C., Sonty, S., Parrish, T. B., and Mesulam, M. M. (2005). Language network specializations: An analysis with parallel task designs and functional magnetic resonance imaging. *NeuroImage*, 26:975–985.
- Goldshmit, Y., Galley, S., Foo, D., Sernagor, E., and Bourne, J. A. (2010). Anatomical changes in the primary visual cortex of the congenitally blind Crx^{-/-} mouse. *Neuroscience*, 166:886–898.
- Goodale, M. A. and Milner, A. D. (1992). Separate visual pathways for perception and action. *Trends in Neurosciences*, 15:20–25.

- Gori, M., Sandini, G., Martinoli, C., and Burr, D. C. (2014). Impairment of auditory spatial localization in congenitally blind human subjects. *Brain : a journal of neurology*, 137(Pt 1):288–293.
- Gough, P. M., Nobre, A. C., and Devlin, J. T. (2005). Dissociating linguistic processes in the left inferior frontal cortex with transcranial magnetic stimulation. *Journal of Neuroscience*, 25:8010–8016.
- Gougoux, F., Belin, P., Voss, P., Lepore, F., Lassonde, M., and Zatorre, R. J. (2009). Voice perception in blind persons: A functional magnetic resonance imaging study. *Neuropsychologia*, 47:2967–2974.
- Gougoux, F., Lepore, F., Lassonde, M., Voss, P., Zatorre, R. J., and Belin, P. (2004). Pitch discrimination in the early blind. *Nature*, 430:309.
- Gougoux, F., Zatorre, R. J., Lassonde, M., Voss, P., and Lepore, F. (2005). A functional neuroimaging study of sound localization: visual cortex activity predicts performance in early-blind individuals. *PLoS Biology*, 3:e27.
- Goyal, M. S., Hansen, P. J., and Blakemore, C. B. (2006). Tactile perception recruits functionally related visual areas in the late-blind. *Neuroreport*, 17:1381–1384.
- Griffiths, T. D., Uppenkamp, S., Johnsrude, I., Josephs, O., and Patterson, R. D. (2001). Encoding of the temporal regularity of sound in the human brainstem. *Nature Neuroscience*, 4:633–637.
- Grill-Spector, K., Kourtzi, Z., and Kanwisher, N. (2001). The lateral occipital complex and its role in object recognition. In *Vision Research*, volume 41, pages 1409–1422.
- Gu, Q. (2003). Contribution of acetylcholine to visual cortex plasticity. *Neurobiology of learning and memory*, 80:291–301.
- Guimaraes, A. R., Melcher, J. R., Talavage, T. M., Baker, J. R., Ledden, P., Rosen, B. R., Kiang, N. Y., Fullerton, B. C., and Weisskoff, R. M. (1998). Imaging subcortical auditory activity in humans. *Human Brain Mapping*, 6:33–41.
- Hall, D. A., Haggard, M. P., Akeroyd, M. A., Palmer, A. R., Summerfield, A. Q., Elliott, M. R., Gurney, E. M., and Bowtell, R. W. (1999). "Sparse" temporal sampling in auditory fMRI. *Human Brain Mapping*, 7:213–223.

- Hamilton, R., Keenan, J. P., Catala, M., and Pascual-Leone, A. (2000). Alexia for Braille following bilateral occipital stroke in an early blind woman. *Neuroreport*, 11:237–240.
- Hamilton, R. H., Pascual-Leone, A., and Schlaug, G. (2004). Absolute pitch in blind musicians. *Neuroreport*, 15:803–806.
- Harms, M. P. and Melcher, J. R. (2002). Sound repetition rate in the human auditory pathway: representations in the waveshape and amplitude of fMRI activation. *Journal of Neurophysiology*, 88:1433–1450.
- Haxby, J. V., Grady, C. L., Horwitz, B., Ungerleider, L. G., Mishkin, M., Carson, R. E., Herscovitch, P., Schapiro, M. B., and Rapoport, S. I. (1991). Dissociation of object and spatial visual processing pathways in human extrastriate cortex. *Proceedings of the National Academy of Sciences of the United States of America*, 88:1621–1625.
- Hensch, T. K., Fagiolini, M., Mataga, N., Stryker, M. P., Baekkeskov, S., and Kash, S. F. (1998). Local GABA circuit control of experience-dependent plasticity in developing visual cortex. *Science*, 282:1504–1508.
- Hickok, G. and Poeppel, D. (2000). Towards a functional neuroanatomy of speech perception. *Trends in Cognitive Sciences*, 4:131–138.
- Hickok, G. and Poeppel, D. (2004). Dorsal and ventral streams: A framework for understanding aspects of the functional anatomy of language. *Cognition*, 92:67–99.
- Hickok, G. and Poeppel, D. (2007). The cortical organization of speech processing. *Nature reviews. Neuroscience*, 8:393–402.
- Holmes, G. (1918). Disturbances of vision by cerebral lesions. *British Journal of Ophthalmology*, 2:353–384.
- Huang, Z., Zhang, J. X., Yang, Z., Dong, G., Wu, J., Chan, A. S., and Weng, X. (2010). Verbal memory retrieval engages visual cortex in musicians. *Neuroscience*, 168:179–189.
- Innocenti, G. M., Berbel, P., and Clarke, S. (1988). Development of projections from auditory to visual areas in the cat. *Journal of Comparative Neurology*, 272:242–259.
- Innocenti, G. M. and Clarke, S. (1984). Bilateral transitory projection to visual areas from auditory cortex in kittens. *Developmental Brain Research*, 14:143–148.

- Izraeli, R., Koay, G., Lamish, M., Heicklen-Klein, A. J., Heffner, H. E., Heffner, R. S., and Wollberg, Z. (2002). Cross-modal neuroplasticity in neonatally enucleated hamsters: structure, electrophysiology and behaviour. *European Journal of Neuroscience*, 15(4):693–712.
- Jamison, H. L., Watkins, K. E., Bishop, D. V. M., and Matthews, P. M. (2006). Hemispheric specialization for processing auditory nonspeech stimuli. *Cerebral Cortex*, 16:1266–1275.
- Jenkinson, M., Bannister, P., Brady, M., and Smith, S. (2002). Improved optimization for the robust and accurate linear registration and motion correction of brain images. *NeuroImage*, 17:825–841.
- Jiang, F., Stecker, G. C., and Fine, I. (2013). Functional localization of the auditory thalamus in individual human subjects. *NeuroImage*, 78:295–304.
- Jiang, F., Stecker, G. C., and Fine, I. (2014). Auditory motion processing after early blindness. *Journal of Vision*, 14(13):1–18.
- Jiang, J., Zhu, W., Shi, F., Liu, Y., Li, J., Qin, W., Li, K., Yu, C., and Jiang, T. (2009). Thick visual cortex in the early blind. *Journal of Neuroscience*, 29:2205–2211.
- Jiang, Z. D., Moore, D. R., and King, A. J. (1997). Sources of subcortical projections to the superior colliculus in the ferret. *Brain Research*, 755:279–292.
- Johnsrude, I. S., Penhune, V. B., and Zatorre, R. J. (2000). Functional specificity in the right human auditory cortex for perceiving pitch direction. *Brain : a journal of neurology*, 123 (Pt 1:155–163.
- Jones, E. G. (2003). Chemically Defined Parallel Pathways in the Monkey Auditory System. *Annals of the New York Academy of Sciences*, 999:218–233.
- Källén, B. and Tornqvist, K. (2005). The epidemiology of anophthalmia and microphthalmia in Sweden. *European Journal of Epidemiology*, 20:345–350.
- Kanowski, M., Kaufmann, J., Braun, J., Bernarding, J., and Tempelmann, C. (2004). Quantitation of simulated short echo time 1H human brain spectra by LCMoel and AMARES. *Magnetic Resonance in Medicine*, 51:904–912.
- Karlen, S. J., Kahn, D. M., and Krubitzer, L. (2006). Early blindness results in abnormal corticocortical and thalamocortical connections. *Neuroscience*, 142:843–858.

- Katz, L. C. and Shatz, C. J. (1996). Synaptic activity and the construction of cortical circuits. *Science*, 274:1133–1138.
- Kauffman, T., Théoret, H., and Pascual-Leone, A. (2002). Braille character discrimination in blindfolded human subjects. *Neuroreport*, 13:571–574.
- Kelly, K. R., McKetton, L., Schneider, K. A., Gallie, B. L., and Steeves, J. K. E. (2014). Altered anterior visual system development following early monocular enucleation. *NeuroImage: Clinical*, 4:72–81.
- Kim, J.-K. and Zatorre, R. J. (2011). Tactile-auditory shape learning engages the lateral occipital complex. *Journal of Neuroscience*, 31:7848–7856.
- King, A. J., Jiang, Z. D., and Moore, D. R. (1998). Auditory brainstem projections to the ferret superior colliculus: anatomical contribution to the neural coding of sound azimuth. *Journal of Comparative Neurology*, 390:342–365.
- Klinge, C., Eippert, F., Röder, B., and Büchel, C. (2010). Corticocortical connections mediate primary visual cortex responses to auditory stimulation in the blind. *Journal of Neuroscience*, 30:12798–12805.
- Krauzlis, R. J., Lovejoy, L. P., and Zénon, A. (2013). Superior colliculus and visual spatial attention. *Annual Review of Neuroscience*, 36:165–82.
- Krumbholz, K., Schönwiesner, M., Rübsem, R., Zilles, K., Fink, G. R., and von Cramon, D. Y. (2005). Hierarchical processing of sound location and motion in the human brainstem and planum temporale. *European Journal of Neuroscience*, 21:230–238.
- Kujala, T., Alho, K., Huotilainen, M., Ilmoniemi, R. J., Lehtokoski, A., Leinonen, A., Rinne, T., Salonen, O., Sinkkonen, J., Standertskjöld-Nordenstam, C. G., and Näätänen, R. (1997). Electrophysiological evidence for cross-modal plasticity in humans with early- and late-onset blindness. *Psychophysiology*, 34:213–216.
- Kujala, T., Palva, M. J., Salonen, O., Alku, P., Huotilainen, M., Järvinen, A., and Näätänen, R. (2005). The role of blind humans’ visual cortex in auditory change detection. *Neuroscience Letters*, 379:127–131.
- Kumar, S., Stephan, K. E., Warren, J. D., Friston, K. J., and Griffiths, T. D. (2007). Hierarchical processing of auditory objects in humans. *PLoS Computational Biology*, 3:0977–0985.

- Laemle, L. K., Strominger, N. L., and Carpenter, D. O. (2006). Cross-modal innervation of primary visual cortex by auditory fibers in congenitally anophthalmic mice. *Neuroscience Letters*, 396:108–112.
- Lambert, S., Sampaio, E., Mauss, Y., and Scheiber, C. (2004). Blindness and brain plasticity: Contribution of mental imagery? An fMRI study. *Cognitive Brain Research*, 20:1–11.
- Landry, S. P., Shiller, D. M., and Champoux, F. (2013). Short-term visual deprivation improves the perception of harmonicity. *Journal of Experimental Psychology: Human Perception and Performance*, 39:1503–7.
- Langers, D. R. M., van Dijk, P., and Backes, W. H. (2005). Lateralization, connectivity and plasticity in the human central auditory system. *NeuroImage*, 28:490–499.
- Laurienti, P. J., Burdette, J. H., Wallace, M. T., Yen, Y.-F., Field, A. S., and Stein, B. E. (2002). Deactivation of sensory-specific cortex by cross-modal stimuli. *Journal of Cognitive Neuroscience*, 14:420–429.
- Lazzouni, L., Voss, P., and Lepore, F. (2012). Short-term crossmodal plasticity of the auditory steady-state response in blindfolded sighted individuals. *European Journal of Neuroscience*, 35:1630–1636.
- Leclerc, C., Saint-Amour, D., Lavoie, M. E., Lassonde, M., and Lepore, F. (2000). Brain functional reorganization in early blind humans revealed by auditory event-related potentials. *Neuroreport*, 11:545–550.
- Leech, R., Braga, R., and Sharp, D. J. (2012). Echoes of the Brain within the Posterior Cingulate Cortex. *Journal of Neuroscience*, 32:215–222.
- Lerens, E., Araneda, R., Renier, L., and De Volder, A. G. (2014). Improved beat asynchrony detection in early blind individuals. *Perception*, 43(10):1083–1096.
- Lessard, N., Paré, M., Lepore, F., and Lassonde, M. (1998). Early-blind human subjects localize sound sources better than sighted subjects. *Nature*, 395:278–280.
- Lewald, J. (2002). Opposing effects of head position on sound localization in blind and sighted human subjects. *European Journal of Neuroscience*, 15:1219–1224.
- Lewald, J. (2007). More accurate sound localization induced by short-term light deprivation. *Neuropsychologia*, 45:1215–1222.

- Lewald, J. (2013). Exceptional ability of blind humans to hear sound motion: Implications for the emergence of auditory space. *Neuropsychologia*, 51:181–186.
- Lewald, J., Meister, I. G., Weidemann, J., and Töpper, R. (2004). Involvement of the superior temporal cortex and the occipital cortex in spatial hearing: evidence from repetitive transcranial magnetic stimulation. *Journal of Cognitive Neuroscience*, 16:828–838.
- Lewis, L. B., Saenz, M., and Fine, I. (2010). Mechanisms of cross-modal plasticity in early-blind subjects. *Journal of Neurophysiology*, 104:2995–3008.
- Liang, M., Mouraux, A., Hu, L., and Iannetti, G. D. (2013). Primary sensory cortices contain distinguishable spatial patterns of activity for each sense. *Nature Communications*, 4:1979.
- Liu, Y., Yu, C., Liang, M., Li, J., Tian, L., Zhou, Y., Qin, W., Li, K., and Jiang, T. (2007). Whole brain functional connectivity in the early blind. *Brain : a journal of neurology*, 130:2085–2096.
- Locke, J. C. (1954). Retrolental fibroplasia definitive role of oxygen administration in its etiology. *AMA Arch Ophthalmol*, 59:73–79.
- MacKay, S., Meyerhoff, D. J., Constans, J. M., Norman, D., Fein, G., and Weiner, M. W. (1996). Regional gray and white matter metabolite differences in subjects with AD, with subcortical ischemic vascular dementia, and elderly controls with 1H magnetic resonance spectroscopic imaging. *Archives of neurology*, 53:167–174.
- McDermott, K. B., Petersen, S. E., Watson, J. M., and Ojemann, J. G. (2003). A procedure for identifying regions preferentially activated by attention to semantic and phonological relations using functional magnetic resonance imaging. *Neuropsychologia*, 41:293–303.
- Mekle, R., Mlynárik, V., Gambarota, G., Hergt, M., Krueger, G., and Gruetter, R. (2009). MR spectroscopy of the human brain with enhanced signal intensity at ultrashort echo times on a clinical platform at 3T and 7T. *Magnetic Resonance in Medicine*, 61:1279–1285.
- Merabet, L. B., Maguire, D., Warde, A., Alterescu, K., Stickgold, R., and Pascual-Leone, A. (2004). Visual hallucinations during prolonged blind-folding in sighted subjects. *Journal of Neuro-Ophthalmology*, 24:109–113.

- Merabet, L. B. and Pascual-Leone, A. (2010). Neural reorganization following sensory loss: the opportunity of change. *Nature reviews. Neuroscience*, 11:44–52.
- Merabet, L. B., Swisher, J. D., McMains, S. A., Halko, M. A., Amedi, A., Pascual-Leone, A., and Somers, D. C. (2007). Combined activation and deactivation of visual cortex during tactile sensory processing. *Journal of Neurophysiology*, 97:1633–1641.
- Meredith, M. A. and Stein, B. E. (1986). Visual, auditory, and somatosensory convergence on cells in superior colliculus results in multisensory integration. *Journal of Neurophysiology*, 56:640–662.
- Micheyl, C. and Oxenham, A. J. (2010). Pitch, harmonicity and concurrent sound segregation: Psychoacoustical and neurophysiological findings. *Hearing Research*, 266:36–51.
- Morales, B., Choi, S.-Y., and Kirkwood, A. (2002). Dark rearing alters the development of GABAergic transmission in visual cortex. *Journal of Neuroscience*, 22:8084–8090.
- Morel, A., Magnin, M., and Jeanmonod, D. (1997). Multiarchitectonic and stereotactic atlas of the human thalamus. *Journal of Comparative Neurology*, 387:588–630.
- Morosan, P., Rademacher, J., Schleicher, A., Amunts, K., Schormann, T., and Zilles, K. (2001). Human primary auditory cortex: cytoarchitectonic subdivisions and mapping into a spatial reference system. *NeuroImage*, 13:684–701.
- Mrsic-Flogel, T. D., Versnel, H., and King, A. J. (2006). Development of contralateral and ipsilateral frequency representations in ferret primary auditory cortex. *European Journal of Neuroscience*, 23:780–792.
- Muchnik, C., Efrati, M., Nemeth, E., Malin, M., and Hildesheimer, M. (1991). Central auditory skills in blind and sighted subjects. *Scandinavian Audiology*, 20:19–23.
- Near, J., Andersson, J., Maron, E., Mekle, R., Gruetter, R., Cowen, P., and Jezard, P. (2013). Unedited in vivo detection and quantification of γ -aminobutyric acid in the occipital cortex using short-TE MRS at 3 T. *NMR in Biomedicine*, 26:1353–62.

- Near, J., Edden, R., Evans, C. J., Paquin, R., Harris, A., and Jezzard, P. (2014). Frequency and phase drift correction of magnetic resonance spectroscopy data by spectral registration in the time domain. *Magnetic Resonance in Medicine*.
- Nhan, H. L. and Callaway, E. M. (2012). Morphology of superior colliculus- and middle temporal area-projecting neurons in primate primary visual cortex. *Journal of Comparative Neurology*, 520:52–80.
- Niemann, K., Mennicken, V. R., Jeanmonod, D., and Morel, A. (2000). The Morel stereotactic atlas of the human thalamus: atlas-to-MR registration of internally consistent canonical model. *NeuroImage*, 12:601–616.
- Noppeney, U., Friston, K. J., Ashburner, J., Frackowiak, R., and Price, C. J. (2005). Early visual deprivation induces structural plasticity in gray and white matter. *Current Biology*, 15(13):R488–R490.
- Noppeney, U., Friston, K. J., and Price, C. J. (2003). Effects of visual deprivation on the organization of the semantic system. *Brain : a journal of neurology*, 126:1620–1627.
- Park, H. J., Lee, J. D., Kim, E. Y., Park, B., Oh, M. K., Lee, S., and Kim, J. J. (2009). Morphological alterations in the congenital blind based on the analysis of cortical thickness and surface area. *NeuroImage*, 47:98–106.
- Pascolini, D. and Mariotti, S. P. (2012). Global estimates of visual impairment: 2010. *British Journal of Ophthalmology*, 96:614–618.
- Pascual-Leone, A. and Hamilton, R. (2001). The metamodal organization of the brain. In *Progress in Brain Research*, volume 134, pages 427–445.
- Pasqualotto, A. and Proulx, M. J. (2012). The role of visual experience for the neural basis of spatial cognition. *Neuroscience and Biobehavioral Reviews*, 36:1179–1187.
- Pellerin, L. (2005). How astrocytes feed hungry neurons. *Molecular Neurobiology*, 32:59–72.
- Petrus, E., Isaiah, A., Jones, A. P., Li, D., Wang, H., Lee, H. K., and Kanold, P. O. (2014). Crossmodal Induction of Thalamocortical Potentiation Leads to Enhanced Information Processing in the Auditory Cortex. *Neuron*, 81:664–673.

- Piché, M., Robert, S., Miceli, D., and Bronchti, G. (2004). Environmental enrichment enhances auditory takeover of the occipital cortex in anophthalmic mice. *European Journal of Neuroscience*, 20:3463–3472.
- Pinto, J. G. A., Hornby, K. R., Jones, D. G., and Murphy, K. M. (2010). Developmental changes in GABAergic mechanisms in human visual cortex across the lifespan. *Frontiers in Cellular Neuroscience*, 4:16.
- Piovesan, E. J., Lange, M. C., Kowacs, P. A., Famelli, H., Werneck, L. C., Yamada, A., and Minguetti, G. (2002). Structural and functional analyses of the occipital cortex in visual impaired patients with visual loss before 14 years old. *Arquivos de neuro-psiquiatria*, 60:949–953.
- Pitskel, N. B., Merabet, L. B., Ramos-Estebanez, C., Kauffman, T., and Pascual-Leone, A. (2007). Time-dependent changes in cortical excitability after prolonged visual deprivation. *Neuroreport*, 18:1703–1707.
- Poirier, C., Collignon, O., Scheiber, C., Renier, L., Vanlierde, A., Tranduy, D., Veraart, C., and De Volder, A. G. (2006). Auditory motion perception activates visual motion areas in early blind subjects. *NeuroImage*, 31:279–285.
- Poldrack, R. A. (2014). Is "efficiency" a useful concept in cognitive neuroscience? *Developmental Cognitive Neuroscience*.
- Poldrack, R. A., Wagner, A. D., Prull, M. W., Desmond, J. E., Glover, G. H., and Gabrieli, J. D. (1999). Functional specialization for semantic and phonological processing in the left inferior prefrontal cortex. *NeuroImage*, 10:15–35.
- Provencher, S. W. (1993). Estimation of metabolite concentrations from localized in vivo proton NMR spectra. *Magnetic Resonance in Medicine*, 30:672–679.
- Ptito, M., Fumal, A., de Noordhout, A. M., Schoenen, J., Gjedde, A., and Kupers, R. (2008). TMS of the occipital cortex induces tactile sensations in the fingers of blind Braille readers. *Experimental Brain Research*, 184:193–200.
- Ptito, M., Matteau, I., Zhi Wang, A., Paulson, O. B., Siebner, H. R., and Kupers, R. (2012). Crossmodal recruitment of the ventral visual stream in congenital blindness. *Neural Plasticity*, 2012.

- Puts, N. A. J. and Edden, R. A. E. (2012). In Vivo Magnetic Resonance Spectroscopy of GABA: a methodological review. *Prog Nucl Magn Reson Spectrosc*, 60:29–41.
- Qin, W., Liu, Y., Jiang, T., and Yu, C. (2013). The Development of Visual Areas Depends Differently on Visual Experience. *PLoS ONE*, 8.
- Rademacher, J., Bürgel, U., and Zilles, K. (2002). Stereotaxic localization, intersubject variability, and interhemispheric differences of the human auditory thalamocortical system. *NeuroImage*, 17:142–160.
- Rauschecker, J. P. (1998). Cortical processing of complex sounds. *Current Opinion in Neurobiology*, 8:516–521.
- Rauschecker, J. P. and Harris, L. R. (1983). Auditory compensation of the effects of visual deprivation in the cat’s superior colliculus. *Experimental Brain Research*, 50:69–83.
- Rauschecker, J. P. and Tian, B. (2000). Mechanisms and streams for processing of ”what” and ”where” in auditory cortex. *Proceedings of the National Academy of Sciences of the United States of America*, 97:11800–11806.
- Raz, N., Amedi, A., and Zohary, E. (2005). V1 activation in congenitally blind humans is associated with episodic retrieval. *Cerebral Cortex*, 15:1459–1468.
- Renier, L. A., Anurova, I., De Volder, A. G., Carlson, S., VanMeter, J., and Rauschecker, J. P. (2009). Multisensory integration of sounds and vibrotactile stimuli in processing streams for ”what” and ”where”. *Journal of Neuroscience*, 29:10950–10960.
- Renier, L. A., Anurova, I., De Volder, A. G., Carlson, S., VanMeter, J., and Rauschecker, J. P. (2010). Preserved functional specialization for spatial processing in the middle occipital gyrus of the early blind. *Neuron*, 68:138–148.
- Ricciardi, E., Bonino, D., Pellegrini, S., and Pietrini, P. (2013). Mind the blind brain to understand the sighted one! Is there a supramodal cortical functional architecture? *Neuroscience and Biobehavioral Reviews*.
- Rockland, K. S. and Ojima, H. (2003). Multisensory convergence in calcarine visual areas in macaque monkey. In *International Journal of Psychophysiology*, volume 50, pages 19–26.

- Röder, B., Demuth, L., Streb, J., and Rösler, F. (2003). Semantic and morpho-syntactic priming in auditory word recognition in congenitally blind adults. *Language and Cognitive Processes*, 18:1–20.
- Röder, B., Rösler, F., and Neville, H. J. (2000). Event-related potentials during auditory language processing in congenitally blind and sighted people. *Neuropsychologia*, 38:1482–1502.
- Röder, B., Stock, O., Bien, S., Neville, H., and Rösler, F. (2002). Speech processing activates visual cortex in congenitally blind humans. *European Journal of Neuroscience*, 16:930–936.
- Röder, B., Teder-Sälejärvi, W., Sterr, A., Rösler, F., Hillyard, S. A., and Neville, H. J. (1999). Improved auditory spatial tuning in blind humans. *Nature*, 400:162–166.
- Sadato, N., Okada, T., Honda, M., and Yonekura, Y. (2002). Critical period for cross-modal plasticity in blind humans: a functional MRI study. *NeuroImage*, 16:389–400.
- Saenz, M., Lewis, L. B., Huth, A. G., Fine, I., and Koch, C. (2008). Visual Motion Area MT+/V5 Responds to Auditory Motion in Human Sight-Recovery Subjects. *Journal of Neuroscience*, 28:5141–5148.
- Sakurabayashi, H., Sato, Y., and Uehara, E. (1956). Auditory discrimination of the blind. *J Psychol Blind*, 1:3–10.
- Satlin, A., Bodick, N., Offen, W. W., and Renshaw, P. F. (1997). Brain proton magnetic resonance spectroscopy (1H-MRS) in Alzheimer’s disease: changes after treatment with xanomeline, an M1 selective cholinergic agonist. *American Journal of Psychiatry*, 154:1459–1461.
- Schepers, I. M., Hipp, J. F., Schneider, T. R., Röder, B., and Engel, A. K. (2012). Functionally specific oscillatory activity correlates between visual and auditory cortex in the blind. *Brain : a journal of neurology*, 135:922–34.
- Schlaug, G., Chen, C., Press, D., Halpernt, A., Chen, Q., Pascual-leone, A., and Warde, A. (2000). Hearing with the minds eye. *NeuroImage*, 5:2000.
- Schmid, M., Nardone, A., De Nunzio, A. M., Schmid, M., and Schieppati, M. (2007). Equilibrium during static and dynamic tasks in blind subjects: no evidence of cross-modal plasticity. *Brain : a journal of neurology*, 130:2097–2107.

- Schneider, K. A., Richter, M. C., and Kastner, S. (2004). Retinotopic organization and functional subdivisions of the human lateral geniculate nucleus: a high-resolution functional magnetic resonance imaging study. *Journal of Neuroscience*, 24:8975–8985.
- Schneider, P., Sluming, V., Roberts, N., Scherg, M., Goebel, R., Specht, H. J., Dosch, H. G., Bleeck, S., Stippich, C., and Rupp, A. (2005). Structural and functional asymmetry of lateral Heschl's gyrus reflects pitch perception preference. *Nature Neuroscience*, 8:1241–1247.
- Schnupp, J., Nelken, I., and King, A. J. (2011). *Auditory Neuroscience - Making Sense of Sound*. MIT Press.
- Schonwiesner, M., Krumbholz, K., Rubsamen, R., Fink, G. R., and von Cramon, D. Y. (2007). Hemispheric asymmetry for auditory processing in the human auditory brain stem, thalamus, and cortex. *Cerebral Cortex*, 17:492–499.
- Schoth, F., Burgel, U., Dorsch, R., Reinges, M. H. T., and Krings, T. (2006). Diffusion tensor imaging in acquired blind humans. *Neuroscience Letters*, 398:178–182.
- Schroeder, C. E., Smiley, J., Fu, K. G., McGinnis, T., O'Connell, M. N., and Hackett, T. A. (2003). Anatomical mechanisms and functional implications of multisensory convergence in early cortical processing. In *International Journal of Psychophysiology*, volume 50, pages 5–17.
- Schwarzkopf, D. S., Song, C., and Rees, G. (2011). The surface area of human V1 predicts the subjective experience of object size. *Nature Neuroscience*, 14:28–30.
- Shaw, G. M., Carmichael, S. L., Yang, W., Harris, J. A., Finnell, R. H., and Lammer, E. J. (2005). Epidemiologic characteristics of anophthalmia and bilateral microphthalmia among 2.5 million births in California, 1989-1997. *American Journal of Medical Genetics. Part A*, 137:36–40.
- Shimony, J. S., Burton, H., Epstein, A. A., McLaren, D. G., Sun, S. W., and Snyder, A. Z. (2006). Diffusion tensor imaging reveals white matter reorganization in early blind humans. *Cerebral Cortex*, 16:1653–1661.
- Shtyrov, Y., Pihko, E., and Pulvermüller, F. (2005). Determinants of dominance: Is language laterality explained by physical or linguistic features of speech? *NeuroImage*, 27:37–47.

- Shu, N., Li, J., Li, K., Yu, C., and Jiang, T. (2009). Abnormal diffusion of cerebral white matter in early blindness. *Human Brain Mapping*, 30:220–227.
- Sliwinska, M. W., Khadilkar, M., Campbell-Ratcliffe, J., Quevenco, F., and Devlin, J. T. (2012). Early and sustained supramarginal gyrus contributions to phonological processing. *Frontiers in Psychology*, 3.
- Smith, S. M. (2002). Fast robust automated brain extraction. *Human Brain Mapping*, 17:143–155.
- Soares, D. P. and Law, M. (2009). Magnetic resonance spectroscopy of the brain: review of metabolites and clinical applications. *Clinical Radiology*, 64:12–21.
- Stagg, C. J. (2013). Magnetic Resonance Spectroscopy as a tool to study the role of GABA in motor-cortical plasticity. *NeuroImage*, pages 1–9.
- Starlinger, I. and Niemeyer, W. (1981). Do the blind hear better? Investigations on auditory processing in congenital or early acquired blindness. I. Peripheral functions. *Audiology*, 20:503–509.
- Stellwagen, D. and Shatz, C. J. (2002). An instructive role for retinal waves in the development of retinogeniculate connectivity. *Neuron*, 33:357–367.
- Stephan, K. E., Penny, W. D., Moran, R. J., den Ouden, H. E. M., Daunizeau, J., and Friston, K. J. (2010). Ten simple rules for dynamic causal modeling. *NeuroImage*, 49:3099–3109.
- Stevens, A. A. and Weaver, K. (2005). Auditory perceptual consolidation in early-onset blindness. *Neuropsychologia*, 43:1901–1910.
- Stoodley, C. J. and Schmahmann, J. D. (2009). Functional topography in the human cerebellum: A meta-analysis of neuroimaging studies. *NeuroImage*, 44:489–501.
- Striem-Amit, E., Cohen, L., Dehaene, S., and Amedi, A. (2012). Reading with Sounds: Sensory Substitution Selectively Activates the Visual Word Form Area in the Blind. *Neuron*, 76:640–652.
- Suh, B. C. and Hille, B. (2002). Recovery from muscarinic modulation of M current channels requires phosphatidylinositol 4,5-bisphosphate synthesis. *Neuron*, 35:507–520.

- Sur, M., Garraghty, P. E., and Roe, A. W. (1988). Experimentally induced visual projections into auditory thalamus and cortex. *Science*, 242:1437–1441.
- Suzuki, M., Kitano, H., Kitanishi, T., Itou, R., Shiino, A., Nishida, Y., Yazawa, Y., Ogawa, F., and Kitajima, K. (2002). Cortical and subcortical activation with monaural monosyllabic stimulation by functional MRI. *Hearing Research*, 163:37–45.
- Symmes, D., Alexander, G. E., and Newman, J. D. (1980). Neural processing of vocalizations and artificial stimuli in the medial geniculate body of squirrel monkey. *Hearing Research*, 3:133–146.
- Szczepanski, S. M., Konen, C. S., and Kastner, S. (2010). Mechanisms of spatial attention control in frontal and parietal cortex. *Journal of Neuroscience*, 30:148–10.
- Tootell, R., Mendola, J., Hadjikhani, N., Ledden, P., Liu, A., Reppas, J., Sereno, M., and Dale, A. (1997). Functional analysis of V3A and related areas in human visual cortex. *Journal of Neuroscience*, 17:7060–78.
- Tucker, P., Laemle, L., Munson, A., Kanekar, S., Oliver, E. R., Brown, N., Schlecht, H., Vetter, M., and Glaser, T. (2001). The eyeless mouse mutation (ey1) removes an alternative start codon from the Rx/rax homeobox gene. *Genesis*, 31:43–53.
- Uhl, F., Franzen, P., Podreka, I., Steiner, M., and Deecke, L. (1993). Increased regional cerebral blood flow in inferior occipital cortex and cerebellum of early blind humans. *Neuroscience Letters*, 150:162–164.
- Ungerleider, L. and Mishkin, M. (1982). Two cortical visual systems. *Analysis of Visual Behavior*, pages 549–586.
- Van Essen, D. C. (2005). Corticocortical and thalamocortical information flow in the primate visual system. In *Progress in Brain Research*, volume 149, pages 173–185.
- Veraart, C., De Volder, A. G., Wanet-Defalque, M. C., Bol, A., Michel, C., and Goffinet, A. M. (1990). Glucose utilization in human visual cortex is abnormally elevated in blindness of early onset but decreased in blindness of late onset. *Brain Research*, 510:115–121.
- Verma, A. S. and Fitzpatrick, D. R. (2007). Anophthalmia and microphthalmia. *Orphanet Journal of Rare Diseases*, 2:47.

- Vidyasagar, T. R. (1978). Possible plasticity in the rat superior colliculus. *Nature*, 275:140–141.
- von Kriegstein, K., Patterson, R. D., and Griffiths, T. D. (2008). Task-Dependent Modulation of Medial Geniculate Body Is Behaviorally Relevant for Speech Recognition. *Current Biology*, 18:1855–1859.
- Voss, P. (2013). Sensitive and critical periods in visual sensory deprivation. *Frontiers in Psychology*, 4:664.
- Voss, P., Gougoux, F., Zatorre, R. J., Lassonde, M., and Lepore, F. (2008). Differential occipital responses in early- and late-blind individuals during a sound-source discrimination task. *NeuroImage*, 40:746–758.
- Voss, P., Lassonde, M., Gougoux, F., Fortin, M., Guillemot, J.-P., and Lepore, F. (2004). Early- and late-onset blind individuals show supra-normal auditory abilities in far-space. *Current Biology*, 14:1734–1738.
- Voss, P., Pike, B. G., and Zatorre, R. J. (2014). Evidence for both compensatory plastic and disuse atrophy-related neuroanatomical changes in the blind. *Brain : a journal of neurology*, 137:1224–1240.
- Voss, P. and Zatorre, R. J. (2012). Occipital cortical thickness predicts performance on pitch and musical tasks in blind individuals. *Cerebral Cortex*, 22:2455–65.
- Wan, C. Y., Wood, A. G., Reutens, D. C., and Wilson, S. J. (2010). Early but not late-blindness leads to enhanced auditory perception. *Neuropsychologia*, 48:344–348.
- Wanet-Defalque, M. C., Veraart, C., De Volder, A., Metz, R., Michel, C., Doms, G., and Goffinet, A. (1988). High metabolic activity in the visual cortex of early blind human subjects. *Brain Research*, 446:369–373.
- Wang, X.-C., Du, X.-X., Tian, Q., and Wang, J.-Z. (2008). Correlation between choline signal intensity and acetylcholine level in different brain regions of rat. *Neurochemical research*, 33:814–819.
- Warner, C. E., Kwan, W. C., and Bourne, J. a. (2012). The early maturation of visual cortical area MT is dependent on input from the retinorecipient medial portion of the inferior pulvinar. *Journal of Neuroscience*, 32:17073–85.

- Warren, J. E., Wise, R. J. S., and Warren, J. D. (2005). Sounds do-able: Auditory-motor transformations and the posterior temporal plane. *Trends in Neurosciences*, 28:636–643.
- Watkins, K. E., Cowey, A., Alexander, I., Filippini, N., Kennedy, J. M., Smith, S. M., Ragge, N., and Bridge, H. (2012). Language networks in anophthalmia: maintained hierarchy of processing in 'visual' cortex. *Brain : a journal of neurology*, 135:1566–77.
- Watkins, K. E., Shakespeare, T. J., O'Donoghue, M. C., Alexander, I., Ragge, N., Cowey, a., and Bridge, H. (2013). Early Auditory Processing in Area V5/MT+ of the Congenitally Blind Brain. *Journal of Neuroscience*, 33:18242–18246.
- Weaver, K. E., Richards, T. L., Saenz, M., Petropoulos, H., and Fine, I. (2013). Neurochemical changes within human early blind occipital cortex. *Neuroscience*, 252:222–33.
- Weeks, R., Horwitz, B., Aziz-Sultan, A., Tian, B., Wessinger, C. M., Cohen, L. G., Hallett, M., and Rauschecker, J. P. (2000). A positron emission tomographic study of auditory localization in the congenitally blind. *Journal of Neuroscience*, 20:2664–2672.
- Weisser, V., Stilla, R., Peltier, S., Hu, X., and Sathian, K. (2005). Short-term visual deprivation alters neural processing of tactile form. *Experimental Brain Research*, 166:572–582.
- Winer, J. A. (1984). The human medial geniculate body. *Hearing Research*, 15:225–247.
- Woldorff, M. G., Tempelmann, C., Fell, J., Tegeler, C., Gaschler-Markefski, B., Hinrichs, H., Heinz, H. J., and Scheich, H. (1999). Lateralized auditory spatial perception and the contralaterality of cortical processing as studied with functional magnetic resonance imaging and magnetoencephalography. *Human Brain Mapping*, 7:49–66.
- Wong, M., Hackeman, E., Hurd, C., and Goldreich, D. (2011). Short-term visual deprivation does not enhance passive tactile spatial acuity. *PLoS ONE*, 6.
- Wong, R. O. (1999). Retinal waves and visual system development. *Annual Review of Neuroscience*, 22:29–47.

- Wong, R. O., Meister, M., and Shatz, C. J. (1993). Transient period of correlated bursting activity during development of the mammalian retina. *Neuron*, 11:923–938.
- Wurtman, R. J., Blustajn, J. K., and Maire, J. C. (1985). 'Autocannibalism' of choline-containing membrane phospholipids in the pathogenesis of Alzheimer's disease - A hypothesis. *Neurochemistry International*, 7:369–372.
- Yaka, R., Yinon, U., and Wollberg, Z. (1999). Auditory activation of cortical visual areas in cats after early visual deprivation. *European Journal of Neuroscience*, 11:1301–1312.
- Yeo, B. T., Krienen, F. M., Sepulcre, J., Sabuncu, M. R., Lashkari, D., Hollinshead, M., Roffman, J. L., Smoller, J. W., Zöllei, L., Polimeni, J. R., Fischl, B., Liu, H., and Buckner, R. L. (2011). The organization of the human cerebral cortex estimated by intrinsic functional connectivity. *Journal of Neurophysiology*, 106:1125–1165.
- Zatorre, R. J. (1988). Pitch perception of complex tones and human temporal-lobe function. *Journal of the Acoustical Society of America*, 84:566–572.
- Zatorre, R. J. and Belin, P. (2001). Spectral and temporal processing in human auditory cortex. *Cerebral Cortex*, 11:946–53.
- Zatorre, R. J., Belin, P., and Penhune, V. B. (2002). Structure and function of auditory cortex: music and speech. *Trends in Cognitive Sciences*, 6:37–46.
- Zatorre, R. J., Evans, A. C., and Meyer, E. (1994). Neural mechanisms underlying melodic perception and memory for pitch. *Journal of Neuroscience*, 14:1908–1919.
- Zeki, S. M. (1978). Functional specialisation in the visual cortex of the rhesus monkey. *Nature*, 274:423–428.
- Zhang, Y., Brady, M., and Smith, S. (2001). Segmentation of brain MR images through a hidden Markov random field model and the expectation-maximization algorithm. *IEEE transactions on medical imaging*, 20:45–57.
- Zwiers, M. P., Van Opstal, A. J., and Cruysberg, J. R. (2001). A spatial hearing deficit in early-blind humans. *Journal of Neuroscience*, 21:RC142:1–5.